Effect of proinflammatory activation on the neurosupportive functions of astrocytes

Megan Leigh Steele

A thesis submitted in fulfilment of the requirements for the degree of Doctor of Philosophy

School of Medicine

University of Western Sydney

2011

Acknowledgements

First of all thank you to my supervisor Associate Professor Gerald Münch. Over the last four and a half years you have provided me with encouragement and guidance. At the same time you have given me the freedom to pursue ideas, try things my own way and make my own mistakes. I feel that I have learnt an enormous amount about what it means to be a scientist as a result of this. I am also grateful for the variety of opportunities that you have provided and for your ongoing support and friendship throughout the course of my PhD.

Thank you to all the past and present members of the lab for your friendship and camaraderie. Special thanks to Grant and also to Katrin and Sonia from the early days back in Townsville. To Annette, Bernie and Kib who all made the move from Townsville to Sydney along side me; and Nicky and Tanja who made the last couple of years so much fun! Thanks also to the rest of the post grad bunch for the numerous laughs, D & Ms, rant sessions, participation in crazy dress days, movie nights, basketball fridays and "write club" nights. Thanks for your company during the many late nights and weekends spent working towards what sometimes felt like a distant light at the end of a very long tunnel.

On the academic front, thanks to Dr Lezanne Ooi for proof reading and for being an exemplary role model. I only wish you were here sooner! Thanks to Professor Nikolaus Sücher for providing the Chinese herbs and for feedback regarding Chapter 6. Thanks to John Truong for providing the chemical antioxidant data and to Stacey Fuller for being a wonderful honours student, whose data slotted nicely into my project. Thanks to Associate Professor Stephen Robinson for his time and tremendous skill in helping me to publish my literature review. Many thanks also to Garry Niedermayer, Shameran Slewa-Younan and Cindy Kersaitis for reading through the final version.

I am very grateful to Alzheimer's Australia for providing me with the Hunter Postgraduate Scholarship Award (2007-2010) and for funding my research through the Dementia grants program.

Thank you to all of my lovely friends and family who are scattered between Townsville, Sydney and around the world for your support, understanding, distractions and motivation. I can't wait to celebrate with you and get back to having a social life!

A couple of special thanks to my temporary housemates, Sam and Maczurek, for helping me get through the last few challenging months. Sam - I can't thank you enough for letting me stay with you, providing me with dinner on numerous occasions, always having wine on hand and for listening to my longwinded stories and progress updates! MacZurek - there's been times over the last couple of months that we've almost killed each other, but I'm extremely grateful for the fact that we've been in this together from the start. Not only are you a good friend, but you've been a great support over the years for bouncing ideas off and working through problems with. Nicksi – thank you for your friendship and support over the last few years and for your encouragement and positivity during the last couple months. I will definitely miss our coffee breaks and wine nights. Mark, Tanja, Paul, Elise, Chris, Elie and Sarah G you've also been great supports to me at various times, thank you.

Last of all, but most importantly, thank you to Mum, Dad and Lisey. I am so very grateful for everything that you've ever done for me. I grew up with the encouragement that I can do whatever I put my mind to. Although I have doubted this many times over the last few years, the strength of your confidence in me and your unconditional love and support has helped me keep on keeping on. I promise that I will get a 'real' job soon…

Statement of Authentication

The work presented in this thesis is, to the best of my knowledge and belief, original except as acknowledged in the text. I hereby declare that I have not submitted this material, either in full or in part, for a degree at this or any other institution.

Megan Steele

August 2011

Table of Contents

List of Figures

List of Tables

List of Publications

Steele ML and Robinson, S. Reactive astrocytes give neurons less support: implications for Alzheimer's disease. Neurobiol. Aging. (In press).

Krautwald M, Leech D, Horne S, **Steele ML**, Forbes J, Rahmadi A, Griffith R and Münch G. The Advanced Glycation End Product-Lowering Agent ALT-711 Is a Low-Affinity Inhibitor of Thiamine Diphosphokinase. Rejuvenation Res. 2011; 14(4):383-91.

Fuller S, **Steele ML** and Muench, G. Activated astroglia during chronic inflammation in Alzheimer's disease – Do they neglect their neurosupportive roles? Mutat. Res. 2010; 690(1-2):40-49.

Hansen E, Krautwald M, Maczurek AE, Stuchbury G, Fromm P, **Steele M**, Schulz O, Garcia OB, Castillo J, Körner H and Münch G. A versatile high throughput screening system for the identification of anti-inflammatory and neuroprotective compounds. J. Alzheimers Dis. 2010; 19(2):451-64.

Shanmugam K, Maczurek A, **Steele M**, Benavente-García O, Castillo J, Münch G. Novel Neuroprotective Therapies for Alzheimer's and Parkinsons's Disease. In: Frontiers in Medicinal Chemistry (edited by Reitz AB, Rahman A, Choudhary MI; Bentham Science Publishers, 2010).

Maczurek AE, Krautwald M, **Steele M**, Hager K, Kenklies M, Sharman M, Martins R, Engel J, Carlson D, Münch G. Lipoic Acid as a Novel Treatment for Mild Cognitive Impairment and Early-Alzheimer's Disease. In: Micronutrients and Brain Health (edited by Packer L, Sies H, Eggersdorfer M, Cadenas E; CRC Press, 2009).

Srikanth V, Maczurek A, Phan T, **Steele ML**, Westcott B, Juskiw D and Münch G. Advanced Glycation Endproducts and their receptor RAGE in Alzheimer's disease. Neurobiol. Aging. 2009; 32(5):763-777.

Fuller S, Muench G and **Steele ML**. Activated astrocytes: a therapeutic target in Alzheimer's disease? Exp. Rev. 2009; 9(11):1585-1594.

Shanmugam K, Holmquist L, **Steele M**, Stuchbury G, Berbaum K, Schulz O, Benavente García O, Castillo J, Burnell J, Garcia Rivas V, Dobson G and Münch G. Plant-derived polyphenols attenuate lipopolysaccharide-induced nitric oxide and tumour necrosis factor production in murine microglia and macrophages. Mol. Nutr. Food Res. 2008; 52(4):427-38.

Steele M, Stuchbury G and Münch G. The molecular basis of the prevention of Alzheimer's disease through healthy nutrition. Exp. Gerontol. 2007; 42:28-36.

Holmquist L, Stuchbury G, **Steele M** and Münch G. Hydrogen peroxide is a true first messenger. J. Neural Transm. Suppl. 2007; 72:39-41.

Steele M, Münch G. Healthy nutrition and selected micronutrients can delay the cognitive decline in the elderly. Exp. Gerontol. 2007; 42:8-9. (editorial).

List of Presentations

Oral presentation "Effect of proinflammatory activation on the neurosupportive functions of astroglia" at UWS Futures Forum – June 2011 (Sydney, Australia)

- awarded prize for best presentation

Poster presentation "Effect of proinflammatiory activation on the neurosupportive functions of astroglia" at the Alzheimer's disease-Parkinson's disease conference – March 2011 (Barcelona, Spain)

Oral presentation "Effect of proinflammatory activation on the neurosupportive functions of astroglia" at the Australian Neuroscience Society Meeting – February 2011 (Auckland, New Zealand)

Poster presentation "Increasing glutathione export by astrocytes – a novel therapeutic principle for the treatment of Alzheimer's disease?" at the International Conference on Alzheimer's Disease – July 2010 (Honolulu, Hawaii)

Poster presentation "Change in glutathione export parameters by activated astrocytes – a novel target for Alzheimer's disease" at the 4th Alzheimer's & Parkinson's Disease Symposium – April 2010 (Sydney, NSW) **- awarded poster prize**

Oral presentation "Change in glutathione export parameters by activated astrocytes – a novel target for Alzheimer's disease" at Kioloa Neuroscience Colloquium – March 2010 (Kioloa, NSW)

Poster presentation "Change in glutathione export parameters by activated astrocytes – a novel target for Alzheimer's disease" at the Australian Neuroscience Society Meeting – February 2010 (Sydney, NSW)

Oral presentation "Change in glutathione export parameters by activated astrocytes – a novel target for Alzheimer's disease" at the Dementia and Neurodegenerative Disease Interest Meeting – January 2010 (Sydney, NSW)

Poster presentation "Change in glutathione export parameters by activated astrocytes – a novel target for Alzheimer's disease" at the Society for Free Radical Research Meeting – December 2009 (Sydney, NSW)

Poster presentation "Change in glutathione export parameters by activated astrocytes – a novel target for Alzheimer's disease" at the Australasian Society of Clinical and Experimental Pharmacologists and Toxicologists Meeting – November 2009 (Sydney, NSW) (co-author)

Abbreviations

AAPH	2,2'azobis(2-amidinopropane)dihydrochloride
ABD-F	4-fluoro-7-aminosulfonylbenzofurazan
ACM	astroglial-conditioned media
ACT	α1-antichymotrypsin
AD	Alzheimer's disease
ANLS	astrocyte-neuron lactate shuttle
ARE	antioxidant response element
ASC system	Alanine-serine-cysteine system
ATP	adenosine triphosphate
CAC	Citric acid cycle
CGL	cysteine glutamate ligase
CNS	central nervous system
CSF	cerebral spinal fluid
Cys	cysteine
Cysgly	cysteinylglycine
DMEM	Dulbeccos's Modified Eagle Medium
DMSO	dimethyl sulfoxide
DNA	deoxyribonucleic acid
DPPH	1,1-Diphenyl-2-picryl-hydrazyl
DTNB	5,5'-dithio-bis(2-nitrobenzoic acid)
EAAT	excitatory amino acid transporter
EC_{50}	50% effective concentration
EDTA	ethylenediaminetetraacetic acid
ELISA	enzyme-linked immunosorbent sandwich assay
FBS	foetal bovine serum
FCR	Folin-Ciocalteu reagent
FDG	2-fluorodeoxy-D-glucose
GA	gallic acid
GABA	γ-aminobutyric acid
GAPDH	glyceraldehyde phosphate dehydrogenase
GFAP	glial fibrillary acidic protein
GLAST/GLT	Na^+-dependent glutamate transporters
GLUT	glucose transporter
GlyT	glycine transporter
GPx	glutathione peroxidase
GR	glutathione reductases
GS	glutamine synthetase
GSH	glutathione
GSSG	glutathione disulfide
GST	glutathione-S-transferase
H_2O_2	hydrogen peroxide

HCl	hydrochloric acid
Hcys	homocysteine
HPLC	high pressure liquid chromatography
IL	interleukin
INF-γ	interferon-γ
Keap1	Kelch like-ECH-associated protein 1
LC_{50}	50% of lethal concentration
LDH	lactate dehydrogenase
LPS	Lipopolysaccharide
MCP	monocyte chemotactic protein
MCT	monocarboxylate transporter
Mrp1	multidrug resistance protein 1
NAC	N-acetylcysteine
NAD(P)H	reduced nicotinamide adenine dinucleotide (phosphate)
$NAD(P)^+$	oxidised nicotinamide adenine dinucleotide (phosphate)
NFκB	nuclear factor kappa B
NFT	neurofibrillary tangles
NMDA	N-methyl-D-aspartate
NO	nitric oxide
Nrf2	nuclear factor erythroid-2-related factor 2
NSAID	non-steroidal anti-inflammatory drugs
ORAC	oxygen radical absorbance capacity
PBS	phosphate buffered saline
PI3	phosphoinositide 3 kinase pathway
PD	Parkinson's disease
PET	positron emission topography
PPP	pentose phosphate pathway
PVDF	polyvinylidene
ROS	reactive oxygen species
RSD	relative standard deviation
SBD-F	4-aminosulfonyl-7-fluoro-2,1,3-benzoxadiazole-4-sulfonate
SD	standard deviation
SEM	standard error of the mean
SSA	5-sulfosalicylic acid
TCA	tricarboxylic acid
TCEP	Tris(2-carboxyethyl)phosphine hydrochloride
TCM	traditional Chinese medicine
TNB	5-thio-2-nitrobenzoic acid
TNF-α	tumour necrosis factor-α
X^-_c system	Na^+-independent glutamate-cystine exchanger
γ-GluCys	γ-glutamylcysteine
γ-GT	γ-glutamyltranspeptidase

Abstract

A complex relationship exists between astrocytes and neurons involving astrocytic uptake of glucose and glutathione (GSH) precursors (cysteine, glycine and glutamate) and the release of lactate and GSH, which are taken up by neurons, either directly or after extracellular degradation. This metabolic exchange between astrocytes and neurons is vital to normal neuronal functions including GSH-dependent cellular antioxidant defence. It is therefore hypothesised that a breakdown in astroglial-neuronal interaction, due to chronically activated astrocytes altering their metabolic phenotype, might lead to neurons becoming energetically challenged and vulnerable to neurodegeneration, as observed in Alzheimer's disease (AD). This thesis examined the affect of proinflammatory activation on two key neurosupportive functions of astrocytes: (1) the supply of GSH and its degradation products and (2) the uptake of glucose and release of lactate. A large portion of the project related to establishment of the conditions of inflammatory activation in U373 cells and the development and validation of a high pressure liquid chromatography (HPLC) method required for the determination of GSH and related thiol compounds. Based on the premise that astrocytes are key modulators in the progression of oxidative stress associated neurodegenerative diseases, thirteen herbal extracts purported to possess anti-ageing or cognitive-enhancing properties by traditional Chinese medicine were tested for their cytoprotective ability in hydrogen peroxide-challenged U373 cells. Findings from this thesis suggest that inflammation activated astrocytes might contribute to neurodegenerative processes through the upregulation of neurotoxic activities (i.e. release of cytokines such as IL-6 and neurotoxic compounds such as homocysteine) as well as decreases in neurosupportive functions (i.e. provision of substrates for GSH synthesis and energy metabolism). The results

presented strongly support the hypothesis that reactive astrocytes play a key role in disease progression. Furthermore, a multi-compound, multi-targeted approach is proposed for the prevention and treatment of AD and drugs capable of restoring astrocytic function or supplementation of astrocyte-derived neuronal nutrients may be especially important.

CHAPTER 1

Literature review

1.1 Introduction

Astrocytes serve an array of important functions, including the regulation of extracellular ion concentrations, synaptic remodelling (addition and removal of synapses), and the maintenance of protective barriers, such as the glia limitans, glial scars and blood-brain barrier. The ensheathment of blood vessels and synapses by astrocytic processes enables these cells to monitor the extracellular ionic environment and to mediate the transfer of metabolites between cerebral blood vessels and neurons. Three crucial interrelated astroglial-neuronal interactions, discussed herein, are glucose uptake and lactate release, glutamate recycling and the synthesis of glutathione.

1.2 Astrocytes take up glucose and release lactate

Glucose is transported from the blood to the abluminal surface of cerebral capillaries by vascular endothelial cells and is then taken up by glucose transporter (GLUT)1, which is located on the endfeet of astrocytes (Benarroch, 2005) and thought to play a constitutive role in basal glucose uptake (Birnbaum et al., 1986). In contrast, neurons predominantly express GLUT3, which is an inducible transporter, commonly described as the "insulin-responsive" transporter (Birnbaum, 1989; Leino et al., 1998; McEwen and Reagan, 2004). In cell culture, glucose taken up by astrocytes and neurons is phosphorylated by hexokinase, thus committing it to breakdown by glycolysis (Brown and Ransom, 2007). In the brain however, astrocytes may have a virtual monopoly over glucose due to the proximity of their endfeet to capillary walls, and the fact that nearly all neuronal processes and cell bodies are ensheathed by astrocytes. Hence most of the metabolic substrates that reach neurons are likely to have first passed through astrocytes (Barros et al., 2005; Rouach et al., 2008). The

direct transfer of glucose from astrocytes to neurons was recently demonstrated in brain slices (Gandhi et al., 2009). The importance of astrocyte mediated glucose uptake is illustrated by a clinical condition termed GLUT1-deficiency syndrome, which results in a 50% decrease in GLUT1 protein expression in vascular endothelial cells and astrocytes, and is associated with a global decrease in cortical glucose uptake and severe neurological deficits (Brockmann, 2009; Pascual et al., 2002).

Astrocytes metabolise glucose to lactate by glycolysis, or store glucose as glycogen; nearly all of the glycogen stores in the brain are located within astrocytes, because neurons lack the enzymes required to metabolise glycogen (Brown and Ransom, 2007). Astrocytes release lactate via the H^+-coupled monocarboxylate transporters (MCT) 1 and 4, and the extracellular lactate is taken up into neurons via MCT2. Neurons convert lactate to pyruvate which can serve as a substrate for oxidative metabolism (Benarroch, 2005). There has been considerable controversy concerning whether lactate released from astrocytes is a major substrate for neuronal energy metabolism during synaptic activity (Bouzier-Sore et al., 2003). Described as the astrocyte-neuron lactate shuttle hypothesis, supporting evidence comes from in vitro demonstrations that astrocytes produce lactate in an activity-dependent, glutamate-mediated manner and that neurons can take up this lactate as a substrate for oxidative metabolism (Pellerin and Magistretti, 1994). Cytological support includes differences in enzyme subtypes and lactate transporter affinities between astrocytes and neurons. For example, astrocytes primarily express lactate dehydrogenase-5 (LDH-5), which catalyses pyruvate to lactate, whereas neurons primarily express LDH-1, which catalyses lactate to pyruvate (Bittar et al., 1996; Laughton et al., 2007).

Evidence against an astrocyte-neuron lactate shuttle is based on observations that astrocytes in culture can completely degrade glucose via the tricarboxylic acid (TCA) cycle (Hertz et al., 2007), that both astrocytes and neurons possess efficient transporters for the uptake of glucose (Vannucci et al., 1997), and that activated neurons are capable of releasing lactate (Dienel and Cruz, 2008). Indeed, Gandhi and colleagues (2009) used a novel fluorometric approach to infer that much of the lactate released during brain activation may originate from neurons, and be transported to capillaries by astrocytes, rather than serving as a metabolic substrate. Despite these objections, it is becoming increasingly accepted that synaptic activity is at least partly fuelled by the transfer of metabolites from astrocytes to neurons, and that lactate is likely to be one of these metabolites (Aubert et al., 2005; Dienel and Cruz, 2008; Erlichman et al., 2008; Hyder et al., 2006). Another point of agreement is that the breakdown of glycogen to lactate provides astrocytes with a source of energy that can be obtained extremely rapidly and without a requirement for oxygen, therefore glycogen represents a valuable substrate during periods of high metabolic demand, when the availability of blood-borne glucose and oxygen are rate-limiting factors (Brown and Ransom, 2007).

Neurons lack another critical step in energy metabolism; pyruvate carboxylase is present in astrocytes and other glial cells but not in neurons (Murin et al., 2009). Pyruvate carboxylase combines a molecule of carbon dioxide with one of pyruvate to form oxaloacetate, which is needed to replenish carbon skeletons in the tricarboxylic acid (TCA) cycle (Serres et al., 2008). Pyruvate carboxylase deficiency is a rare disorder which results in progressive neurologic symptoms including developmental delay, poor muscle tone, abnormal eye movements or seizures (Garcia-Cazorla et al.,

2006). Alternative anaplerotic pathways are present in neurons (eg. carboxylation of pyruvate to malate) but they do not proceed under normal conditions because the energetics of these reactions are not favourable (reviewed by Hertz et al., 2007; Murin et al., 2009). This unusual situation means that astrocytes must provide neurons with a constant supply of TCA intermediates (eg. citrate, malate) or their derivatives (eg. aspartate, glutamine) (Hertz et al., 1999) (Figure 1.1). Without this critical support, the de novo synthesis of glutamate and GABA would rapidly deplete neuronal reserves of TCA intermediates and compromise neuronal viability.

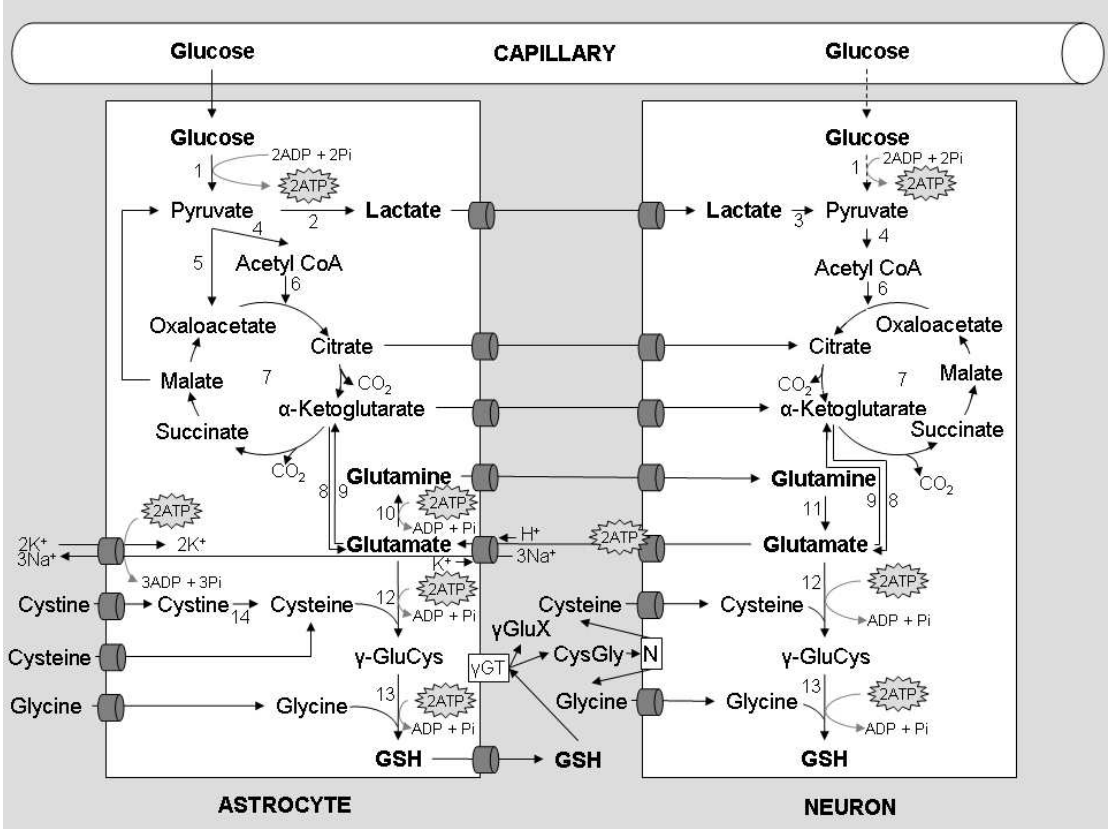

Figure 1.1 Neurosupportive function of astrocytes. Astrocytes and neurons can both take up glucose. Glucose is metabolised to pyruvate via glycolysis (multiple enzymes) [1]. Pyruvate dehydrogenase [4] further catalyses the oxidation of pyruvate to acetyl CoA, which reacts with oxaloacetate to form citrate. This reaction is catalysed by citrate synthase [6] and forms the first step of the tricarboxylic acid (TCA) cycle. In astrocytes, pyruvate can also be converted to oxaloacetate by pyruvate carboxylase [5] or reduced to lactate by lactate dehydrogenase-5 [2]. Neurons can also use lactate that is released by astrocytes as an energy substrate for the TCA cycle, by reconverting lactate to pyruvate through the action of lactate dehydrogenase-1 [3]. It has been suggested that lactate may be the preferred energy substrate of neurons during synaptic activity. Astrocytes also take up glutamate released by pre-synaptic, glutamatergic neurons and can convert glutamate into α-ketoglutarate (another TCA cycle intermediate) by glutamate dehydrogenase and a transaminase [8, 9] (this reaction is reversible under varying metabolic conditions) or into glutamine, by glutamine synthetase [10], to be transported back to neurons. Uptake of glutamate by astrocytes activates the Na+/K+ ATPase, stimulating glucose uptake and metabolism. Both astrocytes and neurons can synthesise glutathione (GSH) by two ATP-consuming reactions, catalysed by γ-glutamylcysteine synthetase [12] and GSH synthetase [13]. Astrocytes can readily take up the required substrates (glutamate, cysteine and glycine) from the extracellular space. However, since extracellular cysteine exists predominantly in its oxidised form as cystine; astrocytes must take up cystine and reduce it to cysteine, via cystine transhydrogenase [14]. Furthermore, astrocytes release GSH, which is subsequently metabolised by γ-glutamyltranspeptidase [γGT] to form cysteinylglycine (cysgly) and a γ-glutamyl derivative. Neurons are able to use cys-gly produced by astrocytes as a precursor for

glutathione synthesis by a mechanism involving the hydrolysis of cys-gly by the ectopeptidase aminopeptidase N [N] and the subsequent uptake of cysteine and glycine. This process is vital for neuronal GSH synthesis due to the inability of neurons to take up sufficient cystine from the extracellular space.

1.3 Astrocytes recycle glutamate for neuronal re-uptake

Glutamate released into the synaptic cleft is mainly taken up by glutamate transporters on adjacent astrocytic processes, and a small amount is taken up by presynaptic neurons for immediate repackaging into vesicles. Astrocytes take up glutamate predominantly by Na^+-dependent glutamate transporters (GLAST and GLT1), but also by Na+-independent glutamate transporters such as the Cl--dependent glutamate-cystine (X-c) antiporter. By taking up glutamate, astrocytes are potentially able to regulate the levels of extracellular glutamate and thereby influence synaptic activity. Astrocytes, but not neurons, contain the enzyme glutamine synthetase (GS), which amidates glutamate to glutamine. Astrocytes release glutamine into the interstitial space for uptake by neurons, which deamidate it via phosphate-activated glutaminase to complete the glutamate-glutamine cycle (Anderson and Swanson, 2000; Hertz et al., 1999).

The functional importance of the glutamate-glutamine cycle is dramatically illustrated when the activity of astrocytic GS is inhibited by methionine sulfoximine. When this drug is administered into the central nervous system, behavioural deficits are observed that correspond to the function of the region injected. Injection of the eye with methionine sulfoximine for example, causes temporary blindness by rapidly depleting retinal neurons of glutamate and glutamine (Barnett et al., 2000; Pow and Robinson, 1994). In another example, this time in chicks, inactivation of GS in the hyperstriatum (homologue of the hippocampus) leaves vision unaffected but prevents the consolidation of new memories for visually-learned discrimination tasks (Gibbs et al., 1996; Ng et al., 1997). In the experiments described above, both the blinding and the amnestic effects of methionine sulfoximine were fully reversed by the

application of exogenous glutamine, indicating that the functional impairments were due to the inhibition of GS, and not to a non-specific action of the drug. Finally, the critical role of astrocytes in the uptake of synaptically-released glutamate uptake is demonstrated by the fact that knockout mice lacking GLT1 undergo spontaneous seizures and premature death as a result of the excitotoxicity caused by high extracellular glutamate concentrations (Tanaka et al., 1997).

The uptake of synaptically-released glutamate into astrocytes is an energetically expensive process, since each molecule of glutamate is co-transported with three sodium ions. These ions then have to be pumped from the astrocytes by exchanging with extracellular potassium, through the action of Na+/K+ ATPase. In addition, the amidation of glutamate to glutamine is ATP-dependent, so each turn of the glutamate-glutamine cycle costs astrocytes a total of four ATP, thereby tightly coupling glucose utilisation in astrocytes to neuronal activity (Hertz et al., 1999; Pellerin et al., 1998).

1.4 Astrocytes maintain the glutathione system

Glutathione (GSH), the main antioxidant thiol in mammalian cells, plays a prominent role in the detoxification of reactive oxygen species and in neutralisation of organic hydroperoxides, particularly of the hydrogen peroxide that is produced as a by-product of metabolism in the electron transport chain (Dringen and Hirrlinger, 2003; Liddell et al., 2006). GSH is a tripeptide consisting of glutamate, cysteine and glycine. Due to the fact that glutamate and glycine are neurotransmitters, they are maintained at low concentrations in the extracellular fluid by high affinity

transporters on astrocytes. Any cysteine that is present extracellularly is rapidly oxidised to cystine which is toxic to neurons and is rapidly accumulated by astrocytes (Dringen et al., 1999b). Astrocytes take up glutamate via GLAST and GLT1, cystine via the X^-_c transporter, cysteine mainly via the Na^+-dependent neutral amino acid transport (ASC) system, and glycine via the glycine transporter (GlyT) 1 (Aschner, 2000; Mallorga et al., 2003). Thus astrocytes have ready access to all three precursors of GSH, whereas neurons have very limited access, particularly to cysteine.

Astrocytes synthesise GSH by two successive, ATP-consuming reactions where the rate-limiting step is the generation of γ-glutamylcysteine (γ-GluCys) from glutamate and cysteine by the action of γ-GluCys synthetase. Glycine is then added to the C-terminal end of γ-GluCys via GSH synthetase. Astrocytes release GSH extracellularly at a rate of 10% of total cellular GSH per hour, whereas neurons and other types of brain cell do not normally release GSH (Dringen and Hirrlinger, 2003). The GSH released by astrocytes is subsequently cleaved by the astrocytic ectoenzyme γ-glutamyltranspeptidase (γ-GT) to generate CysGly and γ-Glu (Dringen and Hirrlinger, 2003). CysGly can then be hydrolysed by a neuronal ectopeptidase (aminopeptidase N) which allows these cells to take up cysteine and glycine for incorporation into GSH, while the glutamate moiety is provided by glutamine, again sourced from astrocytes (Dringen et al., 2000; Dringen and Hirrlinger, 2003).

GSH detoxifies hydrogen peroxide by reducing it to water and oxygen, and in the process GSH is oxidised to glutathione disulphide (GSSG). Astrocytes and neurons can recycle GSSG by reducing it to GSH in a NADPH-dependent reaction that is

catalysed by glutathione reductase. However, during periods of oxidative stress, when there are high rates of GSSG production and a relatively low availability of NADPH, cells release GSSG extracellularly. As a consequence, neurons must continually synthesise GSH to replenish their supplies. Since neuronal stores of GSH are entirely dependent on the provision of precursors to neurons by astrocytes, neurons are more vulnerable than astrocytes to oxidative stress. Numerous co-culture experiments have shown that astrocytes protect neurons from the toxicity of hydrogen peroxide by a GSH-dependent mechanism (Dringen et al., 2000; Gegg et al., 2005).

1.5 Inflammation and oxidative stress modify the metabolic phenotype of astrocytes

This review has discussed three important features of the symbiotic relationship between astrocytes and neurons: metabolic exchange related to energy metabolism, the glutamate cycle and the GSH system. Potential advantages conferred by this complex relationship include: (i) the coupling of glucose utilisation (uptake of glucose from the blood by astrocytes) to neuronal activity; (ii) the existence of multiple points of regulation; (iii) this relationship allows the brain to switch to rapid, local, non-oxidative glucose utilisation (in astrocytes) in order to provide increased substrates for oxidative metabolism in neurons during physiological activation; and (iv) lactate from astrocytes is "clean" energy since astrocytes, which have a higher rate of glycolysis than neurons (Occhipinti et al., 2009), accumulate the cytotoxic, reactive carbonyl compound methylglyoxal, which is a by-product of glycolysis (Desai and Wu, 2008).

Although there seem to be advantages to this glial-neuronal relationship, there is much to be elucidated concerning the causes and consequences of disrupted glial-neuronal communication. Glutamate release by astrocytes is reportedly controlled by inflammatory agents, such as tumour necrosis factor-α (TNF-α) and prostaglandins, thus suggesting that glial-neuronal signalling is sensitive to production of these inflammatory mediators in pathological conditions (Vesce et al., 2007). Additionally, glutamate transporters have been shown to be inhibited by lipid peroxidation in response to various oxidants, leading to neuronal death through glutamate excitotoxicity (Anderson and Swanson, 2000). The inflammatory agents, interferon-γ (IFN-γ) and lipopolysaccharide (LPS), individually and synergistically reduce the levels of intracellular ATP in astrocytes via a nitric oxide-dependent mechanism, without affecting cell viability (Makarov et al., 2006). In the presence of glucose-deficient medium however, LPS and IFN-γ are toxic to astrocytes, thereby demonstrating increased astrocytic vulnerability under low energy conditions (Choi and Kim, 1998). Exposure of primary murine astrocytes to a combination of the proinflammatory cytokines, TNF-α and interleukin (IL)-1β, leads to a 3-fold increase in astrocytic glucose utilization, a marked decrease in intracellular glycogen stores, large increases in the activities of both the pentose phosphate pathway and the TCA cycle, and an increased efflux of GSH and hydrogen peroxide (Gavillet et al., 2008). Furthermore, compared to control astrocytes, those treated with TNF-α and IL-1β, display a 45% decrease in the amount of lactate released in response to glutamate stimulation. Gavillet and colleagues concluded that a pro-inflammatory environment, such as that present in Alzheimer's disease (AD), markedly modifies the metabolic phenotype of astrocytes. Furthermore, this altered astrocytic phenotype may actively increase neuronal vulnerability, both through a disrupted energy metabolism and via

an increased release of hydrogen peroxide (Gavillet et al., 2008). Makarov and colleagues (2006) showed that when cultured astrocytes were exposed to a period of hypoxia followed by re-oxygenation (as a model of ischemia/reperfusion), their GSH levels became depleted and their cellular redox capacity decreased. In a study of primary astrocytes that were exposed to hydrogen peroxide (Liddell et al., 2009a), astrocytes were shown to lower their rate of uptake of glucose by 20% and divert much of their remaining glucose into the pentose phosphate pathway, presumably as a means of regenerating NADPH, which is needed for the reduction of GSSG. As a consequence, the rate of glycolysis in astrocytes was slowed and the rate of lactate release was reduced by 40%. Thus, oxidative stress causes a major shift in the metabolic phenotype of astrocytes. When the preceding findings are transposed to the context of the brain, it can be expected that episodes of oxidative stress will lower the amounts of GSH and lactate released by astrocytes. These changes will subsequently lower the capacity of neurons to produce energy via the TCA cycle and will also limit their capacity to combat oxidative stress.

1.6 Reactive astrocytosis in Alzheimer's disease

The role played by astrocytes in the inflammatory cascade accompanying AD has been well described (Akiyama et al., 2000; Tuppo and Arias, 2005). When astrocytes are stimulated by cytokines such as IL-1β and IL-6, they promote the inflammatory process through the secretion of a wide range of cytokines, chemokines and complement proteins, as well as nitric oxide (Dong and Benveniste, 2001). Other phenotypic changes associated with astrocytes in AD include the upregulation of GFAP (associated with astrocytic activation) (Beach and McGeer, 1988), increased expression of the neurotrophic factor S100β (Marshak DR et al., 1992), and

increased expression of heme oxygenase-1, a marker of oxidative stress (Schipper et al., 2006). In AD, activated astrocytes form a halo around neuritic plaques with their processes covering the neurite layer and interweaving within the plaque (Akiyama et al., 2000; Nagele et al., 2004; Robinson, 2001). Reactive astrocytes in the vicinity of neuritic plaques strongly overexpress the serine protease inhibitor, α1-antichymotrypsin (ACT) (Licastro et al., 1998; Styren et al., 1998). ACT is an acute phase protein that has been implicated as an inhibitor of β-amyloid breakdown, and as a neurotoxin that induces the hyperphosphorylation of neuronal tau protein (Padmanabhan et al., 2006). Hence the release of ACT by reactive astrocytes has the potential both to increase amyloid plaque burden and to increase the incidence of neurofibrillary tangles in AD.

Reactive astrocytes overexpress GFAP, and the expression of GFAP in the AD cortex increases with Braak stage (Wharton et al., 2009), indicating that the extent of astrocytosis increases with the severity of the disease. However, reactive astrocytes are often found some distance away from amyloid deposits (Simpson et al., 2008), indicating that the relationship between astrocyte activation and AD pathology is a complex one. The complexity of this relationship is further illustrated by the fact that the cerebrospinal fluid of AD patients contains significantly increased concentrations of astrocyte-specific proteins, including GS (Tumani et al., 1999), S100β (Petzold et al., 2003), GFAP (Fukuyama et al., 2001) and ACT (Nielsen et al., 2007). It is not yet known whether these increases are due to a greater rate of secretion of these proteins by reactive astrocytes, or whether they are an indicator of astrocyte death. In either case, the increased abundance of these proteins in the cerebrospinal fluid implicates astrocytes in the pathogenesis of the disease.

A triple transgenic mouse model of AD (3xTg-AD) that develops amyloid-β plaques and neurofibrillary tangles was generated through the expression of three major genes associated with familial AD, namely APP_{Swe}, $PS1_{M146V}$, and tau_{P301L} (Oddo et al., 2003). In a histological examination of the hippocampus of these mice, Olabarria and colleagues (2010) confirmed that GFAP+ astrocytes become hypertrophic when they are in the vicinity of β-amyloid plaques. These authors also reported that the numbers of GFAP+ astrocytes in transgenics are similar to those in age-matched control mice, but in transgenic mice the astrocytes located away from plaques are considerably smaller than astrocytes in control mice. This pattern is very different from sporadic AD in humans, where the numbers of GS+ and GFAP+ astrocytes are increased (Robinson, 2001; Vanzani et al., 2005), and hypertrophic GFAP+ astrocytes are often observed in regions away from plaques (Simpson et al., 2010). These differences between AD and the 3xTg-AD mouse indicate that abnormalities in the cellular processing of β-amyloid or tau protein are not the primary cause of reactive astrocytosis in AD. Indeed, in AD, other features of the reactive phenotype, including a downregulation of GS and an upregulation of heme-oxygenase-1, have a spatial distribution that does not reflect that of β-amyloid plaques (Robinson, 2000, 2001; Schipper et al., 2006). Furthermore, while the extent of cognitive impairment is significantly correlated with the extent of heme-oxygenase-1 expression, the upregulation of heme-oxygenase-1 expression begins when patients exhibit mild cognitive impairment, and the extent of heme-oxygenase-1 expression is not correlated with the burden of neuritic plaques or neurofibrillary tangles (Schipper et al., 2006). Thus while hypertrophic astrocytes often occur in the vicinity of β-amyloid plaques, reactive astrocytosis precedes β-amyloid deposition and is more widely distributed. While the primary cause of reactive astrocytosis in AD has not

yet been identified, pro-inflammatory cytokines and/or oxidative stress are promising candidates.

1.7 Abnormal glucose metabolism in Alzheimer's disease

There is potential for the transition of astrocytes from a basal to reactive state to interfere with the metabolic interactions between astrocytes and neurons. Indeed, signs of astrocytic dysfunction relating to the three neuroprotective functions of astrocytes discussed here have been observed in numerous post-mortem and in vivo studies of AD. For example, PET studies show that brain glucose uptake is impaired in AD patients, suggesting that compromised energy metabolism in the brain may be a contributing factor to the neurodegeneration that characterises this disease (Freemantle et al., 2006). The extent of the decrease in glucose uptake rate often exceeds 10%, and since astrocytes constitute as much of the volume of the cerebral cortex as do neurons, it has been suggested that the loss of signal is partly caused by a reduction in glucose uptake by astrocytes (Alexander et al., 2002). Furthermore, it has been shown that disrupted glucose metabolism precedes the appearance of amyloid plaques and neurofibrillary tangles, thus implicating disrupted energy metabolism early in disease progression (Small et al., 2000). Conversely, regions of the AD brain with a high amyloid load do not always exhibit a reduced rate of glucose uptake (Edison et al., 2007). Such observations indicate that while hypometabolism and neuropathological changes are both features of AD, the relationship between these features is not a straightforward one.

1.8 Abnormal glutamate metabolism in Alzheimer's disease

Earlier in this review the glutamate-glutamine cycle was described as an elegant example of a symbiotic relationship between astrocytes and neurons. Many lines of evidence indicate that glutamate recycling is abnormal in AD. For instance, neurons normally express little or no GS, yet it has been detected in sporadic pyramidal neurons in the parahippocampal and inferior temporal regions of the cerebral cortex in end-stage AD (Robinson, 2000). Such neurons are more common in regions of tissue where the expression of GS in nearby astrocytes is abnormally low (Robinson, 2001). This aberrant pattern is consistent with other observations that indicate a major disruption of glutamate metabolism. The activity of GS in cortical homogenates from AD brain for example, is lower than in homogenates from the brains of non-demented individuals (Le Prince et al., 1995; Smith et al., 1991). These changes are mirrored in the cerebrospinal fluid of patients with AD, in which the concentration of glutamate is elevated, while the concentration of glutamine is lowered (Csernansky et al., 1996; Jimenez-Jimenez et al., 1998; Redjems-Bennani et al., 1998; Smith et al., 1985). In this context it is noteworthy that when cultured glutamatergic neurons are deprived of glutamine, they aberrantly express active GS, and this expression can be suppressed by the addition of glutamine or by direct contact with astrocytes (Fernandes et al., 2010).

Astrocytic glutamate transporters are also greatly affected in AD. For instance, the astrocyte-specific glutamate transporter GLT-1/EAAT2 undergoes oxidative modification (Lauderback et al., 2001), and a reduction in its activity (Li et al., 1997; Masliah et al., 1996). This reduction has implications for brain function, because most of the uptake of glutamate from the synaptic cleft is mediated by GLT-1/EAAT2 (Melone et al., 2009). In homogenates of AD cortex, GFAP and EAAT2

expression are inversely correlated, with a trend towards an increased expression of GFAP and a decreased expression of EAAT2 with increasing Braak stage (Simpson et al., 2008). As with GS, the reduced expression of GLT-1/EAAT2 in astrocytes is accompanied by an aberrant expression of this 'glial' glutamate transporter in some AD neurons (Pow and Cook, 2009). Similarly, another astrocytic glutamate transporter, GLAST/EAAT1, is aberrantly expressed in a subset of cortical pyramidal neurons (Scott et al., 2002). Particularly notable is the observation that neuronal GLAST/EAAT1 is only found in neurons that express abnormally phosphorylated tau, suggesting that neuronal EAAT1 expression may be related to neurofibrillary tangle formation in AD (Scott et al., 2002).

Collectively, these observations suggest that AD involves a profound impairment in the capacity of astrocytes to protect neurons from excitotoxicity. In what appears to be a compensatory response, neurons begin to aberrantly express astrocytic transporters and enzymes associated with glutamate metabolism (Pow and Cook, 2009; Robinson, 2000; Scott et al., 2002). Several lines of evidence suggest that cytokines released as part of the inflammatory response are the primary cause of the changes to the glutamate-glutamine cycle in AD. Cytokine levels are greatly increased in AD brains, particularly that of TNF-α, which reaches levels in the cerebrospinal fluid that are 25-fold higher than in cognitively normal individuals (Tarkowski et al., 1999). Among the targets of this proinflammatory cytokine are astrocytes, which are transformed from a resting phenotype to a reactive one (Edwards and Robinson, 2006). It is noteworthy that when astrocytes are exposed to TNF-α, their expression of GLAST is downregulated (Korn et al., 2005; Tilleux and Hermans, 2008) and their expression of GS is reduced to 30% of basal levels (Zou et

al.). These reductions are accompanied by greatly reduced rates of glutamate uptake by astrocytes and by subsequent reductions in their rates of glutamine release (Zou et al.). Furthermore, when co-cultures of astrocytes and neurons are treated with TNF-α, the astrocytes lose their capacity to protect neurons from glutamate excitotoxicity (Zou et al.). These observations suggest that TNF-α may represent a potential therapeutic target in the treatment of AD. Indeed, Etanercept, a drug that specifically targets TNF-α, has been reported to significantly improve cognitive outcomes in AD patients when injected peri-spinally in a six-month pilot trial (Tobinick, 2009).

Ammonia is a potent endogenous neurotoxin that is produced by many metabolic pathways in the brain (Kvamme et al., 2000; Margolis and Lifschitz, 1985). Since the brain lacks a urea cycle, glutamine, which contains two ammonia groups, represents the main route for the clearance of ammonia. For this reason, there is normally a net outflow of glutamine from the brain into the blood (Albrecht et al., 2007). Perturbation of the glutamate-glutamine cycle in AD reduces the brain's capacity to detoxify ammonia, and leads to increased levels of extracellular ammonia. Branconnier and colleagues (1986) examined a group of patients with AD who did not have liver disease, and found that their serum ammonia levels were on average, 3-fold higher than in cognitively normal individuals. While the source of this elevated ammonia was not determined, it is consistent with the diffusion of excess ammonia from the brain. Direct evidence for this possibility was recently provided by Kaiser et al (2010) who reported that the mean concentration of ammonia in the cerebrospinal fluid was 256 μM in mild cognitive impairment and 528 μM in AD. In some individuals with AD, the ammonia concentration in the cerebrospinal fluid was as high as 1.28mM (Kaiser et al., 2010). By contrast, the concentration of ammonia

in the cerebrospinal fluid of normal healthy individuals is approximately 50 μM (Felipo and Butterworth, 2002a). Thus in mild cognitive impairment and AD, the concentrations of extracellular ammonia are five-fold and ten-fold higher than in cognitively normal individuals, respectively. To put these values into context, brain ammonia levels reach 300-500 μM in chronic liver failure, and attain 1-5 mM just prior to death in acute liver failure (reviewed by Felipo and Butterworth, 2002b). Ammonia is hydrophilic and readily substitutes for potassium, so consequently many of its neurotoxic effects are related to a disruption of functions that are normally dependent on potassium, such as the cellular resting potential (Bosoi and Rose, 2009). Since the plasma membranes of astrocytes contain a much higher density of potassium channels than the membranes of neurons (Higashi et al., 2001; Seifert et al., 2009), astrocytes are the major site of ammonia uptake, and in normal circumstances they protect neurons from ammonia toxicity, as has been demonstrated in co-cultures (Rao et al., 2005). In situations where GS activity in astrocytes is diminished, both neurons and astrocytes are exposed to higher concentrations of ammonia. Increased extracellular levels of ammonia in the brain result in increased rates of lactate production, inhibition of the TCA cycle, release of glutamate from astrocytes, decreased expression of glutamate transporters on astrocytes, widespread oxidative and nitrosative stress, and an increased expression of pro-inflammatory cytokines (Bjerring et al., 2009; Felipo and Butterworth, 2002b; Gorg et al., 2010; Norenberg et al., 2009). Seiler (2002) commented on the remarkable similarities between the neuropathological changes and cognitive deficits that occur in AD and those which occur in hepatic encephalopathy, and suggested that elevated cerebral ammonia levels might contribute to the pathogenesis of AD. Two consequences of ammonia intoxication deserve further comment. First, extensive evidence from cell

culture and animal models of acute liver failure has established that elevated ammonia levels activate microglia and increase the cerebral production of inflammatory cytokines, particularly the expression of TNF-α, IL-6 and IL-1β (Jiang et al., 2009). Furthermore, treatment with anti-inflammatory agents, such as indomethacin and minocycline, helps to protect brain cells from ammonia toxicity (Bemeur et al., 2010). Second, these models have also demonstrated that ammonia intoxication results in substantial increases in lipid peroxidation, oxidised mRNA and a depletion of glutathione stores. This oxidative stress is associated with the increased production of superoxide and inducible nitric oxide synthase (Bemeur et al., 2010). There is a strong co-expression of 3-nitrotyrosine in cells that contain GFAP, and furthermore, the GS in these cells is nitrosylated and inactivated, indicating that astrocytes are the principal target of ammonia-induced nitrosative stress (Schliess et al., 2002). Treatment with N-acetylcysteine, an antioxidant and glutathione precursor, reduces oxidative stress in the brains of animals with acute liver failure (Bemeur et al., 2010).

Together the preceding observations suggest that as the activity of GS begins to diminish in early AD (during the phase of mild cognitive impairment), the resulting elevation in extracellular ammonia causes oxidative stress and inflammation which further repress the activity of GS and amplify the neurotoxic cascade. Thus ammonia may represent an important therapeutic target in AD. Elevated serum levels of ammonia in hepatic encephalopathy are commonly treated by the use of non-absorbable disaccharides in the diet and by the administration of non-absorbable antibiotics to reduce ammonia production in the gut (Bass, 2007). If ammonia originating from dietary and bacterial sources could be similarly reduced in AD, this

outcome might facilitate a greater rate of efflux of ammonia from the brain, thereby aiding the clearance of this toxic metabolite. However, such regimes have yet to be trialled as a treatment strategy for AD.

1.9 Oxidative stress in Alzheimer's disease

Compared to the brains of healthy age-matched controls, those in AD are characterised by significantly higher levels of oxidised macromolecules, including lipids, DNA, proteins and sugars (Moreira et al., 2008). This fact is significant in two respects. First it confirms that oxidative stress is a prominent feature of AD and second, since oxidation impairs the function of macromolecules, it will greatly contribute to cellular dysfunction in AD (Butterfield, 2004; Gill et al., 1995). Karelson and colleagues (2001) found that lipid peroxidation (as assessed by diene conjugates and lipid peroxides) was increased in the inferior frontal and inferior temporal cortices of AD patients, while total antioxidant capacity was decreased in the inferior temporal cortex. It was also shown that the ratio of GSSG/GSH (an indicator of oxidative stress) was increased in the inferior frontal and inferior temporal cortices. Interestingly, a comparison between sporadic AD and patients carrying the Swedish K670N/M671L mutation, found that familial AD is associated with a 2-3-fold increase in the cortical levels of diene conjugates, lipid peroxides and protein carbonyls, as well as a significant increase in GSSG levels (Bogdanovic et al., 2001). Thus it appears that familial AD mutations may further increase the brain's sensitivity to oxidative stress.

It is noteworthy that in sporadic AD, the activities of glutathione peroxidase and glutathione reductase are elevated (Aksenov and Markesbery, 2001; Schuessel et al., 2004), indicating that an increased production of pro-oxidants, rather than an impairment of glutathione recycling, is responsible for the increased levels of GSSG. Interestingly, the pentose phosphate pathway is more active in the AD brain, which is consistent with an increased need to regenerate NADPH in response to oxidative stress (Martins et al., 1986; Palmer, 1999). Given that neurons rely on astrocytes for their supply of GSH precursors, the available evidence indicates that in AD, astrocytes are unable to provide neurons with sufficient supplies of glutamine and CysGly to protect them fully from pro-oxidants.

Proteins in which a thiol moiety has been replaced by a disulfide group (protein-SSG) are known as S-glutathionylated proteins. There are several potential sources of the disulphide group, including GSH and GSSG (Mieyal et al., 2008). While S-glutathionylation alters the activity of proteins (generally decreasing activity), it seems to provide an increased level of protection from oxidation, and may also play a role in redox signalling. Hence the level of protein S-glutathionylation is often increased in conditions that involve oxidative stress. Furthermore, S-glutathionylation is a reversible process that is catalysed by glutaredoxin, using GSH as the electron donor (Mieyal et al., 2008). Thus, the S-glutathionylation of proteins may play a role in the antioxidant defence of cells by protecting proteins from irreversible oxidation. Newman and colleagues (2007) have shown that there is a significant increase in the level of S-glutathionylated proteins in the inferior parietal lobe of AD brains. Interestingly, the S-glutathionylated proteins include glyceraldehyde phosphate dehydrogenase (GAPDH) and α-enolase, both of which

catalyse reactions of the glycolytic pathway. Furthermore, in homogenates from the inferior parietal lobe of AD patients, these enzymes were found to have a significantly reduced level of activity compared to that in control brains (Newman et al., 2007). These data suggest that in AD, an increased level of S-glutathionylation of these glycolytic enzymes may contribute to a reduced rate of glucose breakdown, and a subsequent decrease in energy production.

Oxidative stress stimulates astrocytes to switch from a resting to a reactive phenotype, thereby causing them to divert some of their energy away from supporting neurons and into defending the brain. This diversion of metabolic support can leave neurons less able to defend themselves from reactive oxygen species which are generated by their own metabolism. GSH provides an important line of defence against intracellular oxidative stress, and it is therefore significant that the glutathione pathway is perturbed in AD. Since cysteine is the rate-limiting amino acid for the synthesis of GSH, it may be possible to boost intracellular GSH in neurons by increasing the availability of cysteine. Indeed, several analogues of cysteine have been shown to be effective at increasing intracellular GSH in vitro and in vivo (Djurhuus et al., 1990; Issels and Nagele, 1989; Maher et al., 2008).

Another promising group of drugs for the treatment of AD are those which stimulate the synthesis of GSH. The genes coding for key enzymes involved in the synthesis of GSH are regulated by the binding of transcription factor Nrf2 to antioxidant response elements (AREs; also known as electrophile response elements) in their promoter regions. Genes targeted by Nrf2 include glutamate cysteine ligase catalytic subunit, glutathione synthetase and the cystine/glutamate exchanger (Vargas and Johnson, 2009). Drugs which stimulate Nrf2-mediated gene expression can increase the GSH

content of brain cells in vitro and in vivo. Such drugs include tert-butylhydroquinone, sulforaphane (an active ingredient in broccoli), resveratrol (the major polyphenol in red wine) and lipoic acid (Chen and Kunsch, 2004; Suh et al., 2004). It would be interesting to determine whether these drugs can reduce oxidative stress in AD, particularly when used in combination with analogues of cysteine and other antioxidants that can cross the blood-brain barrier (Figure 1.2).

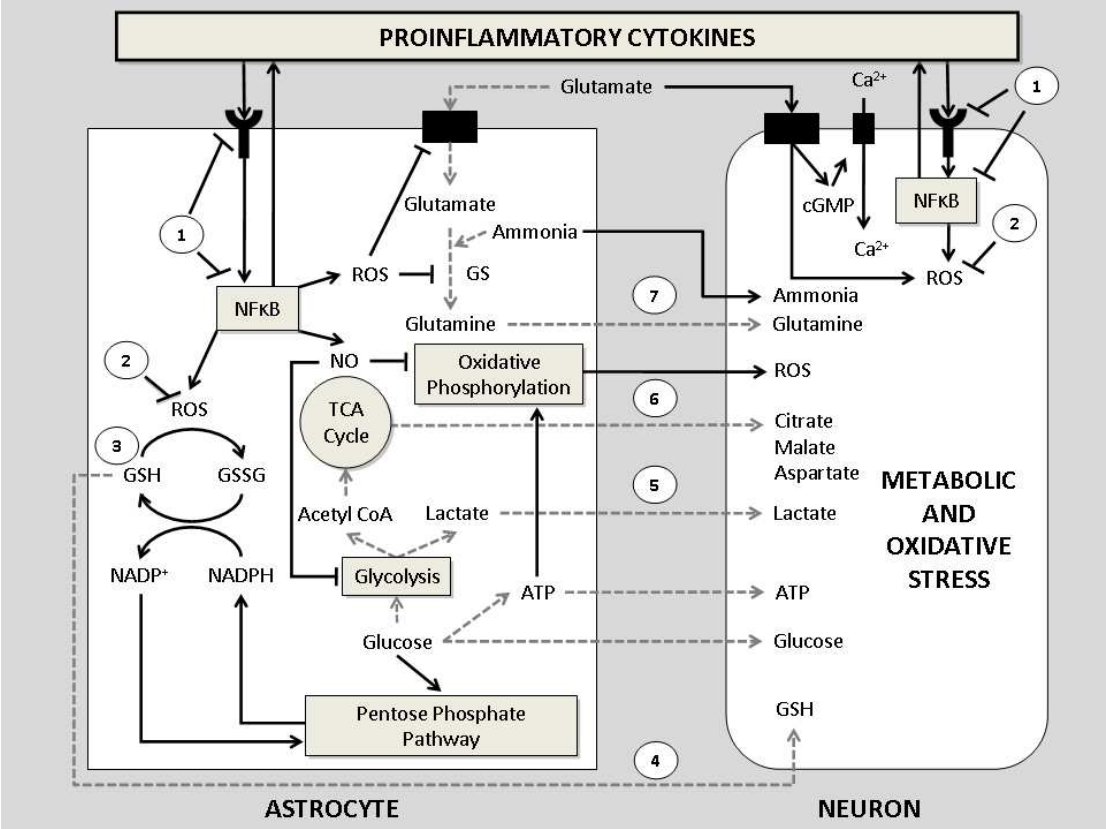

Figure 1.2 Changes induced by inflammation in the metabolic exchange between astrocytes and neurons and potential therapeutic targets. The production and release of some metabolites are downregulated (grey, dashed arrows) while others are upregulated (black arrows) in response to proinflammatory cytokines. Potential therapeutic targets are numbered (1-8). Cytokines activate astrocytes and neurons through cytokine-specific receptors and subsequent signalling via stress kinase pathways leads to NFκB translocation to the nucleus. NFκB induces the expression of cytokines, inducible nitric oxide synthase and cyclooxygenase, enzymes which increase the production of nitric oxide (NO) and other reactive oxygen species (ROS). In addition to reinforcing this inflammatory cycle through further activation of NFκB, ROS can interfere with cellular functions. For example, ROS are neutralised by the oxidation of glutathione (GSH) to glutathione disulfide (GSSG), a process which requires NADPH to recycle GSSG back to GSH. Depletion of NADPH stimulates the pentose phosphate pathway, which provides 2 moles of NADPH per mole of glucose. ROS can also inhibit glutamate transporters and the enzyme glutamine synthetase (GS), resulting in neurotoxic levels of extracellular glutamate and ammonia. Enzymes involved in glycolysis and oxidative phosphorylation are particularly vulnerable to inhibition by NO, which impairs the function of astrocytes and neurons, and also disrupts their exchange of metabolites, causing astrocytes to provide neurons with fewer precursors for energy metabolism (glucose, lactate, tricarboxcylic acid (TCA) intermediates such as citrate, malate and aspartate), glutamatergic signalling (glutamine) and GSH. This combination of increased stress (oxidants, cytokines and glutamate) and decreased protection renders neurons vulnerable to metabolic and oxidative stress. We postulate that this vicious cycle of events can be interrupted by a multifactorial approach to therapeutic

intervention. Treating inflammation (1) and oxidative stress (2) by using non-steroidal antiinflammatories (NSAIDs) and antioxidants, may help to prevent the blockade of glutamate transporters and glutamine synthetase, thereby preventing extracellular glutamate and ammonia from reaching neurotoxic levels, and enabling astrocytes to provide glutamine to neurons (7). Intracellular levels of GSH may be boosted by stimulating the synthesis of enzymes involved in GSH synthesis (3), as well as by the provision of analogues of cysteine, which is the rate-limiting precursor of GSH (4). The replenishment of GSH may reduce activity in the phosphate pentose pathway, and restore the provision of lactate, citrate, malate and aspartate to neurons (5, 6). Dietary changes, combined with antibiotics can be used to reduce serum levels of ammonia, thereby aiding the clearance of this toxic metabolite from the brain (8).

1.10 Conclusion

Twenty one years ago (Hertz, 1989) advanced the radical proposal that AD may constitute *'a cruel demonstration by Nature of the crucial importance of functional* and metabolic interactions between neurons and astrocytes for normal brain *function'.* A considerable body of evidence has accumulated in support of Hertz's proposal. Furthermore, the reason for the breakdown in this symbiosis is becoming clear. It has become evident that the transformation of astrocytes from a basal to a reactive state, in response to inflammation or oxidative stress, can trigger a change in their metabolic phenotype. This change in phenotype appears to provide a basis for many of the metabolic perturbations that occur in AD, and which contribute to the pathogenesis and progression of the disease.

The adoption of a reactive metabolic phenotype is likely to assist the brain to survive in instances of local acute injury, but it could become counterproductive if the response is sustained and widespread. When astrocytes adopt a reactive phenotype, their efforts are redirected towards defensive and repair tasks at the expense of providing adequate metabolic support to neurons. Viewed from this perspective, the targeting of astrocytes with pharmacological agents that are specifically designed to return astrocytes to a quiescent phenotype could represent a fruitful new angle for the therapeutic treatment of AD and other neurodegenerative disorders.

1.11 Hypothesis and Aims

Review of the literature highlights three important neurosupportive functions of astrocytes: uptake of glucose and release of lactate; uptake of glutamate and release of glutamine and provision of glutathione substrates to neurons. It is proposed that disruption of these functions, possibly induced by inflammatory activation of astrocytes, might contribute to the pathogenesis of neurodegenerative diseases. This project aims to provide a better understanding of how inflammatory activation can modulate key astrocytic functions in vitro. The general aims for this project were to:

- Investigate whether U373 cells provide an acceptable model for the study of metabolic changes in inflammation-activated astrocytes (Chapter 2)
- Optimise and validate a method for the measurement of glutathione and related thiol compounds in media (Chapter 3)
- Investigate whether inflammation-activated U373 cells alter their neurosupportive functions:
    - Release of GSH and GSH related metabolites (Chapter 4)
    - Uptake of glucose and release of lactate (Chapter 5)
- Investigate the potential antioxidant and cytoprotective abilities of traditional Chinese herbal medicines purported for their anti-ageing and cognitive-enhancing properties (Chapter 6)

CHAPTER 2

Effect of proinflammatory activation on IL-6 release and intracellular glutathione in U373 astrocytoma cells

2.1 Introduction

Astrocytes possess a wide variety of homeostatic and nutritive functions in the brain. These include regulation of extracellular glutamate (Sonnewald et al., 1997) and ion concentrations (reviewed by Simard and Nedergaard, 2004), modulation of neural synapses (Araque et al., 1998) and cerebral blood flow (Takano et al., 2006), trafficking of metabolites in between neurons and the blood (Gandhi et al., 2009; Pellerin and Magistretti, 1994), involvement in both pro and anti-inflammatory activities (reviewed by Dong and Benveniste, 2001) and the synthesis, storage and distribution of the main thiol antioxidant, glutathione (GSH) (Desagher et al., 1996; Dringen et al., 1999b; Rice and Russo-Menna, 1998). Reactive astrogliosis and glial scar formation are also regarded as normal astroyctic functions (reviewed by Sofroniew, 2009). Reactive astrogliosis can be described as a finely gradatated continuum of progressive changes which includes astrocytic hypertrophy and hyperplasia, process extension and increases in expression of glial fibrillary acidic protein, production of reactive oxygen species (ROS) and release of cytokines in response to central nervous system (CNS) insult and disease (Cui et al., 2011; Gadea et al., 2008; Sofroniew and Vinters, 2010; Wilhelmsson et al., 2006). Severe astrogliosis occurs in response to overt tissue damage and inflammation and involves compact glial scar formation. Scar formation has been described as neuroprotective by means of acting as a barrier against inflammatory cells and infectious agents (Drogemuller et al., 2008; Voskuhl et al., 2009). Although considered as normal astrocytic functions, increasing evidence suggests that dysfunction in the processes of astrogliosis and scar formation could potentially contribute to, or even cause, a wide variety of neurological disorders (Sofroniew and Vinters, 2010). Furthermore, dysfunctional reactive astrocytes might contribute to disease progression both

through the upregulation of neurotoxic substances, such as pro-inflammatory cytokines, as well as through the alteration or failure of their normal neurosupportive functions (Fuller et al., 2009a). It is therefore of interest to investigate the effect of proinflammatory activation on a wide range of astroglial functions in addition to the relatively well characterised changes in cytokine production, proliferation and morphology (Gadea et al., 2008; Johnstone et al., 1999; Park et al., 2006; Selmaj et al., 1990; Wilhelmsson et al., 2006). In particular, the effect of proinflammatory activation on GSH synthesis in astrocytes deserves attention. The major intracellular metabolic reactions of GSH in astrocytes have been thoroughly reviewed by Dringen et al. (2000) and are summarised in Figure 2.1. GSH is the key regulator of intracellular redox state and is required for the detoxification of ROS, peroxides, electrophilic xenobiotic compounds and the regeneration of other endogenous and exogenous antioxidants. A tripeptide consisting of glutamate, cysteine and glycine, GSH is synthesised by the consecutive actions of cysteine glutamate ligase (CGL), which is the rate-limiting enzyme, and glutathione synthetase (Chen et al., 2005). GSH can non-enzymatically detoxify ROS, such as superoxide and hydroxyl radicals, as well as being an electron donor for the reduction of peroxides, catalysed by glutathione peroxidase (Brannan et al., 1980). In both reactions, two GSH molecules become oxidised and join together via a disulfide bond between the cysteine residues to form glutathione disulfide (GSSG) (Meister, 1988). In addition to de novo synthesis, GSH can be regenerated from the oxidised disulfide form back to the reduced form by glutathione reductases, which require NADPH as a cofactor. Another family of glutathione related enzymes is the glutathione-S-transferases, which conjugate GSH moieties to endogenous and xenobiotic compounds to form mixed disulfides (Pr-SH) for transport out of the cell (Dringen, 2000). Astrocytes can

also release GSH, GSSG and PrSH via the multidrug resistant protein 1 (Mrp1) tranporter (Minich et al., 2006).

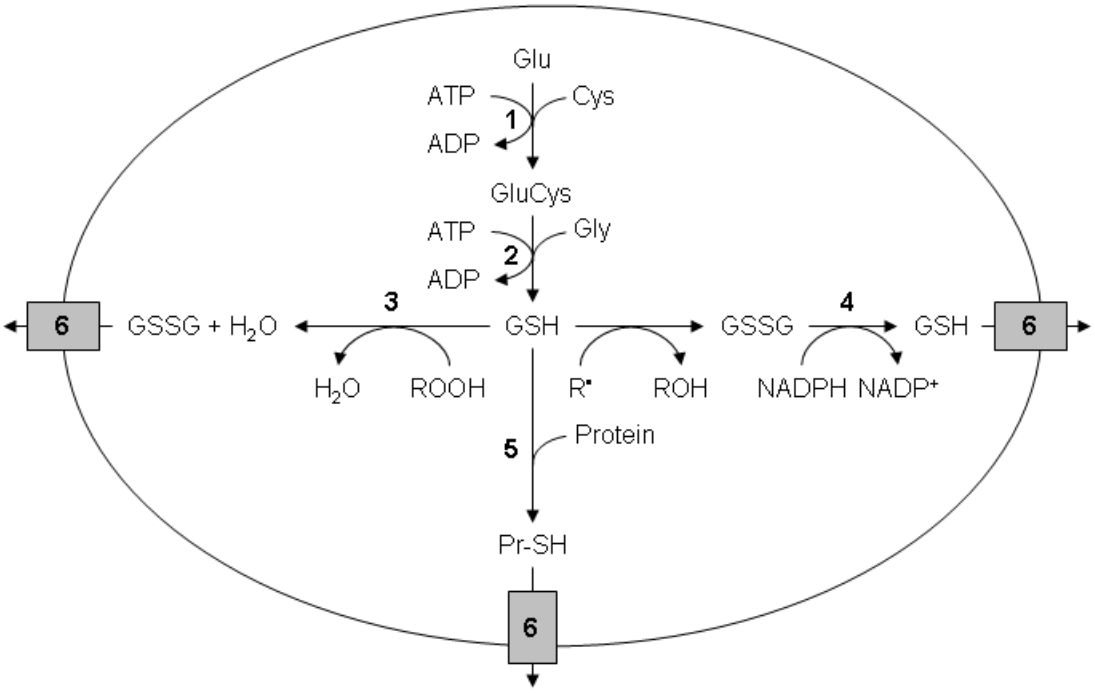

Figure 2.1 Intracellular metabolism and reactions of GSH. GSH is synthesised in two steps catalysed by glutamate cysteine ligase (1) and glutathione synthetase (2). It can react nonenzymatically with radicals (R•) or act as the electron donor for the reduction of peroxides (ROOH) catalysed by glutathione peroxidase (3). GSH is consumed through reaction with proteins or other endogenous or xenobiotic compounds catalysed by glutathione-S-transferase (5). GSH, GSSG and Pr-SH can all be released from the cell via the Multidrug resistance protein 1 transporter (6).

An imbalance between the rates of ROS production and detoxification, caused by depletion of GSH and/or elevated ROS production, results in a state of oxidative stress (reviewed by Mittler, 2002). Oxidative stress leads to the detrimental oxidation of cellular components including DNA, lipids and proteins, which can cause cellular dysfunction and death. Although GSH can be synthesised by all cells in the body, astrocytes are the predominant producers of GSH in the brain and hence play a key role in preventing oxidative stress in the brain (Dringen, 2000). As such, the effect of inflammatory activation on the intracellular GSH content of astrocytes is of critical importance, especially in the context of chronic neuro-inflammatory conditions such as Alzheimer's disease (AD).

The first part of this study involved investigation of the U373 human astrocytoma cell line for its suitability as a model system for researching inflammatory activation in astrocytes. This was done by testing whether increasing concentrations (0.01 – 10 ng/ml) of a combination of two proinflammatory cytokines, Interleukin (IL)-1β and tumour necrosis factor (TNF)-α, could induce a gradatated activation continuum, measured by increased release of another cytokine, IL-6. In addition, the effect of the cytokines on cell viability was assessed in order to determine whether the selected concentrations were toxic to cells. The U373 cell line retains morphological and physiological properties of primary astrocytes and has been frequently exploited as a model for astrocyte function (Gitter et al., 1995; Lieb et al., 1996; Malaplate-Armand et al., 2000). It has previously been demonstrated that U373 cells respond to a range of triggers in a similar manner to primary astrocytes, including activation of the nuclear factor-κB (NFκB) transcriptional pathway and production of IL-6, IL-8, monocyte chemotactic protein 1 (MCP-1), nitric oxide, superoxide and hydrogen

peroxide in response to treatment with IL-1β and TNF-α (Gavillet et al., 2008; Oh et al., 1999; Schwamborn et al., 2003). The pleiotropic cytokines, IL-1β and TNF-α, were chosen as inflammatory activators due to their elevated expression in the post-mortem brains of AD patients (Grammas and Ovase, 2001; Griffin et al., 1989; Tarkowski et al., 1999). Due to difficulties in quantifying cytokine concentrations in the brain, a number of studies have measured IL-1β and TNF-α, along with other inflammatory molecules, in blood or cerebral spinal fluid (CSF) of patients. Reported concentrations, however, vary significantly between patients, and between studies (Swardfager et al., 2010). For example, reported mean levels of IL-1β in the CSF of AD patients range from < 2 pg/ml (Engelborghs et al., 1999) to > 131 pg/ml (Cacabelos et al., 1991), while mean levels of TNF-α in the CSF of AD patients range from < 16 pg/ml (Engelborghs et al., 1999) to > 1 ng/ml (Fillit et al., 1991). A study by Wilms and colleagues (2001) showed that CSF samples collected from patients with AD, Parkinson's disease or amyotrophic lateral sclerosis were not able to activate primary rat microglia and astrocytes in vitro. Neither could IL-1β, TNF-α or IL-6, at concentrations comparable to the amounts found in CSF samples (10-500 pg/ml), induce activation-associated morphological changes or nitric oxide production (Wilms et al., 2001). Cytokine production and products of oxidative stress appear to be quite localised in the CNS and the concentration of inflammatory molecules surrounding astrocytes is likely to be much higher than is found in CSF samples, thus justifying the concentrations of cytokines used in this study. Furthermore, IL-1β and TNF-α have been described as "early response" cytokines due to their rapid expression in response to cellular activation and their ability to induce the expression of a range of inflammatory mediators (Aloisi et al., 1992; Mizgerd et al., 2001; Moynagh, 2005; Saito et al., 1996). One of these, another

multifunctional cytokine IL-6 (Kamimura et al., 2003), is also found at elevated levels in AD brains and is believed to be predominantly produced by reactive astrocytes (Blum-Degen et al., 1995), thus making it an attractive readout for astroglial activation in the present study.

The second aim of this study was to investigate the effect of IL-1β and TNF-α induced activation of U373 cells on total intracellular GSH content. Although GSH can be found in both reduced and oxidised forms, the method used here involved the reduction of GSSG to GSH and thus reported total GSH (Tietze, 1969). GSSG has been shown to make up < 1% of total intracellular GSH, even in activated cells (Gavillet et al., 2008), therefore the determined total GSH represents almost exclusively reduced form GSH. Based on the findings from a study by Gavillet et al. (2008) in which intracellular GSH was depleted in IL-1β and TNF-α primary mouse astrocytes, it was hypothesised that proinflammatory activation of U373 cells with these same cytokines would similarly induce a dose-dependent depletion of intracellular GSH.

2.2 Material and Methods

2.2.1 Materials

The U373-MG human astrocytoma cell line was kindly provided by Dr Peter Locke (The Royal Melbourne Hospital, Australia). Bradford reagent was from Bio-Rad (Gladesville, Australia). The IL-6 enzyme-linked immunosorbent sandwich assay (ELISA) kit was from Peprotech (London, United Kingdom). All cell culture materials were from Invitrogen (Mulgrave, Australia). All other reagents were from Sigma-Aldrich (Castle Hill, Australia).

2.2.2 Cell maintenance

Cells were maintained in Dulbeccos's Modified Eagle Medium (DMEM) containing 25 mM glucose, supplemented with 200 U/ml penicillin, 200 µg/ml streptomycin, 2.6 µg/ml Fungizone, 200 mM glutamine and 5% foetal bovine serum (FBS). Cells were grown in 175 cm^2 tissue culture flasks and incubated at 37°C in 5% CO_2.

2.2.3 Treatment of U373 cells with IL-1β and TNF-α

U373 cells were harvested with a solution containing 0.05% trypsin and 0.02% ethylenediaminetetraacetic acid (EDTA) in phosphate buffered saline (PBS) and seeded into 96-well, flat-bottom, tissue culture plates at a density of 9×10^3 cells/well. FBS concentration was reduced to 3% to minimise proliferation and the total volume of media in each well was 100 µl. Cells were allowed to settle for 24 hours before the media was replaced with fresh media containing 1% FBS and various concentrations of IL-1β and TNF-α (both at 0.01 to 10 ng/ml) and incubated for up to 96 hours.

2.2.4 Resazurin-based assay for determination of cell viability

Cell viability was assessed in terms of the metabolic capability of cells to convert the fluorogenic redox indicator, resazurin, into its highly fluorescent product, resorufin. A modified version of the resazurin reduction assay was used (Buranrat et al., 2008).

Resazurin was dissolved in PBS to give a concentration of 0.001% (w/v). This solution was sterile filtered (0.22 µm), protected from light with aluminium foil and stored at 4°C for up to six months. To determine cell viability, incubation media was aspirated from wells (or collected for IL-6 determination) and replaced with 100 µl of resazurin solution. Plates were incubated at 37°C, with 5% CO_2 for 45 mins and then fluorescence was measured with excitation at 530 nm and emission at 590 nm in a POLARstar Omega microplate reader (BMG Labtech, Mornington, Australia). For every plate, background fluorescence determined in cell-free wells was subtracted from all wells, and values were expressed as a percentage of untreated control cells.

2.2.5 Measurement of IL-6 in conditioned media

Media was taken from U373 cells treated with 0 – 10 ng/ml IL-1β and TNF-α for 12, 24, 36, 48, 60, 72, 84 or 96 hours, placed in fresh 96 well plates and stored at -20°C until analysis. On thawing, supernatants were diluted with distilled water by a factor of 130 and samples assayed for IL-6 by ELISA. The ELISA protocol described by PeproTech was followed, using all recommended reagents and solutions (http://www.peprotech.com). Briefly, capture antibody was used at a concentration of 1 µg/ml in PBS. Serial dilutions of TNF-α standard from 0 to 2000 pg/ml in diluent (0.05% Tween-20, 0.1% bovine serum albumin in PBS) were used for calibration. TNF-α was detected with a biotinylated secondary antibody and an avidin peroxidase

conjugate, with tetra-methyl-benzidine as the detection reagent. Absorbance was determined at 355 nm in a POLARstar Omega microplate reader (BMG Labtech, Mornington, Australia).

2.2.6 Determination of intracellular glutathione by the Teitze assay and total protein by the Bradford assay

The Tietze assay is a kinetic assay based on the reaction of GSH with 5,5'-dithio-bis(2-nitrobenzoic acid) (DTNB) to form GSSG and 5-thio-2-nitrobenzoic acid (TNB). GSSG is converted back to GSH by glutathione reductases (GR) allowing further production of TNB. The rate of TNB formation, which is measurable at an absorbance of 412 nm, is proportional to the concentration of total GSH (GSH + GSSG) in the sample and is expressed as nmol of GSH per mg of protein.

Preparation of cell lysates

Following treatment of U373 cells with 0.01 – 10 ng/ml IL-1β and TNF-α for 24, 48, 72 or 96 hours and removal of conditioned media, cells were lysed by subjection to three freeze-thaw (-80°C and 25°C) cycles. Cell lysates were dissolved in sterile distilled water (100 µl/well) and analysed for total GSH concentration by the Teitze assay (Tietze, 1969) and total protein by the Bradford assay (Bradford, 1976).

Bradford assay for determination of total protein

To determine total protein in cell lysates, 10 µl samples were added to a 96 well plate, followed by 40 µl of Bradford reagent and 150 µl distilled water. Absorbance was measured at 595 nm using a Bio-Rad Model 680 Microplate reader (Bio-Rad, Gladesville, Australia). A standard curve consisting of 0 – 0.125 mg/ml bovine serum albumin (BSA) was used to determine total protein concentration in samples.

Tietze assay for the determination of GSH

GSH standards and samples (20 µl) were added in triplicate to wells of a 96 well plate. Equal volumes of freshly prepared DTNB and GR solutions were mixed together and 120 µl was added to each well. 30 seconds was allowed for the conversion of GSSG to GSH, and then 60 µl of NADPH was added to each well. The velocity of the reaction was then monitored at 5 intervals over 2.5 minutes using a Bio-Rad Model 680 Microplate reader (Bio-Rad, Gladesville, Australia). Total GSH in the samples was determined by use of a standard curve. GSH concentration was then standardised to total protein for each sample and expressed as nmol per mg of protein.

2.2.7 Statistics

Graphpad Prism was used to produce figures and analyse data. Data presented are the mean of three independent experiments and error bars denote standard error of the mean (SEM). Significant differences were assessed by one-way analysis of variance (ANOVA) with Dunnett's post hoc tests and shown as * $p<0.05$, ** $p<0.01$ and *** $p<0.001$.

2.3 Results

2.3.1 Treatment with IL-1β and TNF-α up to 10 ng/ml and 96 hours was not toxic to cells

In order to investigate time-dependent changes in cell viability of U373 cells cultured for 96 hours, the capacity of cells to metabolise resazurin to its highly fluorescent product, resorufin, was assessed at 12 hour intervals (Figure 2.2). Increasing fluorescence, indicative of higher metabolic activity suggesting an increase in the number of viable cells, was observed up to 72 hours incubation. A decrease in fluorescence was observed after 72 hours, suggesting decreased metabolic activity due to cell loss, possibly caused by overcrowding of cells or depletion of media constituents necessary for survival.

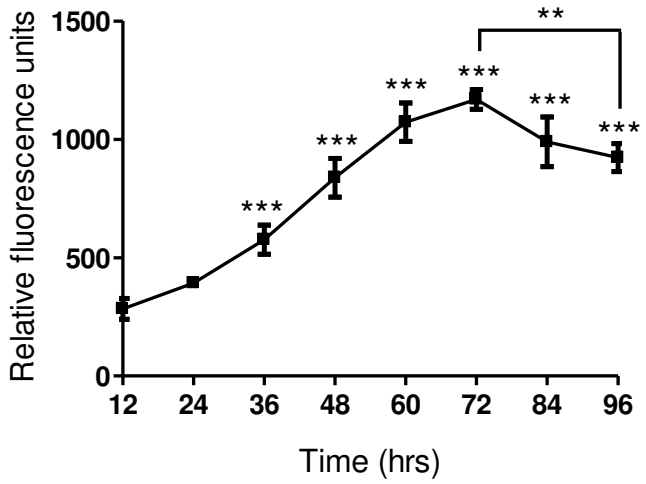

Figure 2.2 Metabolic activity of U373 cells incubated up to 96 hours. U373 cells were cultured for 12, 24, 36, 48, 60, 72, 84 or 96 hours. The metabolic activity of cells was then measured by the resazurin reduction assay and data expressed as mean relative fluorescence units ± SEM of 3 experiments. ** $p<0.01$ and *** $p<0.01$ designate a significant difference to the metabolic activity of cells measured after 12 hours incubation or as otherwise shown.

The cell viability of U373 cells treated with 0.01 – 10 ng/ml IL-1β and TNF-α was compared to non-treated cells after 24, 48, 72 and 96 hours to test for any treatment-induced toxicity (Figure 2.3). A slight reduction in cell viability was seen after 24 hours in cells treated with 5 or 10 ng/ml each of IL-1β and TNF-α. At later time points, however, no statistical differences were observed between metabolic activity of cells treated with different concentrations of IL-1β and TNF-α, indicating that the selected concentrations of IL-1β and TNF-α were not toxic to cells.

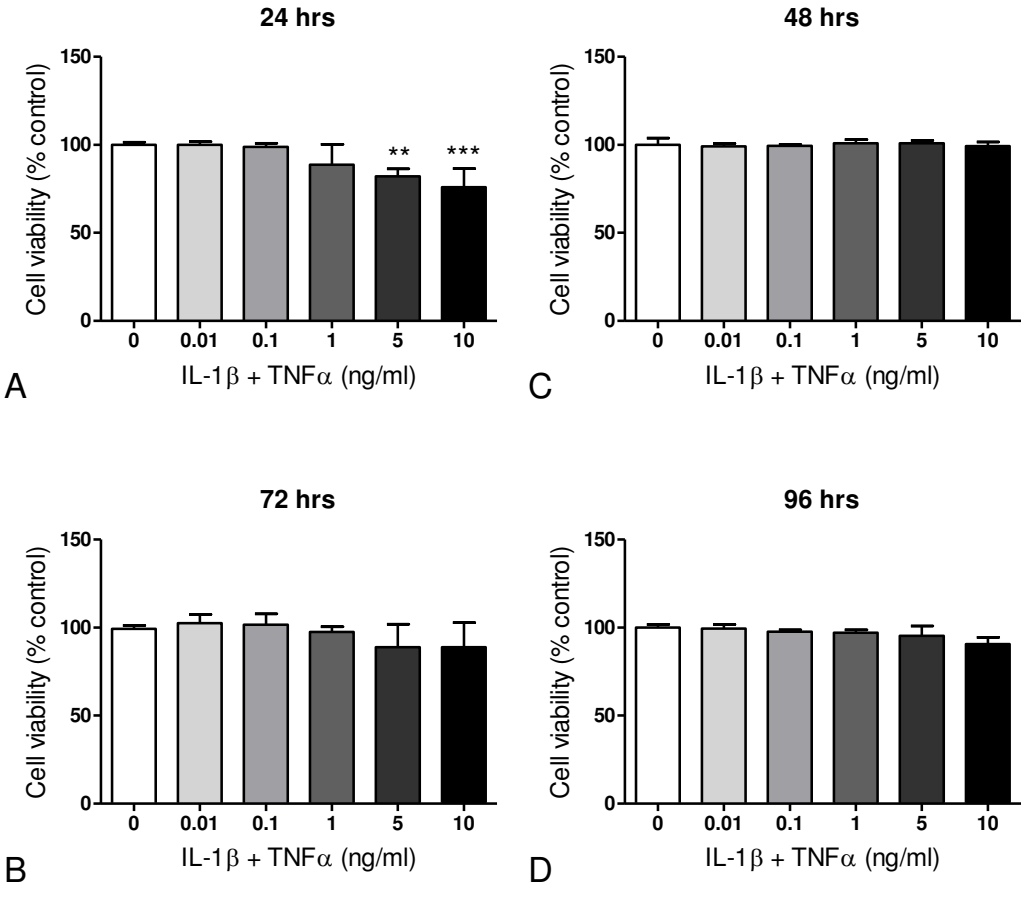

Figure 2.3 Cell viability results for U373 cells treated with IL-1β and TNF-α. U373 cells were treated with 0.01, 0.1, 1, 5 or 10 ng/ml IL-1β and TNF-α for 24, 48, 72 or 96 hours. Cell viability was measured by the resazurin reduction assay and data are expressed as percentage of non-treated control cells ± SEM of 3 experiments. ** $p<0.01$ and *** $p<0.01$ designate a significant difference to the non-treated control (0 ng/ml IL-1β and TNF-α).

2.3.2 IL-1β and TNF-α induce IL-6 release in U373 cells

** IL-6 release was determined together with Stacey Fuller, an Honours student in our laboratory under my direct supervision **

Reactive astrocytes are known to release a range of cytokines in response to pro-inflammatory activation. Levels of IL-6 were determined in the cell culture media of IL-1β and TNF-α treated U373 cells to determine whether increasing concentrations of theses cytokines could be used to achieve a gradated inflammatory response (Figure 2.4). Concentrations of 0.01 – 10 ng/ml of IL-1β and TNF-α induced a significant dose dependent increase in IL-6 release, with the maximal concentration of IL-6 found in the media after 72 hours treatment with 10 ng/ml of IL-1β and TNF-α (493 ± 17 pg/ml). Negligible IL-6 was measured for non-treated cells or cells treated with 0.01 ng/ml IL-1β and TNF-α up to 96 hours.

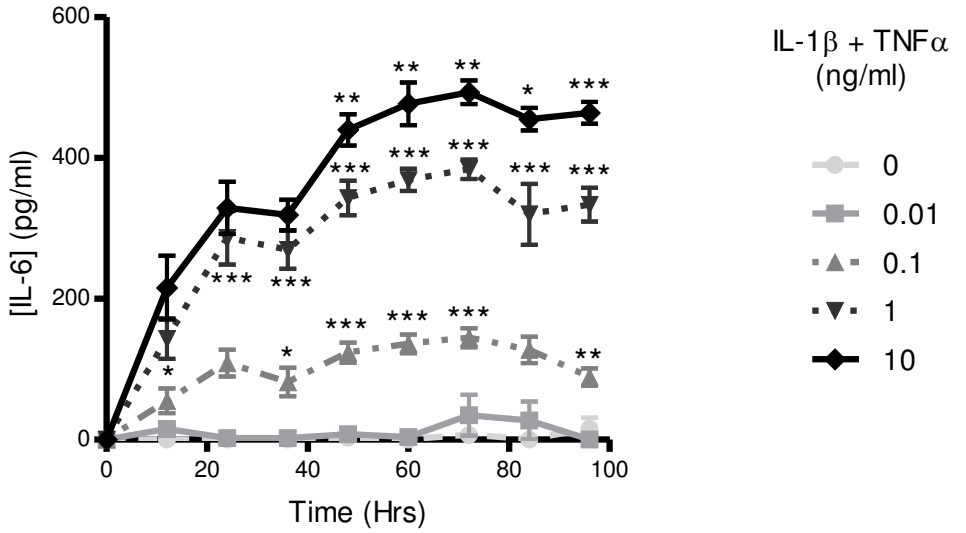

Figure 2.4 IL-6 production by U373 cells treated with IL-1β and TNF-α. U373 cells were incubated with 0.01 – 10 ng/ml IL-1β and TNF-α up to 96 hrs. IL-6 concentration was measured in the media after 0, 12, 24, 36, 48, 60, 72, 84 and 96 hours by ELISA. A standard calibration curve was used to calculate IL-6 concentration. Data are represented as mean ± SEM of 3 experiments and * = $p < 0.05$, ** = $p < 0.05$ and *** = $p < 0.01$ designate significant treatment concentration-dependent increases in IL-6 release measured at different time points.

2.3.3 Effect of IL-1β and TNF-α treatment of U373 cells on intracellular glutathione concentration

** Intracellular GSH was determined together with Stacey Fuller, an Honours student in our laboratory under my direct supervision **

In order to investigate the effect of IL-1β and TNF-α on the oxidative stress status of U373 cells, intracellular GSH was determined by the Tietze assay after 24, 48, 72 and 96 hours treatment (Figure 2.5). Although cells contain both GSH and GSSG, it has been shown previously that GSSG makes up < 1% of total GSH (GSH + GSSG) in both control and cytokine-treated cells (Gavillet et al., 2008). Therefore, total GSH measured here represents almost exclusively GSH. Furthermore, GSH content determined in control cells ranged from 77.6 nmol/mg protein in cells incubated for 24 hours to 52.8 nmol/mg protein in cells incubated for 96 hours. These values are in good agreement with those reported in the literature (Gavillet et al., 2008; Zerarka et al., 2001). In response to treatment with 0.01 – 10 ng/ml IL-1β and TNF-α, no significant changes were observed after 24 or 48 hours. After 72 hours a trend towards increased GSH in response to IL-1β and TNF-α concentrations up to 1 ng/ml was observed, however this was not statistically significant. After 96 hours treatment, GSH concentration measured in U373 cells treated with 1 ng/ml IL-1β and TNF-α was significantly increased compared to non-treated control cells. This increase disappeared however, in response to a higher concentration of 10 ng/ml IL-1β and TNF-α, which appeared to have no effect on GSH concentration compared to control cells.

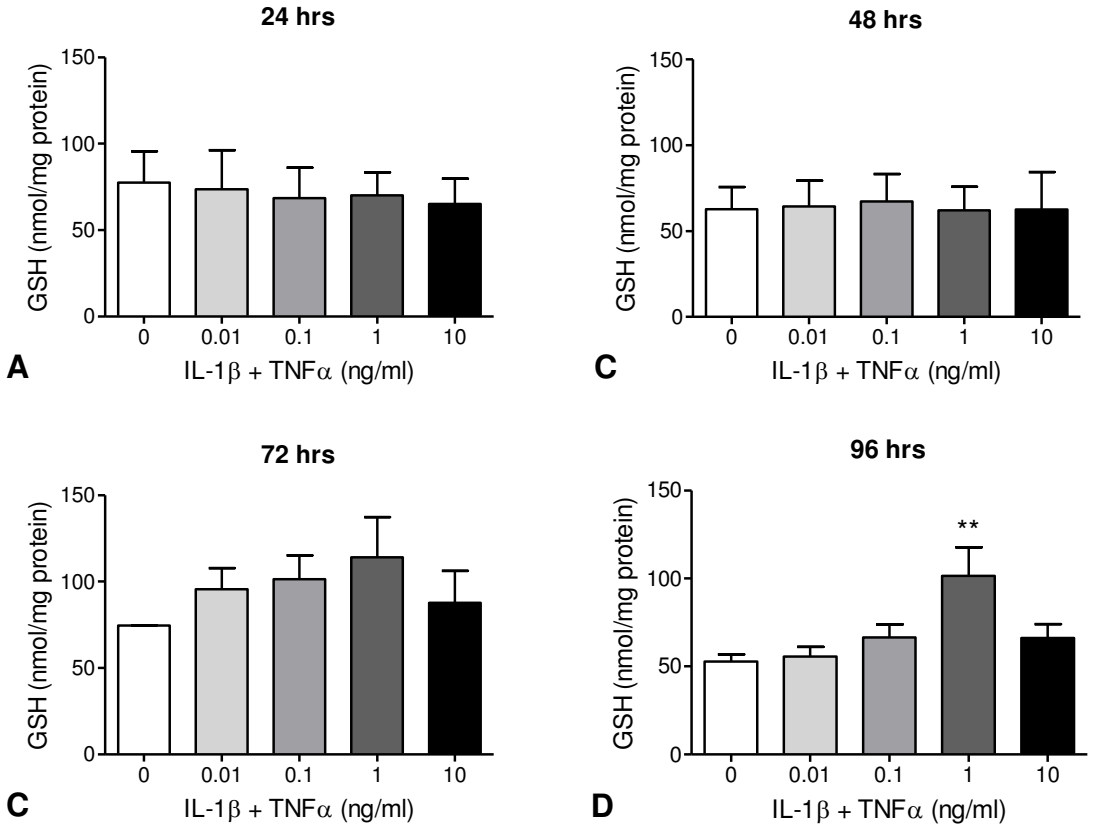

Figure 2.5 Total intracellular GSH in U373 cells after 24, 48, 72 and 96 hours incubation. U373 cells were treated with 0.01 - 10 ng/ml IL-1β and TNF-α for 24 (A), 48 (B), 72 (C) or 96 (D) hours. Levels of total intracellular GSH were determined by the Teitze assay and data are represented by the mean ± SEM of 3 experiments and ** $p<0.01$ designates a significant difference to the non-treated control (0 ng/ml IL-1β and TNF-α).

2.4 Discussion

IL-1β and TNF-α are central regulators of the cellular inflammatory response in astrocytes. Both cytokines induce complex signalling pathways, resulting in the expression of a wide variety of inflammatory mediators including nitric oxide, ROS such as superoxide and hydrogen peroxide, and cytokines such as IL-6 (shown here), IL-8 and macrophage colony stimulating factor, as well as positive feedback expression of IL-1β and TNF-α (Aloisi et al., 1992; Benveniste et al., 1994; Gavillet et al., 2008; Hu et al., 1995). Whilst the roles of IL-1β and TNF-α in the induction and promotion of inflammatory signalling in astrocytes have been well studied, the effects of inflammatory activation on other aspects of the metabolic phenotype of astrocytes are less understood. This study investigated the effect of IL-1β and TNF-α co-treatment on the intracellular GSH content of U373 cells, in addition to monitoring cell viability and IL-6 release. The first aim was to test whether cell viability was effected by the selected concentrations of IL-1β and TNF-α. According to results from the resazurin reduction assay, there were no significant differences between the metabolic activity of cells treated for 48 to 96 hours with 0.01 – 10 ng/ml IL-1β and TNF-α, suggesting that the cytokine concentrations used were not toxic and that other changes in astrocytic phenotype were not simply due to differences in cell number. However, data also suggests that the number of viable cells increased up to 72 hours, after which time a decrease was observed, independent of cytokine treatment. The observed increase in cell viability can be explained by the highly proliferative nature of tumour cells (Gao et al., 2005). Cells were seeded at 90% confluence and FBS concentration reduced to 1% in an attempt to minimise proliferation. The reduction in metabolic activity after 72 hours might be due to cell death caused by overcrowding of cells, accumulation of toxic cellular

metabolic by-products or depletion of medium components. These limitations of long-term cell culture can make the interpretation of in vitro findings concerning the effects of chronic inflammation somewhat difficult. On the other hand, this astrogliotic and nutrient-deficient environment might better reflect the aged and/or diseased brain.

When IL-6 levels were determined in the media of U373 cells treated with IL-β and TNF-α, a dose and time-dependent increase up until 10 ng/ml and 72 hours incubation was observed. After this time, a dose-dependent increase was still observed, however a slight time-dependent decrease was also seen, which probably relates to the treatment-independent reduction in cell viability seen after 72 hours. Therefore co-treatment of U373 cells with 0.01 – 10 ng/ml IL-1β and TNF-α up to 96 hours was not toxic and induced a dose-dependent activation of cells, measured by increased IL-6 release. These results therefore support the use of IL-1β and TNF-α treated U373 cells as an acceptable experimental model for further investigation of the effects of proinflammatory activation on the metabolic phenotype of astrocytes.

In addition to the release of cytokines, IL-1β and TNF-α activated astrocytes have previously been shown to produce large volumes of hydrogen peroxide, superoxide and nitric oxide (Gavillet et al., 2008; Lee et al., 1993). In order to determine whether this proinflammatory induced upregulation of ROS generation leads to a state of oxidative stress, intracellular GSH was measured in U373 cells treated with increasing concentrations of IL-1β and TNF-α. No differences in intracellular GSH were seen in 24 or 48 hour treated cells, suggesting that cells were capable of effectively neutralising any IL-1β and TNF-α induced ROS. After 72 hours

treatment, there was a trend towards a dose-dependent increase in GSH content, which became statistically significant after 96 hours treatment with 1 ng/ml IL-1β and TNF-α. The underlying mechanism of increased GSH seen in "chronically" activated U373 cells is likely to involve activation of the redox-active transcription factor, nuclear factor erythroid-2-related factor 2 (Nrf2) and subsequent expression of antioxidant response element (ARE) regulated genes (Correa et al., 2011). The Nrf2-ARE pathway is the most studied and presumably the most important signalling pathway involved in modulation of GSH metabolism (Vargas and Johnson, 2009). Under basal conditions, Nrf2 interacts with Kelch like-ECH-associated protein 1 (Keap1) in the cytoplasm and undergoes ubiquitin-mediated proteasomal degradation (Itoh et al., 1999). Upon direct modification of cysteine thiols in Keap1 induced by electrophilic or oxidative stress, Nrf2 translocates to the nucleus where it binds to the ARE present in the upstream promoter region of a range of phase II antioxidant defence genes. These include the genes encoding for GCL, GR, glutathione synthetase, glutathione peroxidase and glutathione-S-transferase (Chan and Kwong, 2000; Chanas et al., 2002; Copple et al., 2008; Harvey et al., 2009; Thimmulappa et al., 2002; Wild et al., 1999).

Interestingly, there was no increase in GSH observed in response to treatment with 10 ng/ml IL-1β and TNF-α. The low GSH content of cells treated with 10 ng/ml IL-1β and TNF-α compared to cells treated with 1 ng/ml of the cytokines was not due to cell death, since GSH was normalised to the total amount of protein in each sample. Furthermore there was no significant difference in cell viability between treatment groups, as previously discussed. Possible explanations for this result might include feedback inhibition of GCL through GSH competing with glutamate at the active site

of the GCL-catalytic unit, substrate depletion (e.g. glutamate, cysteine or glycine), elevated efflux of GSH into the medium or failure of the rates of de novo GSH synthesis (through the actions of GCL and GS) and regeneration of GSSG to GSH (through the action of GR) to surpass the rate of GSH consumption. Further studies are required to elucidate the relative contributions of these explanations to the results observed here. In a study by Gavillet et al. (2008) in which mouse primary astrocytes were treated with 0.25 ng/ml IL-1β together with 20 ng/ml TNF-α for 48 hours, a 20% decrease in intracellular GSH was seen. When cells were treated with each of the cytokines individually, however, there was no significant effect on GSH content, demonstrating the synergistic nature of these cytokines. A possible explanation for the discrepancies between the findings by Gavillet et al. (Gavillet et al., 2008) and by the present study is that different ratios and concentrations of IL-1β and TNF-α were used. Additionally, the fact that different cells were used (a human astrocytoma cell line versus mouse primary astrocytes) might be an important contributing factor to the variation observed amongst results. In fact, U373 cells have previously been shown to contain more than double the concentration of GSH measured in mouse primary astrocytes (Jurkowska et al., 2011), suggesting there might be an increased resistance against GSH depletion in U373 cells compared to primary astrocytes. It is possible that higher concentrations of cytokines might induce depletion of GSH in these cells.

In summary, treatment of U373 cells with the proinflammatory cytokines, IL-1β and TNF-α, induced a reactive phenotype, characterised by a dose-dependent increase in IL-6 release. It can be concluded that this model system is useful for basic, first-stage hypothesis testing (preceding replication in primary cells or tissue), as well as for the

high throughput screening of potential drugs. Additionally, results may indeed have direct relevance to astroglioma-mediated pathology. Secondly, cells were found to be resistant to GSH depletion in response to the selected concentrations of cytokines, and even showed an increase in intracellular GSH in response to chronic treatment with 1 ng/ml IL-1β and TNF-α. While this study focused on whether proinflammatory activation affects intracellular GSH content, it did not consider any changes that may have occurred in the levels of extracellular GSH. In the brain, astrocytes release GSH in order to sustain GSH synthesis in neurons (Dringen et al., 1999b), a function that is especially important to neuronal survival and particularly important in inflammatory and oxidative stress characterised conditions such as AD (Aksenov and Markesbery, 2001; Desagher et al., 1996). The hypothesis that reactive astrocytes might successfully maintain their intracellular GSH levels by releasing less GSH and thus providing neurons with limited substrates for GSH synthesis is investigated in the following chapters.

CHAPTER 3

Optimisation and validation of a HPLC method for quantitation of glutathione and related thiols

3.1 Introduction

Oxidative stress and altered antioxidant defence systems have been implicated in the pathophysiology of a wide range of chronic conditions. In particular, alteration in levels of glutathione (GSH), the most abundant mammalian antioxidant, and GSH related enzymes has been linked to neurodegenerative disorders including Parkinson's disease (Pearce et al., 1997) and Alzheimer's disease (AD) (Aksenov and Markesbery, 2001; Karelson et al., 2001; Lovell et al., 1995). In the brain, neurons rely on the supply of GSH by astrocytes (Dringen et al., 1999b). Astrocytic released GSH is metabolised by an ectoenzyme, γ-glutamyltranspeptidase, to form the dipeptide, cysteinylglycine (CysGly) (Dringen et al., 1997a), which is then processed by the neuronal ectopeptidase aminopeptidase N allowing uptake of cysteine (Cys) and glycine by neurons (Dringen et al., 2001). It has been hypothesised that in neurodegenerative diseases, such as AD, reactive astrocytes might be unable to provide neurons with sufficient supplies of GSH substrates to protect them fully from pro-oxidants (Steele and Robinson, 2011). Homocysteine (HCys) is another thiol group-containing compound that is linked to GSH metabolism via the transulfuration pathway (Vitvitsky et al., 2006) and is also released by astrocytes (Huang et al., 2005b). Elevated plasma Hcys has been identified as a strong, independent risk factor for AD (Seshadri et al., 2002). Therefore, the development of accurate methods for the determination of GSH, as well as its related compounds, is extremely important for the investigation of abnormal thiol metabolism in AD. This chapter describes the optimisation and validation of a high performance liquid chromatography (HPLC) method developed for the simultaneous determination of GSH, Cys, CysGly and Hcys.

A derivative of Cys, N-acetylcysteine (NAC), was investigated for its effectiveness as an internal calibration standard. The chemical structures of these compounds are shown in Figure 3.1.

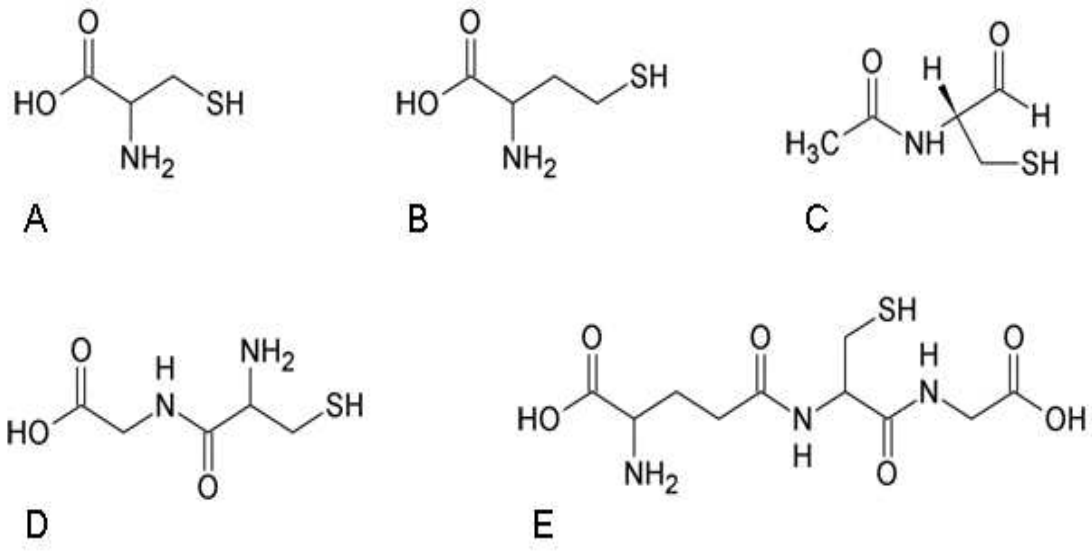

Figure 3.1 Thiol compounds of interest. Chemical structures of Cys (A); Hcys (B); NAC (C); CysGly (D) and GSH (E).

Although there have been numerous methods published for the determination of GSH, many of these have limitations or have not been fully validated. While the classic Tietze reaction (Tietze, 1969) and the monochlorobimane assay (Kamencic et al., 2000) are quick, simple and inexpensive ways to measure GSH, they lack sensitivity and can not determine Cys, CysGly or HCys. Other methods such as HPLC with tandem mass spectrometry show good sensitivity and specificity, but are expensive and involve complex or time-consuming procedures (Bouligand et al., 2006). Therefore, reaction of the thiol group with a fluorophore, followed by

separation by HPLC and subsequent fluorescence detection has become the most popular method for the determination of GSH and other thiol compounds. One of the most widely used and best validated derivatising agents is 4-aminosulfonyl-7-fluoro-2,1,3-benzoxadiazole-4-sulfonate (SBD-F) (McMenamin et al., 2009; Nolin et al., 2007; Oe et al., 1998; Toyo'oka and Imai, 1983). More recently, a closely related fluorogenic reagent, 4-fluoro-7-aminosulfonylbenzofurazan (ABD-F), has been used for measurement of thiols and is reported to have a number of advantages over SBD-F (Akgül et al., 2005). Both SBD-F and ABD-F possess a benzofurazan moiety that produces a highly fluorescent compound through its reaction with a sulfhydryl group (Figure 3.2). The reaction rate of ABD-F, however, is 30 times faster than that of SBD-F. It also takes place under less extreme conditions, with ABD-F reactions with thiol compounds reported to complete within 5 minutes in aqueous conditions at 50°C and pH 8 (Toyo'oka et al., 1989), compared to SBD-F reactions with thiol compounds requiring incubation for 60 minutes in aqueous conditions at 60°C and pH 9.5 (Nolin et al., 2007). Due to these features, ABD-F was selected as the derivatisation agent of choice for this study.

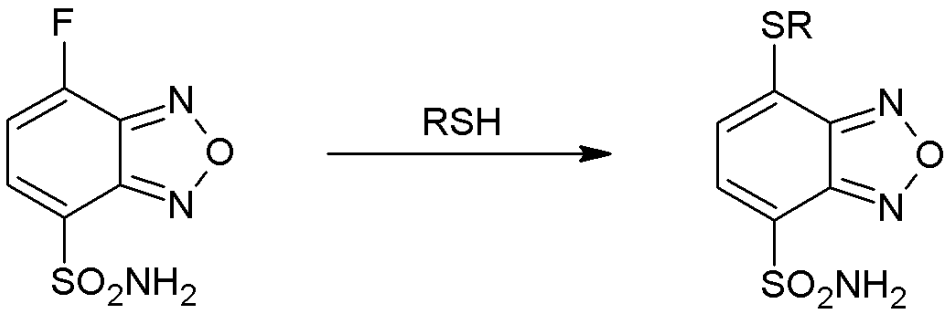

Figure 3.2 ABD-F derivatisation of a thiol group. The benzofurazan moiety of ABD-F reacts with a sulfhydryl group to produce a highly fluorescent compound.

On surveying the literature, however, it was found that none of the published methods utilising ABD-F were suitable for the intended application of quantitating total (reduced and oxidised), soluble thiol compounds in cell culture media. Therefore, it was necessary to design and optimise a suitable method for the simultaneous quantitation of Cys, CysGly, Hcys and GSH, that involved deproteinisation of samples (to exclude non-soluble thiols) and reduction of disulfides (to include reduced and oxidised thiols).

There are three critical components that need to be considered when designing a HPLC method: sample preparation, chromatographic conditions and quantitation. In addition to selection of a derivatisation agent (ABD-F) and introduction of deproteinisation and reduction steps; optimisation of sample preparation involves selection of appropriate sample collection and storage conditions, as well as incubation times, temperature and buffers to enable optimal derivatisation. For chromatographic conditions, a suitable column, mobile phase and flow rate are chosen to produce acceptable separation of all thiol compounds (Sharbir, 2004). Finally, the two most commonly employed techniques for quantitation of analyte in a sample are the external standard method and the internal standard method. Both methods involve construction of a calibration curve covering a relevant concentration range, where standards (usually synthetic versions of the compounds of interest) are dissolved in the same matrix (e.g. cell culture media, plasma) as the sample, where possible. The external standard method involves plotting the response (e.g. peak area of fluorescence) of an analyte against known amounts of the analyte to produce a linear equation which can be used to determine unknown concentrations of analyte in samples (Poole, 2003). Although this method can give a good indication of changes

that may occur from day to day, it does not correct for any errors that may result during sample preparation (Poole, 2003). The internal standard method involves the addition of an 'internal standard' to all standard solutions and samples. The internal standard is a compound that is not present in samples, but is physically and chemically similar to the compounds of interest. Calibration curves are then prepared by calculating the ratio of the response of an analyte to the response of the internal standard and plotting response ratios against analyte concentration. The use of internal standards in chromatography is very common due to the assumption that any changes in the analyte that arise during sample preparation or injection will be reflected in the internal standard, thereby reducing errors and improving precision. Internal standards can also correct for error introduced by matrix differences when it is not possible to prepare standard solutions in the same matrix as samples (Poole, 2003).

In the present study, N-acetylcysteine (NAC) was selected for use as an internal standard due to its similarity to the compounds of interest, its ready availability, ease of chromatographic separation from other thiols under the selected conditions and since it has previously been used as an internal standard for HPLC separation and detection of ABD-thiols (Santa et al., 2006). The performance and suitability of NAC as an internal standard was investigated by comparing the precision and accuracy of results produced by the external and internal standard calibration methods.

Although there are a number of published methods for the quantification of multiple thiols, very few of these have been fully validated (McMenamin et al., 2009).

"Method validation is the process used to confirm that the analytical procedure employed for a specific test is suitable for its intended use. Results from method validation can be used to judge the quality, reliability and consistency of analytical *results; it is an integral part of any good analytical practice"* (Huber, 1998). The International Conference on Harmonisation (ICH) guidelines recommend that all analytical methods be assessed for specificity, linearity, precision, accuracy and limits of quantitation before their introduction into routine use (ICH, 2005). Accordingly, the objective of the present study was to establish and thoroughly validate a simple, sensitive and reliable method for the quantification of GSH and related compounds.

3.2 Materials and Methods

3.2.1 Materials

The U373-MG human astrocytoma cell line was kindly provided by Dr Peter Locke (The Royal Melbourne Hospital, Australia). 4-fluoro-7-aminosulfonylbenzofurazan (ABD-F) was purchased from Novachem (Collingwood, Australia). Chromatography grade methanol was from Merck (Kilsyth, Australia). All buffers were prepared with Millipore water (Kilsyth, Australia). All cell culture materials were from Invitrogen (Mulgrave, Australia). All other reagents were from Sigma-Aldrich (Castle Hill, Australia).

3.2.2 Instrumentation

A Dionex HPLC system consisting of an ASI-100 automated sample injector, a P680 solvent pump, a TCC-100 thermostatted column compartment and an RF-2000 fluorescence detector was used for all chromatographic analyses (Sydney, Australia). The system was equipped with a Luna C18(2) column (150 mm x 4.6 mm id, 3 µm) protected by a Security Guard C18 Cartridge (4.0 x 3.0 mm) in a Security Guard Cartridge Holder supplied by Phenomenex (Sydney, Australia). The Chromeleon 6.8 Chromatography Data System from Dionex was used to control instruments, acquire data and quantify peak areas (Sydney, Australia).

3.2.3 Preparation of standards and calibration curve solutions

Stock solutions of Cys (3,200 µM), CysGly, Hcys and GSH (all 200 µM) were prepared in water or media and then combined to give a top concentration of 800 µM for Cys and 50 µM for each of CysGly, Hcys and GSH. This multiple-thiol solution

was then serially diluted 2-fold to make six additional solutions of decreasing concentration. To mimic sample preparation (described in section 3.2.7) each solution was mixed with an equal volume of 1% 5-sulfosalicylic acid (SSA) containing 1 mM EDTA, centrifuged at 14,000 x g and 4°C for 10 minutes and the supernatant removed to fresh tubes and stored at -80°C. A 50 µM NAC solution was prepared in Millipore water for use as an internal standard.

3.2.4 Derivatisation of GSH and related thiols with ABD-F

Standards and samples were removed from -80°C storage and allowed to thaw. Microcentrifuge vials were placed in a heating block set to 35˚C and 50 µl of sample or standard added. To reduce all disulfide bonds, 30 µl of a 1 mM solution of the reducing agent Tris(2-carboxyethyl)phosphine hydrochloride (TCEP) was added. 30 µl of a 50 µM NAC solution was added as an internal standard. For the derivatisation reaction, vials were incubated for 5 minutes at 35°C before the addition of 100 µl of borate buffer (0.1 M, pH 9.3, with 1 mM EDTA) and 30 µl of the derivatising agent ABD-F (1mg/ml in 0.1 M borate buffer, pH 9.3, with 1 mM EDTA). Incubation at 35°C was continued for 10 minutes, before the reaction was stopped by addition of 50 µl of 2 M hydrochloric acid (HCl). Vials were then centrifuged at 14,000 x g for 5 minutes at 4°C in order to pellet any particulates that could potentially damage the HPLC system. Supernatants were placed into fresh vials and loaded into the autosampler which was set to 8°C to minimise evaporation. The steps involved in sample preparation and derivatisation are summarised in Figure 3.3.

3.2.5 Chromatographic Conditions

An autosampler maintained sample temperatures at 8°C and injected 10 µl aliquots for analysis. The mobile phase used for separation of ABD-derivatised thiols was 0.1 M acetate buffer (pH 4)-methanol [86:14]. An isocratic program with a flow rate of 1 ml/min was used and column temperature was maintained at 35°C. Fluorescence detection was set to excitation at 390 nm and emission at 510 nm, with high level sensitivity.

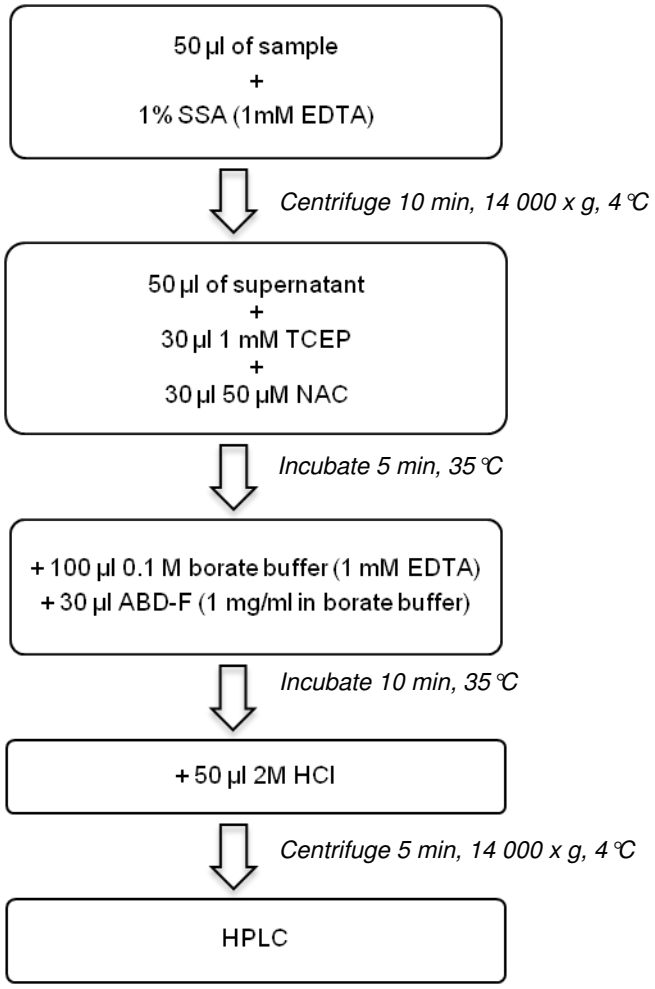

Figure 3.3 Sample preparation and derivatisation reaction for HPLC detection of thiols. SSA: 5-sulfosalicylic acid; EDTA: ethylenediaminetetraacetic acid; TCEP: Tris(2-carboxyethyl)phosphine hydrochloride; NAC: N-acetylcysteine; HCl: hydrochloric acid.

3.2.6 Validation of the method

Validation of the analytical method was carried out according to the guidelines of the International Conference on Harmonization (ICH, 2005). The method was validated for specificity, linearity, precision, accuracy and limits of quantitation.

3.2.7 Application of the method to measure GSH and related thiols in cell conditioned media

U373 cells maintained in Dulbeccos's Modified Eagle Medium (DMEM) containing 25 mM glucose, supplemented with 200 U/ml penicillin, 200 µg/ml streptomycin, 2.6 µg/ml Fungizone, 200 mM glutamine and 5% foetal bovine serum (FBS) were grown in 175 cm^2 tissue culture flasks and incubated at 37°C in 5% CO_2. U373 cells were harvested with a solution containing 0.025 mM trypsin and 1 mM EDTA in PBS and seeded at a density of 9×10^3 cells/well in 96 well plates. FBS concentration was reduced to 1% to minimise proliferation and the total volume of media in each well was 100 µl. After 72 hrs incubation, media was carefully removed from wells and centrifuged at 200 x g for 5 minutes at 4°C to pellet cellular debris. Following centrifugation, 50 µl of supernatant was mixed with an equal volume of 1% SSA containing 1 mM EDTA, centrifuged at 14,000 x g for 10 minutes at 4°C to precipitate protein, and the resultant supernatant placed in fresh tubes and stored at -80°C for later analysis. This acidification step eliminates protein-bound thiols from samples and helps to prevent auto-oxidation of thiols (Williams et al., 2001).

3.2.8 Statistics

Graphpad Prism was used to produce figures and analyse data. Relationships between linear regression data were assessed by using Pearson's correlation test.

3.3 Results

3.3.1 Chromatographic separation of GSH and related compounds

Preliminary experiments to optimise the chromatographic separation of Cys, CysGly, Hcys and GSH involved testing various columns, mobile phase compositions and flow rates. A Luna C18(2) column (150 x 4.6 mm id, 3 µm) produced a better separation compared to a PurospherSTAR RP-18e column (250 x 4 mm id, 5 µm). A methanol-acetate buffer, previously used by Santa et al. (2006) and Nolin et al. (2007), was tested with different buffer to methanol ratios and varying pH. The best separation was achieved with a mobile phase consisting of 14% methanol and 86% 0.1 M acetate buffer at pH 4 and a flow rate of 1.0 ml/min. Retention times and elution order of the thiols were extremely sensitive to changes in the pH of the buffer. Therefore precise repeatability of mobile phase production was very important. Since the concentration of total thiols was of interest, various concentrations of TCEP were tested in order to select the optimal concentration. While too little TCEP (1:1 ratio of TCEP to oxidised GSH) resulted in incomplete reduction of oxidised GSH, too much TCEP (50:1 ratio of TCEP to oxidised GSH) appeared to interfere with the derivatising reaction leading to an underestimation of total GSH. A TCEP concentration of 1 mM (10:1 ratio of TCEP to oxidised GSH) showed the best estimation of total GSH and thus was selected for routine use.

Representative chromatograms of Cys, CysGly, Hcys, GSH and NAC determined in water and DMEM with the method described in Section 3.2 are shown in Figure 3.4. Excellent resolution (≥ 3.47) was achieved with Cys, CysGly, Hcys, GSH and NAC (internal standard) eluting at 4.26 ± 0.03, 4.87 ± 0.03, 6.07 ± 0.04, 7.74 ± 0.06 and

14.46 ± 0.10 minutes ± standard deviation, respectively, under the chromatographic conditions described. There was no interference from endogenous compounds in DMEM, except in the case of Cys, which is included in DMEM in its oxidised form as cystine. Fresh DMEM contains 0.201 mM of cystine, which after reduction with TCEP is roughly equivalent to 0.4 mM of cysteine. This value was used for determining the 'expected' concentrations of Cys in the recovery studies for assessing accuracy of the method (Section 3.3.5).

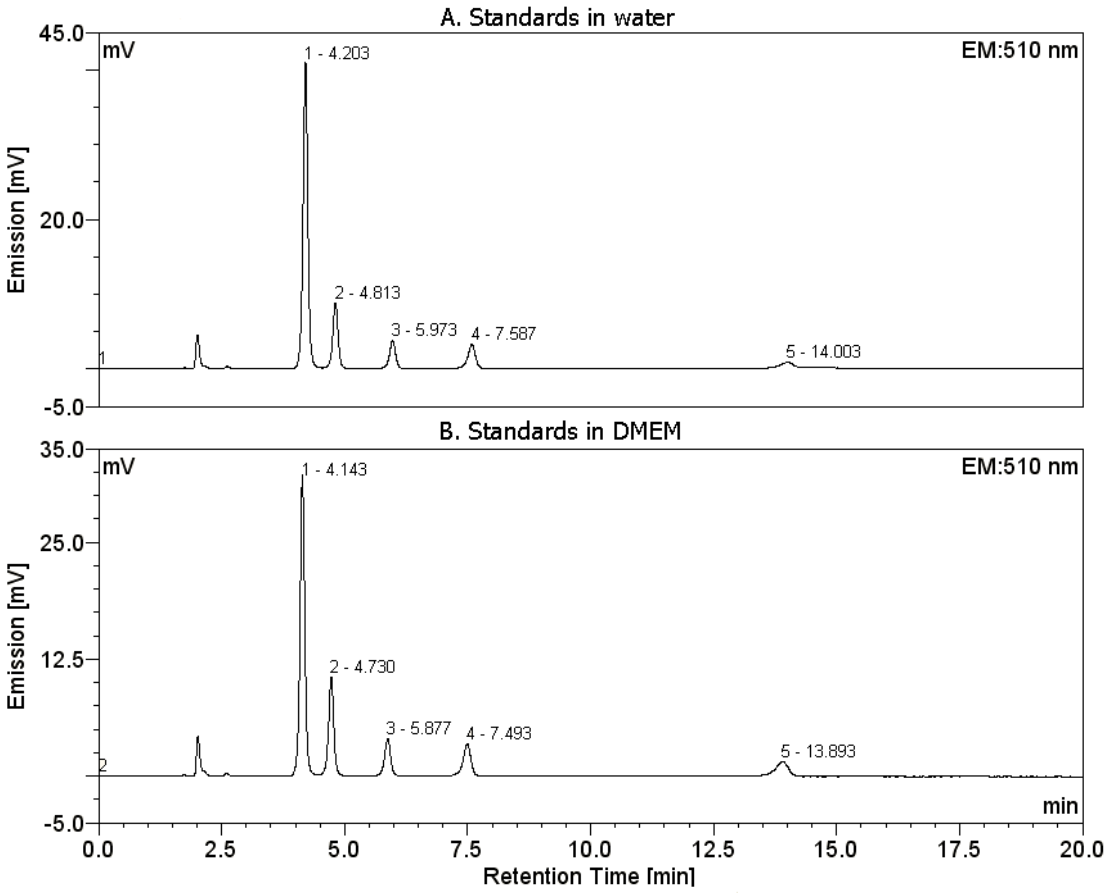

Figure 3.4 Chromatograms of ABD-labelled thiol compounds. Thiol standards dissolved in Millipore water (A) or Dulbecco's Modified Eagle's medium (DMEM) (B) were derivitised with ABD-F and separated on Luna C18(2) column (150 mm x 4.6 mm id, 3 µm) at 35°C with a mobile phase of 0.1 M acetate buffer (pH 4)-methanol [86:14]. Peaks: 1. Cys (400 µM); 2. CysGly (25 µM); 3. Hcys (25 µM); 4. GSH (25 µM); 5. N-acetylcysteine was included as an internal standard.

3.3.2 Linearity of assay

Linear calibration curves were constructed for each analyte dissolved in water and in DMEM using both the external and internal standard calibration curve methods. Concentrations ranged from 12.5 – 800 µM for Cys and from 0.8 – 50 µM for CysGly, Hcys and GSH. When the external standard method was used, peak area responses were plotted against analyte concentration. When the internal standard method was used, a ratio of the analyte signal to the internal standard signal (NAC) was plotted against analyte concentration. Linear responses were observed in water and in DMEM for both quantitation methods and correlation coefficients were > 0.99 for all calibration curves. Linear regression plots and data for calibration curves of all analytes in water and media quantified by either the external standard method or the internal standard method are shown in Figures 3.5 - 3.8 and Tables 3.1 – 3.4.

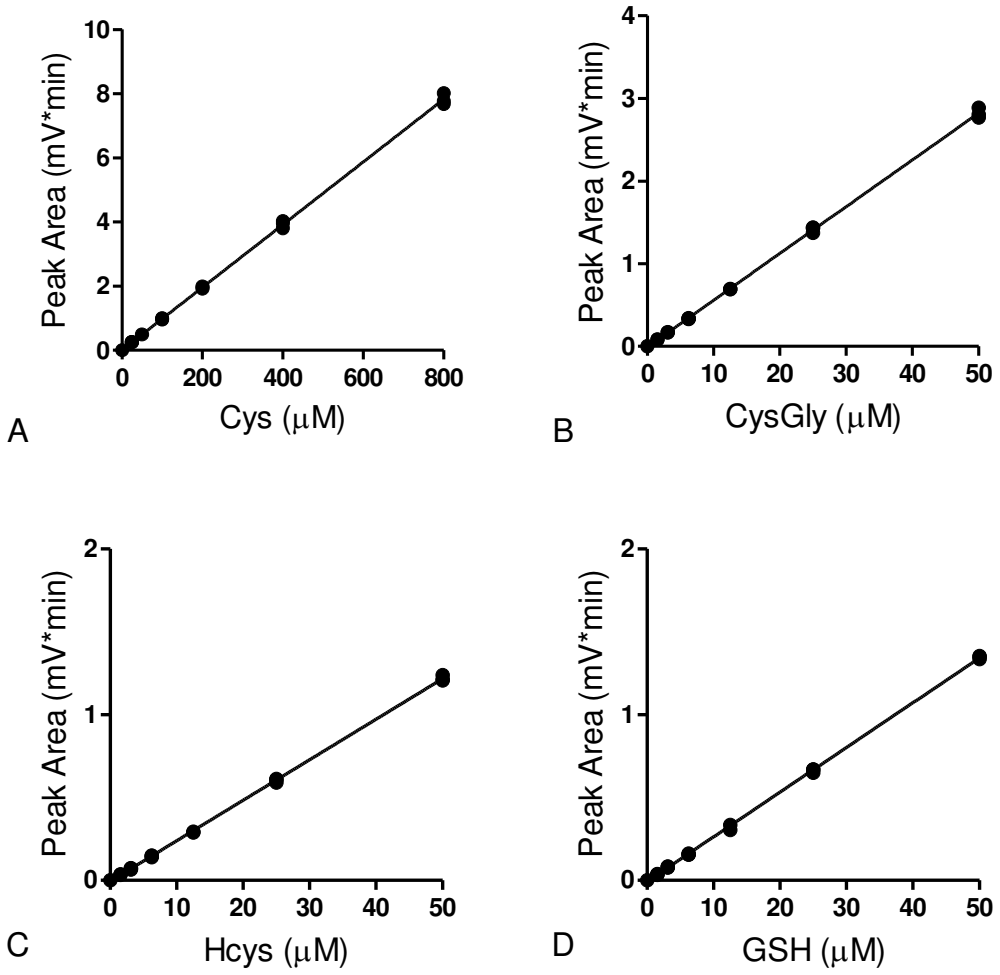

Figure 3.5 Linear regression plots for thiol compounds in water produced by the external standard calibration curve method. Mixtures of 12.5 – 800 µM Cys (A) and 0.78 – 50 µM CysGly (B), Hcys (C) and GSH (D) in water were determined by HPLC with fluorescence detection and linear regression plots produced using the external standard method (n=3).

Table 3.1 Linear regression data for HPLC determination of Cys, CysGly, Hcys and GSH in water by the external standard calibration curve method.

Statistical parameter	Cys	CysGly	Hcys	GSH
Calibration range (µM)	12.5-800	0.78-50	0.78-50	0.78-50
Regression equation slope	0.0098 ± 0.0001	0.0566 ± 0.0003	0.0245 ± 0.0001	0.0269 ± 0.0001
y-Intercept	0.0097 ± 0.0202	-0.0072 ± 0.0072	-0.0061 ± 0.0024	-0.0075 ± 0.0028
Correlation coefficient (r)	0.9994	0.9994	0.9997	0.9996

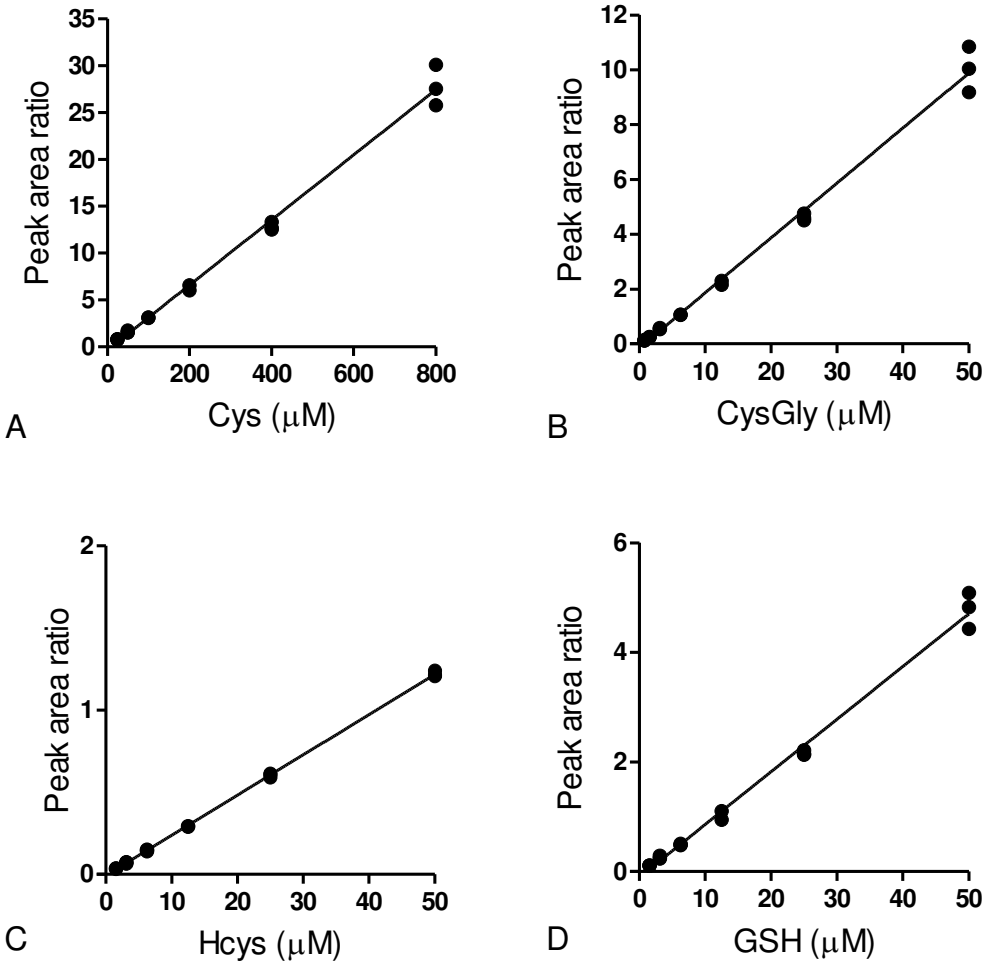

Figure 3.6 Linear regression plots for thiol compounds in water produced by the internal standard calibration curve method. Mixtures of 12.5 – 800 μM Cys (A) and 0.78 – 50 μM CysGly (B), Hcys (C) and GSH (D) in water were determined by HPLC with fluorescence detection and linear regression plots produced using the internal standard calibration curve method. NAC (50 μM) was used as the internal standard and y-axis values were calculated by dividing peak area of the analyte by the peak are of NAC (n=3).

Table 3.2 Linear regression data for HPLC determination of Cys, CysGly, Hcys and GSH in water by the internal standard calibration curve method.

Statistical parameter	Cys	CysGly	Hcys	GSH
Calibration range (μM)	12.5-800	0.78-50	0.78-50	0.78-50
Regression equation slope	0.0346 ± 0.0007	0.2003 ± 0.0042	0.0865 ± 0.0017	0.0955 ± 0.0019
y-Intercept	-0.2867 ± 0.2446	-0.1373 ± 0.0923	-0.0685 ± 0.0373	-0.0778 ± 0.0415
Correlation coefficient (r)	0.9929	0.9923	0.9932	0.9931

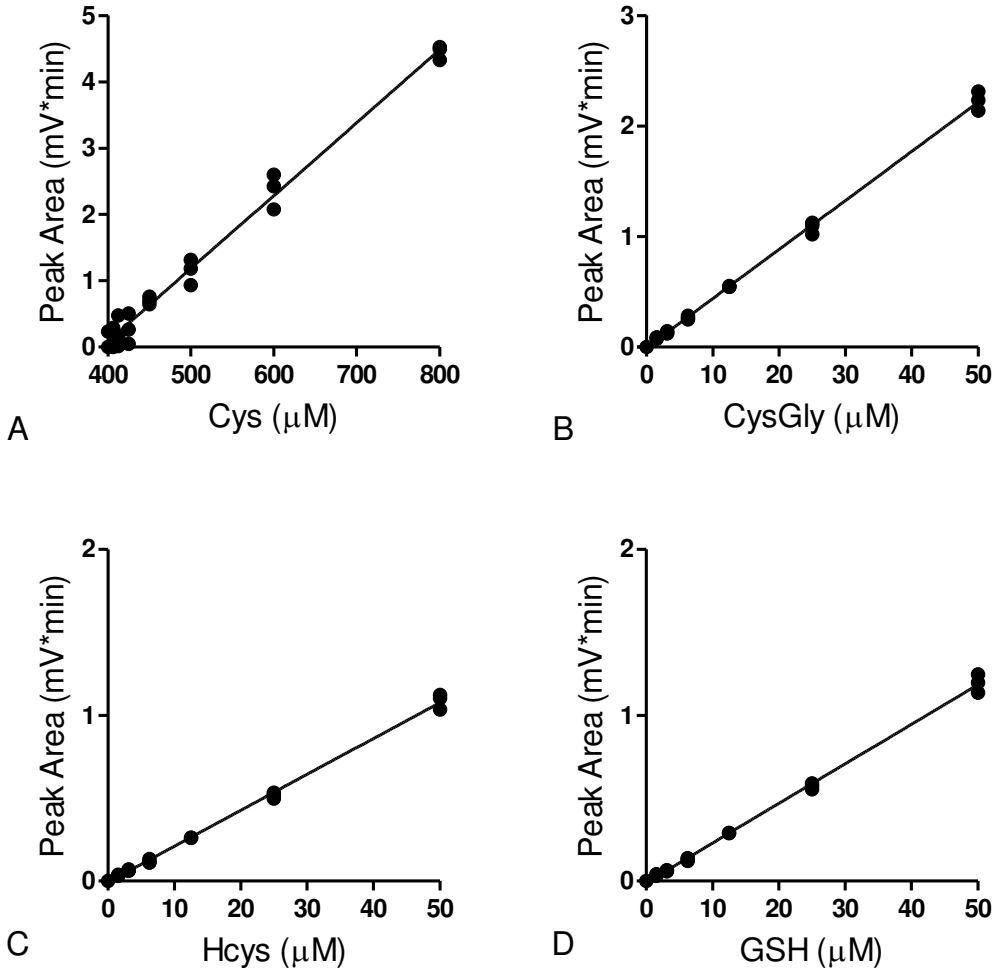

Figure 3.7 Linear regression plots for thiol compounds in media produced by the external standard calibration curve method. Mixtures of 12.5 – 800 μM Cys (A) and 0.78 – 50 μM CysGly (B), Hcys (C) and GSH (D) in media were determined by HPLC with fluorescence detection and linear regression plots produced using the external standard method (n=3).

Table 3.3 Linear regression data for HPLC determination of Cys, CysGly, Hcys and GSH in media by the external standard calibration curve method.

Statistical parameter	Cys	CysGly	Hcys	GSH
Calibration range (μM)	0.00 – 400.00	1.56 – 100.00	1.56 – 100.00	1.56 – 100.00
Regression equation slope	0.0111 ± 0.0003	0.0443 ± 0.0002	0.0216 ± 0.0001	0.0243 ± 0.0001
y-Intercept	0.0660 ± 0.0456	-0.0039 ± 0.0094	-0.0066 ± 0.0049	-0.0141 ± 0.0057
Correlation coefficient (r)	0.9862	0.9994	0.9993	0.9993

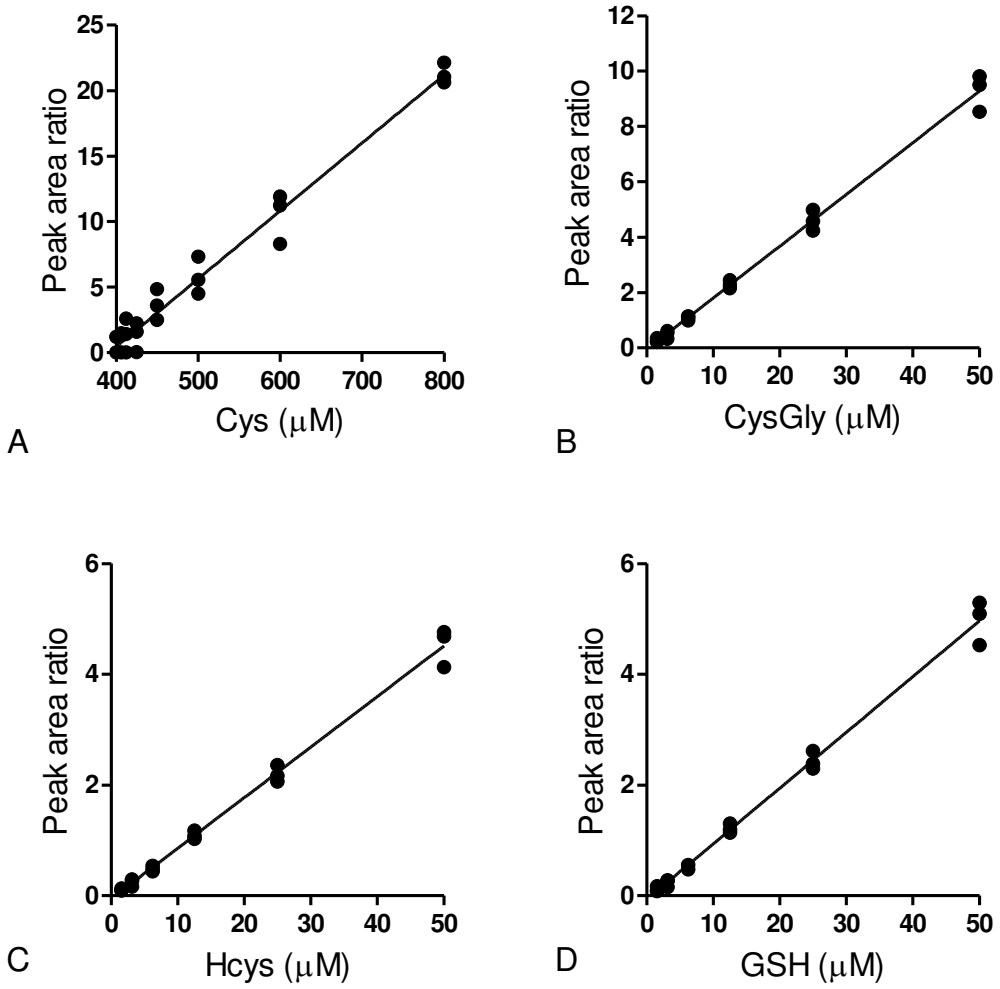

Figure 3.8 Linear regression plots for thiol compounds in media produced by the internal standard calibration curve method. Mixtures of 12.5 – 800 μM Cys (A) and 0.78 – 50 μM CysGly (B), Hcys (C) and GSH (D) in media were determined by HPLC with fluorescence detection and linear regression plots produced using the internal standard calibration curve method. NAC (50 μM) was used as the internal standard and y-axis values were calculated by dividing peak area of the analyte by the peak are of NAC (n=3).

Table 3.4 Linear regression data for HPLC determination of Cys, CysGly, Hcys and GSH in media by the internal standard calibration curve method.

Statistical parameter	Cys	CysGly	Hcys	GSH
Calibration range (μM)	6.25 - 400	1.56 - 100	1.56 - 100	1.56 - 100
Regression equation slope	0.0519 ± 0.0017	0.1963 ± 0.0023	0.0959 ± 0.0011	0.1076 ± 0.0013
y-Intercept	0.4398 ± 0.2822	-0.1870 ± 0.1004	-0.1145 ± 0.0478	-0.1599 ± 0.0583
Correlation coefficient (r)	0.9762	0.9974	0.9975	0.9971

3.3.3 Comparison of thiol calibration curves prepared in water and in media

Concentrations of Cys, CysGly, Hcys and GSH were calculated by using calibration curves prepared in water and in DMEM. These values were then plotted against each other and compared by using Pearson's correlation test (Figure 3.9). Highly significant ($p<0.0001$), strong correlations ($r^2 \geq 0.9968$) were seen for all compounds for both the external standard method and the internal standard calibration method. Therefore intra-day and inter-day precision studies (Section 3.3.4) were carried out using standards dissolved in water only.

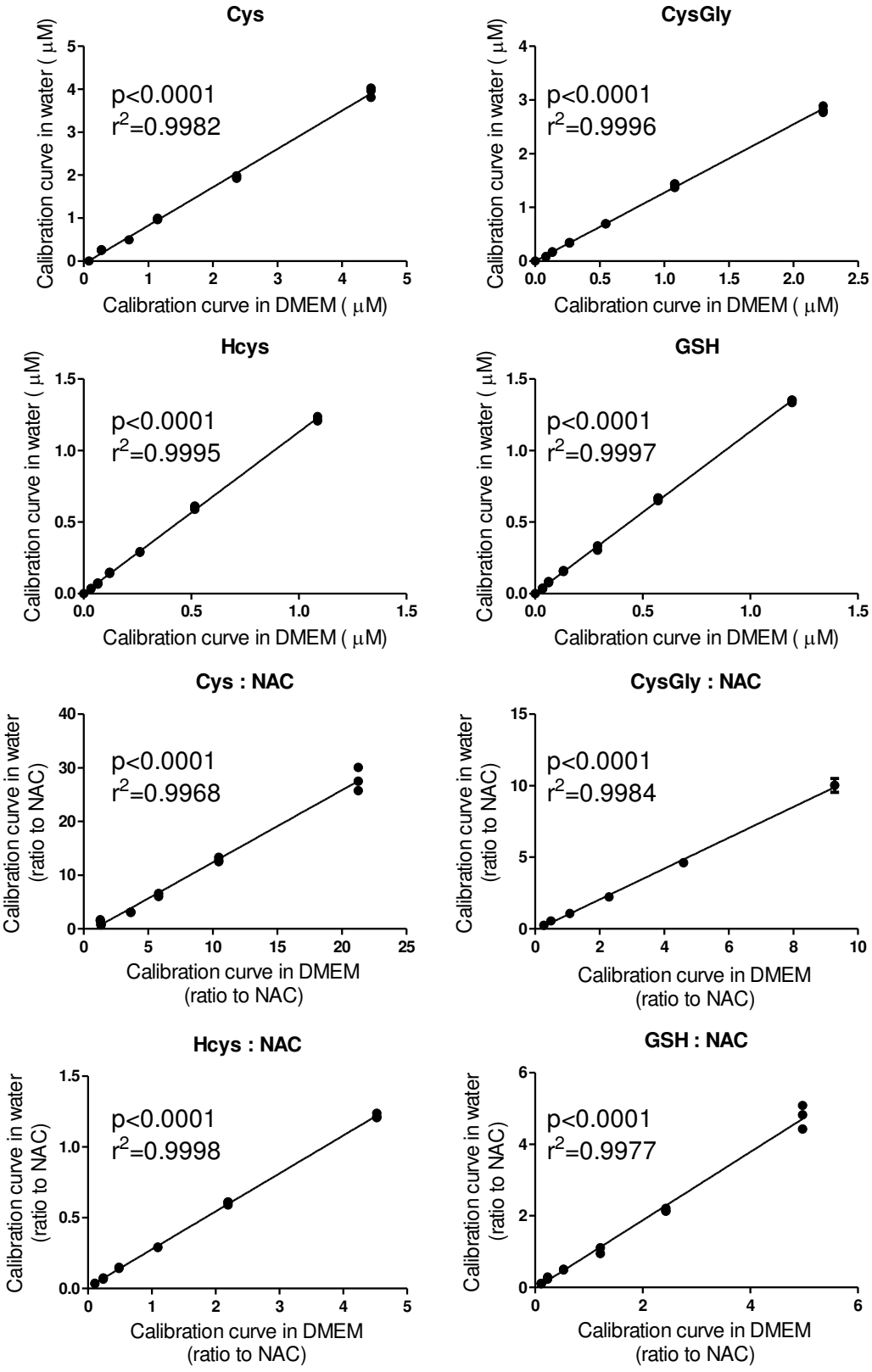

Figure 3.9 Comparison of thiol calibration curves made in water and in DMEM. Calibration curves made in water and DMEM for Cys (12.5 – 800 μM), CysGly, Hcys and GSH (0.78 – 50 μM) were plotted against each other and analysed using Pearson's correlation test. Correlation coefficients (r^2) and significance (p) values are shown on graphs (n=3).

3.3.4 Precision of the HPLC method

The precision of a method can be expressed as the relative standard deviation (RSD) which is calculated by dividing the standard deviation of the response by the mean response (also called the coefficient of variation). Typically, a method that gives RSD values ≤ 15% for all concentrations is considered to have an acceptable level of precision (Shah et al., 2000). Intra and inter-day variability of the HPLC assay for determining Cys, CysGly, Hcys and GSH standards in DMEM was assessed. Results from the external and internal standard calibration curve methods were compared to enable determination of the most precise method.

Intra-day variability

The intra-day variability of the assay was determined by repeated analysis of a combined standard solution over a range of concentrations on the same day. Results are presented in Table 3.5 and indicate that the external standard method is reproducible within the same day (RSD ≤ 6.6%). The internal standard method produced RSD values that were generally higher than that produced by the external standard method suggesting that it was less precise, however all values were within the acceptable range (RSD ≤ 10.2%).

Inter-day variability

The inter-day variability of the assay was determined by analysis of a combined standard solution at low, medium and high concentration on three different days. Samples were prepared on the same day as a single batch by dissolving thiol standards in water. This solution was divided into aliquots and stored at -80°C until analysis. Results are shown in Table 3.6 and indicate that the assay is reproducible

between different days, for both the external (RSD $\leq$ 7.1%) and internal standard (RSD $\leq$ 6.6%) calibration methods.

Table 3.5 Intra-day variability of HPLC method for determining Cys, CysGly, Hcys and GSH concentrations in water.

Standard	Concentration added (µM)	External standard calibration		Internal standard calibration	
		Mean concentration measured ± S.D. (µM)	RSD (%)	Mean concentration measured ± S.D. (µM)	RSD (%)
Cys	12.5	13.0 ± 0.4	2.7	20.0 ± 0.3	1.5
	25.0	25.1 ± 0.8	3.0	30.9 ± 0.5	1.6
	50.0	49.5 ± 0.1	0.2	54.6 ± 3.2	5.9
	100.0	98.9 ± 1.9	1.9	97.4 ± 0.9	0.9
	200.0	198.7 ± 4.2	2.1	190.1 ± 11.6	6.1
	400.0	400.3 ± 11.5	2.9	379.7 ± 12.3	3.2
	800.0	797.2 ± 17.3	2.2	811.7 ± 62.9	7.7
CysGly	0.8	0.9 ± 0.0	4.6	1.3 ± 0.0	2.7
	1.6	1.6 ± 0.1	3.8	1.9 ± 0.1	2.8
	3.1	3.1 ± 0.1	2.1	3.4 ± 0.1	3.9
	6.3	6.1 ± 0.1	1.5	6.0 ± 0.0	0.4
	12.5	12.4 ± 0.1	0.4	11.8 ± 0.5	4.4
	25.0	25.1 ± 0.6	2.5	23.7 ± 0.6	2.7
	50.0	50.0 ± 1.1	2.2	50.7 ± 4.2	8.2
Hcys	0.8	1.0 ± 0.0	3.2	1.4 ± 0.0	1.5
	1.6	1.7 ± 0.1	5.7	2.0 ± 0.1	4.3
	3.1	3.2 ± 0.2	5.8	3.5 ± 0.3	9.7
	6.3	6.2 ± 0.2	2.9	6.1 ± 0.2	3.5
	12.5	12.1 ± 0.2	1.3	11.6 ± 0.3	2.8
	25.0	24.9 ± 0.5	1.9	23.5 ± 0.6	2.4
	50.0	50.1 ± 0.7	1.3	50.9 ± 3.6	7.1
GSH	0.8	1.0 ± 0.1	6.6	1.4 ± 0.1	3.6
	1.6	1.6 ± 0.1	4.9	2.0 ± 0.1	2.8
	3.1	3.3 ± 0.1	4.2	3.5 ± 0.3	8.9
	6.3	6.1 ± 0.1	2.2	6.0 ± 0.1	1.9
	12.5	12.1 ± 0.8	6.5	11.6 ± 1.2	10.2
	25.0	24.8 ± 0.4	1.7	23.5 ± 0.5	1.9
	50.0	50.2 ± 0.4	0.7	50.9 ± 3.5	6.8

Mixtures of Cys (12.5 – 800 µM), CysGly, Hcys and GSH (0.8 – 50 µM) in water were determined on the same day by HPLC with fluorescence detection and quantified by the external and internal standard calibration curve methods, where 50 µM NAC was used as the internal standard (n=3). RSD: relative standard deviation; S.D.: standard deviation.

Table 3.6 Inter-day variability of HPLC method for determining Cys, CysGly, Hcys and GSH concentrations in water.

Standard	Concentration added (µM)	External standard calibration		Internal standard calibration	
		Mean concentration measured ± S.D. (µM)	RSD (%)	Mean concentration measured ± S.D. (µM)	RSD (%)
Cys	25.0	26.0 ±1.5	5.9	31.1 ± 2.0	6.3
	100.0	98.2± 1.1	1.1	95.7 ± 3.0	3.2
	400.0	403.9± 6.4	1.6	374.4 ± 15.2	4.1
CysGly	1.6	1.6 ± 0.0	2.8	1.9 ± 0.1	2.9
	6.3	6.0 ± 0.1	2.3	5.9 ± 0.2	3.2
	25.0	25.0 ± 0.5	2.2	23.2 ± 1.0	4.3
Hcys	1.6	1.7 ± 0.1	7.1	2.0 ± 0.1	6.6
	6.3	6.1 ± 0.3	5.1	6.0 ± 0.4	5.9
	25.0	25.0 ± 0.5	2.0	23.2 ± 0.9	3.8
GSH	1.6	1.7 ± 0.1	7.0	2.0 ± 0.1	6.3
	6.3	6.0 ± 0.2	3.5	5.8 ± 0.2	4.0
	25.0	25.0 ± 0.4	1.8	23.2 ± 0.7	3.1

Mixtures of Cys (25 – 400 µM), CysGly, Hcys and GSH (1.6 – 25 µM) in water were determined on 3 different days by HPLC with fluorescence detection and quantified by the external and internal standard calibration curve methods, where 50 µM NAC was used as the internal standard (n=3). RSD: relative standard deviation; S.D.: standard deviation.

3.3.5 Accuracy of the HPLC method

Since the intended application of the developed HPLC method was determination of thiols in cell culture media, the method was assessed for its accuracy at determining thiol compounds in DMEM. Known amounts of thiol standards were added to DMEM to produce sample mixtures ranging in concentration from 6.5 – 800 μM for Cys and from 0.8 – 50 μM for CysGly, Hcys and GSH. Triplicate samples were analysed by the developed method and the percentage recovered was calculated for each compound (Table 3.7). Linear regression equations obtained from calibration curves prepared in DMEM (Tables 3.3 and 3.4) were used to assess the accuracy of the method for CysGly, Hcys and GSH. Due to cystine being a constituent of DMEM, the linear regression equations from calibration curves prepared in water (Tables 3.1 and 3.2) were used to assess the accuracy of the method for determining total Cys in DMEM. Recovery rates ranged from 93.7 – 125.0% for the external standard calibration curve method and from 87.5 – 175.0% for the internal standard calibration curve method. The generally accepted level of accuracy for bioanalytic methods is ± 15% of the true value. Surprisingly, the present findings suggest that the external standard method is more accurate than the internal standard method of calibration.

Table 3.7 Accuracy of HPLC method for determining standard thiols in media.

Standard	Concentration		External standard calibration		Internal standard calibration	
	Added (μM)	Expected (μM)	Measured Mean ± S.D. (μM)	Recovered (%)	Measured Mean ± S.D. (μM)	Recovered (%)
Cys*	0.0	400.0	395.9 ± 18.3	99.0	391.5 ± 21.3	97.9
	6.3	406.3	410.5 ± 16.1	101.0	355.7 ± 55.7	87.5
	12.5	412.5	415.3 ± 21.3	100.7	388.6 ± 73.0	94.2
	25	425.0	420.4 ± 20.7	98.9	416.4 ± 21.9	98.0
	50	450.0	459.1 ± 5.1	102.0	461.6 ± 22.6	102.6
	100	500.0	499.0 ± 17.3	99.8	503.3 ± 27.8	100.7
	200.0	600.0	609.2 ± 24.1	101.5	593.2 ± 37.1	98.9
	400.0	800.0	796.3 ± 9.5	99.6	801.5 ± 15.0	100.2
CysGly	0.8	0.8	0.9 ± 0.1	112.5	1.3 ± 0.0	162.5
	1.6	1.6	1.6 ± 0.1	100.0	2.1 ± 0.1	131.3
	3.1	3.1	3.1 ± 0.2	100.0	3.5 ± 0.7	112.9
	6.3	6.3	6.1 ± 0.4	96.8	6.4 ± 0.4	101.6
	12.5	12.5	12.5 ± 0.1	100.0	12.6 ± 0.7	100.8
	25.0	25.0	24.5 ± 1.2	98.0	24.4 ± 1.9	97.6
	50.0	50.0	50.4 ± 2.0	100.8	48.2 ± 3.4	96.4
Hcys	0.8	0.8	0.9 ± 0.1	112.5	1.4 ± 0.0	175.0
	1.6	1.6	1.7 ± 0.1	106.3	2.2 ± 0.1	137.5
	3.1	3.1	3.3 ± 0.2	109.7	3.7 ± 0.7	119.4
	6.3	6.3	5.9 ± 0.5	93.7	6.3 ± 0.5	100.0
	12.5	12.5	12.4 ± 0.5	99.2	12.6 ± 0.8	100.8
	25.0	25.0	24.2 ± 0.8	96.8	24.1 ± 1.5	96.4
	50.0	50.0	50.6 ± 2.1	101.2	48.4 ± 3.6	96.8
GSH	0.8	0.8	1.0 ± 0.1	125.0	1.4 ± 0.1	175.0
	1.6	1.6	1.7 ± 0.1	106.25	2.3 ± 0.0	143.8
	3.1	3.1	3.1 ± 0.2	100.0	3.6 ± 0.6	116.1
	6.3	6.3	6.0 ± 0.4	95.2	6.4 ± 0.4	101.6
	12.5	12.5	12.5 ± 0.0	100.0	12.8 ± 0.7	102.4
	25.0	25.0	24.1 ± 0.8	96.4	24.1 ± 1.5	96.4
	50.0	50.0	49.8 ± 2.3	99.6	47.7 ± 3.7	95.4

Mixtures of Cys (6.3 – 400 μM), CysGly, Hcys and GSH (1.6 – 50 μM) in DMEM were determined by HPLC with fluorescence detection. Cys was quantified using a standard curve in water. CysGly, Hcys and GSH were quantified using standard curves in DMEM. External and internal standard calibration methods are compared, where 50 μM NAC was used as the internal standard (n=3). RSD: relative standard deviation; S.D.: standard deviation. *DMEM contains 400 μM Cys.

3.3.6 Limits of quantitation of the HPLC method

The lowest limit of quantitation (LLOQ) of an assay can be defined as the lowest concentration for which the method was validated yielding an acceptable precision (RSD $\leq$ 15 %) and accuracy (180 - 120 %) of theoretical value (Shah et al., 2000). Therefore, the LLOQ of the HPLC method determined for Cys, CysGly, Hcys and GSH was 6.3 μM, 0.8 μM, 0.8 μM and 1.6 μM, respectively, when the external standard calibration method was used. When the internal standard calibration curve method was used, the LLOQ of the method for Cys, CysGly, Hcys and GSH was 6.3 μM, 3.1 μM, 3.1 μM and 3.1 μM, respectively. The upper limit of quantitation (ULOQ) is defined by the highest concentration for which the method was validated yielding an acceptable precision (RSD $\leq$ 15 %) and accuracy (180 - 120 %) of theoretical value (Shah et al., 2000). Therefore the ULOQ was determined as 800 μM for Cys and as 50 μM for CysGly, Hcys and GSH for both the external and internal standard calibration methods.

3.3.7 Application of method to the determination of thiols in cell-conditioned media

While the external standard calibration curve method and the internal standard calibration method appeared equal regarding intra and inter-day precision, the external standard method appeared to be the superior method in terms of accuracy and was also found to have lower LLOQ values for all analytes. As a result, the external standard method was selected as the calibration method of choice. In order to test the developed HPLC method on a biologically relevant sample, media was collected from an in vitro cell culture preparation of U373 cells after 72 hours incubation. On analysis of the media, Cys, CysGly, Hcys and GSH were determined at concentrations of 85.1 ± 12.7 µM, 3.6 ± 0.2 µM, 3.5 ± 0.3 µM and 12.1 ± 0.4 µM, respectively (Figure 3.10).

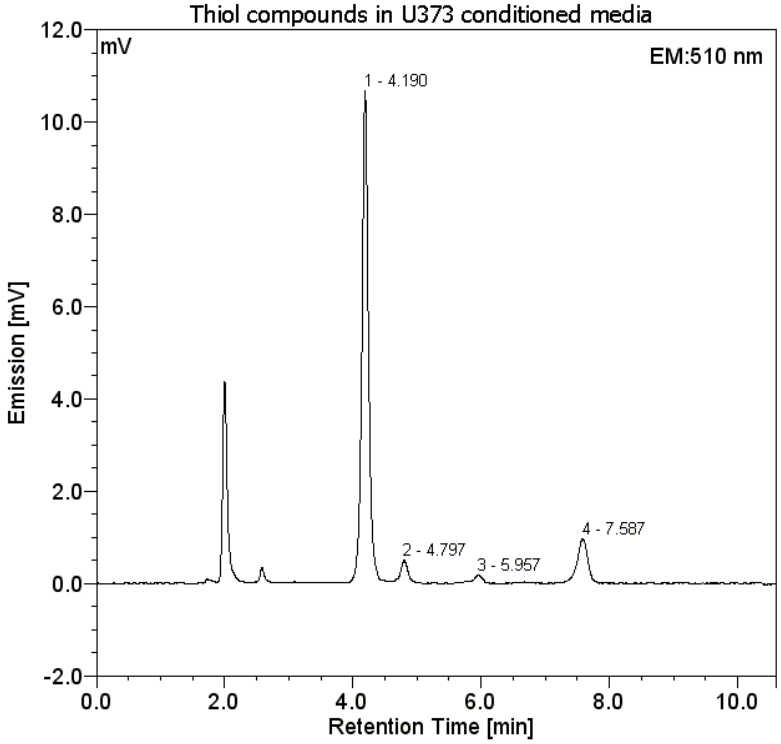

Figure 3.10 Thiol compounds detected in media from U373 cells cultured for 72 hours. Media collected from U373 cells incubated for 72 hours was derivatised with ABD-F and separated on Luna C18(2) column (150 mm x 4.6 mm id, 3 µm) at 35°C with a mobile phase of 0.1 M acetate buffer (pH 4)-methanol [86:14]. Labelled peaks represent Cys (1) CysGly (2), Hcys (3) and GSH (4).

3.4 Discussion

Increased levels of Cys and Hcys and decreased levels of GSH have been implicated in the pathogenesis of neurodegenerative diseases such as AD (Liu et al., 2004; McCaddon et al., 2003; Popp et al., 2009), making the investigation of changes in thiol metabolism an important focus for future research into such diseases. Previous published methods for the determination of thiols have focused on analysis of only one or two compounds, used less appropriate derivatisation agents (e.g. low specificity or sensitivity, time consuming) or did not involve thiol reduction or deproteinisation steps (Kamencic et al., 2000; Nolin et al., 2007; Oe et al., 1998; Santa et al., 2006; Tietze, 1969). This study described the development and validation of a practical HPLC method suitable for application to the simultaneous analysis of multiple thiol compounds. Cys, CysGly, Hcys and GSH were selected for investigation due to their notable appearance in astrocyte conditioned media (Dringen et al., 1997a; Huang et al., 2005b). In addition, the effectiveness of using NAC as an internal standard was addressed by comparing results determined by the external and internal standard calibration methods. Generally, the inclusion of an internal standard is thought to improve precision due to the assumption that any changes in the analyte that arise during sample preparation or injection into the analytic instrument, will also be reflected in the internal standard (Poole, 2003). In the present study, both the external and internal standard calibration methods showed acceptable intra-day and inter-day precision and there was no improvement demonstrated by inclusion of an internal standard. In the past, internal standardisation of chromatographic techniques was especially important to account for variations in sample volume due to manual injection. The use here of an automatic injector with excellent repeatability (RSD < 1%), might explain the failure

of the internal standard method to improve method precision compared to the external standard method.

When accuracy was assessed for the determination of thiol standards in DMEM at concentrations > 3.1 μM, both calibration methods showed good recovery rates ranging from 87.5 – 102.5%. For thiol concentrations between 0.8 μM and 3.1 μM, only the external standard method produced acceptable recovery rates (100.0 – 112.5%), with the exception of 0.8 μM GSH (125%). Recovery rates of thiol concentrations between 0.8 μM and 3.1 μM produced by the internal standard method ranged from 112.9 - 175.0%. As a result, the LLOQ values determined for each compound were lower for the external standard method compared to those determined for the internal standard method. The poor accuracy that was observed for the internal standard calibration method was probably due to the fact that the relative responses of low level concentrations of the thiol compounds were much smaller than the response of the internal standard (50 μM NAC). In order to improve method performance, the amount of internal standard added should be similar to the amount of analyte in the standard (Chan, 2004). In fact, as appears to be the case here, non-comparable responses between analyte and internal standard can actually introduce error rather than minimise it (Hewavitharana, 2009). As shown in Figure 3.10, there is a large variation in the responses (peak areas) of the different thiol compounds present in cell conditioned media. Therefore it is especially challenging to select an internal standard concentration that is capable of yielding precise and accurate results for all four thiol compounds simultaneously. In addition, not adding NAC to samples enabled chromatographic run times to be halved. This is an

important consideration in the application of the HPLC method to medium throughput analysis.

In conclusion a simple, sensitive and reliable HPLC method was developed and validated for specificity, linearity, accuracy, precision and lower and upper limits of quantitation. When quantitated by the external standard calibration curve method, the HPLC method here showed similar precision and accuracy to other published methods (reviewed by McMenamin et al., 2009). Due to being fully validated for the detection of Cys, CysGly, Hcys and GSH in media, this method is particularly useful for researching changes in extracellular thiol metabolism in vitro or for medium throughput screening of putative GSH boosters or antioxidants. It also has the potential for other applications, including analysis of thiols in plasma, cerebrospinal fluid or urine samples. Furthermore slight modification of the method would allow determination of the ratio between reduced and oxidised thiols (by analysing samples without the addition of TCEP), analysis of soluble and/or protein bound thiols (by reducing disulfides before precipitating protein) or determination of thiols at lower or higher concentration ranges (by increasing or decreasing the sensitivity of fluorescence detection respectively).

CHAPTER 4

Effect of proinflammatory activation on the release of glutathione and related thiols by U373 astrocytoma cells

4.1 Introduction

Intracellular levels of glutathione (GSH) in the brain have been reported to range from 1 to 20 mM in astrocytes to less than 1 mM in neurons (Aschner et al., 1994; Mokrasch and Teschke, 1984; Raps et al., 1989). Cysteine, the rate limiting substrate for GSH synthesis, is taken up rapidly by both neurons and astrocytes, but its oxidised form, cystine, is taken up much more efficiently by astrocytes (Kranich et al., 1996). Since extracellular cysteine is readily oxidised to form cystine, cystine transport mechanisms are essential to provide cells with cysteine (Yoshiba-Suzuki et al., 2011). Cystine uptake is mediated by the X_c^- system, a Na^+-independent cystine/glutamate antiporter, and it appears that this antiporter is expressed at lower levels in neurons compared to astrocytes (Bannai, 1984; Sagara et al., 1993; Shanker and Aschner, 2001). To reconcile this apparent shortcoming, astrocytes release approximately 10% of their intracellular GSH content per hour, via the multidrug resistance protein 1 transporter (Dringen et al., 1997a; Minich et al., 2006). Extracellular GSH is metabolised by γ-glutamyltranspeptidase (γ-GT) to form the dipeptide, cysteinylglycine (CysGly), which is then processed by the neuronal ectopeptidase aminopeptidase N, allowing neurons to immediately take up the resultant cysteine and glycine (Figure 4.1). Therefore, neurons rely on the release and cleavage of GSH by astrocytes in order to maintain optimal intracellular GSH levels (Dringen et al., 1999b).

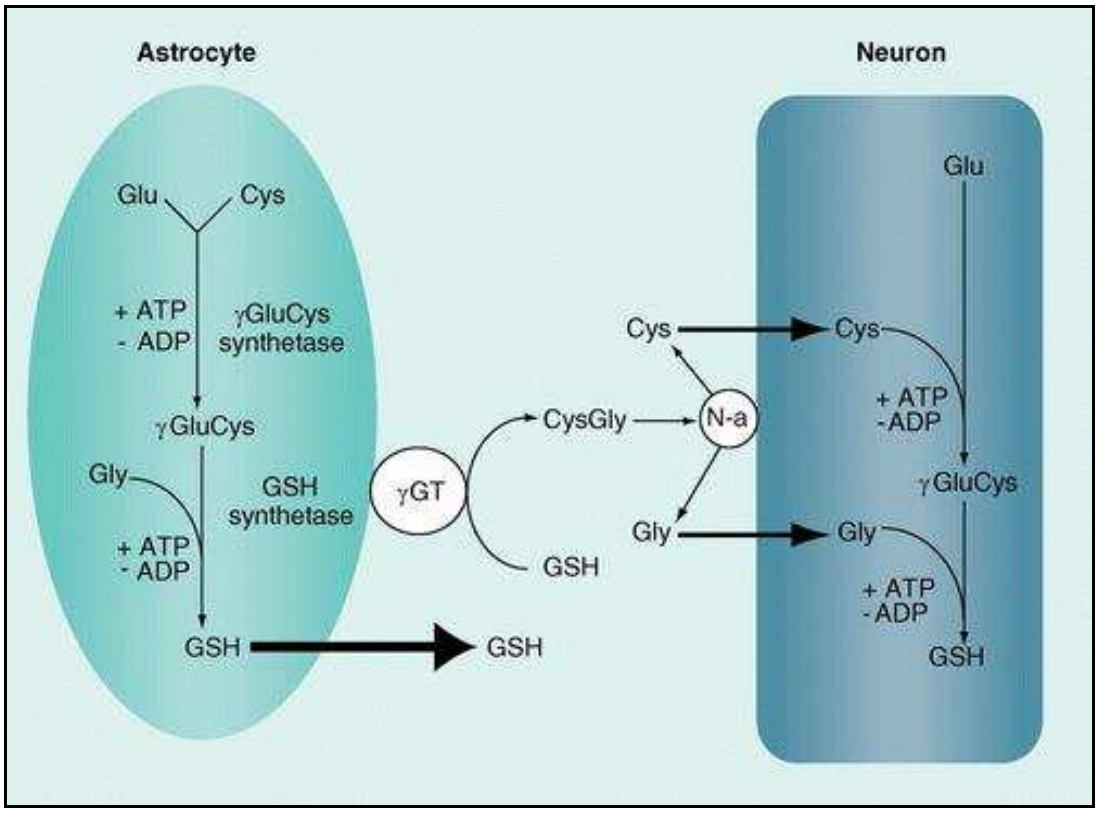

Figure 4.1 Astroglial-neuronal GSH metabolism. Glutamate cysteine ligase (also called γGluCys synthetase) uses glutamate and cysteine as substrates for the dipeptide γGluCys, which is combined with glycine by glutathione synthetase to generate glutathione (GSH). GSH is then exported from the astrocyte. Extracellular GSH serves as a substrate for the astroglial ectoenzyme γ-glutamyl transpeptidase (γGT), producing the dipeptide CysGly, which is an important exogenous precursor of neuronal GSH (This figure was adapted from Dringen, 2000; and is published in Fuller et. al., 2009).

Oxidative stress refers to an imbalance between the production of reactive oxygen species (ROS) and their metabolism by GSH and other antioxidants. Inadequate detoxification of ROS can lead to detrimental oxidation of DNA, lipids and proteins, which can cause cellular dysfunction and death. The brain appears to be particularly vulnerable to oxidative stress. Possible reasons for this include a high oxygen usage compared to the rest of the body (20% of total), a high iron content (which can increase the generation of ROS) and relatively low levels of superoxide dismutase, catalase and glutathione peroxidase (Dringen and Hirrlinger, 2000). Oxidative stress is thought to be involved in the neuronal degeneration evident in Parkinson's disease (PD) (Pearce et al., 1997) and Alzheimer's disease (AD) (Karelson et al., 2001). Another characteristic of these diseases is the presence of a chronic inflammatory reaction in the brain (DiPatre and Gelman, 1997; McGeer et al., 1989; McGeer and McGeer, 1999; Orr et al., 2002). Due to the widespread and early appearance of both inflammation and oxidative stress related modifications in PD and AD, it has been proposed that inflammation induced oxidative stress, or vice versa, might be central to the pathogenesis of such diseases (Butterfield et al., 2006; Hald and Lotharius, 2005; Markesbery, 1997; Nunomura et al., 2006). Furthermore astrocytes are thought to be key players or even instigators of these processes (Aschner, 2000; Steele and Robinson, 2011). As discussed in Chapter 2 of this thesis, astrocytes respond to inflammation by adopting a reactive metabolic phenotype. Although this reactive phenotype is likely to assist the brain to survive in instances of local acute injury, it could become counterproductive if the response is sustained and widespread. The effect of chronic inflammation on the neurosupportive function of astrocytes providing neurons with substrates for GSH synthesis is of particular interest.

This study investigated the effect of proinflammatory activation on the release and extracellular metabolism of GSH in the U373 human astrocytoma cell line. This was done by treating cells with various concentrations of the pro-inflammatory cytokines, Interleukin (IL)-1β and tumour necrosis factor (TNF)-α for 24 or 72 hours and measuring extracellular concentrations of GSH and the related thiol compounds CysGly, cysteine and homocysteine (Hcys), using the HPLC method developed in Chapter 3. Incubation times of 24 and 72 hours were selected in order to examine possible "short term" and "chronic" changes in the concentrations of thiols in the media of activated cells. The developed HPLC method is capable of quantitating total (reduced + oxidised) thiols by inclusion of a thiol reduction step before analysis, or reduced thiols only, by exclusion of the thiol reduction step. The intracellular ratio of oxidised to reduced GSH is a commonly used indicator of oxidative stress. For this study, however, the decision was made to measure total extracellular thiols only for the following reasons:

(1) Oxidised GSH (GSSG) has been reported to make up < 0.3% of total brain GSH (Cooper et al., 1980). As a result, accurate measurement of the GSSG/GSH ratio has proved difficult and GSSG is often overestimated (Senft et al., 2000). Furthermore, despite use of acidic pH, chelating agents (ethylenediaminetetraacetic acid, EDTA) and keeping samples on ice, some auto-oxidation of GSH to GSSG during sample collecting is unavoidable, thus introducing further error to GSSG/GSH estimation (McMenamin et al., 2009).

(2) The aim of this project was to study the release and extracellular processing of GSH which meant measuring GSH and related thiols in the media. Cell culture media, such as Dulbecco's Eagle Medium (DMEM), is used universally to provide appropriate conditions for cell growth. Despite attempts to mimic the in vivo

environment, however, cells in culture are exposed to higher oxygen concentrations than those found in the body and are therefore subject to oxidative stress (Rubin, 1997). In addition, the total antioxidant capacity of DMEM is lower than that of plasma and CSF (Lewinska et al., 2007) and the concentration of cystine in DMEM (2 mM) is approximately 1000 times higher than would be expected in vivo (Murphy et al., 1989). As a result, the ratio of reduced to oxidised thiols in cell culture media is probably not very useful in terms of extrapolating findings to the in vivo environment.

(3) Finally, not only GSH but also GSSG, γ-glutamylglutathione and other γ-glutamyl-containing compounds can react with γ-GT to provide substrates for neuronal GSH synthesis (Deneke and Fanburg, 1989).

Therefore, measuring total thiols in the media is not only more accurate, but also reflects the total thiol pool potentially available for neuronal uptake (in the case that neurons were present).

A similar study by Gavillet et al. (2008) has shown that GSH in the media of primary mouse astrocytes treated with IL-1β and TNF-α was increased after 48 hours. The present study differs, in that a range of concentrations of IL-1β and TNF-α were used for short term (24 hours) and long term (72 hours) treatment of cells, thus enabling identification of possible concentration and/or time dependent difference in GSH release. It was hypothesised that early stage activation (24 hours) might involve a defensive response with increased GSH release by astrocytes, as described by Gavillet et al. (2008), while extended activation (72 hours) might lead to a decrease in GSH release.

4.2 Materials and Methods

4.2.1 Materials

The U373-MG human astrocytoma cell line was kindly provided by Dr Peter Locke (The Royal Melbourne Hospital, Australia). 4-fluoro-7-aminosulfonylbenzofurazan (ABD-F) was purchased from Novachem (Collingwood, Australia). Chromatography grade methanol was from Merck (Kilsyth, Australia). All buffers were prepared with Millipore water (Kilsyth, Australia). All cell culture materials were from Invitrogen (Mulgrave, Australia). All other reagents were from Sigma-Aldrich (Castle Hill, Australia).

4.2.2 Instrumentation

A Dionex HPLC system consisting of an ASI-100 automated sample injector, a P680 solvent pump, a TCC-100 thermostatted column compartment and an RF-2000 fluorescence detector was used for all chromatographic analyses (Sydney, Australia). The system was equipped with a Luna C18(2) column (150 mm x 4.6 mm id, 3 µm) protected by a SecurityGuardC18 Cartridge (4.0 x 3.0 mm) in a SecurityGuardCartridge Holder supplied by Phenomenex (Sydney, Australia). The Chromeleon 6.8 Chromatography Data System from Dionex was used to control instruments, acquire data and quantify peak areas (Sydney, Australia).

4.2.3 Cell maintenance

U373 cells were maintained in Dulbeccos's Modified Eagle Medium (DMEM) containing 25 mM glucose, supplemented with 200 U/ml penicillin, 200 µg/ml streptomycin, 2.6 µg/ml Fungizone, 200 mM glutamine and 5% foetal bovine serum

(FBS). Cells were grown in 175 cm^2 tissue culture flasks and incubated at 37°C in 5% CO_2.

4.2.4 Treatment of U373 cells with IL-1β and TNF-α

U373 cells were harvested with a solution containing 0.05% trypsin and 0.02% EDTA in PBS, and seeded into 96-well, flat-bottom, tissue culture plates at a density of 9×10^3 cells/well. FBS concentration was reduced to 3% to minimise cell proliferation and the total volume of media in each well was 100 µl. Cells were allowed to settle for 24 hours, before the media was removed and replaced with fresh media with 1% FBS, containing various concentrations of IL-1β and TNF-α up to 10 ng/ml and incubated for 24 or 72 hours. At each time point, media was carefully removed from wells and centrifuged at 200 x g for 5 minutes at 4°C to pellet cellular debris. Following centrifugation, the supernatant was mixed with an equal volume of 1% 5-sulfosalicylic acid (SSA) containing 1 mM EDTA, centrifuged at 14,000 x g for 10 minutes at 4°C to precipitate protein, and the resulting supernatant placed in fresh tubes and stored at -80°C for later analysis of non-protein thiols.

4.2.5 Preparation of standards and calibration curve solutions

In order to quantify Cys, CysGly, HCys and GSH in media samples, several 'mixed thiol' solutions over a range of concentrations were prepared for the production of calibration curves. Stock solutions of cysteine (3,200 µM), CysGly, Hcys and GSH (all 200 µM) were prepared in water or media and then combined to give a top concentration of 800 µM for cysteine and 50 µM for each of CysGly, Hcys and GSH. This solution was then serially diluted 2-fold to make six additional solutions of

decreasing concentration. To mimic sample preparation (described in section 4.2.4) each solution was mixed with an equal volume of 1% SSA containing 1 mM EDTA, centrifuged at 14,000 x g and 4°C for 10 minutes and the supernatant removed to fresh tubes and stored at -80°C.

4.2.6 Derivatisation of GSH and related thiols with ABD-F

Samples and standards were removed from -80°C storage and allowed to thaw. Microcentrifuge vials were placed in a heating block set to 35˚C and 50 µl of sample or standard added. To reduce all disulfide bonds, 30 µl of a 1 mM solution of the reducing agent Tris(2-carboxyethyl)phosphine hydrochloride (TCEP) was added. For the derivatisation reaction, vials were incubated for 5 minutes at 35°C before the addition of 100 µl of borate buffer (0.1 M, pH 9.3, with 1 mM EDTA) and 30 µl of the derivatising agent ABD-F (1mg/ml in 0.1 M borate buffer, pH 9.3, with 1 mM EDTA). Incubation at 35°C was continued for 10 minutes, before the reaction was stopped by addition of 50 µl of 2 M hydrochloric acid (HCl). Vials were then centrifuged at 14,000 x g for 5 minutes at 4°C in order to pellet any particulates that could potentially damage the HPLC system. Supernatants were placed into fresh vials and loaded into the autosampler which was set to 8°C to minimise evaporation.

4.2.7 Chromatographic Conditions

An autosampler maintained sample temperatures at 8°C and injected 10 µl aliquots for analysis. The mobile phase used for separation of ABD-derivatised thiols was 0.1 M acetate buffer (pH 4)-methanol [86:14]. An isocratic program with a flow rate of 1 ml/min was used and column temperature was maintained at 35°C. Fluorescence detection was set to excitation at 390 nm and emission at 510 nm, with high level sensitivity.

4.2.8 Statistics

Graphpad Prism was used to produce figures and analyse data. Data presented are the mean of three independent experiments and error bars denote standard error of the mean (SEM). Significant differences were assessed by one-way ANOVA with Dunnett's post hoc tests and shown as * $p<0.05$, ** $p<0.01$ and *** $p<0.001$.

4.3 Results

4.3.1 Changes in extracellular levels of GSH and related thiols in non-activated cells

GSH, CysGly, cysteine and Hcys were measured in the cell culture media of non-activated U373 cells to determine the normal changes in thiol concentrations after 0, 24, 48 and 72 hours incubation (Figure 4.2). According to the manufacturer (Invitrogen, Mulgrave, Australia), the concentration of cystine in DMEM is 200 μM. Considering that the media was slightly diluted by the addition of FBS and antibiotics, and since the method used for determination of thiols involved the reduction of disulfides using TCEP, the concentration of cysteine in fresh, supplemented media was expected to be slightly less than 400 μM. Due to cystine being a constituent of DMEM, a calibration curve of cysteine standards in water was used to quantitate cysteine in media samples. As determined by this method, the concentration of cysteine decreased 4.4-fold from 374.9 ± 8.1 μM in fresh media to 85.1 ± 12.7 μM after 72 hours incubation with U373 cells. In contrast, no GSH, CysGly or Hcys was detected in fresh media. Calibration curves for GSH, CysGly and Hcys were therefore constructed in fresh, supplemented media. The concentration of GSH increased up to 12.6 ± 0.5 μM after 48 hours and then appeared to plateau between 48 and 72 hours. CysGly and Hcys accumulated in the media over time, reaching concentrations of 3.6 ± 0.2 μM and 3.5 ± 0.3 μM after 72 hours, respectively.

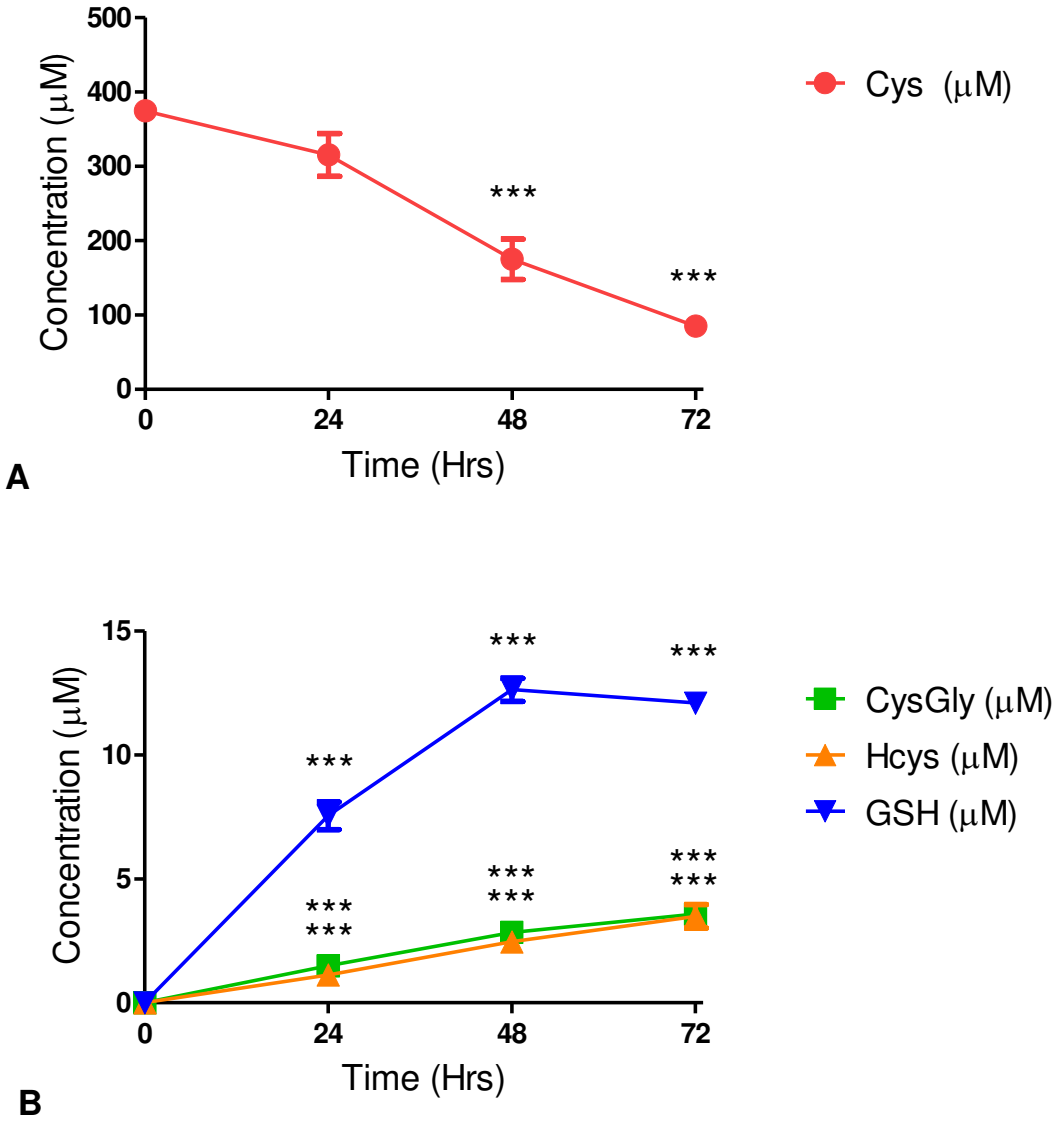

Figure 4.2 Concentrations of total Cys, CysGly, Hcys and GSH found in media collected from U373 cells after 24, 48 and 72 hours incubation. Total cysteine, CysGly, Hcys and GSH were measured in the collected incubation media by HPLC with fluorescence detection. A calibration curve of standards made in water was used to quantify cysteine and calibration curves made in media (DMEM) were used to quantify CysGly, Hcys and GSH. The 0 hrs time point shows concentrations of compounds found in the media before the addition of cells. Mean ± SEM are plotted from 3 experiments and *** $p<0.001$ designates significant difference to measurements taken at 0 hrs.

4.3.2 U373 cells were treated with IL-1β and TNF-α to investigate activation induced changes in levels of extracellular GSH and related thiols

In order to activate U373 cells to a reactive phenotype (measured by increased IL-6 release), the proinflammatory cytokines IL-1β and TNF-α were used to treat cells at concentrations of 0.01, 0.1, 1 and 10 ng/ml. Cell viability was determined by the resazurin reduction assay which measures the metabolic activity of cells. The viability of cells treated for 24 hours with 5 or 10 ng/ml IL-1β and TNF-α, decreased to 82% and 72% of control cells. After 48, 72 or 96 hours treatment, however, cells treated with different concentrations of IL-1β and TNF-α showed 100% cell viability compared to control cells, indicating that the selected concentrations of cytokines were not toxic to cells (Figure 2.3). IL-6 release, determined by an enzyme-linked immunosorbent sandwich assay (ELISA), was used as a measure of cellular activation. Extracellular IL-6 levels increased dose-dependently in cytokine treated U373 cells, with the maximal concentration of IL-6 in the media reaching 493 ± 17 pg/ml after 72 hours treatment with 10 ng/ml of IL-1β and TNF-α (Figure 2.4). Cell viability and IL-6 release results are presented in Chapter 2 of this thesis. To investigate how proinflammatory activation influences astrocytic GSH release and the conversion of GSH into metabolites, the effect of short term (24 hours) and long term (72 hours) treatment with 0.01 - 10 ng/ml IL-1β and TNF-α on the extracellular levels of GSH, Cys, CysGly and Hcys was determined. Data are presented as percentage of control so that the effect of treatment with IL-1β and TNF-α at different concentrations could effectively be compared to the non-treated cells. Data were not normalised to protein concentration since the total concentration of thiols in the media, independent of proliferation, was of interest.

4.3.3 Effect of IL-1β and TNF-α on levels of extracellular GSH

IL-1β and TNF-α treatment had no significant effect on GSH concentration in the media after 24 hours incubation (Figure 4.3). When the incubation time was extended to 72 hours, however, a dose-dependent increase in GSH was observed with 1 ng/ml IL-1β and TNF-α producing a 49% increase in GSH concentration (18 ± 0.6 μM) compared to the non-treated control (12.1 ± 0.4 μM). Cells treated with 10 ng/ml of the cytokines however showed no significant difference in GSH concentration (12.9 ± 1.6 μM) when compared to control cells (12.1 ± 0.4 μM).

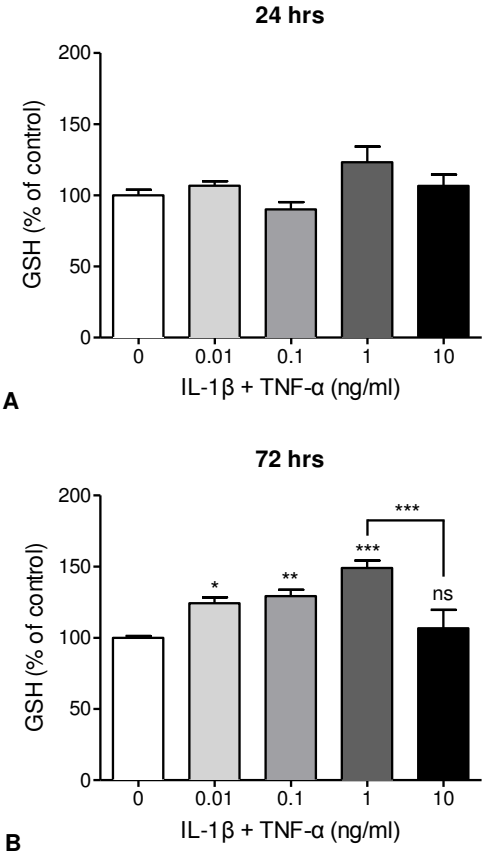

Figure 4.3 Concentration of total GSH in media collected from U373 cells after 24 and 72 hours incubation. U373 cells were treated with IL-1β and TNF-α (0.01-10 ng/ml) for either 24 (A) or 72 (B) hours. Levels of total GSH in the media were then determined by HPLC with fluorescence detection. Mean ± S.E. are plotted from 3 independent experiments and * $p<0.05$, ** $p<0.01$ or *** $p<0.001$ designates a significant difference from the non-treated control (0 ng/ml IL-1β and TNF-α).

4.3.4 Effect of IL-1β and TNF-α on extracellular CysGly levels

Most of the GSH released by astrocytes is metabolised by the astroglial ectoenzyme γ-GT to produce CysGly, an important substrate for neuronal GSH synthesis (Dringen et al., 1999b). Therefore, total CysGly levels were measured in U373 media after 24 and 72 hours treatment with IL-1β and TNF-α (Figure 4.4). No significant changes were seen after 24 hours incubation, but after 72 hours a dose-dependent decrease was observed. Treatment of U373 cells with 10 ng/ml IL-1β and TNF-α induced a 36% reduction in extracellular CysGly (2.3 ± 0.1 μM) compared to control cells (3.6 ± 0.2 μM).

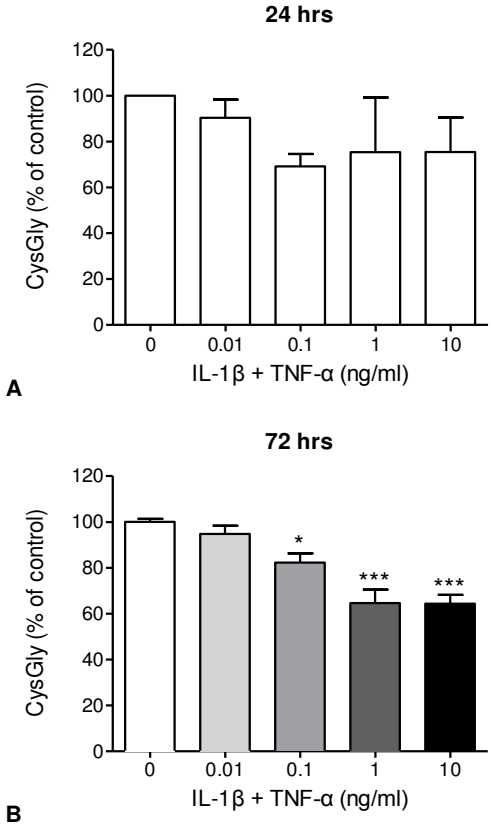

Figure 4.4 Concentration of total CysGly in media collected from U373 cells after 24 and 72 hours incubation. U373 cells were treated with IL-1β and TNF-α (0.01-10 ng/ml) for either 24 (A) or 72 (B) hours. Levels of total CysGly in the media were then determined by HPLC with fluorescence detection. Mean ± S.E. are plotted from 3 independent experiments and * $p<0.05$ or *** $p<0.001$ designates significant difference from the non-treated control (0 ng/ml IL-1β and TNF-α).

4.3.5 Effect of IL-1β and TNF-α on extracellular cysteine levels

In order to investigate whether the observed decrease in CysGly might be due to depletion of cystine in the media, total cysteine (cysteine + cystine) was determined (Figure 4.5). While there appeared to be some fluctuation in cysteine levels in response to different concentrations of IL-1β and TNF-α, there were no significant differences found when compared to non-treated control cells after 24 hours (374.9 ± 8.1 μM) or 72 hours (85.1 ± 12.7 μM) incubation. Importantly, the fact there were no significant decreases in total cysteine suggests that the observed decrease in CysGly was not due to depletion of Cys.

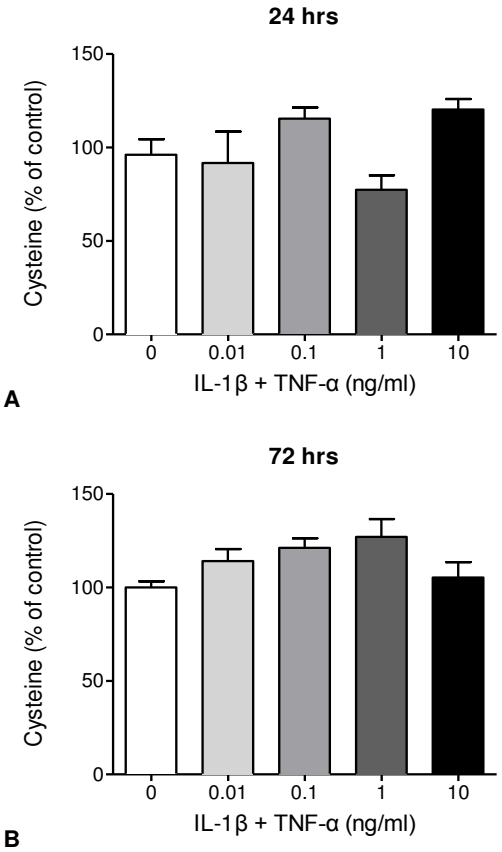

Figure 4.5 Concentration of total cysteine in media collected from U373 cells after 24 and 72 hours incubation. U373 cells were treated with IL-1β and TNF-α (0.01-10 ng/ml) for either 24 (A) or 72 (B) hours. Levels of total cysteine in the media were then determined by HPLC with fluorescence detection. Mean ± SEM are plotted from 3 independent experiments.

4.3.6 Effect of IL-1β and TNF-α on extracellular Hcys levels

Hcys is a sulphydryl-containing amino acid, whose metabolism is closely linked to that of GSH. No significant changes were observed after 24 hours incubation with IL-1β and TNF-α (Figure 4.6). After 72 hours incubation, there appeared to be a cytokine concentration-dependent increase in Hcys. The concentration of Hcys in the media of cells treated with 10 ng/ml IL-1β and TNF-α for 72 hours was significantly elevated to 189% (6.6 ± 0.9 μM) of the non-treated control (3.5 ± 0.3 μM).

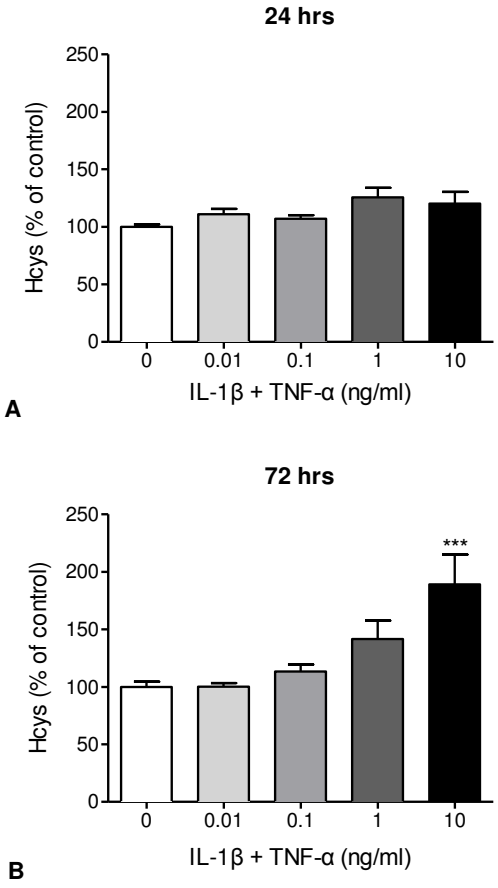

Figure 4.6 Concentration of total Hcys in media collected from U373 cells after 24 and 72 hours incubation. U373 cells were treated with IL-1β and TNF-α (0.01-10 ng/ml) for either 24 (A) or 72 (B) hours. Levels of total Hcys in the media were then determined by HPLC with fluorescence detection. Mean ± SEM are plotted from 3 independent experiments and *** $p<0.001$ designates significant difference from the non-treated control (0 ng/ml IL-1β and TNF-α).

4.4 Discussion

Neurons rely on astroglial provision of GSH and its degradation product, CysGly, which can be further processed by neurons into cysteine and glycine. Both amino acids are then taken up by neurons and used for GSH synthesis (Dringen et al., 2001; Dringen et al., 1999b). The aim of this study was to investigate whether proinflammatory activation can disrupt this partnership, by treating U373 cells with IL-1β and TNF-α and measuring extracellular levels of GSH, CysGly and cysteine by HPLC. In addition levels of the cysteine homologue Hcys, which is also released by U373 cells, were monitored.

Initial experiments involved measuring the levels of GSH, CysGly, cysteine and Hcys in the media of non-activated U373 cells after 24, 48 and 72 hours incubation. In media collected from cells incubated for 24 hours, GSH, CysGly, cysteine and Hcys were found at concentrations of 7.55 ± 0.55 μM, 1.50 ± 0.06 μM, 374.9 ± 8.1 μM and 1.14 μM ± 0.05 μM, respectively. All four compounds were easily detectable and fell within the lower and upper limits of quantitation that were determined during validation of the HPLC method in Chapter 4. When U373 cell conditioned media collected from later time points was analysed, the concentration of total cysteine decreased with increasing incubation time, as expected. Astrocytic uptake of cystine occurs predominantly via the X_c^- system which exchanges intracellular glutamate for extracellular cystine (Bender et al., 2000). Antiporters of the X_c^- system are known to be abundantly expressed in astrocytes and astrocytoma cell lines resulting in rapid accumulation of cystine from the media (Savaskan et al., 2011), as was seen here. Once inside the cell, cystine is rapidly reduced to cysteine

and either reacts with glutamate to form γ-glutamylcysteine, as the first and rate-limiting step of GSH synthesis, or is released from the cell via the alanine-serine-cysteine (ASC) system (Bannai, 1984). Although the ASC system mediates both the inward and outward flow of neutral amino acids, such as alanine, serine, glutamine and Cys, in the presence of high extracellular concentrations of amino acids other than cysteine (such as in DMEM), efflux of cysteine is stimulated (Bannai and Tateishi, 1986). Free cysteine in cell culture media has been shown to be oxidised back to cystine or to react with components of the cell culture media, such as bovine serum albumin (BSA) which is a constituent of both DMEM and FBS (Yoshiba-Suzuki et al., 2011). Since total soluble thiols were analysed in this study, the main routes of cystine disappearance were most likely to be incorporation into GSH and reaction with media components such as BSA. In contrast to levels of Cys, the concentrations of GSH, CysGly and Hcys increased over time, as was expected based on previous published data (Dringen et al., 1999b; Huang et al., 2005b).

In order to investigate the possible "short term" and "chronic" effects of IL-1β and TNF-α induced activation of U373 cells on extracellular thiol levels, conditioned media collected from cells incubated for 24 and 72 hours was analysed. No significant changes were observed for any of the examined thiols after 24 hours incubation. This suggests that 24 hours might be too early for significant changes in extracellular thiol metabolism to appear.

Treatment of U373 cells with IL-1β and TNF-α for 72 hours induced a number of significant changes in different thiol levels. For instance, a dose dependent increase

in GSH in the media was observed, with 1 ng/ml IL-1β and TNF-α treatment inducing a 49% increase compared to non-treated control cells. This result supports similar findings by Gavillet et al. (2008), who showed that 48 hours treatment with 0.25 ng/ml IL-1β and 20 ng/ml TNF-α induced a 257% increase in extracellular GSH, and that this was due to a net increase in GSH efflux. In response to 72 hours treatment with 10 ng/ml of IL-1β and TNF-α, the level of GSH found in the media was not significantly different to that found in the media of non-treated control cells and was significantly lower than in media from cells treated with 1 ng/ml. This finding is interesting since it can be theorised that neurons in a highly stressful environment (e.g. in the presence of 10 ng/ml IL-1β and TNF-α) might require more GSH substrates than those in low or non-stressful environments (0 - 1 ng/ml IL-1β and TNF-α). The reported results suggest, however, that astrocytes might reach an activation threshold point where an increased release of GSH is not able to be sustained.

As already mentioned, astrocytes release approximately 10% of their intracellular GSH content per hour (Dringen et al., 1997a). As such, extracellular GSH levels are largely dependent on intracellular GSH levels, as well as on the rate of extracellular degradation by γ-GT. Modulation of intracellular GSH was discussed in Chapter 2 of this thesis. As seen here with extracellular GSH, intracellular GSH increased in response to treatment with IL-1β and TNF-α up to a concentration of 1 ng/ml, but treatment with 10 ng/ml of the cytokines showed no significant difference in GSH level to that of non-treated control cells. Together, these findings suggest that the changes seen in extracellular GSH are directly related to changes in intracellular

GSH. This observation is supported by data demonstrating that activation of the nuclear factor erythroid-2-related factor 2 (Nrf 2)-antioxidant response element (ARE) pathway, not only upregulates the expression of enzymes involved in GSH synthesis, but also induces the expression of multidrug resistant protein (Mrp) 1 transporters, thus promoting increased GSH release (Hayashi et al., 2003; Shih et al., 2003). In addition, the activity of γ-GT can affect extracellular levels of GSH. In the event of increased γ-GT activity, elevated levels of CysGly would be expected. However, when total CysGly in the media was investigated a significant dose-dependent decrease was observed, with 10 ng/ml of the cytokines inducing a 36% reduction compared to the control. The fact that increasing cytokine concentration had opposite effects on extracellular GSH and CysGly levels up to 1 ng/ml, suggests a dose-dependent inhibition of γ-GT. Indeed Malaplate-Armand and colleagues (2000) have shown that IL-1β induces a dose-dependent reduction in γ-GT activity in U373 cells after 48 or 72 hours, but not after 24 hours. In a similar study by Ruedig and Dringen (2004), however, astrocytes isolated from neonatal Wistar rats and treated with TNF-α concentrations up to 50 ng/ml, resulted in a dose-dependent increase in specific γ-GT activity up to 48 hours, followed by a plateau effect observed between 48 and 72 hours.

No significant decreases in total cysteine levels after IL-1β and TNF-α treatment suggests that the decreases seen in GSH (in response to 10 ng/ml) and CysGly were not caused by depletion of cystine in the media. Given that primary murine astrocytes treated with IL-1β have been shown to upregulate X_c^- system antiporters in order to increase intracellular cysteine availability for GSH synthesis (Jackman et al.,

2011), a depletion of extracellular total cysteine might have been expected in response to increasing IL-1β and TNF-α concentration. However, it is has also been shown that cystine uptake via the X_c^- system is inhibited by elevated extracellular glutamate levels (Bannai and Kitamura, 1980). U373 cells in culture display a net release of glutamate (Ye and Sontheimer, 1999), which can be explained by an abundance of X_c^- system antiporters and relatively low expression of excitatory amino acid transporters that normally mediate glutamate uptake, both characteristics of astrocytoma cells lines (Ye et al., 1999). It has also been shown that TNF-α can induce enhanced release of glutamate by astrocytes (Bezzi et al., 2001) and that X_c^- system antiporters are inhibited by elevated intracellular GSH levels (Seib et al., 2011). Therefore, it is possible that increased extracellular glutamate and intracellular GSH (Chapter 2) concentrations in 72 hour cytokine-treated U373 cells, might have led to an inhibition of cystine uptake. Additionally, the ASC system releases cysteine partly replenishing total cysteine in the media (Bannai, 1984; Yoshiba-Suzuki et al., 2011). As a result, the specific dynamics of cystine and cysteine uptake and release are far too complex to be understood through simply measuring total cysteine in the media.

Whether cystine uptake and GSH release increase or decrease and whether γ-GT activity is up or down-regulated appears to be especially variable depending on incubation time, cytokine combination and perhaps cell type, for example U373 cells versus primary rat or mice astrocytes (Gavillet et al., 2008; Jackman et al., 2011; Malaplate-Armand et al., 2000; Ruedig and Dringen, 2004). Although similar studies have examined the effects of various cytokine treatments on GSH release up to 24 or 48 hours (Bélanger et al., 2011; Gavillet et al., 2008), this study appears to be the

first to investigate changes in GSH, as well as CysGly, after a longer incubation period of 72 hours. From the findings here, it is proposed that astrocytes exposed to extended, high level stress, such as chronic inflammation, are unable to maintain adequate provision of GSH substrates to neurons.

When levels of Hcys were analysed in media collected from cultures of U373 cells treated with IL-1β and TNF-α for 72 hours, a striking dose-dependent increase was observed, with 10 ng/ml of the cytokines increasing Hcys to 189% of the control. Hcys is a sulphadryl-containing, non-essential amino acid that is derived from the breakdown of dietary-obtained methionine, by a multi-step process involving removal of a methyl group. The two primary fates of Hcys are reversible methylation back to methionine, or trans-sulfuration to form cystathionine and then cysteine, the rate limiting substrate for GSH synthesis (Vitvitsky et al., 2006). Astrocytes are deficient in cystathionine β-synthase, the enzyme that catalyses the conversion of Hcys to cystathionine (Kohl and Quay, 1979; Robert et al., 2003). Furthermore, it has been shown that exogenous Hcys does not stimulate total GSH synthesis in rat astrocytes (Jin and Brennan, 2008) and that activation of catechol-O-methyltransferase (enzyme involved in methionine-Hcys conversion) in astrocytes stimulates Hcys synthesis and export (Huang et al., 2005b). Together, these findings suggest that astrocytes have a reduced capacity for trans-sulfuration and therefore must export Hcys and take up cysteine and cystine for maintenance of GSH levels. This phenomenon may explain the high levels of extracellular Hcys observed in the culture media of cytokine-treated U373 cells. Notably, it has also been shown that Hcys exported from astrocytes is harmful to adjacent neurons, through the activation

of neuronal NMDA-type glutamatergic receptors and induction of oxidative stress and apoptosis (Althausen and Paschen, 2000; Ho et al., 2002; Lipton et al., 1997).

In summary, it appears that chronic exposure (72 hours) and increasing concentration of inflammatory stimulus (IL-1β and TNF-α) can induce non-favourable changes in astrocytic thiol metabolism. Although these results can not be directly extrapolated to an in vivo situation, it is tempting to consider the possibility that chronically activated astrocytes, such as those found in AD brains, might show similar changes to those observed here. In particular, decreased provision of the neuronal GSH substrate, CysGly, and increased release of the neuro-toxic compound, Hcys, may contribute to neuronal stress and degeneration.

On examination of AD brains, increased levels of oxidatively modified proteins, lipids, sugars and DNA are found compared to age-matched, healthy control brains (Moreira et al., 2008). In addition, the activities of glutathione peroxidase and glutathione reductase are elevated (Aksenov and Markesbery, 2001) and the ratio of GSSG/GSH increased (Karelson et al., 2001), confirming the presence of oxidative stress as a prominent feature of AD. As for the dynamics of biologically important thiols in vivo, elevated levels of cysteine and Hcys have been found in plasma (McCaddon et al., 2003) and CSF samples (Popp et al., 2009) of AD patients. In fact, an elevated plasma level of Hcys, termed hyperhomocysteinemia, is now recognised as an independent risk factor for AD (Dwyer et al., 2004), as well as for other oxidative stress associated conditions like ischemic stroke (Li et al., 2003b) and cardiovascular diseases (Pietrzik, 2006). Contradicting results have been published

suggesting increased, decreased or unchanged plasma or CSF levels of GSH (Konings et al., 1999; Liu et al., 2004; McCaddon et al., 2003), whilst plasma levels of CysGly were found to be decreased in AD patients compared to controls (Hernanz et al., 2007). While further studies are needed in order to better understand the significance of altered thiol profiles to disease progression, together, the current in vitro and in vivo data suggest a role for inflammation-induced impaired thiol metabolism in the pathogenesis of AD. If indeed inflammation-induced impaired thiol metabolism is a key contributor to the neurodegeneration seen in diseases such as AD, it might be possible to affect disease outcomes by modulation of GSH levels. For example, through the use of astroglial-targeted GSH boosters (e.g. Nrf2 activators), direct supplementation with neuronal GSH substrates (e.g. CysGly and γ-GluCys) or administration of exogenous antioxidants or anti-inflammatory agents (Steele et al., 2007; Steele and Robinson, 2011).

CHAPTER 5

Effect of proinflammatory activation on energy metabolism in U373 cells

5.1 Introduction

Initial hypotheses about the functions of astrocytes were based on studies of their morphology in the brain. Although popularly considered to be most important for their structural support of neurons, Camillo Golgi (1885) speculated over a century ago that astrocytes may act as a link permitting the transfer of metabolic substrates from the blood to neurons. More recently, a range of different studies have provided support for astrocytes being the primary uptakers of glucose from the blood (Stuart et al., 2011; Tsacopoulos et al., 1988; Voutsinos-Porche et al., 2003), as well as being able to directly regulate cerebral blood flow (Filosa et al., 2004; Harder et al., 1998; Mulligan and MacVicar, 2004; Zonta et al., 2003). Protoplasmic astrocytes, the most abundant type of astrocyte in humans, generally have small cell bodies (~ 10 μM in diameter) with up to 100,000 process endings that span 100 - 200 μM and occupy separate, essentially non-overlapping territories (Oberheim et al., 2006). While some processes surround neuronal synapses, and are involved in sensing and modulating synaptic activity, others contribute to the blood-brain barrier by almost completely covering the surface of intraparenchymal capillaries with specialised endfeet (Abbott, 2002). Glucose is transported from the blood to the abluminal surface of cerebral capillaries by vascular endothelial cells and is then taken up by glucose transporter (GLUT)1, which is located on the endfeet of astrocytes (Benarroch, 2005) and thought to play a constitutive role in basal glucose uptake (Birnbaum et al., 1986). By contrast, neurons predominantly express GLUT3, which is an inducible transporter, commonly described as the "insulin-responsive" transporter (Birnbaum, 1989; Leino et al., 1998; McEwen and Reagan, 2004). The importance of astroglial mediated glucose uptake is illustrated by a clinical condition termed GLUT1-deficiency syndrome, which results in a 50% decrease in GLUT1 protein expression

in vascular endothelial cells and astrocytes, and is associated with a global decrease in cortical glucose uptake and severe neurological deficits (Brockmann, 2009; Pascual et al., 2002). Whether astrocytes distribute unmetabolised glucose directly to neurons, or another metabolic intermediate of glucose, is still of great debate (Kimelberg, 2011). In 1994, Pellerin and Magistretti defined the concept of an astrocyte-neuron lactate shuttle (ANLS), based on the coupling of glutamate-mediated synaptic activity to glucose utilisation (Pellerin and Magistretti, 1994). This concept is summarised in Figure 5.1.

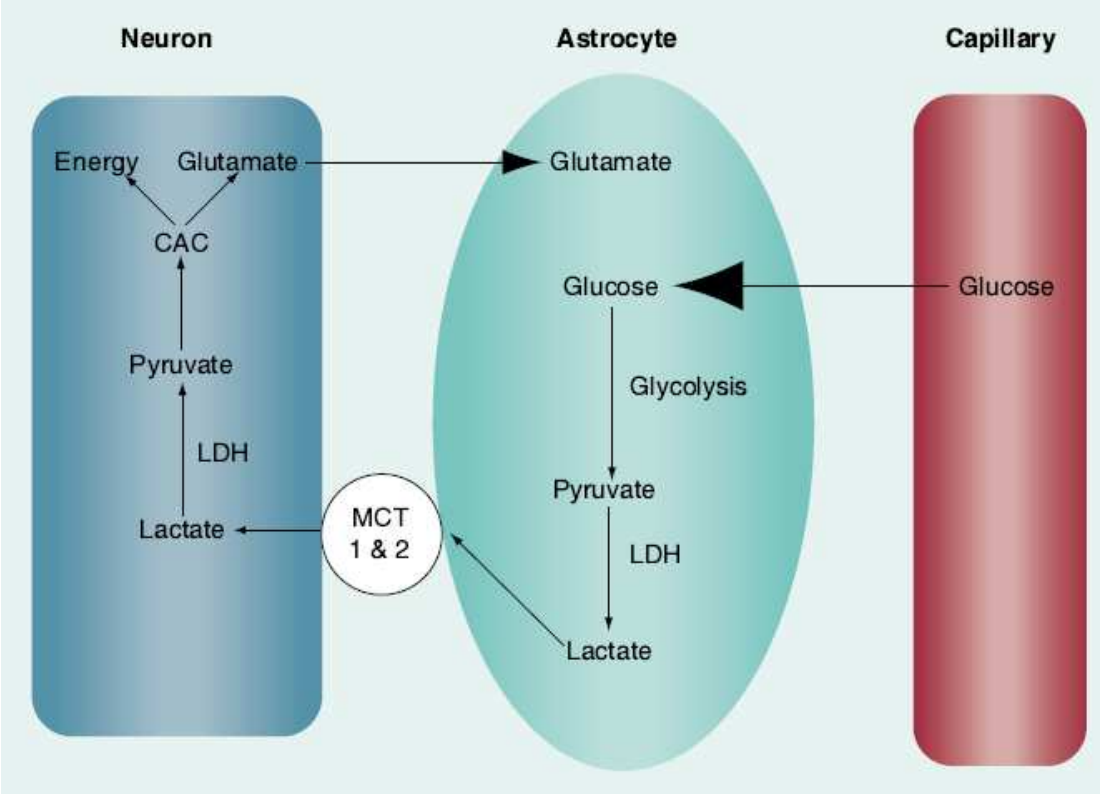

Figure 5.1 Energy metabolism in astrocytes and neurons. Glutamate uptake into the astrocyte triggers increased glucose uptake from capillaries via activation of Na+/K+-ATPase. Glucose is then processed via glycolysis, which results in lactate production. Lactate is then exchanged between astrocytes and neurons by the H+-coupled monocarboxylate transporters. Within the neuron, lactate is converted to pyruvate, which is then used in oxidative metabolism. CAC: Citric acid cycle; LDH: Lactate dehydrogenase; MCT: Monocarboxylate transporter (Fuller et al., 2009a).

The uptake of glutamate, which has been well described in astrocytes (Anderson and Swanson, 2000), is an energetically expensive process. According to the ANLS hypothesis, glutamate uptake in astrocytes results in the co-uptake of Na^+ ions, which induces Na^+/K^+-ATPase activity to pump out the extra Na^+ ions. This process requires ATP and so induces astrocytic glucose uptake predominantly via GLUT1, as well as the process of glycogenolysis. Astroglial glycolysis results in the production of lactate, owing to the conversion of pyruvate to lactate by the action of lactate dehydrogenase (LDH)-5. Lactate released by astrocytes via H^+-coupled monocarboxylate transporters (MCT)-1 and 4 is subsequently taken up by neurons via MCT2. Neurons convert lactate to pyruvate via LDH-1, allowing pyruvate to serve as a substrate for oxidative metabolism (Benarroch, 2005). There has been considerable controversy concerning whether lactate released from astrocytes is a major substrate for neuronal energy metabolism during synaptic activity (Bouzier-Sore et al., 2003). Although Simpson and colleagues (2007) support the idea that there is a flow of lactate between these two cell types, they disagree with Pellerin and Magistretti (1994) on the direction of energy flow. The neuron-astrocyte lactate shuttle hypothesis describes a similar mechanism for energy metabolism in the brain, however the main difference is that it is based on the transfer of lactate from neurons to astrocytes. Conversely, DiNuzzo and colleagues (2010) have recently suggested that any flow of lactate between astrocytes and neurons is secondary to direct neuronal glucose uptake. Despite this controversy, it is becoming increasingly accepted that synaptic activity is at least partly fuelled by the transfer of metabolites from astrocytes to neurons and that lactate is likely to be one of these metabolites (Aubert et al., 2005; Dienel and Cruz, 2008; Erlichman et al., 2008; Hyder et al., 2006).

One reason why elucidation of the pathways involved in cerebral energy metabolism is so important is that many neurodegenerative diseases, including Alzheimer's disease (AD), are characterised by perturbed glucose metabolism (Kalaria and Harik, 1989a, b). Regional changes in brain glucose uptake are readily studied using positron emission topography (PET) to monitor cerebral uptake of labeled 2-fluorodeoxy-D-glucose (FDG). FDG-PET studies have shown that impaired brain glucose uptake in AD patients precedes the appearance of pathological hallmarks, such as amyloid plaques and neurofibrillary tangles, thus implicating disrupted energy metabolism early in disease progression (Small et al., 2000). Furthermore, the fact that FDG-PET primarily reflects an astrocyte-based signal (Magistretti and Pellerin, 1996), suggests that astrocytic dysfunction might contribute to impaired energy metabolism in AD (Steele and Robinson, 2011). Another early perturbation that is observed in AD brains is the presence of a chronic inflammatory reaction (Ferretti and Cuello, 2011; McGeer et al., 1989). Therefore, it is proposed that chronic inflammatory stress might impair astrocytic glucose uptake, resulting in decreased provision of lactate or other metabolic substrates for neuronal uptake. This chapter investigates changes in extracellular glucose and lactate levels in the U373 human astrocytoma cell line, upon treatment with the proinflammatory mediators IL-1β and TNF-α for up to 96 hours.

5.2 Material and Methods

5.2.1 Materials

The U373-MG human astrocytoma cell line was kindly provided by Dr Peter Locke (The Royal Melbourne Hospital, Australia). All cell culture materials were from Invitrogen (Mulgrave, Australia). All other reagents were from Sigma-Aldrich (Castle Hill, Australia).

5.2.2 Cell maintenance

Cells were maintained in Dulbeccos's Modified Eagle Medium (DMEM) containing 25 mM glucose, supplemented with 200 U/ml penicillin, 200 µg/ml streptomycin, 2.6 µg/ml Fungizone, 200 mM glutamine and 5% foetal bovine serum (FBS). Cells were grown in 175 cm^2 tissue culture flasks and incubated at 37°C in 5% CO_2.

5.2.3 Treatment of U373 cells with IL-1β and TNF-α

U373 cells were harvested with a solution containing 0.05% trypsin and 0.02% EDTA in PBS and seeded into 96-well, flat-bottom, tissue culture plates at a density of $9x10^3$ cells/well. FBS concentration was reduced to 3% to minimise proliferation and the total volume of media in each well was 100 µl. Cells were allowed to settle for 24 hours before the media was replaced with fresh media containing 1% FBS and various concentrations of IL-1β and TNF-α (both at 0.01 to 10 ng/ml) and incubated for up to 96 hours. After 24, 48, 72 and 96 hours incubation, media was carefully removed from wells and centrifuged at 200 x g for 10 mins at 4°C to pellet cellular debris. Supernatant was transferred to fresh 96 well plates and stored at -80°C. On

thawing, supernatants were diluted with distilled water by a factor of 10 and samples assayed as below.

5.2.4 Measurement of glucose in media

Samples were assayed for glucose concentration by a modified version of the hexokinase/glucose-6-phosphate dehydrogenase (HK/G6PD) based assay used by Peterson and Young (1968). In a 96 well plate, 20 µl samples and glucose standards were mixed with 180 µl of a reaction mixture consisting of 1 U/ml HK/G6PD, 6 mM ATP and 2 mM $NADP^+$ in a 0.3 M triethanolamine solution containing 3 mM $MgSO_4$. Plates were incubated for 2 hours and then absorbance measured at 340 nm in a POLARstar Omega microplate reader (BMG Labtech, Mornington, Australia). The change in absorbance of NADPH is linearly proportional to the concentration of glucose in samples, determined by standard curve.

5.2.5 Measurement of lactate in media

Samples were assayed for lactate concentration by a modified version of the lactate dehydrogenase based assay used by Allman et al. (2004). In a 96 well plate, 20 µl samples and lactate standards were mixed with 180 µl of a reaction mixture consisting of 7 U/ml lactate dehydrogenase and 6 mM NAD^+ in a 163.4 mM hydrazine-62.2 mM glycine buffer. Plates were incubated for 2 hours and then absorbance measured at 340 nm in a POLARstar Omega microplate reader (BMG Labtech, Mornington, Australia). The change in absorbance of NADH is linearly proportional to the concentration of lactate in samples, determined by standard curve.

5.2.6 Statistics

Graphpad Prism was used to produce figures and analyse data. Data presented are the mean of three independent experiments and error bars denote standard error of the mean (SEM). Significant differences were assessed by one-way ANOVA with Dunnett's post hoc tests and shown as * = $p < 0.05$, ** = $p < 0.01$ and *** = $p < 0.001$.

5.3 Results

5.3.1 Effect of IL-1β and TNF-α treatment of U373 cells on extracellular glucose levels

Glucose consumption in differentially activated U373 cells was investigated by determining the concentration of glucose remaining in the media after 24, 48, 72 or 96 hours treatment with 0.01 – 10 ng/ml IL-1β and TNF-α (Figure 5.2). The initial concentration of glucose in the media (DMEM) was 25 mM, as stated by the manufacturer, and this concentration was confirmed by experiments using a standard curve. The amount of remaining glucose quantitated in the media post-incubation was subtracted from the original concentration (25 mM). Thus the data shown here represents the total amount of glucose consumed by the cells over a defined time period. There was no significant difference in the amount of glucose consumed by cells in response to 24 or 48 hours treatment with 0.01 – 10 ng/ml IL-1β and TNF-α. Extended treatment of cells induced an initial dose-dependent increase in glucose consumption up to 7.83 ± 0.66 mM (72 hours) and 10.72 ± 0.66 mM (96 hours) by 0.1 ng/ml IL-1β and TNF-α. In contrast, cells treated with higher concentrations of IL-1β and TNF-α (5 – 10 ng/ml) showed no significant difference in glucose consumption compared to control cells.

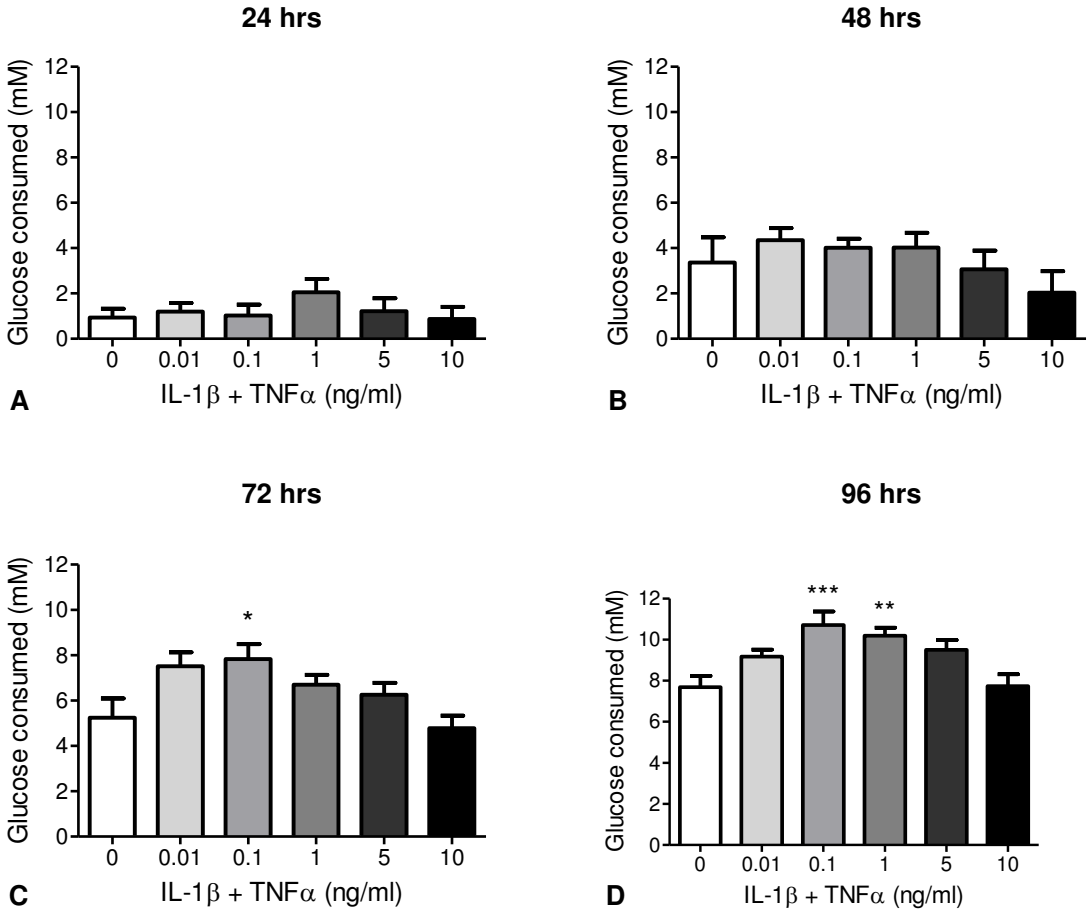

Figure 5.2 Glucose consumption by U373 cells treated with IL-1β and TNF-α. U373 cells were treated with 0.01-10 ng/ml IL-1β and TNF-α for either 24 (A), 48 (B), 72 (C) or 96 (D) hours. Concentration of glucose in the media was determined using a colorimetric, hexokinase and glucose-6-phosphate dehydrogenase-based assay. Data are expressed as the amount of glucose consumed, calculated by subtracting the remaining glucose concentration determined in the media from the initial glucose concentration of 25 mM. Data are represented by the mean ± SEM of 3 experiments and * $p<0.05$, ** $p<0.01$ or *** $p<0.001$ designates a significant difference to the non-treated control (0 ng/ml IL-1β and TNF-α).

5.3.2 Effect of IL-1β and TNF-α treatment of U373 cells on extracellular lactate levels

In order to better understand the effect of proinflammatory activation on energy metabolism in astrocytes, lactate was measured in the media of U373 cells treated with 0.01 – 10 ng/ml IL-1β and TNF-α for 24, 48, 72 and 96 hours (Figure 5.3). Lactate is not a constituent of DMEM but accumulated in the media over time, reaching a maximum of 18.02 ± 2.32 mM after 96 hours incubation in non-treated control cells. Treatment of U373 cells with 10 ng/ml IL-1β and TNF-α induced a significant decrease in lactate release (71% of control) after only 24 hours of incubation. As incubation time increased a dose-dependent decrease in lactate release was observed with a 96 hour treatment of U373 cells with 10 ng/ml IL-1β and TNf-α inducing a decrease in lactate release corresponding to 12% of that released by control cells.

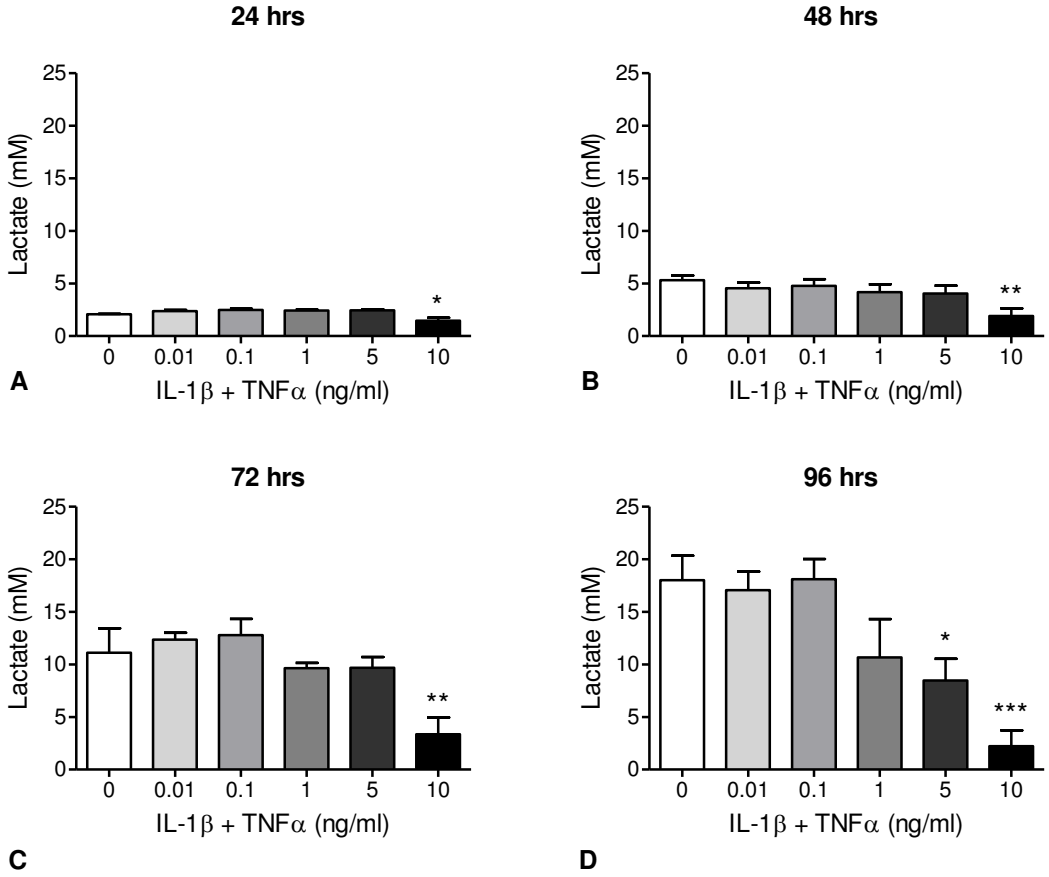

Figure 5.3 Lactate release byU373 cells treated with IL-1β and TNF-α. U373 cells were treated with 0.01 - 10 ng/ml IL-1β and TNF-α for 24 (A), 48 (B), 72 (C) or 96 (D) hours. The concentration of lactate in the media was determined using a colorimetric, lactate dehydrogenase-based assay. Data are expressed as lactate concentration in cell media, which was calculated using a calibration curve. Data are represented by the mean ± SEM of 3 experiments and * $p<0.05$, ** $p<0.01$ or *** $p<0.001$ designates a significant difference to the non-treated control (0 ng/ml IL-1β and TNF-α).

5.3.3 Ratio of lactate release to glucose consumption by U373 cells treated with IL-1β and TNF-α

Due to the knowledge that glycolytic processing of one glucose molecule generates two lactate molecules (Garrett and Grisham, 2005), it was assumed that the ratio of lactate release to glucose consumption would be approximately 2:1. Data from figures 5.2 and 5.3 were used to investigate the effect of treatment with 0.01 – 10 ng/ml IL-1β and TNF-α on the lactate release-glucose consumption ratio of U373 cells (Table 5.1). While no significant differences were observed at early time points, a significant decrease in the ratio of lactate release to glucose consumption was observed in cells treated with > 0.01 ng/ml IL-1β and TNF-α for 72 hours and > 1 ng/ml IL-1β and TNF-α for 96 hours.

Table 5.1 Ratios of lactate release to glucose consumption for U373 cells treated with IL-1β and TNF-α.

IL-1β and TNF-α (ng/ml)	Treatment time (hrs)			
	24	48	72	96
0	1.27 ± 0.28	1.44 ± 0.40	2.78 ± 0.71	2.30 ± 0.23
0.01	1.99 ± 0.53	1.09 ± 0.13	1.70 ± 0.2 ***	1.86 ± 0.17
0.1	2.57 ± 0.80	1.17 ± 0.12	1.64 ± 0.25 ***	1.73 ± 0.23
1	2.50 ± 0.84	1.12 ± 0.22	1.40 ± 0.11 ***	1.29 ± 0.35 *
5	1.10 ± 0.25	1.54 ± 0.38	1.57 ± 0.24 ***	0.85 ± 0.19 ***
10	1.06 ± 0.30	1.01 ± 0.18	1.28 ± 0.23 ***	0.86 ± 0.19 *

Values were calculated by dividing total lactate release by total glucose consumption and * $p<0.05$ or *** $p<0.001$ designates a significant difference to the non-treated control (0 ng/ml IL-1β and TNF-α).

5.4 Discussion

This study investigated the effect of proinflammatory activation on astrocytic energy metabolism by measuring changes in glucose consumption and lactate release in IL-1β and TNF-α treated U373 cells. Described as the "Warburg effect", tumour cells are known to maintain elevated rates of glycolysis and release large quantities of lactate, even in the presence of oxygen (Warburg et al., 1927). Coinciding with this, non-activated U373 cells showed significant glucose consumption (7.68 ± 0.56 mM) and lactate release (18.02 ± 2.32 mM) after 96 hours. These values are in good agreement with those reported elsewhere (Bouzier et al., 1998a; Bouzier et al., 1998b; Lu et al., 2002). A time-dependent increase in glucose consumption by U373 cells was observed up to 96 hours, independent of whether or not cells were treated with IL-1β and TNF-α. Although no significant changes were observed between treatment groups after 24 or 48 hours, there was a trend towards a biphasic response in glucose consumption, which became statistically significant after 72 and 96 hours. Cells treated with 0.1 ng/ml IL-1β and TNF-α for 96 hours showed an increased consumption of glucose relative to 140% of non-treated control cells. This elevation in glucose consumption disappeared in response to higher concentrations of 5 and 10 ng/ml IL-1β and TNF-α. In addition, a striking, dose-dependent decrease in lactate accumulation in the media was observed, with a reduction of 88% in cells treated with 10 ng/ml IL-1β and TNF-α for 96 hours, compared to non-treated control cells. Moreover, when the ratio of lactate release to glucose consumption was calculated, a decrease from 2.30 molecules of lactate released per molecule of glucose consumed to 0.86 occurred in response to 96 hours treatment with IL-1β and TNF-α. Since glycolytic processing of 1 mol of glucose results in 2 mol of lactate (Garrett and Grisham, 2005), the results in Table 5.1 suggest that extended

incubation of non-activated cells led to excess lactate accumulation in the media by mechanisms other than glycolysis. For example, lactate can be produced in astrocytes from precursors other than glucose, such as cellular lipids, fatty acids, ketone bodies and proteins or amino acids present in the media (Gibson, 2007). In addition, astrocytes have a high glycogen content which can be accessed as an alternative to glucose uptake (Suh et al., 2007). When U373 cells were treated with IL-1β and TNF-α however, a dose-dependent decrease in the ratio of lactate release to glucose consumption was observed, with a 63% reduction caused by 10 ng/ml. This observation suggests that chronically activated astrocytes not only take up less glucose but they also direct less glucose into lactate production. Fates of astrocytic consumed glucose that is not glycolytically converted to lactate, include oxidative phosphorylation of pyruvate, glycogen synthesis and entry into the pentose phosphate pathway (PPP) to generate NADPH required to recycle oxidised glutathione (Prebil et al., 2011). A study by Gavillet and colleagues (2008) showed that an increase in the latter pathway, appeared to be the most quantitatively important deviation in inflammation-stressed astrocytes. Furthermore, this explanation is supported by the observation in Chapter 2 that intracellular glutathione was elevated in cells treated with 1 ng/ml IL-1β and TNF-α (Figure 2.5).

Therefore, from the findings in this study it can be postulated that chronic inflammation is able to impair energy metabolism in astrocytes. These findings are somewhat in agreement with similar studies by Gavillet et al. (2008) and Liddel et al. (2009a). In the prior study, the effect of individual and co-application of 0.25 ng/ml IL-1β and 20 ng/ml TNF-α for 48 hours was determined for glucose uptake and lactate release, among other metabolic functions, in primary astrocyte

cultures from mice. As was shown here, a 48 hour treatment with IL-1β and TNF-α showed a slight, but not statistically significant, reduction in extracellular lactate (85%) compared to non-treated control cells. When glucose uptake was studied in the same cells by the [3H]-2-deoxyglucose method, glucose utilisation was found to increase to 337% of control. Interestingly, when these experiments were repeated in the presence of 200 µM glutamate (in order to mimic neuronal synaptic activity), IL-1β and TNF-α treatment not only induced a 43% reduction in lactate release but also a 44% reduction in glucose consumption. Although differences in the concentrations of IL-1β and TNF-α used here and by Gavillet et al. make it difficult to compare results, a possible explanation for the findings here being better reflected by the findings of Gavillet et al. when glutamate was added to cells, is that a characteristic of astroglioma cells is that they are capable of releasing large amounts of glutamate into the media. Ye and Sontheimer (1999) have shown that glutamate release by cultured STTG-1 astroglioma cells resulted in an extracellular glutamate concentration of almost 400 µM within 12 hours.

In a study by Liddell and colleagues (2009a), cultured primary rat astrocytes were incubated for two hours with 50 µM hydrogen peroxide (H_2O_2) in the presence of [U-^{13}C]glucose. Rates of glucose consumption and lactate release were found to be reduced by 20% and 39%, respectively. Furthermore, when extracellular levels of glucose and lactate were determined and compared to non-treated control cells, glucose was found to be significantly increased (135%), while lactate was significantly decreased (83%). These studies, together with the present study, suggest that although short term inflammatory activation might slightly modulate energy metabolism, the induction of cellular oxidative stress, either through chronic

exposure of cytokines, co-application of cytokines and glutamate or direct application of reactive oxygen species (ROS), such as H_2O_2, is required in order to induce significant impairment of astrocytic energy metabolism (Gavillet et al., 2008; Liddell et al., 2009b).

Although the mechanism behind cytokine-induced altered glucose consumption was not investigated here, a study by Vega et al. (2002) showed that IL-1β and TNF-α induced upregulation of glucose utilisation was dependent on activation of the phosphoinositide 3-kinase (PI3) pathway. In addition, activation of the ERK pathway, was also involved in IL-1β mediated modulation of glucose utilisation. While both cytokines were shown to increase glucose utilisation independently over 24 hours, combined treatment with the cytokines elicited a strong synergistic effect. Interestingly, IL-1β and TNF-α induced upregulation of glucose utilisation was completely inhibited when cells were pre-treated with oubain, a specific inhibitor of the Na^+/K^+ ATPase (Vega et al., 2002). Since Na^+/K^+ ATPase activity is known to be sensitive to oxidative stress, it is possible that the reduction in glucose consumption that was observed in cells treated with high levels of cytokines (5-10 ng/ml) compared to moderate levels of cytokines (0.1 – 1 ng/ml) might involve oxidative stress mediated inhibition of the Na^+/K^+ ATPase. Furthermore, studies by Muneer et al. (2011a; 2011b) into the effects of the pro-oxidants methamphetamine and ethanol on cultured astrocytes reported concentration and time-dependent decreases in glucose uptake and associated decreases in GLUT1 expression. In addition, Liddell et al. (2009a) demonstrated that decreased glucose consumption and lactate release by rat primary astrocytes treated with H_2O_2 was accompanied by a 90% inhibition of

the glycolytic enzyme, glyceraldehyde phosphate dehydrogenase, after only 90 minutes.

Taken together, the findings from this study along with the other studies mentioned, suggest that sustained low level inflammation may increase glucose uptake by astrocytes, via a mechanism involving activation of the PI3 pathway (Bélanger et al., 2011; Gavillet et al., 2008; Yu et al., 1993). Moreover, it is likely that excess glucose was processed by the PPP, resulting in increased NADPH-dependent regeneration of glutathione. In contrast, sustained high level inflammation may lead to an imbalance between ROS generation and detoxification, thus inducing cellular oxidative stress and subsequent inhibition of a range of ROS-sensitive metabolic enzymes and transporters leading to impaired energy metabolism (Abdul Muneer et al., 2011a; Abdul Muneer et al., 2011b; Liddell et al., 2009a). Although findings from the present study can not be directly extrapolated to the brain, they provide support for the hypothesis that astrocytes contribute to the energy impairment observed in AD (Gavillet et al., 2008; Slosman et al., 2001; Steele and Robinson, 2011). Considering that astrocytes and neurons are metabolically coupled, it is conceivable that inflammation-induced impairment of astrocytic energy metabolism would also be harmful to neurons. If neurons do indeed rely on delivery of lactate (or other energy substrates) by astrocytes as is widely supported (Bittner et al., 2010; Ivanov et al., 2011; Magistretti, 2006; Pellerin, 2003; Suzuki et al., 2011), then impaired astrocytic energy metabolism might in turn lead to "energy-starved" neurons, thus increasing vulnerability to neurodegeneration. In addition, as described by the ANLS hypothesis, glutamate uptake by astrocytes is an energetically costly process (Pellerin and Magistretti, 1994). It has been shown that energy failure in astrocytes (caused by

glucose deprivation or inhibition of glycolysis) induces reversal of Na^+-dependent glutamate uptake, resulting in neurotoxic levels of extracellular glutamate (Huang et al., 1993; Kauppinen et al., 1988; Longuemare and Swanson, 1995). Furthermore, abnormal glutamate metabolism has also been implicated in the pathogenesis of AD (Lauderback et al., 2001; Robinson, 2000, 2001; Scott et al., 2002). Therefore, the emergence of a dysfunctional reactive astrocytic phenotype in response to chronic inflammation provides a viable link between a number of the key pathological perturbations observed in AD. The extent to which activation-induced changes in astrocytic function observed in vitro mimic changes in reactive astrocytes in vivo remains to be determined.

CHAPTER 6

Cytoprotective properties of traditional Chinese medicinal herbal extracts in hydrogen peroxide challenged U373 astrocytoma cells

6.1 Introduction

For millenia, herbal medicines consisting mostly of the leaves, stems, roots and seeds of plants have been used in traditional Chinese medicine (TCM) for the treatment of specific ailments, to maintain and restore body balance and to increase longevity (Suk, 2005). Many of the drugs available in Western medicine have been directly isolated from plants or are synthetic molecules based upon the molecular skeletons of natural products. For example, galantamine is an anticholinesterase drug licensed in Australia, Europe, United Kingdom, United States and in some Asian countries for the treatment of mild to moderate Alzheimer's disease (AD) (Heinrich and Lee Teoh, 2004). It can be isolated from several plants including the red spider lily, Lycoris radiata, which is used in TCM to promote memory and cognitive function, as well as produced synthetically (Howes and Houghton, 2003; Suk, 2005). Galantamine, however, like all of the drugs currently licensed for the treatment of AD, only treats the symptoms of AD and is not a cure (Hull et al., 2006). In fact relief of symptoms is often the only achievable goal in the treatment of many chronic diseases. While Western medicine mainly focuses on the identification and isolation of active constituents from plants that interact with single therapeutic targets, TCM aims to reverse the underlying "imbalance" between the body and the environment that is thought to cause disease (Cheng, 2000). This often involves the use of complex mixtures of herbs containing numerous chemical components with diverse biological and pharmacological actions. It is believed that different compounds not only act synergistically with other compounds from the same plant, but also may enhance the activity or counteract the toxicity of compounds from other plants (Howes and Houghton, 2003). A recent study investigating the antioxidant properties of one widely used herb in TCM, Polygonum multiflorum, found that the radical scavenging

abilities of two of its main active components, emodin and quercetin, were lower than crude leaf, stem and root extracts of the herb (Lin et al., 2010). Furthermore, while studies with traditional herbal medicines such as Fuzhisan (Bi et al., 2011) and herbal extracts such as Panax ginseng (Lee et al., 2008) have shown success in slowing cognitive decline; results of clinical trials with isolated or synthetically produced "active" compounds, such as curcumin from Curcuma longa (Hamaguchi et al., 2011) and huperzine A from Huperzia serrata (Rafii et al., 2011) have been disappointing. These findings may be explained by the fact the AD is a complex, multifactorial disease, which starts years or decades before the onset of symptoms. As such, the purported success of herbal remedies may be due to their inherent multi-compound, multi-targeting nature.

Oxidative stress has long been implicated in the pathogenesis of AD (Markesbery, 1997) and is also believed to play a role in ageing, which is the key risk factor for AD (Finkel and Holbrook, 2000). Since many of the constituents of herbal extracts are known antioxidants, it is believed that restoring oxidative balance may be at least one of the underlying mechanisms by which medicinal herbs can protect against ageing and cognitive decline (Ho et al., 2010). Astrocytes are important determinants of oxidative stress in the brain due to their roles in storage of glutathione (GSH) and delivery of substrates for neuronal GSH synthesis; and their ability to produce a wide variety of pro and anti-inflammatory mediators and reactive oxygen species (ROS) (Dringen et al., 2000). Although astrocytes are generally regarded as being much better than neurons at defending themselves against oxidative stress (Desagher et al., 1996; Dringen et al., 1999a), it has been shown that prolonged inflammatory activation can induce a state of oxidative stress (Gavillet et al., 2008; Malaplate-

Armand et al., 2000). Furthermore, as discussed in Chapters 4 and 5, induction of oxidative stress in astrocytes might also be detrimental to neurons and therefore present a potential therapeutic target for the prevention of inflammation or oxidative stress related neurodegeneration.

The aim of this study was to investigate thirteen TCM herbal extracts, shown in Table 6.1, for their ability to protect U373 human astrocytoma cells from hydrogen peroxide induced cell death. Herbs were selected based on their history of use as anti-ageing and cognitive-enhancing agents or their inclusion in tonic herbal remedies. Tonic herbs are also called "adaptogens" and have been described as *"remarkable natural substances that help the body adapt to stress, support normal* metabolic functio*ns, and restore balance. They increase the body's resistance to physiological, biological, emotional and chronic stress"* (Winston and Maimes, 2007). In order to determine the contribution of antioxidant activity to the cytoprotective ability of extracts, total phenol content (Singleton and Rossi, 1965; Waterhouse, 2002), 2,2-diphenyl-1-picrylhydrazyl (DPPH) radical scavenging capacity (Blois, 1958; Molyneux, 2004) and oxygen radical absorbance capacity (ORAC) (Ganske and Dell, 2006) were also examined.

Table 6.1 Traditional Chinese medicinal herbs.

Scientific name	Family name	Chinese name	Other names	Part used	Traditional uses
Astragalus membranaceus	Leguminosae	Huang qi	Astragalus root, Milk Vetch root	root	Liver tonic to help protect body against physical, mental and emotional stress; enhance immune system; prevent and treat exhaustion (Hou and Jin, 2005)
Codonopsis pilosula	Campanulaceae	dang shen	Poor man's ginsgeng	root	Treatment of hypertension; used to increase red and white blood cell count and boost the immune system (Wang et al., 1996)
Eucommia ulmoides	Eucommiaceae	Du zhong	Chinese rubber tree	bark	Kidney, liver and blood tonic; promote longevity; prevent miscarriage (Hou and Jin, 2005)
Ganoderma lucidum	Polyporaceae	ling zhi	Reishi mushroom	mushroom	Treatment of forgetfulness; cough; breathing difficulty; insomnia; indigestion and general weakness (Li et al., 2007)
Glycyrrhiza glabra	Leguminosae	Gan Cao	Liquorice	root	Used as an expectorant and laxative; treatment of hepatitis, sore throat and muscle spasms (Davis and Morris, 1991)
Gynostemma pentaphyllum	Cucurbitaceae	Jiaogulan	Southern ginseng	herb	Boost resistance to stress, trauma, anxiety and fatigue; anti-ageing; regulate blood pressure; lower cholesterol (Winston and Maimes, 2007)
Lycium barbarum	Solanaceae	gou qi zi	Wolf berry, goji	fruit	Liver and kidney tonic; promote vision and anti-ageing (Hou and Jin, 2005)
Panax ginseng	Araliaceae	Ren shen	Gingseng root	root	Tonic to enhance stamina and capacity to cope with fatigue and physical stress (Gillis, 1997)
Polygonum multiflorum	Polygonaceae	He shou wu	Fo-ti root	root	Blood, liver and kidney tonic; promote longevity; laxative and detoxification (Hou and Jin, 2005)
Rehmannia glutinosa	Scrophulariaceae	Sheng Di huang	Chinese foxglove	root	Blood and kidney tonic; treat tinnitus and hearing loss (Zhang et al., 2008)
Rhodiola rosea	Crassulaceae	hong jing tian	Rose root	root	Increase resistance to chemical, biological and physical stressors; enhance mental functioning; (Kelly, 2001)
Schizandra chinesis	Magnoliaceae	Wu wei zi	Schizandra berries	fruit	Kidney tonic; astringe the lungs; treat sweating and diarrhea; calm the heart and soothe the mind (Quan, 2000)
Polygonum cuspidatum	Polygonaceae	Hu Zhang	Japanese knotweed	root	Treatment of arthritis; urinary disease; dermatitis and hyperlipidemia (Han et al., 2011)

6.2 Materials and Methods

6.2.1 Materials

The U373-MG human astrocytoma cell line was kindly provided by Dr Peter Locke (The Royal Melbourne Hospital, Australia). All cell culture materials were from Invitrogen (Mulgrave, Australia). Solvents (AR grade), (2,2-diphenyl-1-picryl hydrazyl (DPPH), gallic acid, fluorescein, 2,2'azobis(2-amidinopropane) dihydrochloride (AAPH), Folin-Ciocalteu reagent, sodium carbonate and resazurin were from Sigma-Aldrich (Castle Hill, Australia). Elga Pure Lab Prima 7 water purification unit was the source of water (>18.2 M) (Scoresby, Australia).

6.2.2 Plant extracts

Commercial dried extracts of Astragalus membranaceus root, Codonopsis pilosula root, Eucommia ulmoides bark, Ganoderma lucidum mushroom, Glycyrrhiza glabra root, Gynostemma pentaphyllum herb, Lycium barbarum fruit, Panax ginseng root, Polygonum multiflorum root, Rehmannia glutinosa root, Rhodiola rosea root, Schisandra chinensis fruit and Polygonum cuspidatum root (50% trans-resveratrol) were provided by LIPA Pharmaceuticals (Minto, Australia).

6.2.3 Extraction of samples

Sample extraction involved sonication of 5 g of powdered dried extract in approximately 50 ml 80% aqueous methanol for 2 x 30 minutes with a 15 minute cooling interval between sonications. The mixture was centrifuged at 4000 g for 5 minutes and the supernatant was filtered using a polyvinylidene fluoride (PVDF) syringe filter. The particle free filtrate was concentrated to dryness in a rotary

evaporator at 60°C under vacuum. The residue was further freeze dried for 12 hours to remove any residual water and stored at 4°C.

6.2.4 Non-cell based antioxidant assays

Folin-Ciocalteau Reagent assay

The methods of Singleton et al. (1965) and Waterhouse et al. (2002), using gallic acid as the reference standard, were followed for the determination of total phenols by the Folin-Ciocalteau reagent (FCR) assay. All reagents were prepared in 80% aqueous methanol. The gallic acid standard curve was made by diluting a gallic acid stock (3 mM) to form 0.3, 0.6, 0.9 and 1.5 mM working standards. Samples were prepared by dissolving 1 mg of the extract in 10 ml. Serial dilutions (1 in 10 and 1 in 100) of the stock sample solution were also prepared. An 80% aqueous methanol solution was used as the reagent blank. 140 µl of water, 10 µl of Folin-Ciocalteau reagent, 20 µl of sample, standard or blank and 30 µl of sodium carbonate (0.7 M) were added to wells of a 96 well plate. The plate was vortexed briefly and incubated for 30 minutes in the dark prior to measurement of absorbance at 765 nm (POLARstar OPTIMA; BMG). The total phenol content for each herb is reported as the gallic acid equivalent.

DPPH radical scavenging assay

A method adapted from Blois et al. (1958) and Molyneux et al. (2004) was used to estimate the DPPH radical scavenging capacity of the thirteen extracts compared to a gallic acid standard. All reagents were prepared in 80% aqueous methanol. The gallic acid standard curve was made by diluting a gallic acid stock (6 mM) to form 0.3, 0.6,

1.5 and 3 mM working standards. Samples were prepared by dissolving 100 mg of the extract in 10 ml. Serial dilutions (1 in 10 and 1 in 100) of the stock sample solution were also prepared. An 80% aqueous methanol solution was used as the reagent blank. 180 µl of the DPPH reagent (250 µM) was applied to each well of a 96 well plate. In triplicate, 20 µl of each working standard, sample or blank was added to the DPPH reagent to make a total volume of 200 µl in each well. To correct for sample absorbance (i.e. absorbance not due to the DPPH), sample blanks were made in triplicate by adding 180 µl of 80% aqueous methanol to the well and adding 20 µl of sample. The plate was shaken at 700 rpm for 30 minutes in the dark prior to measuring absorbance at 515 nm (POLARstar OPTIMA; BMG). The sample antioxidant scavenging capacity is reported as the gallic acid equivalent.

Oxygen Radical Absorbance Capacity assay

The oxygen radical absorbance capacity (ORAC) assay was used to measure the ability of the 13 extracts to protect fluorescein from degradation by peroxyl radicals. A modified version of the method described in the BMG LABTECH application note was used (http://www.bmglabtech.com). All reagents were prepared in pH 7.4 phosphate buffer (10 mM). A gallic acid standard curve was made by diluting a gallic acid stock (3 mM) to form 0.3, 0.6, 0.9 and 1.5 mM working standards. Samples were prepared by dissolving 2 mg of extract in 10 ml of 80% aqueous methanol. An 80% aqueous methanol solution was used as the reagent blank. 150 µl of fluorescein (10 nM) and 25 µl of either gallic acid standard, sample or blank were mixed in wells of a 96 well plate. Plates were vortexed briefly and incubated at 37ºC for 30 minutes. Following incubation 25 µl of the radical generator 2,2'-azobis(2-amidinopropane) dihydrochloride (AAPH, 240 mM) was rapidly added to each well.

Fluorescence was determined every 80 seconds for 2 hours, with excitation at 485 nm and emission at 520 nm (POLARstar OPTIMA; BMG). The area under the signal degradation curves of the samples were compared to the gallic acid standard and the results expressed as gallic acid equivalents.

6.2.5 Cell maintenance

Cells were maintained in Dulbeccos's Modified Eagle Medium (DMEM) containing 25 mM glucose, supplemented with 200 U/ml penicillin, 200 µg/ml streptomycin, 2.6 µg/ml Fungizone, 200 mM glutamine and 5% foetal bovine serum (FBS). Cells were grown in 175 cm^2 tissue culture flasks and incubated at 37°C in 5% CO_2. For experiments, cells were harvested with a solution containing 0.025 mM trypsin and 1 mM EDTA in PBS, plated in 96 well plates at a density of 9×10^3 cells/well and incubated for 24 hours before treatment.

6.2.6 Cell based assays

For cell-based experiments, extracts were dissolved in dimethyl sulfoxide (DMSO) to give a stock concentration of 100 mg/ml. Herbs were then diluted in DMEM (1% FBS) to a concentration of 1000 µg/ml and filtered using a PVDF syringe filter before immediate use. To determine the cytotoxicity of the extracts, herbal solutions were diluted in DMEM (1% FBS) to give concentrations from 3.9 – 1000 µg/ml and applied to U373 cells for 24 hours treatment. Cell viability was then determined as described below. GraphPad Prism was used to calculate the 50% lethal concentration (LC_{50}) values where appropriate and enable selection of non-toxic concentrations of herbs for assessment of their cytoprotective properties.

Cell viability assay

For determination of cell viability, media was aspirated from wells and 100 µl of resazurin solution (0.001% resazurin in PBS) was added. Plates were incubated at 37°C with 5% CO_2 for 45 minutes and then fluorescence was measured with excitation at 530 nm and emission at 590 nm (POLARstar OPTIMA; BMG). For every plate, background fluorescence determined in cell-free wells was subtracted from all wells and values were expressed as a percentage of untreated control cells (Buranrat et al, 2008).

Treatment of U373 cells with hydrogen peroxide

U373 cells were treated with solutions containing 7.8 - 200 µM hydrogen peroxide in DMEM with 1% FBS for 24 hours. Cell viability was then assessed by the resazurin reduction assay described above and values expressed as a percentage of untreated control cells.

Determination of protective ability of extracts against hydrogen peroxide toxicity

Chinese herbs dissolved in DMEM (1% FBS) were applied to U373 cells for 12 hours incubation. Media was then removed and replaced with 100 µl of a solution containing 90 µM hydrogen peroxide in DMEM with 1% FBS. Following 24 hour hydrogen peroxide treatment of cells, cell viability was assessed by the resazurin reduction assay described above. Data are expressed as percentage of untreated

control cells and GraphPad Prism was used to calculate the concentration effective at returning cell viability to 50% (EC_{50}) where appropriate.

6.2.7 Statistics

Graphpad Prism was used to produce figures and analyse data. The mean and standard error of the mean (SEM) values were calculated from two or three independent experiments for each analysis, as stated. Graphpad Prism was used to calculate the EC_{50} and LC_{50} values using the sigmoidal dose-response function and relationships between antioxidant capacity, cytotoxicity and cytoprotective data were assessed by calculation of Spearman's correlation coefficients.

6.3 Results

6.3.1 Effect of herbal extracts on cell viability

In order to test for any potential cytotoxicity of thirteen herbal extracts, U373 cells were incubated for 24 hours with concentrations of extract ranging from 3.9 µg/ml up to 1000 µg/ml. Cell viability was assessed using the resazurin assay and LC_{50} values were calculated for extracts that resulted in a decrease in cell viability of 50% or greater. Results are shown in Figures 6.1 and 6.2 and LC_{50} values are reported in Table 6.2. The extracts displayed a large variation in cytotoxicity, with LC_{50} values ranging from 35.4 ± 1.2 µg/ml for Polygonum (P.) multiflorum to > 1000 µg/ml for Astragalus (A.) membranaceus, Codonopsis (C.) pilosula and Rehmannia (R.) glutinosa. In addition, Lycium (L.) barbarum and Panax (P.) ginseng showed an increase in cell viability in response to concentrations up to 250 µg/ml, thus suggesting a proliferative effect of these extracts. Maximal concentrations with no observed toxicity were chosen for each extract to test their ability to protect against hydrogen peroxide-induced death in U373 cells.

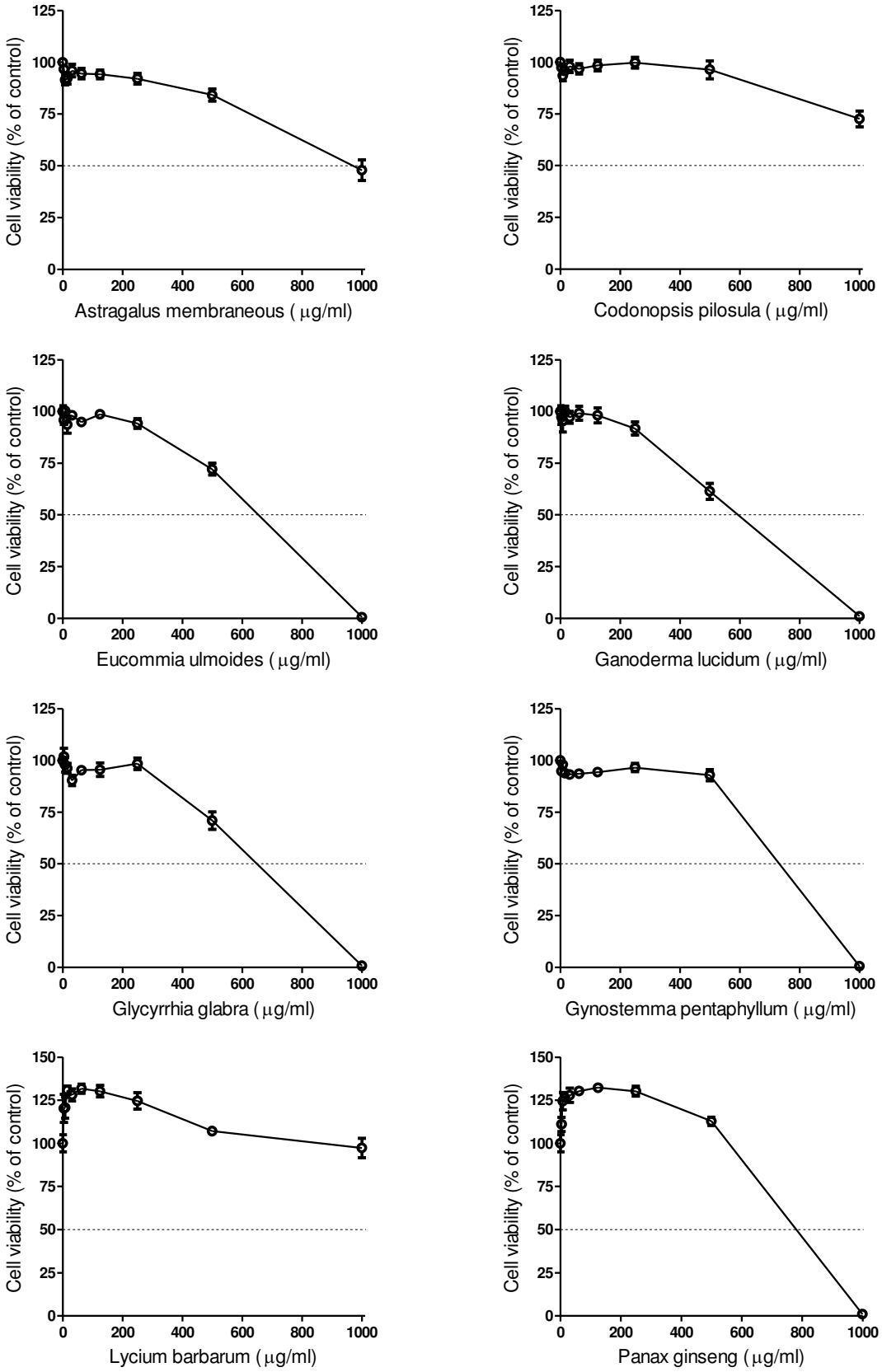

Figure 6.1 Cytotoxic effects of Chinese herbal extracts on U373 cells. Extracts at concentrations from 3.9 - 1000 μg/ml were incubated with U373 cells for 24 hours. Cell viability was then determined by the resazurin assay. Data are presented as percentage of control cells and represented as the mean ± SEM of 3 experiments.

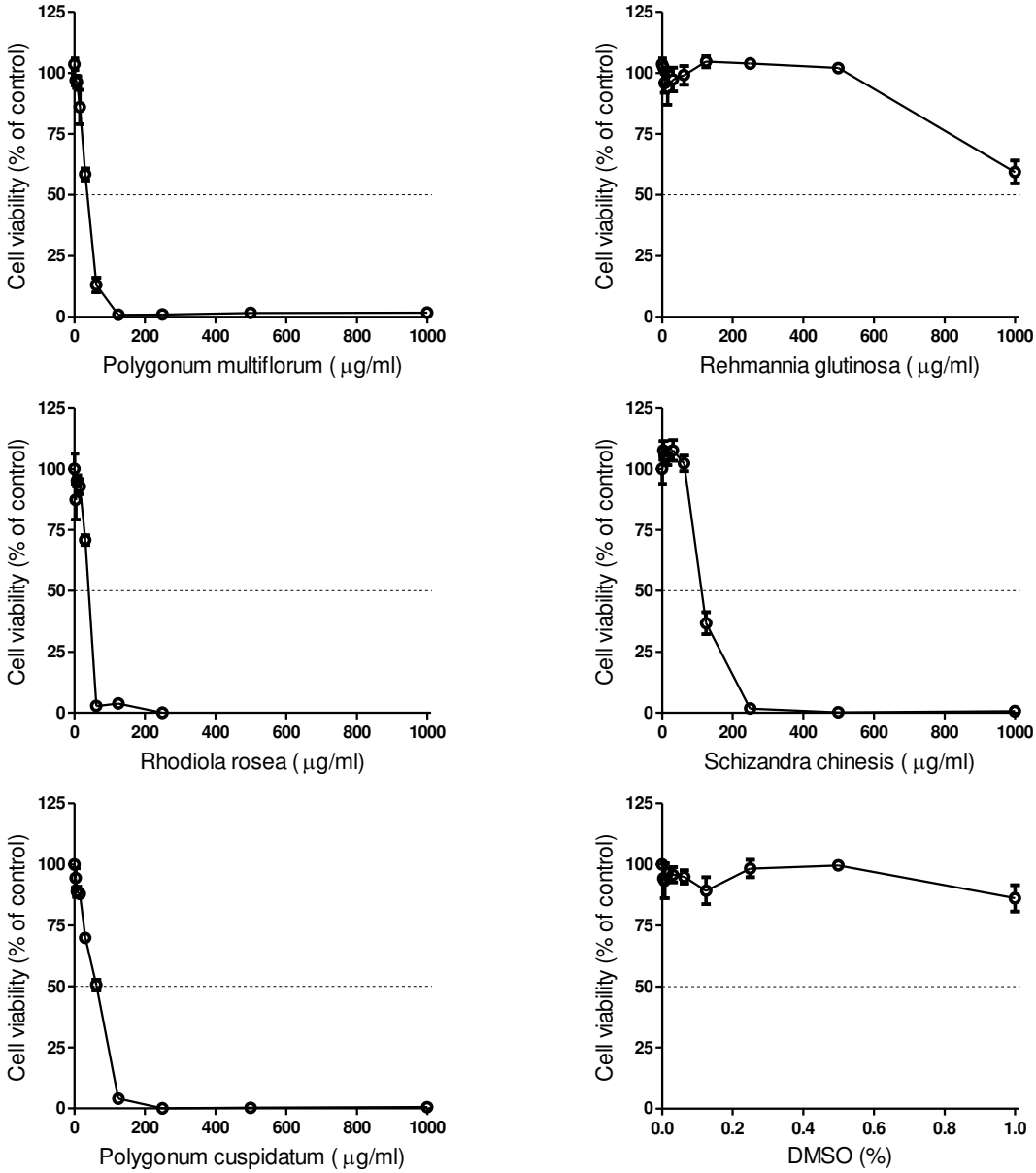

Figure 6.2 Cytotoxic effects of Chinese herbal extracts on U373 cells. Extracts at concentrations from 3.9 - 1000 μg/ml were incubated with U373 cells for 24 hours. Cell viability was then determined by the resazurin assay. Data are presented as percentage of control cells and represented as the mean ± SEM of 3 experiments.

6.3.2 Effect of hydrogen peroxide treatment on U373 cells

Hydrogen peroxide induced death of U373 cells was investigated in order to establish a cell culture based oxidative stress model for assessment of the cytoprotective properties of herbal extracts. U373 cells were treated with concentrations of hydrogen peroxide ranging from 3.9 μM up to 200 μM for 24 hours. Cell viability was then assessed using the resazurin assay and results are shown in Figure 6.3. A dose-dependent decrease in cell viability was observed, with an LC_{50} value of 87.0 μM and a 95% confidence interval of 81.1 to 93.3 μM (R^2 = 0.974). Therefore, a concentration of 90 μM hydrogen peroxide was selected for investigating the cytoprotective abilities of extracts.

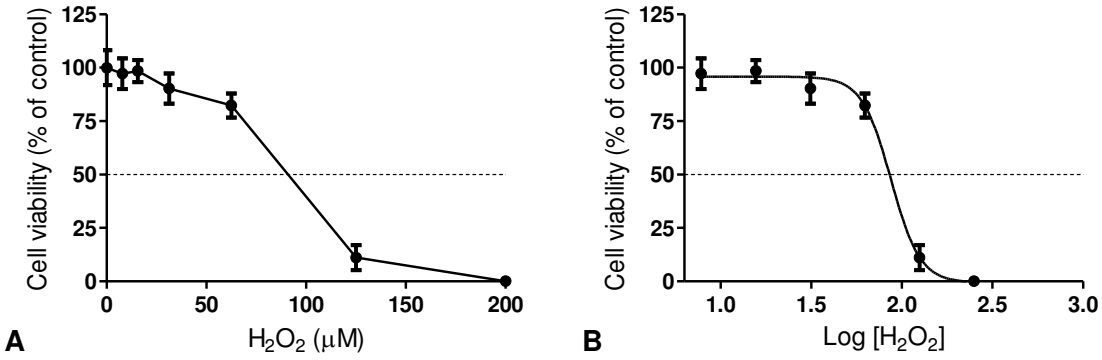

Figure 6.3 Effect of hydrogen peroxide treatment on U373 cell viability. U373 cells were treated with 7.8 - 200 μM hydrogen peroxide (H_2O_2) for 24 hours. Cell viability was then determined by the resazurin assay. Raw data (A) and Log transformed data (B) are shown as percentage of control cells and represented as the mean ± SEM of 3 experiments. Graphpad Prism was used to fit a sigmoidal dose-response curve to the Log transformed data for calculation of LC50 as 87.0 μM.

6.3.3 Cytoprotective effect of herbal extracts

In order to analyse the cytoprotective effects of herbal extracts, U373 cells were supplemented with non-toxic concentrations of extracts for 12 hours, after which time extract-containing media was replaced with a 90 µM hydrogen peroxide solution. After 24 hours hydrogen peroxide treatment, cell viability was assessed using the resazurin assay and EC_{50} values were calculated for extracts capable of maintaining cell viability to greater than 50% of non-hydrogen peroxide treated control cells. Results are shown in Figures 6.4 and 6.5 and EC_{50} values are reported in Table 6.2. As with cytotoxicity, a large variation in the cytoprotective ability of herbs was observed. P. multiflorum, R. rosea and Schizandra (S.) chinesis exhibited the strongest protection against hydrogen peroxide induced cell death, with EC_{50} values of < 0.2, < 0.5 and 1.4 ± 0.7 µg/ml, respectively. In contrast, P. ginseng showed a less potent cytoprotective effect with an EC_{50} value of 66.6 ± 10.4 µg/ml; and pre-incubation with P. cuspidatum at concentrations between 0.1 and 3.9 µg/ml was not able to protect cells. Although the maximal concentrations selected for assessment of cytoprotective effects of extracts were shown to be non-toxic in the initial cytotoxicity screening, some toxicity was seen at the highest concentration for most extracts. This might have been due to the addition of hydrogen peroxide or to the extended incubation time (12 hour pre-incubation with or without extract, followed by 24 hour incubation with or without hydrogen peroxide). A vehicle control, consisting of DMSO diluted in DMEM to reflect concentrations of DMSO present in extract solutions (< 0.5 %), showed no protection against hydrogen peroxide induced cell death, as well as no reduction of cell viability in the absence of hydrogen peroxide.

In addition, the therapeutic index for each extract was calculated by dividing the LC_{50} for an extract by its determined EC_{50} (Table 6.2). A higher therapeutic index is preferable to a lower one, since having little difference between toxic and therapeutic concentrations of a drug can be dangerous and lead to difficulties in effective dosage determination in an in vivo situation. In this cell based model of oxidative stress induced death, P. multiflorum, S. chinesis and Lycium (L.) barbarum were identified as having the largest therapeutic indexes of > 177.0, 83.8 and > 73.0, respectively.

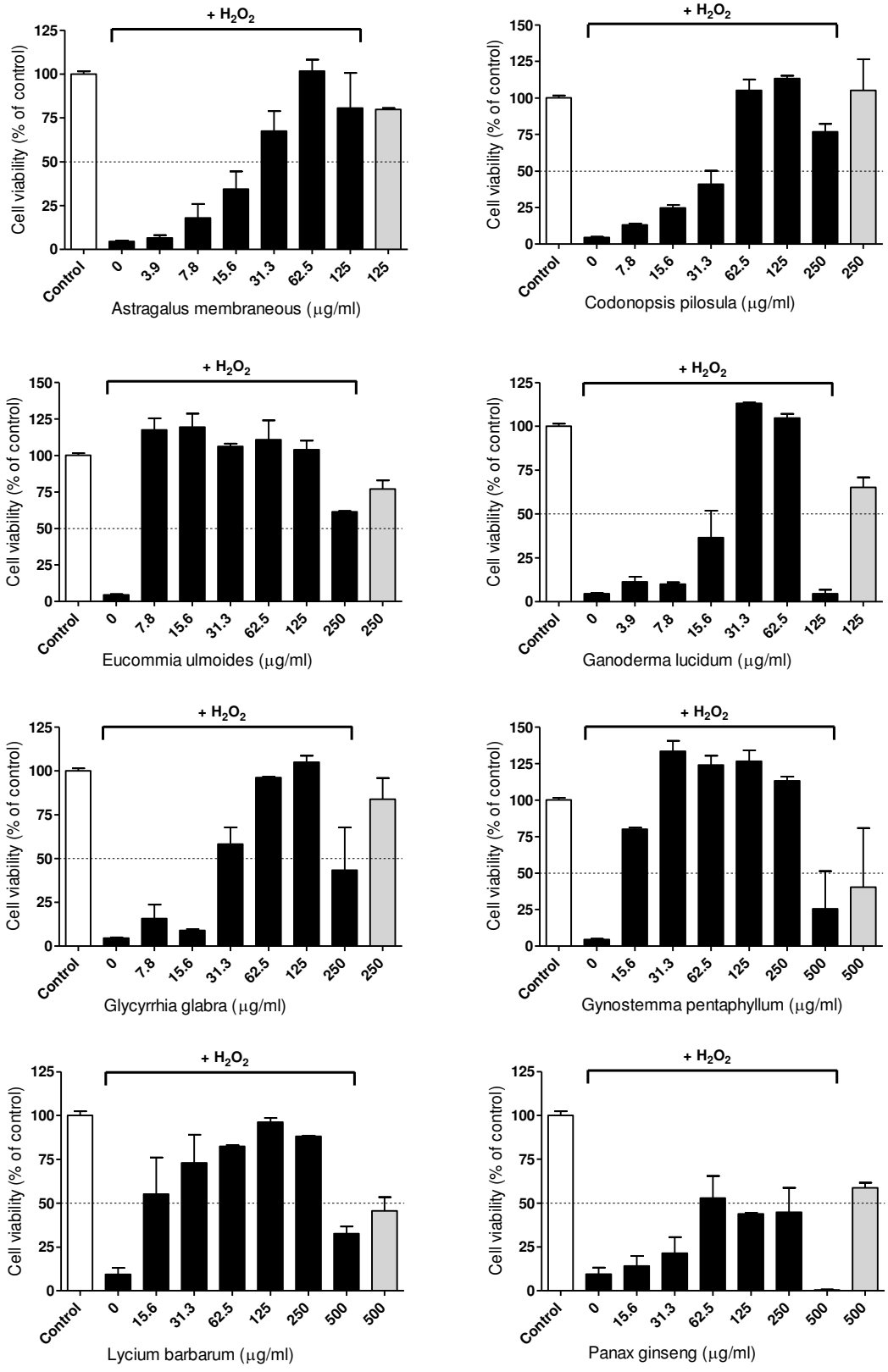

Figure 6.4 Cytoprotective effects of Chinese herbs on U373 cells. Herbs at various concentrations were incubated with U373 cells for 12 hours. Herb-containing media was replaced with fresh media containing 90 μM hydrogen peroxide for 24 hours. Cell viability was then determined by the resazurin assay. Data are presented as percentage of control cells and represent the mean ± SEM of 2 experiments.

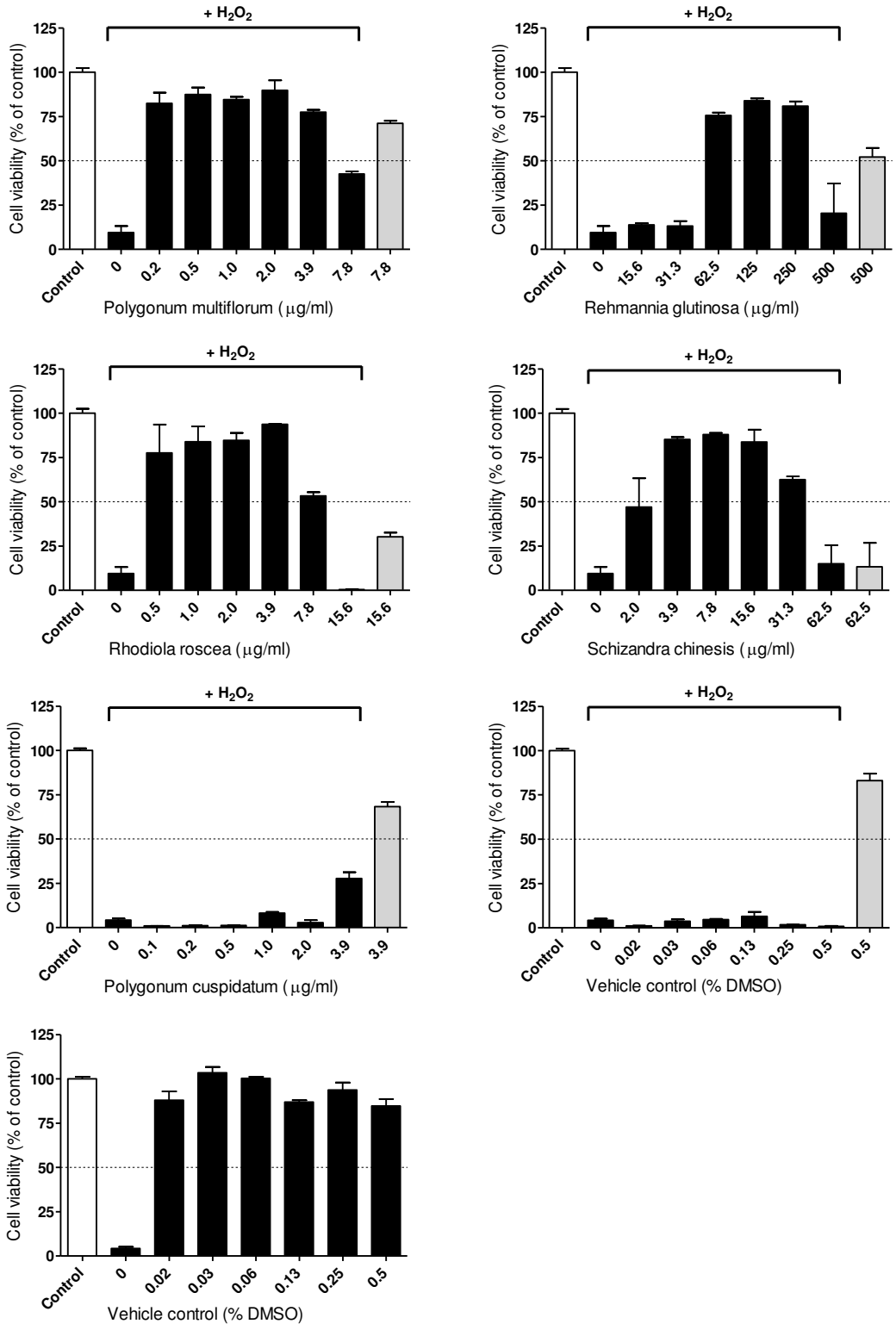

Figure 6.5 Cytoprotective effects of Chinese herbs on U373 cells. Herbs at various concentrations were incubated with U373 cells for 12 hours. Herb-containing media was replaced with fresh media containing 90 μM hydrogen peroxide for 24 hours. Cell viability was then determined by the resazurin assay. Data are presented as percentage of control cells and represent the mean ± SEM of 2 experiments.

6.3.4 Non-cell based determinations of antioxidant capacity of extracts

** Non-cell based antioxidant assays were performed by John Truong from the Complementary Medicine Laboratory headed by Professor Nikolaus Sucher **

In order to find out whether the cytoprotective properties of herbal extracts might be due to their free radical scavenging ability, results from three non-cell based antioxidant assays were considered.

Total phenol content of herbal extracts

The FCR assay measures a sample's reducing capacity, however results from this assay are commonly presented as a measure of total phenol content. Therefore, total phenol content was determined for each extract and normalised against a gallic acid standard curve enabling results to be presented as the gallic acid equivalent (mmol/g GAE). The results are shown in Figure 1 (Appendix) and summarised in Table 6.2. R. rosea, P. cuspidatum and P. multiflorum showed the highest phenol contents with values of 5.55 ± 0.55, 2.57 ± 0.10 and 1.75 ± 0.02 mmol/g GAE, respectively. In contrast, P. ginseng had the lowest phenol content with 0.06 ± 0.00 mmol/g GAE.

Antioxidant capacity of herbal extracts

Antioxidant capacity of herbal extracts was determined by the commonly used DPPH and ORAC chemical assays. The results are shown in Figures 2 - 3 (Appendix) and summarised in Table 6.2. The DPPH assay is an electron transfer based assay and measures the reducing capacity of samples, using copper as an oxidant (Huang et al., 2005a). Results from this assay were well aligned with those from the FCR assay identifying R. rosea, P. cuspidatum and P. multiflorum as the most potent extracts

with values of 4.20 ± 0.05, 3.28 ± 0.01 and 2.56 ± 0.02 mmol/g GAE, respectively. The ORAC assay, on the other hand, is a hydrogen atom transfer based assay and measures radical chain-breaking capacity, involving peroxyl radicals as the oxidant (Huang et al., 2005a). Results from the ORAC assay were also well aligned with the results from the FCR and DPPH assays except that R. rosea did not perform as well in this assay. P. cuspidatum, P. multiflorum and Schizandra (S.) chinesis were the most potent extracts with values of 1.30 ± 0.01, 1.25 ± 0.01 and 1.19 ± 0.05 mmol/g GAE, respectively.

Table 6.2 Results from chemical and cell based antioxidant assays of thirteen traditional Chinese herbs.

Sample Name	DPPH	ORAC	FCR	Cytotoxicity (LC_{50})	Cytoprotection (EC_{50})	Therapeutic Index
	Mean ± SEM (mmol GAE/g)			Mean ± SEM (µg/ml)		LC_{50} / EC_{50}
Astragalus membranaceus	0.04 ± 0.00	0.19 ± 0.00	0.21 ± 0.01	> 1000	20.6 ± 0.5	> 48.5
Codonopsis pilosula	0.03 ± 0.00	0.09 ± 0.00	0.14 ± 0.01	> 1000	23.1 ± 2.2	> 43.3
Eucommia ulmoides	0.05 ± 0.01	0.53 ± 0.01	0.26 ± 0.00	566.3 ± 9.0	< 7.8	> 72.6
Ganoderma lucidum	0.05 ± 0.00	0.26 ± 0.00	0.13 ± 0.00	536.7 ± 21.3	8.0 ± 6.0	67.1
Glycyrrhiza glabra	0.78 ± 0.00	0.87 ± 0.03	0.76 ± 0.03	558.4 ± 24.8	28.6 ± 1.8	19.5
Gynostemma pentaphyllum	0.64 ± 0.01	0.61 ± 0.00	0.18 ± 0.01	631.0 ± 32.0	< 15.6	> 40.4
Lycium barbarum	0.04 ± 0.00	0.24 ± 0.01	0.15 ± 0.01	> 1000	13.7 ± 7.7	> 73.0 $^{+}$
Panax ginseng	0.02 ± 0.00	0.27 ± 0.01	0.06 ± 0.00	862.5 ± 15.4	66.6 ± 10.4	13.0
Polygonum multiflorum	2.56 ± 0.02 $^{+}$	1.25 ± 0.01 $^{++}$	1.75 ± 0.02 $^{+}$	35.4 ± 1.2 $^{+++}$	< 0.2 $^{+++}$	> 177.0 $^{+++}$
Rehmannia glutinosa	0.09 ± 0.00	0.16 ± 0.02	0.10 ± 0.01	> 1000	48.3 ± 0.9	> 20.7
Rhodiola rosea	4.20 ± 0.05 $^{+++}$	1.13 ± 0.02	5.55 ± 0.55 $^{+++}$	36.3 ± 1.0 $^{++}$	< 0.5 $^{++}$	> 72.6
Schizandra chinesis	0.46 ± 0.00	1.19 ± 0.05 $^{+}$	0.59 ± 0.03	117.3 ± 7.5	1.4 ± 0.7 $^{+}$	83.8 $^{++}$
Polygonum cuspidatum	3.28 ± 0.01 $^{++}$	1.30 ± 0.01 $^{+++}$	2.57 ± 0.10 $^{++}$	51.0 ± 2.4 $^{+}$	n/a	n/a

$^{+++}$ = best; $^{++}$ second best; $^{+}$ third best; GAE = gallic acid equivalent; n/a = not applicable.

6.3.5 Relationships between antioxidant activity and cytoprotective ability of herbal extracts

In order to investigate the relationships between total phenol content, antioxidant capacity (determined by the DPPH and ORAC assays), cytoprotective ability and cytotoxicity of extracts, results from the different assays were plotted against each other (Figure 6.6) and correlation coefficients (r) determined using the non-parametric Spearman's Rank Order Correlation test (Table 6.3). Total phenol content (FRC assay) showed a strong positive correlation with antioxidant capacities measured by the DPPH ($r = 0.808$; $p < 0.001$) and ORAC ($r = 0.791$; $p = 0.001$) assays. DPPH and ORAC measurements were also strongly and positively correlated ($r = 0.780$; $p = 0.002$).

To test whether there is a relationship between the antioxidant activity of extracts, as determined by the non-cell based chemical assays, and the cytoprotective ability of extracts in a cell based oxidative stress model, results from the FCR, DPPH and ORAC assays were compared to the determined EC_{50} values. Moderately strong negative correlations were found between cytoprotection and total phenol content, as determined by the FCR assay ($r = -0.699$; $p = 0.011$); and between cytoprotection and antioxidant activity, as measured by the ORAC assay ($r = -0.643$; $p = 0.024$). Therefore, as phenol content and ORAC of extracts increased, the concentration of extract needed to protect 50% of cells decreased. On the other hand, the association between cytoprotection and antioxidant activity determined by the DPPH assay was found to be non-significant.

In addition, the relationship between results of non cell based antioxidant assays and the cytotoxicity of extracts was examined. Strong negative correlations were seen between the LC_{50} values calculated for each extract and values for total phenol content ($r = -0.741$; $p = 0.004$), DPPH ($r = -0.791$; $p = 0.001$) and ORAC ($r = -0.897$; $p < 0.001$). A strong positive correlation was seen when LC_{50} and EC_{50} values were compared ($r = 0.733$; $p = 0.007$). This indicates that the extracts that showed the best protection at low concentrations (low EC_{50} values) were the most toxic when used at high concentrations.

Table 6.3 Correlation coefficients between antioxidant capacity, cytotoxicity and cytoprotection data for herbal extracts.

	DPPH	ORAC	Toxicity LC50	Cytoprotection EC50
Total phenols	0.808 ***	0.791 **	-0.741 **	-0.699 *
DPPH		0.780 **	-0.791 **	-0.545
ORAC			-0.897 ***	-0.643 *
Cytotoxicity LC50				0.733 **

Relationships between results were analysed using the Spearman's Rank Order Correlation Test. Correlation coefficients (r) are presented and statistical significance is designated by * = p< 0.05; ** = p < 0.01 and *** = p < 00.01.

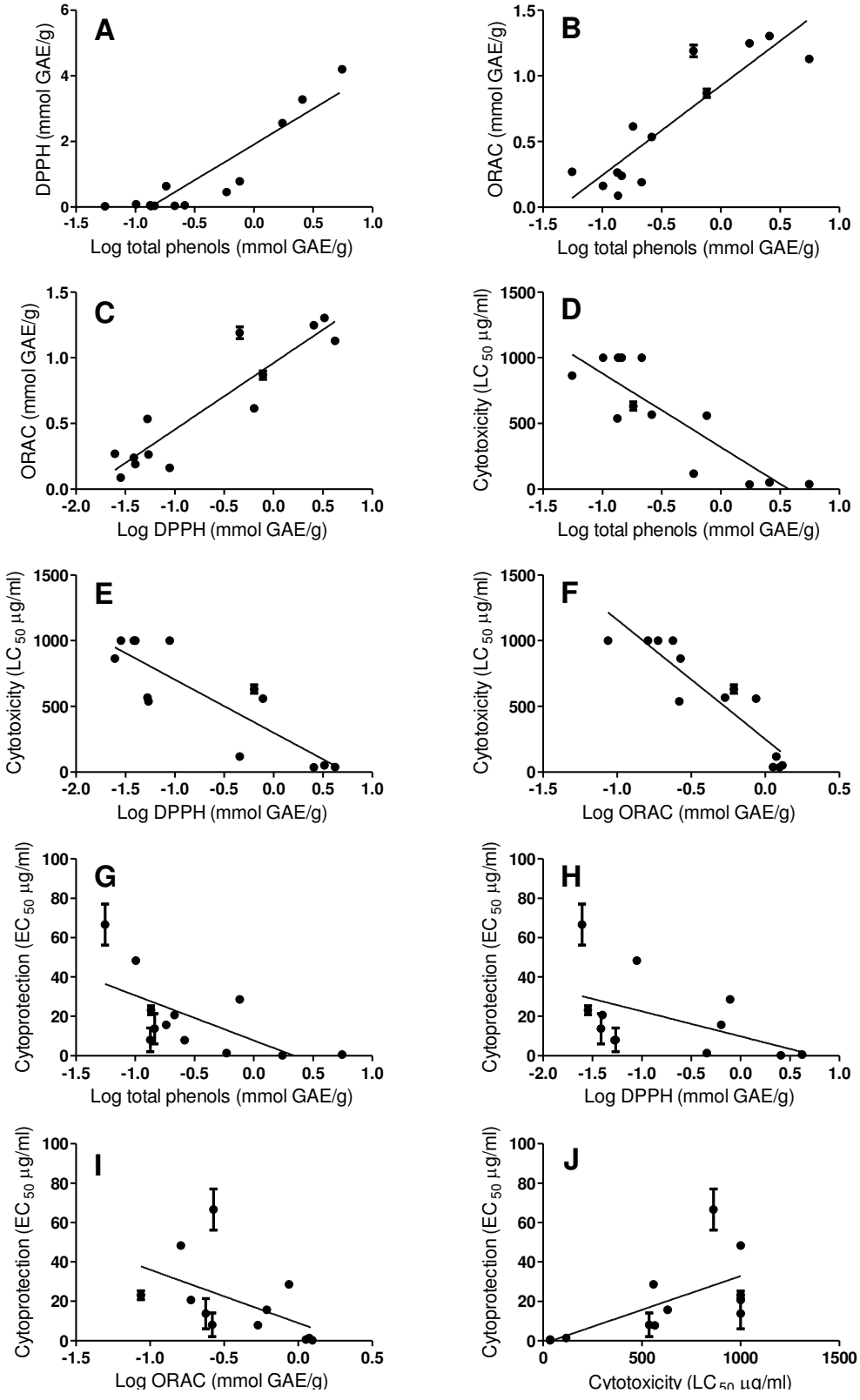

Figure 6.6 Relationships between antioxidant capacity, cytotoxicity and cytoprotection. Scatter plots show Log total phenols versus DPPH (A) and ORAC (B); Log DPPH versus ORAC (C); Log total phenols (D), Log DPPH (E) and Log ORAC (F) versus cytotoxicity; and Log total phenols (G), Log DPPH (H), Log ORAC (I) and cytotoxicity versus cytoprotection.

6.4 Discussion

This study tested thirteen TCM herbal extracts for their ability to protect U373 cells from hydrogen peroxide induced cell death. Total phenol contents and antioxidant capacities of extracts were also investigated by non-cell based chemical assays. P. multiflorum, R. rosea and S. chinesis were amongst the most potent extracts in both the non-cell chemical antioxidant assays as well as in the cytoprotection assay. A major difference between results from the chemical assays and the cytoprotection assays was that while P. cuspidatum performed exceptionally well in the FCR, DPPH and ORAC assays, it appeared to have no protective effect towards hydrogen peroxide treated U373 cells. P. cuspidatum and P. multiflorum are both members of the Polygonaceae family, commonly known as Hu Zhang or Japanese knotwood and He Shou Wu or Fo-Ti root, respectively. In addition to a wide variety of other medicinal uses, P. multiflorum and P. cuspidatum have been valued for their anti-inflammatory, anti-pyretic, hypotensive, antioxidant and anticancer properties for centuries (Unschuld, 1986). P. multiflorum is especially well known for its reputed anti-ageing benefits and is believed to be longevity promoting when consumed daily for an extended period (Bensky et al., 2004), while P. cuspidatum is better known for its anticancer properties (Kimura and Okuda, 2001). Both species have similar phytochemical compositions, with the most important constituents of P. cuspidatum thought to be emodin, physicon, chrysophanol, resveratrol and polydatin; and for P. multiflorum emodine, physicon and 2,3,5,4'-tetrahydroxystilbene-2-O-β-D-glucoside (Frederich et al., 2011). The two Polygonum extracts used here, however, were very different to each other since the P. cuspidatum extract was standardised to contain 50% trans-resveratrol, while P. multiflorum was a crude extract. Trans-resveratrol is a polyphenol thought to be largely responsible for the antioxidant capacity of

P. cuspidatum. Because of this, P. cuspidatum extracts are commonly standardised to contain anywhere from 10% up to >99% trans-resveratrol. Reported concentrations of trans-resveratrol determined in crude extracts of P. cuspidatum have ranged from 0.08% to 0.18% (Chu et al., 2005; Zhao et al., 2005). Therefore, the P. cuspidatum extract standardised to 50% trans-resveratrol that was used in this study contained more than 270 times the amount of trans-resveratrol normally found in non-standardised extracts of P. cuspidatum. This means that the concentration of trans-resveratrol in the P. cuspidatum solutions that were tested for their cytoprotective effects against hydrogen peroxide treated U373 cells ranged from 0.2 - 6.6 µM. Purified trans-resveratrol (> 99%) was investigated for its cytoprotective ability in hydrogen peroxide challenged C6 glioma cells by Quincozes-Santos and colleagues (2007). Interestingly, they observed that a one hour pre-incubation with 10 µM trans-resveratrol could protect against cellular DNA damage induced by an acute thirty minute hydrogen peroxide treatment (1 mM H_2O_2), but that this protection was abolished when a less intense, six hour treatment (0.1 - 0.5 mM H_2O_2) was administered (Quincozes-Santos et al., 2007). Protection was returned however, when cells were pre-incubated with trans-resveratrol at concentrations > 50 µM, suggesting that trans-resveratrol, and possibly P. cuspidatum, may be less effective at protecting against low intensity, chronic oxidative stress than moderate, acute oxidative stress. Trans-resveratrol, can also act as a pro-oxidant itself and was shown to cause DNA damage in C6 glioma cells, when used at a concentration of 250 µM for more than 12 hours. These findings might help to explain the observation here that P. cuspidatum was found to be one of the most potent antioxidants amongst the extracts screened (chemical assays), yet showed negligible protection against extended (24 hour) hydrogen peroxide treatment in U373 cells. Another explanation

for this finding might be related to the reported potent anticancer properties of trans-resveratrol and P. cuspidatum (Kimura and Okuda, 2001). Both the U373 cells used in this study, as well as the C6 cells used by Quincozes-Santos et al. (2007) are tumour cells and therefore may be particularly vulnerable to P. cuspidatum. P. multiflorum, as opposed to P. cuspidatum, performed well in all of the chemical antioxidant assays, as well as being the most potent extract in the cytoprotective assay and having the largest therapeutic index. Furthermore, P. multiflorum has been shown to be protective against cognitive deficits in mice injected with amyloid-β peptide 25-35 (Um et al., 2006); and to improve learning and memory ability and reduce pathological changes in the brains of senescence accelerated mice (Chan et al., 2003). In both cases, it is thought that the antioxidant properties of P. multiflorum were responsible for its beneficial effects.

In order to investigate the relationship between antioxidant activity of extracts and cytoprotection more closely, correlation coefficients were calculated for comparisons between specific assays. When measurements of total phenol content were compared to measurements of antioxidant capacity, determined by the DPPH and ORAC assays, both showed strong positive correlations, indicating that phenols had a major contribution to the antioxidant activity of extracts. This finding is not surprising due to the fact that highly linear relationships between total phenol content and antioxidant activity of medicinal herbs have been reported in the past (Cai et al., 2004; Zheng and Wang, 2001), although this is not always the case (Ghimire et al., 2011). Moreover phenols, such as phenolic acids and flavonoids, have been widely implicated as natural antioxidants in all types of plants including fruits and vegetables (Kahkonen et al., 1999). Interestingly, however, when total phenol

content and ORAC values for extracts were compared to the cytoprotective abilities of extracts, only moderately strong negative correlations were observed. Furthermore the association between DPPH scavenging ability and cytoprotection was found to be non-significant. This difference might be explained by the fact that the ORAC method has been reported to mimic antioxidant activity of phenolics in biological systems better than the DPPH method (Cao et al., 1993), since the ORAC assay uses biologically relevant free radicals (peroxyl radicals), while DPPH is a long-lived, nitrogen radical, bearing no resemblance to the highly reactive peroxyl radicals involved in lipid peroxidation in cells (Huang et al., 2005a). Overall, these findings suggest that although the antioxidant activity of extracts contributes partially to the cytoprotective effect of extracts, there might be other non-radical scavenging related mechanisms involved in protection of cells against hydrogen peroxide toxicity. These might include protection through anti-apoptotic effects (Jawan et al., 2003), anti-inflammatory effects (Li et al., 2003a), enhancement of mitochondrial ATP generation (Ko et al., 2006) and induction of Phase II detoxification genes, including glutathione related genes, superoxide dismutase, catalase and heme oxygenase-1 (Lavoie et al., 2009; Li, 1991; Surh, 2008). Furthermore, not only are there multiple mechanisms involved in cytoprotection, the importance of synergism between different compounds has been demonstrated in a number of studies (Andrews et al., 2007; Li, 1991).

Another interesting finding from this study was that the extracts that showed the best protection at low concentrations (low EC_{50} values), were the most toxic when used at high concentrations (low LC_{50} values). This outcome might be due to an overall higher content of active constituents (including total phenols) in the "potent"

extracts, thus increasing protective efficacy; but also resulting in lower thresholds in terms of toxicity. To quote Paracelsus, the medieval alchemist and physician: *''Poison is in everything, and no thing is without poison. The dosage makes it either a poison or a remedy"*.

In summary, this study has shown that total phenol content and antioxidant activity of extracts are moderately correlated with their cytoprotective ability, suggesting the involvement of multiple protective mechanisms in the beneficial effects of medicinal herbs. It has also highlighted the thin line that can exist between protection and toxicity, thus making the use of medicinal herbs or defined "drug cocktails" consisting of low concentrations of synergistic compounds more attractive than using high concentrations of an individual active constituent. Finally, P. multiflorum, amongst others, was identified as possessing potent cytoprotective properties. Future studies are required to investigate whether the observed cytoprotective abilities of medicinal herbs can be translated to protecting cells against oxidative stress in vivo. The fact that total phenol content of extracts was only moderately correlated with cytoprotection provides support to the multi-compound, multi-targeting approach used in TCM and suggests that medicinal herbs might provide potential therapeutic options for complex, multi-factorial diseases, such as AD and other neurodegenerative and oxidative stress related disorders.

CHAPTER 7

Summary and conclusions

7.1 Summary

This thesis aimed to determine whether inflammatory activation of astrocytes leads to perturbation of their neurosupportive functions, such as the supply of glutathione (GSH) and its degradation products (Chapter 4) and the uptake of glucose and release of lactate (Chapter 5). A large portion of the results presented relate to establishment of the conditions of inflammatory activation (Chapter 2) and the development and validation of a HPLC method that was required for the determination of GSH and related thiol compounds (Chapter 3). Based on the premise that astrocytes are key modulators in the progression of oxidative stress associated neurodegenerative diseases, thirteen herbal extracts purported to possess anti-ageing or cognitive-enhancing properties by traditional Chinese medicine were tested for their cytoprotective ability in hydrogen peroxide-challenged U373 cells (Chapter 6). This chapter will summarise the main findings from this thesis and suggest future work required to build on the results reported here. The findings from this study will be discussed in regards to their possible implications on the understanding and treatment of the pathogenic processes involved in Alzheimer's disease (AD).

The overall hypotheses underpinning this thesis were that (1) chronically activated astrocytes neglect their neurosupportive functions and (2) decreased astrocytic support contributes to neurodegeneration in Alzheimer's disease (AD). These hypotheses were largely based on the following observations in the brains of AD patients:

- AD is characterised by reactive hypertrophic astrocytes that form a halo around neuritic plaques with their processes covering the neurite layer and interweaving within the plaque (Akiyama et al., 2000; Nagele et al., 2004; Robinson, 2001), but are also observed in regions away from plaques (Simpson et al., 2010).
- AD is associated with increased expression of a range of inflammatory mediators including IL-1β, TNF-α, IL-6, IL-8 and MCP-1 (Grammas and Ovase, 2001).
- Reduced energy metabolism is recognised as an early metabolic perturbation in the brains of AD patients (Small et al., 2000).
- Oxidative stress is implicated in AD due to significantly higher levels of oxidised macromolecules, including lipids, DNA, proteins and sugars, compared to control brains (Moreira et al., 2008)
- The concentration of glutamate is elevated, while the concentration of glutamine is lowered in the cerebrospinal fluid of patients with AD (Csernansky et al., 1996; Jimenez-Jimenez et al., 1998; Redjems-Bennani et al., 1998; Smith et al., 1985).

Interestingly, the above mentioned characteristics of AD pathology can all be explained by either upregulation of normal astrocytic functions or by astrocytic dysfunction, thus strongly implicating astrocytes in the pathogenesis of AD. Due to the early and widespread involvement of inflammation in AD, chronic inflammatory activation of astrocytes has been identified as a possible cause of dysfunctional astrocytes in AD (Steele and Robinson, 2011).

7.1.1 Astrocytes, release of neurotoxic compounds and AD

In the present study, reactive U373 astrocytoma cells were shown to release large quantities of the pro-inflammatory cytokine, IL-6 (Chapter 2). IL-6 has been measured at elevated levels in the cerebral spinal fluid (CSF) of AD patients compared to controls (Blum-Degen et al., 1995) and has been shown to cause cell damage and death in primary cultures of rodent cerebellar granule neurons, partly mediated by excessive activation of NMDA-type glutamate receptors (Conroy et al., 2004). Studies on a transgenic mice model in which IL-6 expression is under the control of the glial fibrially acidic protein showed that high levels of cerebral IL-6 led to astrogliosis, neurodegeneration and impaired learning (Campbell et al., 1993; Heyser et al., 1997). In addition to the upregulation of IL-6 release, U373 cells treated with IL-1β and TNF-α were found to increase their release of homocysteine (Chapter 4). Interestingly, elevated plasma and CSF levels of homocysteine are also strongly associated with AD (McCaddon et al., 2003; Popp et al., 2009). Furthermore, in vitro investigations have revealed that homocysteine induces oxidative stress and apoptosis in rodent neuronal cultures through the activation of neuronal NMDA receptors (Althausen and Paschen, 2000; Ho et al., 2002; Lipton et al., 1997). Together, these findings indicate that reactive astrocytes might contribute to neurodegeneration through the upregulation of inflammatory mediators such as IL-6 and neurotoxic substances such as homocysteine.

7.1.2 Astrocytes, altered glutathione metabolism and AD

Along with increased inflammation, the AD brain is characterised by significantly higher levels of oxidised lipids, DNA, proteins and sugars compared to healthy age-matched control brains (Moreira et al., 2008). Additionally, the ratio of oxidised

GSH (GSSG) to GSH was increased in the inferior frontal and inferior temporal cortices of AD patients (Karelson et al., 2001), further indicating that oxidative stress is a predominant feature of AD. Levels of glutathione peroxidase and glutathione reductase are also elevated, suggesting that there is an attempt made by cells to combat oxidative stress. Measurements of GSH levels in the brains of AD patients, however, have yielded contradictory results. While reported to be lowered in some studies (Gu et al., 1998), other studies report increases (Adams et al., 1991) or no significant differences in levels of GSH compared to controls (Perry et al., 1987). This variation in results makes the interpretation of the involvement of GSH in AD somewhat confusing. Use of standardised post mortem analysis techniques and improved analytical methods, such as the HPLC method developed in Chapter 3 of this thesis, may help to elucidate changes in GSH levels of AD brains. In addition, it would be interesting to monitor changes in GSH content in the brains of AD patients using two-photon imaging with monochlorobimane as a GSH probe, a technique which has been successfully used in stroke patients (Bragin et al., 2010). It is possible that GSH level in AD patients, is dependent on disease stage or years since disease onset. One study that measured 8-hydrooxyguanosine (an oxidised nucleoside) and nitrotyrosine (a product of tyrosine nitration, both markers of oxidative stress) in neurons of patients with AD found that oxidative damage was not only an early event in AD, but was quantitatively greatest early in the disease and decreased with disease progression and lesion formation. Surprisingly, increases in amyloid-β deposition were associated with decreases in oxidative damage, and neurofibrillary tangles (NFT)-containing neurons showed 40 – 56% lower levels of 8-hydrooxyguanosine compared to neurons without NFT (Nunomura et al., 2001). These findings suggest that oxidative stress is thus important in disease progression

and not simply a consequence of neurodegeneration. In addition, AD may be associated with compensatory changes that reduce oxidative damage and this may account for the contradictory results concerning variations in levels of GSH reported in AD patients (Adams et al., 1991; Gu et al., 1998; Perry et al., 1987).

The findings presented in Chapter 4 of this thesis showed that U373 cells treated with low to moderate levels of IL-1β and TNF-α increased their intracellular and extracellular levels of GSH. In response to the highest concentration of IL-1β and TNF-α (10 ng/ml) however, there was no change in intracellular or extracellular GSH content compared to controls cells. These findings suggest that astrocytes are capable of "answering the call" so to speak, until a certain activation intensity threshold is reached. It is plausible that if higher concentrations of cytokines were used, then depletion of GSH would have occurred. Preliminary experiments, in which incubation time of cells was extended up to 140 hours, showed a cytokine concentration-dependent depletion of extracellular GSH, which was evident even at low concentrations of IL-1β and TNF-α (0.01 ng/ml). There was also a significant cytokine concentration-dependent reduction in cell viability observed after 140 hours however, making interpretation of the results more complicated. The present findings, that GSH metabolism is sensitive to inflammatory activation and that intracellular and extracellular levels increase or decrease dependent on cytokine concentration and exposure time, may further help to explain the variations observed in GSH levels in AD patients. An important finding from this thesis, also presented in Chapter 4, was that IL-1β and TNF-α treatment of U373 cells produced a concentration-dependent decrease in extracellular cysteinylglycine (CysGly). Since neurons are not able to take up GSH directly, but rely on the supply of CysGly by

astrocytes, it is possible that changes in extracellular concentrations of CysGly might be more important than changes in GSH. To the best of our knowledge, the levels of CysGly in brains of AD patients have not been measured yet. One study that measured total plasma thiols in patients with mild cognitive impairment (MCI) or AD, found that both GSH and CysGly were decreased in MCI and AD patients compared to healthy controls (Hernanz et al., 2007). Another study measured levels of free transthyretin (TTR) as well as TTR-CysGly and TTR-cysteine conjugates in the CSF of AD patients (Biroccio et al., 2006). TTR in the CSF is primarily synthesised by the choroid plexus and functions as a carrier of the thyroid hormone thyroxine and retinol. It has a free reactive sulphydryl moiety and readily binds free cysteine and CysGly in CSF. Interestingly, both CysGly-TTR and cysteine-TTR were strongly diminished in the CSF of AD patients compared to controls (Dickson et al., 1985). The authors suggest that these results might indicate a depletion of these thiols in the brain (Biroccio et al., 2006). The findings from this thesis implicate chronic proinflammatory activation of astrocytes as a possible underlying mechanism contributing to depletion of thiols in AD.

7.1.3 Astrocytes, impaired energy metabolism and AD

Reduced energy metabolism is recognised as an early metabolic perturbation in the brains of AD patients (Small et al., 2000). It is widely believed that astrocytes are predominantly responsible for glucose uptake from the blood (Magistretti and Pellerin, 1996), thus suggesting that astrocytic dysfunction might contribute to the impaired energy metabolism observed in AD (Allaman et al., 2011; Steele and Robinson, 2011). In the current study, extended treatment of U373 cells with the proinflammatory cytokines, IL-1β and TNF-α, led to impaired energy metabolism

(Chapter 5), implicating a role for inflammation in the induction of a dysfunctional astrocytic phenotype. As with GSH synthesis, astrocytic glucose uptake increased in response to low to moderate activation (< 1 ng/ml IL-1β and TNF-α), but showed no significant difference to control cells in response to high level activation (5 – 10 ng/ml). It was suggested that the simultaneous increases seen in GSH synthesis and glucose uptake were metabolically linked by an increase in glucose oxidation by the pentose phosphate pathway, which produces NADPH, the co-substrate required for glutathione reductase mediated regeneration of GSH from GSSG. Experiments showed that not only did the highly activated cells take up less glucose than moderately activated cells, they also released less lactate. Interestingly, however, the reduction in lactate release was far greater than the reduction in glucose uptake, indicating perhaps that astrocytes were using more glucose for themselves. It is likely that reactive astrocytes use increased glucose to fund the energetically costly activities of enhanced cytokine production, elevation of GSH levels and proliferation. Therefore, if neurons do indeed rely on astrocytes for supply of lactate in the brain (Pellerin et al., 1998), these findings suggest that reactive astrocytes become "energetically selfish", a transformation that might result in energy-starved neurons.

7.1.4 Potential therapies for the prevention of AD

The involvement of glial cells in AD was described as early as 1906 by Alois Alzheimer himself: *"The glia have formed substantial threads, and alongside them, many glial cells show large fatty deposits"* (Alzheimer, 1910). It has only been in the last twenty or so years, however, that the important roles of astrocytes, and indeed all glial cells, in normal brain function and dysfunction have been recognised. This

under appreciation of glial cell function has meant that therapeutic interventions for neurodegenerative diseases, including AD, have so far almost entirely focused on the modulation of neurons. There are currently two classes of drugs approved for the treatment of AD in Australia. These are acetylcholinesterase inhibitors (e.g. Rivastigmine and Galantamine) and an NMDA receptor antagonist (Memantine). Whilst capable of ameliorating symptoms in patients with AD, these medications are not curative and do not significantly change the course of the disease. More recently, potential therapies have aimed to reduce the build up of amyloid-β peptide and tau protein-associated NFT in the brains of AD patients. Although numerous amyloid-β targeted interventions in model animals of AD have shown promising results (Chen et al., 2007; Schenk et al., 1999), there has been limited success regarding clinical trials in humans to date (Holmes et al., 2008). Therefore a growing feeling amongst many in the AD research community is that it is time to pursue novel avenues of investigation. Astrocyte targeted therapies for the treatment of neurodegenerative diseases represent one such relatively novel area of research.

As already mentioned, reactive astrocytes in AD release a myriad of inflammatory mediators which can activate or reinforce already activated microglia and astrocytes leading to proliferation and even more inflammatory mediators and ROS, as well as having indirect and direct neurotoxic effects (Akiyama et al., 2000). Inflammation, involving reactive astrocytes and microglia, is thought to precede the presence of the classical pathological characteristics of AD, amyloid-β plaques and NFT-containing neurons (Eikelenboom et al., 2006; van Exel et al., 2009). Furthermore, epidemiological studies have reported a reduced risk of AD associated with non-steroidal anti-inflammatory drug (NSAID) use (Breitner et al., 1994; McGeer et al.,

1996). Together, these findings suggest that inflammation may be a promising target to prevent the onset or delay the progression of AD. Clinical trials with NSAIDs, including cyclooxygenase (COX) inhibitors and steroids, however, have not supported a protective benefit of NSAIDs against progression of AD (Aisen et al., 2000; Gilgun-Sherki et al., 2006). Conversely, a small, six month pilot trial of the TNF-α inhibitor, etanercept, produced an improvement in cognitive test scores in 15 out of 15 AD patients (Tobinick et al., 2006), and more recently was shown to rapidly improve verbal fluency and aphasia in AD patients within minutes (Tobinick, 2008). The authors propose that the rapid clinical improvements observed may be due to synaptic effects related to the role of TNF-α as a gliotransmitter, and the ability of astrocytes to exert widespread effects on multiple synapses through their extensive projections. In addition, it is possible that inhibition of TNF-α might have improved cognition through alleviating activation-induced decreases in astrocytic neurosupportive functions, such as provision of energy metabolites and GSH substrates.

Based on the results from this thesis and the present related literature, it is proposed that novel therapeutic approaches based on the upregulation or supplementation of astrocytic neurosupportive functions be investigated. For example, if chronically activated astrocytes in the brain do indeed deprive neurons of GSH substrates (CysGly) and energy metabolites (lactate), it might be beneficial to administrate exogenous neuron-accessible GSH substrates and energy metabolites. Since the availability of cysteine is the rate limiting step in the synthesis of GSH, increasing the concentration of this substrate would allow continued synthesis of GSH (Fuller et al., 2009a). Cysteine, like GSH however, is not able to penetrate the blood brain

barrier. Furthermore, extracellular cysteine is readily oxidised to cystine and also like GSH, cannot be taken up directly by neurons (Kranich et al., 1996). Therefore provision of cysteine derivatives might be more appropriate than providing GSH or cysteine. In vitro studies utilising primary astroglial or neuronal cultures have demonstrated that supplementation of culture media with CysGly, γ-glutamylcysteine (γ-GluCys) or N-acetylcysteine (NAC) leads to significantly elevated intracellular GSH content (Dringen and Hamprecht, 1999; Dringen et al., 1997b; Dringen et al., 1999b; Hultberg and Hultberg, 2006). In addition, compounds that can "boost" GSH synthesis through the upregulation of GSH enzymes represent interesting candidates for elevating endogenous GSH levels. For example, α-lipoic acid, curcumin, quercetin, tert-butylhydroquinone and sulforaphane increase intracellular GSH via activation of the nuclear factor erythroid-2-related factor 2-antioxidant response element (Nrf2-ARE) pathway (Kraft et al., 2004; Lavoie et al., 2009). Activation of Nrf2-ARE increases the expression of cysteine glutamate ligase (GCL), the rate limiting enzyme of GSH synthesis, amongst a batch of other cellular defence-related genes (Lavoie et al., 2009).

Currently, a limited number of in vivo studies have been carried out to investigate the efficacy and usefulness of providing GSH substrates or boosters for protection against oxidative stress or AD. Intraperitoneal administration of γ-GluCys ethyl ester was shown to increase GSH in rat brain and prevented oxidative stress mediated by administration of the chemotherapeutic drug adriamycin (Joshi et al., 2007). Additionally, intraperitoneal injection of NAC into rats was shown to increase total levels of GSH in the brain and demonstrated protection against hydroxyl radical induced oxidative stress (Pocernich et al., 2001; Pocernich et al., 2000). In a

controlled trial of NAC for patients with probable AD, patients received NAC or placebo for 6 months. Upon testing for efficacy after three and six months of treatment, the interval change favoured NAC treatment on nearly every outcome measure, although significant differences were obtained only for a subset of cognitive tasks (Adair et al., 2001). In a small open pilot trial in Germany, patients with probable AD were given 600 mg α-lipoic acid daily in addition to standard treatment with acetylcholine inhibitors. Cognitive performance of patients treated with α-lipoic acid stabilised for almost a year, demonstrated by constant scores in two neuropsychological tests, and progressed extremely slowly thereafter (Hager et al., 2007; Hager et al., 2001). Authors concluded that treatment with α-lipoic acid might be a successful neuroprotective therapy option for AD and that a state-of-the-art phase II trial is urgently needed. Increasing the endogenous levels of GSH is proposed to reduce oxidative and carbonyl stress and therefore may represent a promising pharmacological treatment strategy in AD and many other disease states.

The replenishment of GSH by GSH substrates or boosters may reduce elevated activity in the phosphate pentose pathway (needed to recycle GSSG), and thus restore the provision of lactate, citrate, malate and aspartate to neurons. Furthermore prevention or attenuation of oxidative stress in the brain might also prevent ROS-mediated inhibition of key metabolic enzymes involved in energy metabolism, therefore decreasing AD associated impaired energy metabolism. Additionally, some studies have reported beneficial effects on cognition after lactate or pyruvate administration to rats after traumatic brain injury or severe hypoglycaemia, respectively (Rice et al., 2002; Suh et al., 2005). Meanwhile, consumption of a drink containing emulsified medium chain triglycerides resulted in elevated plasma levels

of the ketone body β-hydroxybutyrate and was able to improve cognitive performance in a subset of MCI and AD patients (apolipoprotein E 4-negative patients only) (Reger et al., 2004). Whether the supply of alternative energy substrates represents a beneficial approach to the prevention or attenuation of cognitive impairment in AD remains to be investigated.

While some clinical trials involving anti-inflammatory drugs, antioxidants or other approaches might have indicated small beneficial effects in AD patients, it is probable that modulation of one pathogenic process in AD is not adequate for disease modification. Given the complexity of AD, approaches that combine multiple compounds with divergent targets are required for effective prevention or treatment of the disease. Furthermore, it is anticipated that safe concentrations of ingredients in a drug "cocktail" would work synergistically to counteract many of the pathways that contribute to disease progression, whilst having minimal side affects. This would also allow the option of such medicines to be used for decades as "preventative medicines". A recent study using the triple transgenic (3xTg-AD) mouse model of AD tested a medical food cocktail consisting of curcumin, piperine, epigallocatechin gallate, α-lipoic acid, NAC, vitamins C and E, B-vitamins and folate. Constituents were selected based on their anti-inflammatory, antioxidant, anti-glycation or anti-amyloid properties. Administration of the medical food cocktail for six months decreased soluble amyloid-β in the brains of transgenic mice and significantly improved learning and memory (Parachikova et al., 2010). In addition to the current focus on dietary intervention approaches for the treatment of AD, there is a growing interest in the use of traditional Chinese medicines (TCM) for preventing and treating age-related diseases (May et al., 2009; Reddy and Anekonda, 2005). In

particular, deciphering how exactly TCM work and identification of active components as well as synergistic effects of the active components is of importance. Results from Chapter 6 of this thesis suggest that while antioxidant activity is important to the cytoprotective effects of herbal extracts, there are probably other mechanisms involved in cytoprotection. Further elucidation of the beneficial effects of medicinal plants represents an exciting and rapidly growing area of research.

7.2 Future directions

Most importantly, future research related to the findings in this thesis should focus on determining whether the identified changes in astrocytes are physiologically relevant and whether they are in fact detrimental to neuronal viability. Preliminary experiments in our laboratory showed that incubating neurons with astrocyte conditioned media (ACM) from non-treated U373 cells increased neuronal intracellular GSH and viability. When ACM from highly activated cells was used, however, decreased neuronal intracellular GSH and viability was observed. It will therefore be interesting to find out whether supplying neurons with GSH substrates (e.g. CysGly), GSH boosters (e.g. α-lipoic acid), alternative energy metabolites (e.g. lactate) or other compounds can prevent depletion of neuronal intracellular GSH and cell death. Furthermore, by using specific agonists or antagonists, the contribution of various perturbed astrocytic functions to neurodegeneration can begin to be elucidated.

One of the limitations of this work is that all cell experiments were performed in the U373 astrocytoma cell line. As such, repetition in primary cells is required. The use of primary human astrocytes would be preferable due to the findings by Oberheim and colleagues (2009) indicating the large variance between rodent and humans astrocytes. On the other hand, rodent organotypic brain slices provide a good model for investigation of astrocytic changes in the presence of other brain cells. Advantages of this model system include the presence of microglia, which are believed to initiate and perpetuate the inflammatory cycle that occurs in AD brains (Janelsins et al., 2005; LaFerla et al., 2004). Moreover the preserved brain architecture and close association of astrocytes and neurons in slice cultures would

allow the possibility of observing resultant neuronal changes. If indeed the results observed here in U373 cells are reproducible in primary cells and organotypic slice cultures, then some stronger assumptions about the nature of the pathogenic involvement of astrocytes in neurodegenerative diseases can begin to be made. Ultimately, however, future work should focus on the design of studies that investigate the role of astrocytic changes in model animals and most importantly in AD patients.

This thesis focused on astrocytic changes in response to the proinflammatory cytokines, L-1β and TNF-α, due to their increased expression in AD. A wide range of other inflammatory mediators, including IL-6, IL-8 and MCP-1 are also upregulated in AD (Grammas and Ovase, 2001). In a recent study by Bélanger and colleagues (2011), it was shown that the metabolic phenotype of activated astrocytes varied drastically, depending on the inflammatory activator used. For example, whilst the pro-inflammatory cytokines IL-1β, TNF-α, IL-6 and IFN-γ increased glucose utilisation by primary mouse astrocytes, the anti-inflammatory cytokines IL-4 and IL-10 decreased glucose utilisation. Furthermore, various additive and synergistic effects were observed when astrocytes were treated by different pairs of cytokines. These finding suggest that although it is important to understand the pathways and cellular responses induced by individual cytokines and by defined combinations of cytokines, the observed changes may not be physiologically relevant, unless the treatment stimulus used reflects the complex mix of inflammatory mediators found in vivo. For this reason experiments utilising microglial conditioned media as the activating stimulus, co-culture experiments, organotypic brain slice experiments and inflammatory mouse models, such as the IL-

6 over-expressing transgenic mouse (Campbell et al., 1993), are likely to be important in the future elucidation of inflammation and oxidative stress induced changes in astrocytic phenotype. In addition, artificially created media mimicking approximate levels of inflammatory mediators found in AD brains might be useful for determining relevant astrocytic changes and for the identification of key stimuli or combinations of stimuli involved in the induction of these changes.

In addition to the supply of GSH substrates and energy metabolites to neurons, astrocytes play key roles in regulation of extracellular ion concentrations, brain pH, cholesterol metabolism, synaptic levels of glutamate and provision of growth factors (reviewed by Fuller et al., 2009b). It should therefore be of interest to investigate the effect of inflammatory activation on other astrocytic functions in order to further elucidate the role of astrocytes in the progression of AD.

This study identified changes in the extracellular concentration of various metabolites involved in energy metabolism and antioxidant defence. An extension of this research might therefore be to investigate changes in the expression and activity levels of enzymes and transporters involved in these and other neurosupportive functions of astrocytes. Furthermore, once identified, they could be analysed in the brains of AD patients to see if the changes are relevant to disease progression.

Finally, in regards to the TCM herbal extracts that were tested for their cytoprotective abilities, further characterisation of their beneficial effects and activity-based fractionation of extracts to identify active constituents is required.

Currently, the effect of selected extracts on astrocytic intracellular GSH levels is being studied in order to determine whether the GSH boosting ability of extracts positively correlates to cytoprotective ability of the extracts.

7.3 Conclusion

In conclusion, the findings from this thesis suggest that inflammation activated astrocytes might contribute to neurodegenerative processes through the upregulation of neurotoxic activities (i.e. release of cytokines such as IL-6 and neurotoxic compounds such as homocysteine) as well as decreases in neurosupportive or protective functions (i.e. provision of substrates for GSH synthesis and energy metabolism). Although the timing and extent to which the identified changes in astrocytic neurosupportive functions might fit into the pathogenic cascade of AD is not known, results from this thesis strongly support the hypothesis that astrocytes play a key role in disease progression. Furthermore, utilisation of a multi-compound, multi-target approach is proposed for the prevention and treatment of AD and drugs capable of restoring astrocytic function or supplementation of astrocyte-derived neuronal nutrients may be especially important.

Appendix

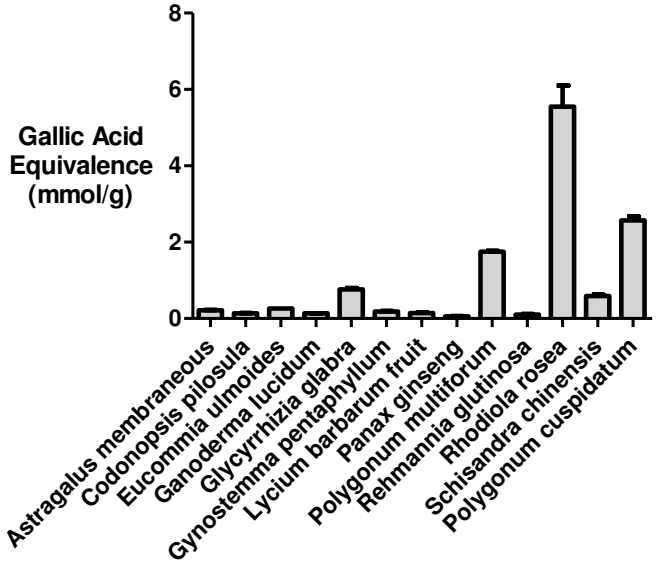

Figure 1 Results from the Folin-Ciocalteau reagent (FCR) assay. The FCR assay was used to calculate total phenols in thirteen traditional Chinese herb extracts. Data are presented as gallic acid equivalents (mean ± SEM; n = 3).

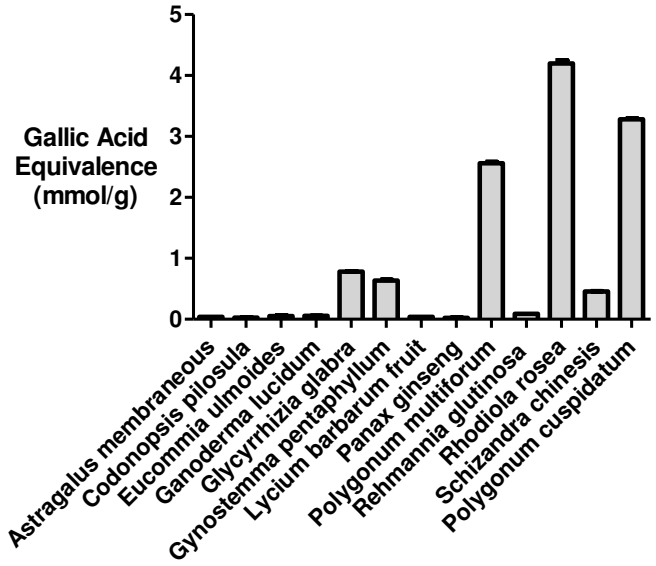

Figure 2 Results from the 2,2-diphenyl-1-picryl hydrazyl (DPPH) assay. The DPPH assay was used to estimate the DPPH radical scavenging capacity of thirteen traditional Chinese herb extracts (mean ± SEM; n = 3).

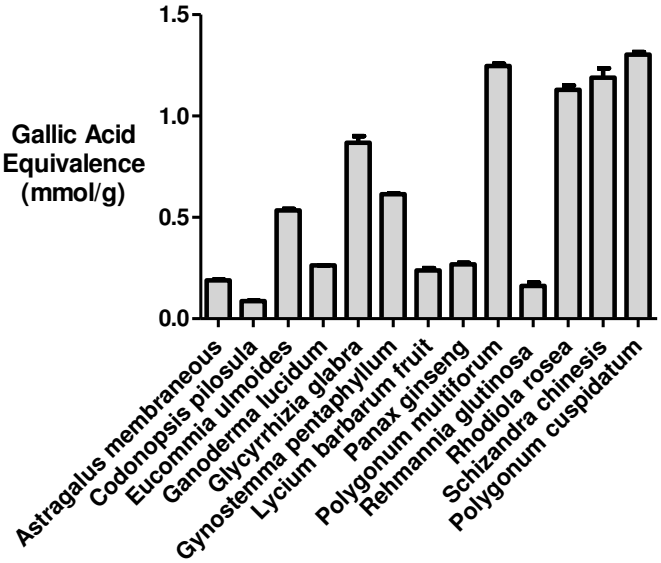

Figure 3 Results from the oxygen radical absorbance capacity (ORAC) assay. The ORAC assay was used to assess the ability of thirteen traditional Chinese herb extracts to protect fluorescein from degradation by peroxyl radicals. Data are presented as gallic acid equivalents (mean ± SEM; n = 3).

References

Abbott, N.J., 2002. Astrocyte-endothelial interactions and blood-brain barrier permeability. J Anat 200, 629-638.

Abdul Muneer, P.M., Alikunju, S., Szlachetka, A.M., Haorah, J., 2011a. Methamphetamine inhibits the glucose uptake by human neurons and astrocytes: stabilization by acetyl-L-carnitine. PLoS One 6, e19258.

Abdul Muneer, P.M., Alikunju, S., Szlachetka, A.M., Mercer, A.J., Haorah, J., 2011b. Ethanol impairs glucose uptake by human astrocytes and neurons: protective effects of acetyl-L-carnitine. Int J Physiol Pathophysiol Pharmacol 3, 48-56.

Adair, J.C., Knoefel, J.E., Morgan, N., 2001. Controlled trial of N-acetylcysteine for patients with probable Alzheimer's disease. Neurology 57, 1515-1517.

Adams, J.D., Jr., Klaidman, L.K., Odunze, I.N., Shen, H.C., Miller, C.A., 1991. Alzheimer's and Parkinson's disease. Brain levels of glutathione, glutathione disulfide, and vitamin E. Mol Chem Neuropathol 14, 213-226.

Aisen, P.S., Davis, K.L., Berg, J.D., Schafer, K., Campbell, K., Thomas, R.G., Weiner, M.F., Farlow, M.R., Sano, M., Grundman, M., Thal, L.J., 2000. A randomized controlled trial of prednisone in Alzheimer's disease. Alzheimer's Disease Cooperative Study. Neurology 54, 588-593.

Akgül, E.Ö., Cakir, E., Zcan, Ö., Yaman, H., Bilgi, C., Erbil, M.K., 2005. A Comparison of Three High Performance Liquid Chromatographic (HPLC) Methods for Measurement of Plasma Total Homocysteine. Turk J Med Sci 35, 289-295.

Akiyama, H., Barger, S., Barnum, S., Bradt, B., Bauer, J., Cole, G., Cooper, N., Eikelenboom, P., Emmerling, M., Fiebich, B., Finch, C., Frautschy, S., Griffin, W., Hampel, H., Hull, M., Landreth, G., Lue, L., Mrak, R., Mackenzie, I., McGeer, P., O'Banion, M., Pachter, J., Pasinetti, G., Plata-Salaman, C., Rogers, J., Rydel, R., Shen, Y., Streit, W., Strohmeyer, R., Tooyoma, I., Muiswinkel, F.V., Veerhuis, R., Walker, D., Webster, S., Wegrzyniak, B., Wenk, G., Wyss-Coray, T., 2000. Inflammation and Alzheimer's disease. Neurobiol Aging 21, 383-421.

Aksenov, M., Markesbery, W., 2001. Changes in thiol content and expression of glutathione redox system genes in the hippocampus and cerebellum in Alzheimer's disease. Neurosci Lett 302, 141-145.

Albrecht, J., Sonnewald, U., Waagepetersen, H.S., Schousboe, A., 2007. Glutamine in the central nervous system: function and dysfunction. Front Biosci 12, 332-343.

Alexander, G., Chen, K., Pietrini, P., Rapoport, S., Reiman, E., 2002. Longitudinal PET Evaluation of Cerebral Metabolic Decline in Dementia: A Potential Outcome Measure in Alzheimer's Disease Treatment Studies. Am J Psychiatry 159, 738-745.

Allaman, I., Belanger, M., Magistretti, P.J., 2011. Astrocyte-neuron metabolic relationships: for better and for worse. Trends Neurosci 34, 76-87.

Allaman, I., Pellerin, L., Magistretti, P.J., 2004. Glucocorticoids modulate neurotransmitter-induced glycogen metabolism in cultured cortical astrocytes. J Neurochem 88, 900-908.

Aloisi, F., Care, A., Borsellino, G., Gallo, P., Rosa, S., Bassani, A., Cabibbo, A., Testa, U., Levi, G., Peschle, C., 1992. Production of hemolymphopoietic cytokines (IL-6, IL-8, colony- stimulating factors) by normal human astrocytes in response to IL-1 beta and tumor necrosis factor-alpha. J Immunol 149, 2358-2366.

Althausen, S., Paschen, W., 2000. Homocysteine-induced changes in mRNA levels of genes coding for cytoplasmic- and endoplasmic reticulum-resident stress proteins in neuronal cell cultures. Brain Res Mol Brain Res 84, 32-40.

Alzheimer, A., 1910. Beiträge zur Kenntnis der pathologischen Neuroglia und ihrer Beziehungen zu den Abbauvorgängen im Nervengewebe. In: Nissl, F., Alzheimer, A. (Eds.), Histologische und histopathologische Arbeiten über die Grosshirnrinde mit besonderer Berücksichtigung der pathologischen Anatomie der Geisteskrankheiten. Gustav Fischer, Jena, pp. 401–562.

Anderson, C.M., Swanson, R.A., 2000. Astrocyte glutamate transport: review of properties, regulation, and physiological functions. Glia 32, 1-14.

Andrews, C., Matthias, A., Agnew, L., Reinke, N., Watson, K., Bone, K.M., Lehmann, R.P., 2007. Enhanced antioxidant effect of a herbal-nutrient complex including ascorbic acid and Polygonum cuspidatum extract (containing resveratrol). Aust J Med Med Herbalism 19, 157-161.

Araque, A., Parpura, V., Sanzgiri, R.P., Haydon, P.G., 1998. Glutamate-dependent astrocyte modulation of synaptic transmission between cultured hippocampal neurons. Eur J Neurosci 10, 2129-2142.

Aschner, M., 2000. Neuron-astrocyte interactions: implications for cellulalr energetics and antioxidant levels. Neurotoxicology 21, 1101-1107.

Aschner, M., Mullaney, K.J., Wagoner, D., Lash, L.H., Kimelberg, H.K., 1994. Intracellular glutathione (GSH) levels modulate mercuric chloride (MC)- and methylmercuric chloride (MeHgCl)-induced amino acid release from neonatal rat primary astrocytes cultures. Brain Res 664, 133-140.

Aubert, A., Costalat, R., Magistretti, P.J., Pellerin, L., 2005. Brain lactate kinetics: Modeling evidence for neuronal lactate uptake upon activation. PNAS 102, 16448-16453.

Bannai, S., 1984. Transport of cystine and cysteine in mammalian cells. Biochim Biophys Acta 779, 289-306.

Bannai, S., Kitamura, E., 1980. Transport interaction of L-cystine and L-glutamate in human diploid fibroblasts in culture. J Biol Chem 255, 2372-2376.

Bannai, S., Tateishi, N., 1986. Role of membrane transport in metabolism and function of glutathione in mammals. J Membr Biol 89, 1-8.

Barnett, N.L., Pow, D.V., Robinson, S.R., 2000. Inhibition of Müller cell glutamine synthetase rapidly impairs the retinal response to light. Glia 30, 64-73.

Barros, L.F., Porras, O.H., Bittner, C.X., 2005. Why glucose transport in the brain matters for PET. Trends in Neurosci. 28, 117-119.

Bass, N.M., 2007. Review article: the current pharmacological therapies for hepatic encephalopathy. Aliment Pharmacol Ther 25 Suppl 1, 23-31.

Beach, T., McGeer, E., 1988. Lamina-specific arrangement of astrocytic gliosis and senile plaques in Alzheimer's disease visual cortex. Brain Res 463, 357-361.

Bélanger, M., Allaman, I., Magistretti, P.J., 2011. Differential effects of pro- and anti-inflammatory cytokines alone or in combinations on the metabolic profile of astrocytes. J Neurochem 116, 564-576.

Bemeur, C., Vaquero, J., Desjardins, P., Butterworth, R.F., 2010. N-acetylcysteine attenuates cerebral complications of non-acetaminophen-induced acute liver failure in mice: antioxidant and anti-inflammatory mechanisms. Metab Brain Dis 25, 241-249.

Benarroch, E.E., 2005. Neuron-astrocyte interactions: partnership for normal function and disease in the central nervous system. Mayo Clin. Proc. 80, 1326-1338.

Bender, A.S., Reichelt, W., Norenberg, M.D., 2000. Characterization of cystine uptake in cultured astrocytes. Neurochem Int 37, 269-276.

Bensky, D., Clavey, S., Stoger, E., 2004. Chinese Herbal Medicine: Materia Medica, 3rd Edn. Eastland Press, Seattle.

Benveniste, E.N., Kwon, J., Chung, W.J., Sampson, J., Pandya, K., Tang, L.P., 1994. Differential modulation of astrocyte cytokine gene expression by TGF-beta. J Immunol 153, 5210-5221.

Bezzi, P., Domercq, M., Brambilla, L., Galli, R., Schols, D., De Clercq, E., Vescovi, A., Bagetta, G., Kollias, G., Meldolesi, J., Volterra, A., 2001. CXCR4-activated astrocyte glutamate release via TNFalpha: amplification by microglia triggers neurotoxicity. Nat Neurosci 4, 702-710.

Bi, M., Tong, S., Zhang, Z., Ma, Q., Zhang, S., Luo, Z., Zhang, Y., Li, X., Wang, D., 2011. Changes in cerebral glucose metabolism in patients with mild-to-moderate Alzheimer's disease: A pilot study with the Chinese herbal medicine fuzhisan. Neurosci Lett.

Birnbaum, M.J., 1989. Identification of a novel gene encoding an insulin-responsive glucose transporter protein. Cell 57, 305-315.

Birnbaum, M.J., Haspel, H.C., Rosen, O.M., 1986. Cloning and characterization of a cDNA encoding the rat brain glucose-transporter protein. Proc Natl Acad Sci U S A 83, 5784-5788.

Biroccio, A., Del Boccio, P., Panella, M., Bernardini, S., Di Ilio, C., Gambi, D., Stanzione, P., Sacchetta, P., Bernardi, G., Martorana, A., Federici, G., Stefani, A., Urbani, A., 2006. Differential post-translational modifications of transthyretin in Alzheimer's disease: a study of the cerebral spinal fluid. Proteomics 6, 2305-2313.

Bittar, P.G., Charnay, Y., Pellerin, L., Bouras, C., Magistretti, P.J., 1996. Selective distribution of lactate dehydrogenase isoenzymes in neurons and astrocytes of human brain. J Cereb Blood Flow Metab 16, 1079-1089.

Bittner, C.X., Loaiza, A., Ruminot, I., Larenas, V., Sotelo-Hitschfeld, T., Gutierrez, R., Cordova, A., Valdebenito, R., Frommer, W.B., Barros, L.F., 2010. High resolution measurement of the glycolytic rate. Front Neuroenergetics 2.

Bjerring, P.N., Eefsen, M., Hansen, B.A., Larsen, F.S., 2009. The brain in acute liver failure. A tortuous path from hyperammonemia to cerebral edema. Metab Brain Dis 24, 5-14.

Blois, M.S., 1958. Antioxidant determinations by the use of a stable free radical. Nature 181, 1199-1200.

Blum-Degen, D., Muller, T., Kuhn, W., Gerlach, M., Przuntek, H., Riederer, P., 1995. Interleukin-1 beta and interleukin-6 are elevated in the cerebrospinal fluid of Alzheimer's and de novo Parkinson's disease patients. Neurosci Lett 202, 17-20.

Bogdanovic, N., Zilmer, M., Zilmer, K., Rehema, A., Karelson, E., 2001. The Swedish APP670/671 Alzheimer's disease mutation: the first evidence for strikingly increased oxidative injury in the temporal inferior cortex. Dement Geriatr Cogn Disord 12, 364-370.

Bosoi, C.R., Rose, C.F., 2009. Identifying the direct effects of ammonia on the brain. Metab Brain Dis 24, 95-102.

Bouligand, J., Deroussent, A., Paci, A., Morizet, J., Vassal, G., 2006. Liquid chromatography-tandem mass spectrometry assay of reduced and oxidized glutathione and main precursors in mice liver. J Chromatogr B Analyt Technol Biomed Life Sci 832, 67-74.

Bouzier-Sore, A.K., Serres, S., Canioni, P., Merle, M., 2003. Lactate involvement in neuron-glia metabolic interaction: 13C-NMR spectroscopy contribution. Biochimie 85, 841-848.

Bouzier, A.K., Goodwin, R., de Gannes, F.M., Valeins, H., Voisin, P., Canioni, P., Merle, M., 1998a. Compartmentation of lactate and glucose metabolism in C6 glioma cells. A 13c and 1H NMR study. J Biol Chem 273, 27162-27169.

Bouzier, A.K., Voisin, P., Goodwin, R., Canioni, P., Merle, M., 1998b. Glucose and lactate metabolism in C6 glioma cells: evidence for the preferential utilization of lactate for cell oxidative metabolism. Dev Neurosci 20, 331-338.

Bradford, M.M., 1976. A rapid and sensitive method for the quantitation of microgram quantities of protein utilizing the principle of protein-dye binding. Anal Biochem 72, 248-254.

Bragin, D.E., Zhou, B., Ramamoorthy, P., Muller, W.S., Connor, J.A., Shi, H., 2010. Differential changes of glutathione levels in astrocytes and neurons in ischemic brains by two-photon imaging. J Cereb Blood Flow Metab 30, 734-738.

Branconnier, R.J., Dessain, E.C., McNiff, M.E., Cole, J.O., 1986. Blood ammonia and Alzheimer's disease. Am J Psychiatry 143, 1313-1314.

Brannan, T.S., Maker, H.S., Weiss, C., Cohen, G., 1980. Regional distribution of glutathione peroxidase in the adult rat brain. J Neurochem 35, 1013-1014.

Breitner, J.C., Gau, B.A., Welsh, K.A., Plassman, B.L., McDonald, W.M., Helms, M.J., Anthony, J.C., 1994. Inverse association of anti-inflammatory treatments and Alzheimer's disease: initial results of a co-twin control study. Neurology 44, 227-232.

Brockmann, K., 2009. The expanding phenotype of GLUT1-deficiency syndrome. Brain Dev 31, 545-552.

Brown, A.M., Ransom, B.R., 2007. Astrocyte glycogen and brain energy metabolism. Glia 55, 1263-1271.

Buranrat, B., Prawan, A., Kukongviriyapan, V., 2008. Optimization of resazurin-based assay for cytotoxicity test in cholangiocarcinoma cells. KKU Res J 8, 73-80.

Butterfield, D., 2004. Proteomics: a new approach to investigate oxidative stress in Alzheimer's disease brain. Brain Res 1000, 1-7.

Butterfield, D.A., Perluigi, M., Sultana, R., 2006. Oxidative stress in Alzheimer's disease brain: new insights from redox proteomics. Eur J Pharmacol 545, 39-50.

Cacabelos, R., Barquero, M., Garcia, P., Alvarez, X.A., Varela de Seijas, E., 1991. Cerebrospinal fluid interleukin-1 beta (IL-1 beta) in Alzheimer's disease and neurological disorders. Methods Find Exp Clin Pharmacol 13, 455-458.

Cai, Y., Luo, Q., Sun, M., Corke, H., 2004. Antioxidant activity and phenolic compounds of 112 traditional Chinese medicinal plants associated with anticancer. Life Sci 74, 2157-2184.

Campbell, I.L., Abraham, C.R., Masliah, E., Kemper, P., Inglis, J.D., Oldstone, M.B., Mucke, L., 1993. Neurologic disease induced in transgenic mice by cerebral overexpression of interleukin 6. Proc Natl Acad Sci U S A 90, 10061-10065.

Cao, G., Alessio, H.M., Cutler, R.G., 1993. Oxygen-radical absorbance capacity assay for antioxidants. Free Radical Biology and Medicine 14, 303-311.

Chan, C.C., 2004. Analytical method validation and instrument performance verification. John Wiley & Sons, Inc., New Jersey.

Chan, J.Y., Kwong, M., 2000. Impaired expression of glutathione synthetic enzyme genes in mice with targeted deletion of the Nrf2 basic-leucine zipper protein. Biochim Biophys Acta 1517, 19-26.

Chanas, S.A., Jiang, Q., McMahon, M., McWalter, G.K., McLellan, L.I., Elcombe, C.R., Henderson, C.J., Wolf, C.R., Moffat, G.J., Itoh, K., Yamamoto, M., Hayes, J.D., 2002. Loss of the Nrf2 transcription factor causes a marked reduction in constitutive and inducible expression of the glutathione S-transferase Gsta1, Gsta2, Gstm1, Gstm2, Gstm3 and Gstm4 genes in the livers of male and female mice. Biochem J 365, 405-416.

Chen, G., Chen, K.S., Kobayashi, D., Barbour, R., Motter, R., Games, D., Martin, S.J., Morris, R.G., 2007. Active beta-amyloid immunization restores spatial learning in PDAPP mice displaying very low levels of beta-amyloid. J Neurosci 27, 2654-2662.

Chen, X.L., Kunsch, C., 2004. Induction of cytoprotective genes through Nrf2/antioxidant response element pathway: a new therapeutic approach for the treatment of inflammatory diseases. Curr Pharm Des 10, 879-891.

Chen, Y., Shertzer, H.G., Schneider, S.N., Nebert, D.W., Dalton, T.P., 2005. Glutamate cysteine ligase catalysis: dependence on ATP and modifier subunit for regulation of tissue glutathione levels. J Biol Chem 280, 33766-33774.

Cheng, J.T., 2000. Review: drug therapy in Chinese traditional medicine. J Clin Pharmacol 40, 445-450.

Choi, J.J., Kim, W.K., 1998. Potentiated glucose deprivation-induced death of astrocytes after induction of iNOS. J Neurosci Res 54, 870-875.

Chu, X., Sun, A., Liu, R., 2005. Preparative isolation and purification of five compounds from the Chinese medicinal herb Polygonum cuspidatum Sieb. et Zucc by high-speed counter-current chromatography. J Chromatogr A 1097, 33-39.

Conroy, S.M., Nguyen, V., Quina, L.A., Blakely-Gonzales, P., Ur, C., Netzeband, J.G., Prieto, A.L., Gruol, D.L., 2004. Interleukin-6 produces neuronal loss in developing cerebellar granule neuron cultures. J Neuroimmunol 155, 43-54.

Cooper, A.J., Pulsinelli, W.A., Duffy, T.E., 1980. Glutathione and ascorbate during ischemia and postischemic reperfusion in rat brain. J Neurochem 35, 1242-1245.

Copple, I.M., Goldring, C.E., Kitteringham, N.R., Park, B.K., 2008. The Nrf2-Keap1 defence pathway: role in protection against drug-induced toxicity. Toxicology 246, 24-33.

Correa, F., Ljunggren, E., Mallard, C., Nilsson, M., Weber, S.G., Sandberg, M., 2011. The Nrf2-inducible antioxidant defense in astrocytes can be both up- and down-regulated by activated microglia:Involvement of p38 MAPK. Glia 59, 785-799.

Csernansky, J.G., Bardgett, M.E., Sheline, Y.I., Morris, J.C., Olney, J.W., 1996. CSF excitatory amino acids and severity of illness in Alzheimer's disease. Neurology 46, 1715-1720.

Cui, M., Huang, Y., Tian, C., Zhao, Y., Zheng, J., 2011. FOXO3a inhibits TNF-alpha- and IL-1beta-induced astrocyte proliferation:Implication for reactive astrogliosis. Glia 59, 641-654.

Davis, E.A., Morris, D.J., 1991. Medicinal uses of licorice through the millennia: the good and plenty of it. Mol Cell Endo 78, 1-6.

Desagher, S., Glowinski, J., Premont, J., 1996. Astrocytes protect neurons from hydrogen peroxide toxicity. J Neurosci 16, 2553-2562.

Desai, K.M., Wu, L., 2008. Free radical generation by methylglyoxal in tissues. Drug Metabol Drug Interact 23, 151-173.

Dickson, P.W., Howlett, G.J., Schreiber, G., 1985. Rat transthyretin (prealbumin). Molecular cloning, nucleotide sequence, and gene expression in liver and brain. J Biol Chem 260, 8214-8219.

Dienel, G.A., Cruz, N.F., 2008. Imaging brain activation: simple pictures of complex biology. Ann N Y Acad Sci 1147, 139-170.

DiNuzzo, M., Mangia, S., Maraviglia, B., Giove, F., 2010. Glycogenolysis in astrocytes supports blood-borne glucose channeling not glycogen-derived lactate shuttling to neurons: evidence from mathematical modeling. J Cereb Blood Flow Metab 30, 1895-1904.

DiPatre, P.L., Gelman, B.B., 1997. Microglial cell activation in aging and Alzheimer disease: partial linkage with neurofibrillary tangle burden in the hippocampus. J Neuropathol Exp Neurol 56, 143-149.

Djurhuus, R., Svardal, A.M., Ueland, P.M., 1990. Cysteamine increases homocysteine export and glutathione content by independent mechanisms in C3H/10T1/2 cells. Mol Pharmacol 38, 327-332.

Dong, Y., Benveniste, E., 2001. Immune function of astrocytes. Glia 36, 180-190.

Dringen, R., 2000. Metabolism and functions of glutathione in brain. Prog Neurobiol 62, 649-671.

Dringen, R., Gutterer, J.M., Gros, C., Hirrlinger, J., 2001. Aminopeptidase N mediates the utilization of the GSH precursor CysGly by cultured neurons. J Neurosci Res 66, 1003-1008.

Dringen, R., Gutterer, J.M., Hirrlinger, J., 2000. Glutathione in brain metabolic interaction between astrocytes and neurons in the defense against reactive oxygen species. Eur. J. Biochem. 267, 4912-4916.

Dringen, R., Hamprecht, B., 1999. N-acetylcysteine, but not methionine or 2-oxothiazolidine-4-carboxylate, serves as cysteine donor for the synthesis of glutathione in cultured neurons derived from embryonal rat brain. Neurosci Lett 259, 79-82.

Dringen, R., Hirrlinger, J., 2003. Glutathione pathways in the brain. Biol Chem 384, 505-516.

Dringen, R., Kranich, O., Hamprecht, B., 1997a. The gamma-glutamyl transpeptidase inhibitor acivicin preserves glutathione released by astroglial cells in culture. Neurochem Res 22, 727-733.

Dringen, R., Kranich, O., Loschmann, P.A., Hamprecht, B., 1997b. Use of dipeptides for the synthesis of glutathione by astroglia-rich primary cultures. J Neurochem 69, 868-874.

Dringen, R., Kussmaul, L., Gutterer, J.M., Hirrlinger, J., Hamprecht, B., 1999a. The glutathione system of peroxide detoxification is less efficient in neurons than in astroglial cells. J Neurochem 72, 2523-2530.

Dringen, R., Pfeiffer, B., Hamprecht, B., 1999b. Synthesis of the antioxidant glutathione in neurons: supply by astrocytes of CysGly as precursor for neuronal glutathione. J Neurosci 19, 562-569.

Drogemuller, K., Helmuth, U., Brunn, A., Sakowicz-Burkiewicz, M., Gutmann, D.H., Mueller, W., Deckert, M., Schluter, D., 2008. Astrocyte gp130 expression is critical for the control of Toxoplasma encephalitis. J Immunol 181, 2683-2693.

Dwyer, B.E., Raina, A.K., Perry, G., Smith, M.A., 2004. Homocysteine and Alzheimer's disease: a modifiable risk? Free Radic Biol Med 36, 1471-1475.

Edison, P., Archer, H.A., Hinz, R., Hammers, A., Pavese, N., Tai, Y.F., Hotton, G., Cutler, D., Fox, N., Kennedy, A., Rossor, M., Brooks, D.J., 2007. Amyloid, hypometabolism, and cognition in Alzheimer disease: an [11C]PIB and [18F]FDG PET study. Neurology 68, 501-508.

Edwards, M.M., Robinson, S.R., 2006. TNF alpha affects the expression of GFAP and S100B: implications for Alzheimer's disease. J Neural Transm 113, 1709-1715.

Eikelenboom, P., Veerhuis, R., Scheper, W., Rozemuller, A.J., van Gool, W.A., Hoozemans, J.J., 2006. The significance of neuroinflammation in understanding Alzheimer's disease. J Neural Transm 113, 1685-1695.

Engelborghs, S., De Brabander, M., De Cree, J., D'Hooge, R., Geerts, H., Verhaegen, H., De Deyn, P.P., 1999. Unchanged levels of interleukins, neopterin, interferon-gamma and tumor necrosis factor-alpha in cerebrospinal fluid of patients with dementia of the Alzheimer type. Neurochem Int 34, 523-530.

Erlichman, J.S., Hewitt, A., Damon, T.L., Hart, M., Kurascz, J., Li, A., Leiter, J.C., 2008. Inhibition of monocarboxylate transporter 2 in the retrotrapezoid nucleus in rats: a test of the astrocyte-neuron lactate-shuttle hypothesis. J Neurosci 28, 4888-4896.

Felipo, V., Butterworth, R.F., 2002a. Mitochondrial dysfunction in acute hyperammonemia. Neurochem Int 40, 487-491.

Felipo, V., Butterworth, R.F., 2002b. Neurobiology of ammonia. Prog Neurobiol 67, 259-279.

Fernandes, S.P., Dringen, R., Lawen, A., Robinson, S.R., 2010. Neurones express glutamine synthetase when deprived of glutamine or interaction with astrocytes. J Neurochem, 1527-1536.

Ferretti, M.T., Cuello, A.C., 2011. Does a pro-inflammatory process precede Alzheimer's disease and mild cognitive impairment? Curr Alzheimer Res 8, 164-174.

Fillit, H., Ding, W.H., Buee, L., Kalman, J., Altstiel, L., Lawlor, B., Wolf-Klein, G., 1991. Elevated circulating tumor necrosis factor levels in Alzheimer's disease. Neurosci Lett 129, 318-320.

Filosa, J.A., Bonev, A.D., Nelson, M.T., 2004. Calcium dynamics in cortical astrocytes and arterioles during neurovascular coupling. Circ Res 95, e73-81.

Finkel, T., Holbrook, N.J., 2000. Oxidants, oxidative stress and the biology of ageing. Nature 408, 239-247.

Frederich, M., Wauters, J.N., Tits, M., Jason, C., de Tullio, P., Van der Heyden, Y., Fan, G., Angenot, L., 2011. Quality assessment of Polygonum cuspidatum and Polygonum multiflorum by 1H NMR metabolite fingerprinting and profiling analysis. Planta Med 77, 81-86.

Freemantle, E., Vandal, M., Tremblay-Mercier, J., Tremblay, S., Blachère, J.C., Bégin, M.E., Brenna, J.T., Windust, A., Cunnane, S.C., 2006. Omega-3 fatty acids, energy substrates, and brain function during aging. Prostaglandins Leukot Essent Fatty Acids 75, 213-220.

Fukuyama, R., Izumoto, T., Fushiki, S., 2001. The cerebrospinal fluid level of glial fibrillary acidic protein is increased in cerebrospinal fluid from Alzheimer's disease patients and correlates with severity of dementia. Eur Neurol 46, 35-38.

Fuller, S., Munch, G., Steele, M., 2009a. Activated astrocytes: a therapeutic target in Alzheimer's disease? Expert Rev Neurother 9, 1585-1594.

Fuller, S., Steele, M., Munch, G., 2009b. Activated astroglia during chronic inflammation in Alzheimer's disease--do they neglect their neurosupportive roles? Mutat Res 690, 40-49.

Gadea, A., Schinelli, S., Gallo, V., 2008. Endothelin-1 regulates astrocyte proliferation and reactive gliosis via a JNK/c-Jun signaling pathway. J Neurosci 28, 2394-2408.

Gandhi, G.K., Cruz, N.F., Ball, K.K., Dienel, G.A., 2009. Astrocytes are poised for lactate trafficking and release from activated brain and for supply of glucose to neurons. J Neurochem 111, 522-536.

Ganske, F., Dell, E.J., 2006. ORAC assay on the FLUOstar OPTIMA to determine antioxidant capacity. Application Note 148. BMG LABTECH, Offenburg.

Gao, C.F., Xie, Q., Su, Y.L., Koeman, J., Khoo, S.K., Gustafson, M., Knudsen, B.S., Hay, R., Shinomiya, N., Vande Woude, G.F., 2005. Proliferation and invasion: plasticity in tumor cells. Proc Natl Acad Sci U S A 102, 10528-10533.

Garcia-Cazorla, A., Rabier, D., Touati, G., Chadefaux-Vekemans, B., Marsac, C., de Lonlay, P., Saudubray, J.M., 2006. Pyruvate carboxylase deficiency: metabolic characteristics and new neurological aspects. Ann Neurol 59, 121-127.

Garrett, R.H., Grisham, C.M., 2005. Biochemistry 3rd Ed. Thomson Brooks-Cole, Belmont.

Gavillet, M., Allaman, I., Magistretti, P., 2008. Modulation of astrocytic metabolic phenotype by proinflammatory cytokines. Glia 56, 975-989.

Gegg, M.E., Clark, J.B., Heales, S.J., 2005. Co-culture of neurones with glutathione deficient astrocytes leads to increased neuronal susceptibility to nitric oxide and increased glutamate-cysteine ligase activity. Brain Res 1036, 1-6.

Ghimire, B.K., Seong, E.S., Kim, E.H., Ghimeray, A.K., Yu, C.Y., Ghimire, B.K., Chung, I.M., 2011. A comparative evaluation of the antioxidant activity of some medicinal plants popularly used in Nepal. J Med Plant Res 5, 1884-1891.

Gibbs, M.E., O'Dowd, B.S., Hertz, L., Robinson, S.R., Sedman, G.L., Ng, K.T., 1996. Inhibition of glutamine synthetase activity prevents memory consolidation. Brain Res Cogn Brain Res 4, 57-64.

Gibson, G.E. (Ed.), 2007. Brain energetics: integration of molecular and cellular processes. Springer.

Gilgun-Sherki, Y., Melamed, E., Offen, D., 2006. Anti-inflammatory drugs in the treatment of neurodegenerative diseases: current state. Curr Pharm Des 12, 3509-3519.

Gill, J., McKenna, W., Camm, A., 1995. Free radicals irreversibly decrease Ca2+ currents in isolated guinea-pig ventricular myocytes. Eur J Pharmacol 292, 337-340.

Gillis, C.N., 1997. Panax ginseng pharmacology: A nitric oxide link? Biochemical Pharmacology 54, 1-8.

Gitter, B.D., Cox, L.M., Rydel, R.E., May, P.C., 1995. Amyloid beta peptide potentiates cytokine secretion by interleukin-1 beta-activated human astrocytoma cells. Proc Natl Acad Sci U S A 92, 10738-10741.

Golgi, C., 1885. Sulla fina anatomia degli organi centrali del sisterma nervoso. Riv Sper Fremiat Med Leg Alienazione

Ment 11, 72-123.

Gorg, B., Morwinsky, A., Keitel, V., Qvartskhava, N., Schror, K., Haussinger, D., 2010. Ammonia triggers exocytotic release of L-glutamate from cultured rat astrocytes. Glia 58, 691-705.

Grammas, P., Ovase, R., 2001. Inflammatory factors are elevated in brain microvessels in Alzheimer's disease. Neurobiol Aging 22, 837-842.

Griffin, W.S., Stanley, L.C., Ling, C., White, L., MacLeod, V., Perrot, L.J., White, C.L., 3rd, Araoz, C., 1989. Brain interleukin 1 and S-100 immunoreactivity are elevated in Down syndrome and Alzheimer disease. Proc Natl Acad Sci U S A 86, 7611-7615.

Gu, M., Owen, A.D., Toffa, S.E., Cooper, J.M., Dexter, D.T., Jenner, P., Marsden, C.D., Schapira, A.H., 1998. Mitochondrial function, GSH and iron in neurodegeneration and Lewy body diseases. J Neurol Sci 158, 24-29.

Hager, K., Kenklies, M., McAfoose, J., Engel, J., Munch, G., 2007. Alpha-lipoic acid as a new treatment option for Alzheimer's disease-a 48 months follow-up analysis. J Neural Transm Suppl, 189-193.

Hager, K., Marahrens, A., Kenklies, M., Riederer, P., Munch, G., 2001. Alpha-lipoic acid as a new treatment option for Azheimer type dementia. Arch Gerontol Geriatr 32, 275-282.

Hald, A., Lotharius, J., 2005. Oxidative stress and inflammation in Parkinson's disease: is there a causal link? Exp Neurol 193, 279-290.

Hamaguchi, T., Ono, K., Yamada, M., 2011. REVIEW: Curcumin and Alzheimer's disease. CNS Neurosci Ther 16, 285-297.

Han, J.H., Koh, W., Lee, H.J., Lee, E.O., Lee, S.J., Khil, J.H., Kim, J.T., Jeong, S.J., Kim, S.H., 2011. Analgesic and anti-inflammatory effects of ethyl acetate fraction of Polygonum cuspidatum in experimental animals. Immunopharmacol Immunotoxicol [Epub ahead of print].

Harder, D.R., Alkayed, N.J., Lange, A.R., Gebremedhin, D., Roman, R.J., 1998. Functional hyperemia in the brain: hypothesis for astrocyte-derived vasodilator metabolites. Stroke 29, 229-234.

Harvey, C.J., Thimmulappa, R.K., Singh, A., Blake, D.J., Ling, G., Wakabayashi, N., Fujii, J., Myers, A., Biswal, S., 2009. Nrf2-regulated glutathione recycling independent of biosynthesis is critical for cell survival during oxidative stress. Free Radic Biol Med 46, 443-453.

Hayashi, A., Suzuki, H., Itoh, K., Yamamoto, M., Sugiyama, Y., 2003. Transcription factor Nrf2 is required for the constitutive and inducible expression of multidrug resistance-associated protein 1 in mouse embryo fibroblasts. Biochem Biophys Res Commun 310, 824-829.

Heinrich, M., Lee Teoh, H., 2004. Galanthamine from snowdrop--the development of a modern drug against Alzheimer's disease from local Caucasian knowledge. J Ethnopharmacol 92, 147-162.

Hernanz, A., De la Fuente, M., Navarro, M., Frank, A., 2007. Plasma aminothiol compounds, but not serum tumor necrosis factor receptor II and soluble receptor for advanced glycation end products, are related to the cognitive impairment in

Alzheimer's disease and mild cognitive impairment patients. Neuroimmunomodulation 14, 163-167.

Hertz, L., 1989. Is Alzheimer's disease an anterograde degeneration, originating in the brainstem, and disrupting metabolic and functional interactions between neurons and glial cells? Brain Res Brain Res Rev 14, 335-353.

Hertz, L., Dringen, R., Schousboe, A., Robinson, S.R., 1999. Astrocytes: glutamate producers for neurons. J Neurosci Res 57, 417-428.

Hertz, L., Peng, L., Dienel, G.A., 2007. Energy metabolism in astrocytes: high rate of oxidative metabolism and spatiotemporal dependence on glycolysis/glycogenolysis. J Cereb Blood Flow Metab 27, 219-249.

Hewavitharana, A.K., 2009. Internal Standard - Friend or Foe? Critical Reviews in Analytical Chemistry 39, 272-275.

Heyser, C.J., Masliah, E., Samimi, A., Campbell, I.L., Gold, L.H., 1997. Progressive decline in avoidance learning paralleled by inflammatory neurodegeneration in transgenic mice expressing interleukin 6 in the brain. Proc Natl Acad Sci U S A 94, 1500-1505.

Higashi, K., Fujita, A., Inanobe, A., Tanemoto, M., Doi, K., Kubo, T., Kurachi, Y., 2001. An inwardly rectifying K(+) channel, Kir4.1, expressed in astrocytes surrounds synapses and blood vessels in brain. Am J Physiol Cell Physiol 281, C922-931.

Ho, P.I., Ortiz, D., Rogers, E., Shea, T.B., 2002. Multiple aspects of homocysteine neurotoxicity: glutamate excitotoxicity, kinase hyperactivation and DNA damage. J Neurosci Res 70, 694-702.

Ho, Y.S., So, K.F., Chang, R.C., 2010. Anti-aging herbal medicine--how and why can they be used in aging-associated neurodegenerative diseases? Ageing Res Rev 9, 354-362.

Holmes, C., Boche, D., Wilkinson, D., Yadegarfar, G., Hopkins, V., Bayer, A., Jones, R.W., Bullock, R., Love, S., Neal, J.W., Zotova, E., Nicoll, J.A., 2008. Long-term effects of Abeta42 immunisation in Alzheimer's disease: follow-up of a randomised, placebo-controlled phase I trial. Lancet 372, 216-223.

Hou, J.P., Jin, Y., 2005. The healing power of Chinese herbs and medicinal recipes. The Haworth Integrative Healing Press, Binghamton.

Howes, M.J., Houghton, P.J., 2003. Plants used in Chinese and Indian traditional medicine for improvement of memory and cognitive function. Pharmacol Biochem Behav 75, 513-527.

Hu, S., Sheng, W.S., Peterson, P.K., Chao, C.C., 1995. Differential regulation by cytokines of human astrocyte nitric oxide production. Glia 15, 491-494.

Huang, D., Ou, B., Prior, R.L., 2005a. The chemistry behind antioxidant capacity assays. J Agric Food Chem 53, 1841-1856.

Huang, G., Dragan, M., Freeman, D., Wilson, J.X., 2005b. Activation of catechol-O-methyltransferase in astrocytes stimulates homocysteine synthesis and export to neurons. Glia 51, 47-55.

Huang, R., Shuaib, A., Hertz, L., 1993. Glutamate uptake and glutamate content in primary cultures of mouse astrocytes during anoxia, substrate deprivation and simulated ischemia under normothermic and hypothermic conditions. Brain Res 618, 346-351.

Huber, L., 1998. Validation and Qualification in Analytical Laboratories. Interpharm Press, East Englewood, CO, USA.

Hull, M., Berger, M., Heneka, M., 2006. Disease-modifying therapies in Alzheimer's disease: how far have we come? Drugs 66, 2075-2093.

Hultberg, M., Hultberg, B., 2006. The effect of different antioxidants on glutathione turnover in human cell lines and their interaction with hydrogen peroxide. Chem. Biol. Interact. 163, 192-198.

Hyder, F., Patel, A.B., Gjedde, A., Rothman, D.L., Behar, K.L., Shulman, R.G., 2006. Neuronal-glial glucose oxidation and glutamatergic-GABAergic function. J Cereb Blood Flow Metab 26, 865-877.

ICH, 2005. Validation of Analytical Procedures: Text and Methodology. CPMP/ICH281/95.

Issels, R.D., Nagele, A., 1989. Promotion of cystine uptake, increase of glutathione biosynthesis, and modulation of glutathione status by S-2-(3-aminopropylamino)ethyl phosphorothioic acid (WR-2721) in Chinese hamster cells. Cancer Res 49, 2082-2086.

Itoh, K., Wakabayashi, N., Katoh, Y., Ishii, T., Igarashi, K., Engel, J.D., Yamamoto, M., 1999. Keap1 represses nuclear activation of antioxidant responsive elements by Nrf2 through binding to the amino-terminal Neh2 domain. Genes Dev 13, 76-86.

Ivanov, A., Mukhtarov, M., Bregestovski, P., Zilberter, Y., 2011. Lactate Effectively Covers Energy Demands during Neuronal Network Activity in Neonatal Hippocampal Slices. Front Neuroenergetics 3, 2.

Jackman, N.A., Uliasz, T.F., Hewett, J.A., Hewett, S.J., 2011. Regulation of system x(c)(-)activity and expression in astrocytes by interleukin-1beta: implications for hypoxic neuronal injury. Glia 58, 1806-1815.

Janelsins, M.C., Mastrangelo, M.A., Oddo, S., LaFerla, F.M., Federoff, H.J., Bowers, W.J., 2005. Early correlation of microglial activation with enhanced tumor necrosis factor-alpha and monocyte chemoattractant protein-1 expression specifically within the entorhinal cortex of triple transgenic Alzheimer's disease mice. J Neuroinflammation 2, 23.

Jawan, B., Goto, S., Pan, T.L., Lai, C.Y., Luk, H.N., Eng, H.L., Lin, Y.C., Chen, Y.S., Lan, K.M., Hsieh, S.W., Wang, C.C., Cheng, Y.F., Chen, C.L., 2003. The

protective mechanism of magnolol, a Chinese herb drug, against warm ischemia-reperfusion injury of rat liver. J Surg Res 110, 378-382.

Jiang, W., Desjardins, P., Butterworth, R.F., 2009. Direct evidence for central proinflammatory mechanisms in rats with experimental acute liver failure: protective effect of hypothermia. J Cereb Blood Flow Metab 29, 944-952.

Jimenez-Jimenez, F.J., Molina, J.A., Gomez, P., Vargas, C., de Bustos, F., Benito-Leon, J., Tallon-Barranco, A., Orti-Pareja, M., Gasalla, T., Arenas, J., 1998. Neurotransmitter amino acids in cerebrospinal fluid of patients with Alzheimer's disease. J Neural Transm 105, 269-277.

Jin, Y., Brennan, L., 2008. Effects of homocysteine on metabolic pathways in cultured astrocytes. Neurochem Int 52, 1410-1415.

Johnstone, M., Gearing, A.J., Miller, K.M., 1999. A central role for astrocytes in the inflammatory response to beta-amyloid; chemokines, cytokines and reactive oxygen species are produced. J Neuroimmunol 93, 182-193.

Joshi, G., Hardas, S., Sultana, R., St Clair, D.K., Vore, M., Butterfield, D.A., 2007. Glutathione elevation by gamma-glutamyl cysteine ethyl ester as a potential therapeutic strategy for preventing oxidative stress in brain mediated by in vivo administration of adriamycin: Implication for chemobrain. J Neurosci Res 85, 497-503.

Jurkowska, H., Uchacz, T., Roberts, J., Wrobel, M., 2011. Potential therapeutic advantage of ribose-cysteine in the inhibition of astrocytoma cell proliferation. Amino Acids 41, 131-139.

Kahkonen, M.P., Hopia, A.I., Vuorela, H.J., Rauha, J.P., Pihlaja, K., Kujala, T.S., Heinonen, M., 1999. Antioxidant activity of plant extracts containing phenolic compounds. J Agric Food Chem 47, 3954-3962.

Kaiser, E., Schoenknecht, P., Kassner, S., Hildebrandt, W., Kinscherf, R., Schroeder, J., 2010. Cerebrospinal fluid concentrations of functionally important amino acids and metabolic compounds in patients with mild cognitive impairment and Alzheimer's disease. Neurodegener Dis 7, 251-259.

Kalaria, R.N., Harik, S.I., 1989a. Abnormalities of the glucose transporter at the blood-brain barrier and in brain in Alzheimer's disease. Prog Clin Biol Res 317, 415-421.

Kalaria, R.N., Harik, S.I., 1989b. Reduced glucose transporter at the blood-brain barrier and in cerebral cortex in Alzheimer disease. J Neurochem 53, 1083-1088.

Kamencic, H., Lyon, A., Paterson, P.G., Juurlink, B.H., 2000. Monochlorobimane fluorometric method to measure tissue glutathione. Anal Biochem 286, 35-37.

Kamimura, D., Ishihara, K., Hirano, T., 2003. IL-6 signal transduction and its physiological roles: the signal orchestration model. Rev Physiol Biochem Pharmacol 149, 1-38.

Karelson, E., Bogdanovic, N., Garlind, A., Winblad, B., Zilmer, K., Kullisaar, T., Vihalemm, T., Kairane, C., Zilmer, M., 2001. The cerebrocortical areas in normal brain aging and in Alzheimer's disease: noticeable differences in the lipid peroxidation level and in antioxidant defense. Neurochem Res 26, 353-361.

Kauppinen, R.A., Enkvist, K., Holopainen, I., Akerman, K.E., 1988. Glucose deprivation depolarizes plasma membrane of cultured astrocytes and collapses transmembrane potassium and glutamate gradients. Neuroscience 26, 283-289.

Kelly, G.S., 2001. Rhodiola rosea: a possible plant adoptogen. Altern Med Rev 6, 293-302.

Kimelberg, H.K., 2011. Functions of mature mammalian astrocytes: a current view. Neuroscientist 16, 79-106.

Kimura, Y., Okuda, H., 2001. Resveratrol isolated from Polygonum cuspidatum root prevents tumor growth and metastasis to lung and tumor-induced neovascularization in Lewis lung carcinoma-bearing mice. J Nutr 131, 1844-1849.

Ko, K.M., Leon, T.Y., Mak, D.H., Chiu, P.Y., Du, Y., Poon, M.K., 2006. A characteristic pharmacological action of 'Yang-invigorating' Chinese tonifying herbs: enhancement of myocardial ATP-generation capacity. Phytomedicine 13, 636-642.

Kohl, R.L., Quay, W.B., 1979. Cystathionine synthase in rat brain: regional and time-of-day differences and their metabolic implications. J Neurosci Res 4, 189-196.

Konings, C.H., Kuiper, M.A., Teerlink, T., Mulder, C., Scheltens, P., Wolters, E.C., 1999. Normal cerebrospinal fluid glutathione concentrations in Parkinson's disease, Alzheimer's disease and multiple system atrophy. J Neurol Sci 168, 112-115.

Korn, T., Magnus, T., Jung, S., 2005. Autoantigen specific T cells inhibit glutamate uptake in astrocytes by decreasing expression of astrocytic glutamate transporter GLAST: a mechanism mediated by tumor necrosis factor-alpha. FASEB J 19, 1878-1880.

Kraft, A.D., Johnson, D.A., Johnson, J.A., 2004. Nuclear factor E2-related factor 2-dependent antioxidant response element activation by tert-butylhydroquinone and sulforaphane occurring preferentially in astrocytes conditions neurons against oxidative insult. J Neurosci 24, 1101-1112.

Kranich, O., Hamprecht, B., Dringen, R., 1996. Different preferences in the utilization of amino acids for glutathione synthesis in cultured neurons and astroglial cells derived from rat brain. Neurosci Lett 219, 211-214.

Kvamme, E., Roberg, B., Torgner, I.A., 2000. Phosphate-activated glutaminase and mitochondrial glutamine transport in the brain. Neurochem Res 25, 1407-1419.

LaFerla, F.M., Kitazawa, M., Yamasaki, T.R., 2004. Microglia as a potential bridge between the amyloid beta-peptide and tau. Ann Ny Acad Sci 1035, 85-103.

Lauderback, C.M., Hackett, J.M., Huang, F.F., Keller, J.N., Szweda, L.I., Markesbery, W.R., Butterfield, D.A., 2001. The glial glutamate transporter, GLT-1,

is oxidatively modified by 4-hydroxy-2-nonenal in the Alzheimer's disease brain: the role of Abeta1-42. J Neurochem 78, 413-416.

Laughton, J.D., Bittar, P., Charnay, Y., Pellerin, L., Kovari, E., Magistretti, P.J., Bouras, C., 2007. Metabolic compartmentalization in the human cortex and hippocampus: evidence for a cell- and region-specific localization of lactate dehydrogenase 5 and pyruvate dehydrogenase. BMC Neurosci 8, 35.

Lavoie, S., Chen, Y., Dalton, T.P., Gysin, R., Cuenod, M., Steullet, P., Do, K.Q., 2009. Curcumin, quercetin, and tBHQ modulate glutathione levels in astrocytes and neurons: importance of the glutamate cysteine ligase modifier subunit. J Neurochem 108, 1410-1422.

Le Prince, G., Delaere, P., Fages, C., Lefrancois, T., Touret, M., Salanon, M., Tardy, M., 1995. Glutamine synthetase (GS) expression is reduced in senile dementia of the Alzheimer type. Neurochem Res 20, 859-862.

Lee, S.C., Dickson, D.W., Liu, W., Brosnan, C.F., 1993. Induction of nitric oxide synthase activity in human astrocytes by interleukin-1 beta and interferon-gamma. J Neuroimmunol 46, 19-24.

Lee, S.T., Chu, K., Sim, J.Y., Heo, J.H., Kim, M., 2008. Panax ginseng enhances cognitive performance in Alzheimer disease. Alzheimer Dis Assoc Disord 22, 222-226.

Leino, R.L., Gerhart, D.Z., van Bueren, A.M., McCall, A.L., Drewes, L.R., 1998. Ultrastructural localization of GLUT 1 and GLUT 3 glucose transporters in rat brain. Journal of Neuroscience Research 49, 617-626.

Lewinska, A., Wnuk, M., Slota, E., Bartosz, G., 2007. Total anti-oxidant capacity of cell culture media. Clin Exp Pharmacol Physiol 34, 781-786.

Li, E.K., Tam, L.S., Wong, C.K., Li, W.C., Lam, C.W., Wachtel-Galor, S., Benzie, I.F., Bao, Y.X., Leung, P.C., Tomlinson, B., 2007. Safety and efficacy of Ganoderma lucidum (lingzhi) and San Miao San supplementation in patients with rheumatoid arthritis: a double-blind, randomized, placebo-controlled pilot trial. Arthritis Rheum 57, 1143-1150.

Li, R.W., David Lin, G., Myers, S.P., Leach, D.N., 2003a. Anti-inflammatory activity of Chinese medicinal vine plants. J Ethnopharmacol 85, 61-67.

Li, S., Mallory, M., Alford, M., Tanaka, S., Masliah, E., 1997. Glutamate transporter alterations in Alzheimer disease are possibly associated with abnormal APP expression. J Neuropathol Exp Neurol 56, 901-911.

Li, X.P., 1991. Experimental study on anti-senility of the 4 famous Chinese herbs produced in Huaiqing area. Zhong Xi Yi Jie He Za Zhi 11, 486-487, 454.

Li, Z., Sun, L., Zhang, H., Liao, Y., Wang, D., Zhao, B., Zhu, Z., Zhao, J., Ma, A., Han, Y., Wang, Y., Shi, Y., Ye, J., Hui, R., 2003b. Elevated plasma homocysteine was associated with hemorrhagic and ischemic stroke, but methylenetetrahydrofolate

reductase gene C677T polymorphism was a risk factor for thrombotic stroke: a Multicenter Case-Control Study in China. Stroke 34, 2085-2090.

Licastro, F., Mallory, M., Hansen, L.A., Masliah, E., 1998. Increased levels of alpha-1-antichymotrypsin in brains of patients with Alzheimer's disease correlate with activated astrocytes and are affected by APOE 4 genotype. J Neuroimmunol 88, 105-110.

Liddell, J.R., Dringen, R., Crack, P.J., Robinson, S.R., 2006. Glutathione peroxidase 1 and a high cellular glutathione concentration are essential for effective organic hydroperoxide detoxification in astrocytes. Glia 54, 873-879.

Liddell, J.R., Zwingmann, C., Schmidt, M.M., Thiessen, A., Leibfritz, D., Robinson, S.R., Dringen, R., 2009a. Sustained hydrogen peroxide stress decreases lactate production by cultured astrocytes. J Neurosci Res 87, 2696-2708.

Liddell, J.R., Zwingmann, C., Schmidt, M.M., Thiessen, A., Leibfritz, D., Robinson, S.R., Dringen, R., 2009b. Sustained hydrogen peroxide stress decreases lactate production by cultured astrocytes. J Neurosci Res 87, 2696-2708.

Lieb, K., Kaltschmidt, C., Kaltschmidt, B., Baeuerle, P.A., Berger, M., Bauer, J., Fiebich, B.L., 1996. Interleukin-1 beta uses common and distinct signaling pathways for induction of the interleukin-6 and tumor necrosis factor alpha genes in the human astrocytoma cell line U373. J Neurochem 66, 1496-1503.

Lin, H., Nah, S., Huang, Y., Wu, S., 2010. Potential antioxidant components and characteristics of fresh polygonum multiflorum. J. Food Drug Anal. 18, 120-127.

Lipton, S.A., Kim, W.K., Choi, Y.B., Kumar, S., D'Emilia, D.M., Rayudu, P.V., Arnelle, D.R., Stamler, J.S., 1997. Neurotoxicity associated with dual actions of homocysteine at the N-methyl-D-aspartate receptor. Proc Natl Acad Sci U S A 94, 5923-5928.

Liu, H., Wang, H., Shenvi, S., Hagen, T.M., Liu, R.M., 2004. Glutathione metabolism during aging and in Alzheimer disease. Ann N Y Acad Sci 1019, 346-349.

Longuemare, M.C., Swanson, R.A., 1995. Excitatory amino acid release from astrocytes during energy failure by reversal of sodium-dependent uptake. J Neurosci Res 40, 379-386.

Lovell, M.A., Ehmann, W.D., Butler, S.M., Markesbery, W.R., 1995. Elevated thiobarbituric acid-reactive substances and antioxidant enzyme activity in the brain in Alzheimer's disease. Neurology 45, 1594-1601.

Lu, H., Forbes, R.A., Verma, A., 2002. Hypoxia-inducible factor 1 activation by aerobic glycolysis implicates the Warburg effect in carcinogenesis. J Biol Chem 277, 23111-23115.

Magistretti, P.J., 2006. Neuron-glia metabolic coupling and plasticity. J Exp Biol 209, 2304-2311.

Magistretti, P.J., Pellerin, L., 1996. The contribution of astrocytes to the 18F-2-deoxyglucose signal in PET activation studies. Mol Psychiatry 1, 445-452.

Maher, P., Lewerenz, J., Lozano, C., Torres, J.L., 2008. A novel approach to enhancing cellular glutathione levels. J Neurochem 107, 690-700.

Makarov, P., Kropf, S., Wiswedel, I., Augustin, W., Schild, L., 2006. Consumption of redox energy by glutathione metabolism contributes to hypoxia/reoxygenation-induced injury in astrocytes. Mol Cell Biochem 286, 95-101.

Malaplate-Armand, C., Gueguen, Y., Bertrand, P., Ferrari, L., Batt, A.M., 2000. U373-MG response to interleukin-1beta-induced oxidative stress. Cell Biol Toxicol 16, 155-163.

Mallorga, P.J., Williams, J.B., Jacobson, M., Marques, R., Chaudhary, A., Conn, P.J., Pettibone, D.J., Sur, C., 2003. Pharmacology and expression analysis of glycine transporters GlyT1 with [3H]-(N-[3-(4′-fluorophenyl)-3-(4′phenylphenoxy)propyl])sarcosine. Neuropharmacology 45, 585-593.

Margolis, B.L., Lifschitz, M.D., 1985. Ammonia production and amino acid metabolism by rat renal papillary epithelial cells in culture. J Biol Chem 260, 501-507.

Markesbery, W.R., 1997. Oxidative stress hypothesis in Alzheimer's disease. Free Radic Biol Med 23, 134-147.

Marshak DR, Pesce SA, Stanley LC, WS, G., 1992. Increased S100 beta neurotrophic activity in Alzheimer's disease temporal lobe. Neurobiol Aging 13, 1-7.

Martins, R.N., Harper, C.G., Stokes, G.B., Masters, C.L., 1986. Increased cerebral glucose-6-phosphate dehydrogenase activity in Alzheimer's disease may reflect oxidative stress. J Neurochem 46, 1042-1045.

Masliah, E., Alford, M., DeTeresa, R., Mallory, M., Hansen, L., 1996. Deficient glutamate transport is associated with neurodegeneration in Alzheimer's disease. Ann Neurol 40, 759-766.

May, B.H., Lit, M., Xue, C.C., Yang, A.W., Zhang, A.L., Owens, M.D., Head, R., Cobiac, L., Li, C.G., Hugel, H., Story, D.F., 2009. Herbal medicine for dementia: a systematic review. Phytother Res 23, 447-459.

McCaddon, A., Hudson, P., Hill, D., Barber, J., Lloyd, A., Davies, G., Regland, B., 2003. Alzheimer's disease and total plasma aminothiols. Biol Psychiatry 53, 254-260.

McEwen, B.S., Reagan, L.P., 2004. Glucose transporter expression in the central nervous system: relationship to synaptic function. Eur J Pharmacol 490, 13-24.

McGeer, P.L., Akiyama, H., Itagaki, S., McGeer, E.G., 1989. Activation of the classical complement pathway in brain tissue of Alzheimer patients. Neurosci Lett 107, 341-346.

McGeer, P.L., McGeer, E.G., 1999. Inflammation of the brain in Alzheimer's disease: implications for therapy. J Leukoc Biol 65, 409-415.

McGeer, P.L., Schulzer, M., McGeer, E.G., 1996. Arthritis and anti-inflammatory agents as possible protective factors for Alzheimer's disease: a review of 17 epidemiologic studies. Neurology 47, 425-432.

McMenamin, M.E., Himmelfarb, J., Nolin, T.D., 2009. Simultaneous analysis of multiple aminothiols in human plasma by high performance liquid chromatography with fluorescence detection. J Chromatogr B Analyt Technol Biomed Life Sci 877, 3274-3281.

Meister, A., 1988. Glutathione metabolism and its selective modification. J Biol Chem 263, 17205-17208.

Melone, M., Bellesi, M., Conti, F., 2009. Synaptic localization of GLT-1a in the rat somatic sensory cortex. Glia 57, 108-117.

Mieyal, J.J., Gallogly, M.M., Qanungo, S., Sabens, E.A., Shelton, M.D., 2008. Molecular mechanisms and clinical implications of reversible protein S-glutathionylation. Antioxid Redox Signal 10, 1941-1988.

Minich, T., Riemer, J., Schulz, J.B., Wielinga, P., Wijnholds, J., Dringen, R., 2006. The multidrug resistance protein 1 (Mrp1), but not Mrp5, mediates export of glutathione and glutathione disulfide from brain astrocytes. J Neurochem 97, 373-384.

Mittler, R., 2002. Oxidative stress, antioxidants and stress tolerance. Trends Plant Sci 7, 405-410.

Mizgerd, J.P., Spieker, M.R., Doerschuk, C.M., 2001. Early response cytokines and innate immunity: essential roles for TNF receptor 1 and type I IL-1 receptor during Escherichia coli pneumonia in mice. J Immunol 166, 4042-4048.

Mokrasch, L.C., Teschke, E.J., 1984. Glutathione content of cultured cells and rodent brain regions: a specific fluorometric assay. Anal Biochem 140, 506-509.

Molyneux, P., 2004. The use of the stable free radical diphenylpicryl-hydrazyl (DPPH) for estimating antioxidant activity. Songklanakarin J Sci Technol 26, 211-219.

Moreira, P.I., Santos, M.S., Oliveira, C.R., Shenk, J.C., Nunomura, A., Smith, M.A., Zhu, X., Perry, G., 2008. Alzheimer disease and the role of free radicals in the pathogenesis of the disease. CNS Neurol Disord Drug Targets 7, 3-10.

Moynagh, P.N., 2005. The interleukin-1 signalling pathway in astrocytes: a key contributor to inflammation in the brain. J Anat 207, 265-269.

Mulligan, S.J., MacVicar, B.A., 2004. Calcium transients in astrocyte endfeet cause cerebrovascular constrictions. Nature 431, 195-199.

Murin, R., Cesar, M., Kowtharapu, B.S., Verleysdonk, S., Hamprecht, B., 2009. Expression of pyruvate carboxylase in cultured oligodendroglial, microglial and ependymal cells. Neurochem Res 34, 480-489.

Murphy, T.H., Miyamoto, M., Sastre, A., Schnaar, R.L., Coyle, J.T., 1989. Glutamate toxicity in a neuronal cell line involves inhibition of cystine transport leading to oxidative stress. Neuron 2, 1547-1558.

Nagele, R.G., Wegiel, J., Venkataraman, V., Imaki, H., Wang, K., Wegiel, J., 2004. Contribution of glial cells to the development of amyloid plaques in Alzheimer's disease. Neurobiol Aging 25, 663-674.

Newman, S., Sultana, R., Perluigi, M., Coccia, R., Cai, J., Pierce, W., Klein, J., Turner, D., Butterfield, D., 2007. An increase in S-glutathionylated proteins in the Alzheimer's disease inferior parietal lobule, a proteomics approach. J Neurosci Res 85, 1506-1514.

Ng, K.T., O'Dowd, B.S., Rickard, N.S., Robinson, S.R., Gibbs, M.E., Rainey, C., Zhao, W.Q., Sedman, G.L., Hertz, L., 1997. Complex roles of glutamate in the Gibbs-Ng model of one-trial aversive learning in the new-born chick. Neurosci Biobehav Rev 21, 45-54.

Nielsen, H.M., Minthon, L., Londos, E., Blennow, K., Miranda, E., Perez, J., Crowther, D.C., Lomas, D.A., Janciauskiene, S.M., 2007. Plasma and CSF serpins in Alzheimer disease and dementia with Lewy bodies. Neurology 69, 1569-1579.

Nolin, T.D., McMenamin, M.E., Himmelfarb, J., 2007. Simultaneous determination of total homocysteine, cysteine, cysteinylglycine, and glutathione in human plasma by high-performance liquid chromatography: application to studies of oxidative stress. J Chromatogr B Analyt Technol Biomed Life Sci 852, 554-561.

Norenberg, M.D., Rama Rao, K.V., Jayakumar, A.R., 2009. Signaling factors in the mechanism of ammonia neurotoxicity. Metab Brain Dis 24, 103-117.

Nunomura, A., Castellani, R.J., Zhu, X., Moreira, P.I., Perry, G., Smith, M.A., 2006. Involvement of oxidative stress in Alzheimer disease. J Neuropathol Exp Neurol 65, 631-641.

Nunomura, A., Perry, G., Aliev, G., Hirai, K., Takeda, A., Balraj, E.K., Jones, P.K., Ghanbari, H., Wataya, T., Shimohama, S., Chiba, S., Atwood, C.S., Petersen, R.B., Smith, M.A., 2001. Oxidative damage is the earliest event in Alzheimer disease. J Neuropathol Exp Neurol 60, 759-767.

Oberheim, N.A., Takano, T., Han, X., He, W., Lin, J.H., Wang, F., Xu, Q., Wyatt, J.D., Pilcher, W., Ojemann, J.G., Ransom, B.R., Goldman, S.A., Nedergaard, M., 2009. Uniquely hominid features of adult human astrocytes. J Neurosci 29, 3276-3287.

Oberheim, N.A., Wang, X., Goldman, S., Nedergaard, M., 2006. Astrocytic complexity distinguishes the human brain. Trends Neurosci 29, 547-553.

Occhipinti, R., Somersalo, E., Calvetti, D., 2009. Astrocytes as the glucose shunt for glutamatergic neurons at high activity: an in silico study. J Neurophysiol 101, 2528-2538.

Oddo, S., Caccamo, A., Shepherd, J.D., Murphy, M.P., Golde, T.E., Kayed, R., Metherate, R., Mattson, M.P., Akbari, Y., LaFerla, F.M., 2003. Triple-transgenic model of Alzheimer's disease with plaques and tangles: intracellular Abeta and synaptic dysfunction. Neuron 39, 409-421.

Oe, T., Ohyagi, T., Naganuma, A., 1998. Determination of gamma-glutamylglutathione and other low-molecular-mass biological thiol compounds by isocratic high-performance liquid chromatography with fluorimetric detection. J Chromatogr B Biomed Sci Appl 708, 285-289.

Oh, J.W., Schwiebert, L.M., Benveniste, E.N., 1999. Cytokine regulation of CC and CXC chemokine expression by human astrocytes. J Neurovirol 5, 82-94.

Olabarria, M., Noristani, H.N., Verkhratsky, A., Rodriguez, J.J., 2010. Concomitant astroglial atrophy and astrogliosis in a triple transgenic animal model of Alzheimer's disease. Glia 58, 831-838.

Orr, C.F., Rowe, D.B., Halliday, G.M., 2002. An inflammatory review of Parkinson's disease. Prog Neurobiol 68, 325-340.

Padmanabhan, J., Levy, M., Dickson, D.W., Potter, H., 2006. Alpha1-antichymotrypsin, an inflammatory protein overexpressed in Alzheimer's disease brain, induces tau phosphorylation in neurons. Brain 129, 3020-3034.

Palmer, A.M., 1999. The activity of the pentose phosphate pathway is increased in response to oxidative stress in Alzheimer's disease. J Neural Transm 106, 317-328.

Parachikova, A., Green, K.N., Hendrix, C., LaFerla, F.M., 2010. Formulation of a medical food cocktail for Alzheimer's disease: beneficial effects on cognition and neuropathology in a mouse model of the disease. PLoS One 5, e14015.

Park, C., Lee, S., Cho, I.H., Lee, H.K., Kim, D., Choi, S.Y., Oh, S.B., Park, K., Kim, J.S., Lee, S.J., 2006. TLR3-mediated signal induces proinflammatory cytokine and chemokine gene expression in astrocytes: differential signaling mechanisms of TLR3-induced IP-10 and IL-8 gene expression. Glia 53, 248-256.

Pascual, J.M., van Heertum, R.L., Wang, D., Engelstald, K., De Vivo, D.C., 2002. Imaging the metabolic footprint of Glut1 deficiency on the brain. Ann Neurol 52, 458-464.

Pearce, R.K., Owen, A., Daniel, S., Jenner, P., Marsden, C.D., 1997. Alterations in the distribution of glutathione in the substantia nigra in Parkinson's disease. J Neural Transm 104, 661-677.

Pellerin, L., 2003. Lactate as a pivotal element in neuron-glia metabolic cooperation. Neurochemistry International 43, 331-338.

Pellerin, L., Magistretti, P.J., 1994. Glutamate uptake into astrocytes stimulates aerobic glycolysis: a mechanism coupling neuronal activity to glucose utilization. Proc Natl Acad Sci 91, 10625-10629.

Pellerin, L., Pellegri, G., Bittar, P.G., Charnay, Y., Bouras, C., Martin, J.L., Stella, N., Magistretti, P.J., 1998. Evidence supporting the existence of an activity-dependent astrocyte-neuron lactate shuttle. Dev Neurosci 20, 291-299.

Perry, T.L., Yong, V.W., Bergeron, C., Hansen, S., Jones, K., 1987. Amino acids, glutathione, and glutathione transferase activity in the brains of patients with Alzheimer's disease. Ann Neurol 21, 331-336.

Peterson, J.I., Young, D.S., 1968. Evaluation of the hexokinase-glucose-6-phosphate dehydrogenase method of determination of glucose in urine. Anal Biochem 23, 301-316.

Petzold, A., Jenkins, R., Watt, H.C., Green, A.J., Thompson, E.J., Keir, G., Fox, N.C., Rossor, M.N., 2003. Cerebrospinal fluid S100B correlates with brain atrophy in Alzheimer's disease. Neurosci Lett 336, 167-170.

Pietrzik, K., 2006. [Homocysteine as a cardiovascular marker and risk factor]. Clin Res Cardiol 95 Suppl 6, VI28-33.

Pocernich, C.B., Cardin, A.L., Racine, C.L., Lauderback, C.M., Butterfield, D.A., 2001. Glutathione elevation and its protective role in acrolein-induced protein damage in synaptosomal membranes: relevance to brain lipid peroxidation in neurodegenerative disease. Neurochem Int 39, 141-149.

Pocernich, C.B., La Fontaine, M., Butterfield, D.A., 2000. In-vivo glutathione elevation protects against hydroxyl free radical-induced protein oxidation in rat brain. Neurochem Int 36, 185-191.

Poole, C.F., 2003. General Concepts in Column Chromatography. The Essence of Chromatography. Elsevier Science, Amsterdam, pp. 1-78.

Popp, J., Lewczuk, P., Linnebank, M., Cvetanovska, G., Smulders, Y., Kolsch, H., Frommann, I., Kornhuber, J., Maier, W., Jessen, F., 2009. Homocysteine metabolism and cerebrospinal fluid markers for Alzheimer's disease. J Alzheimers Dis 18, 819-828.

Pow, D.V., Cook, D.G., 2009. Neuronal Expression of Splice Variants of "Glial" Glutamate Transporters in Brains Afflicted by Alzheimer's Disease: Unmasking an Intrinsic Neuronal Property. Neurochem Res 34, 1748-1757.

Pow, D.V., Robinson, S.R., 1994. Glutamate in some retinal neurons is derived solely from glia. Neuroscience 60, 355-366.

Prebil, M., Jensen, J., Zorec, R., Kreft, M., 2011. Astrocytes and energy metabolism. Arch Physiol Biochem 117, 64-69.

Quan, L.D., 2000. Chinese Medicine. Shanghai Scientific and Technical Publishers, Shanghai.

Quincozes-Santos, A., Andreazza, A.C., Nardin, P., Funchal, C., Goncalves, C.A., Gottfried, C., 2007. Resveratrol attenuates oxidative-induced DNA damage in C6 Glioma cells. Neurotoxicology 28, 886-891.

Rafii, M.S., Walsh, S., Little, J.T., Behan, K., Reynolds, B., Ward, C., Jin, S., Thomas, R., Aisen, P.S., 2011. A phase II trial of huperzine A in mild to moderate Alzheimer disease. Neurology 76, 1389-1394.

Rao, K.V., Panickar, K.S., Jayakumar, A.R., Norenberg, M.D., 2005. Astrocytes protect neurons from ammonia toxicity. Neurochem Res 30, 1311-1318.

Raps, S.P., Lai, J.C., Hertz, L., Cooper, A.J., 1989. Glutathione is present in high concentrations in cultured astrocytes but not in cultured neurons. Brain Res 493, 398-401.

Reddy, P.H., Anekonda, T.S., 2005. Can herbs provide a new generation of drugs for treating Alzheimer's disease? Brain Research Reviews 50, 361-376.

Redjems-Bennani, N., Jeandel, C., Lefebvre, E., Blain, H., Vidailhet, M., Gueant, J.L., 1998. Abnormal substrate levels that depend upon mitochondrial function in cerebrospinal fluid from Alzheimer patients. Gerontology 44, 300-304.

Reger, M.A., Henderson, S.T., Hale, C., Cholerton, B., Baker, L.D., Watson, G.S., Hyde, K., Chapman, D., Craft, S., 2004. Effects of beta-hydroxybutyrate on cognition in memory-impaired adults. Neurobiol Aging 25, 311-314.

Rice, A.C., Zsoldos, R., Chen, T., Wilson, M.S., Alessandri, B., Hamm, R.J., Bullock, M.R., 2002. Lactate administration attenuates cognitive deficits following traumatic brain injury. Brain Res 928, 156-159.

Rice, M.E., Russo-Menna, I., 1998. Differential compartmentalization of brain ascorbate and glutathione between neurons and glia. Neuroscience 82, 1213-1223.

Robert, K., Vialard, F., Thiery, E., Toyama, K., Sinet, P.M., Janel, N., London, J., 2003. Expression of the cystathionine beta synthase (CBS) gene during mouse development and immunolocalization in adult brain. J Histochem Cytochem 51, 363-371.

Robinson, S.R., 2000. Neuronal expression of glutamine synthetase in Alzheimer's disease indicates a profound impairment of metabolic interactions with astrocytes. Neurochem Int 36, 471-482.

Robinson, S.R., 2001. Changes in the cellular distribution of glutamine synthetase in Alzheimer's disease. J Neurosci Res 66, 972-980.

Rouach, N., Koulakoff, A., Abudara, V., Willecke, K., Giaume, C., 2008. Astroglial metabolic networks sustain hippocampal synaptic transmission. Science 322, 1551-1555.

Rubin, H., 1997. Cell aging in vivo and in vitro. Mech Ageing Dev 98, 1-35.

Ruedig, C., Dringen, R., 2004. TNF alpha increases activity of gamma-glutamyl transpeptidase in cultured rat astroglial cells. J Neurosci Res 75, 536-543.

Sagara, J.I., Miura, K., Bannai, S., 1993. Maintenance of neuronal glutathione by glial cells. J Neurochem 61, 1672-1676.

Saito, K., Suyama, K., Nishida, K., Sei, Y., Basile, A.S., 1996. Early increases in TNF-alpha, IL-6 and IL-1 beta levels following transient cerebral ischemia in gerbil brain. Neurosci Lett 206, 149-152.

Santa, T., Aoyama, C., Fukushima, T., Imai, K., Funatsu, T., 2006. Suppression of thiol exchange reaction in the determination of reduced-form thiols by high-performance liquid chromatography with fluorescence detection after derivatization with fluorogenic benzofurazan reagent, 7-fluoro-2,1,3-benzoxadiazole-4-sulfonate and 4-aminosulfonyl-7-fluoro-2,1,3-benzoxadiazole. Biomed Chromatogr 20, 656-661.

Savaskan, N.E., Seufert, S., Hauke, J., Trankle, C., Eyupoglu, I.Y., Hahnen, E., 2011. Dissection of mitogenic and neurodegenerative actions of cystine and glutamate in malignant gliomas. Oncogene 30, 43-53.

Schenk, D., Barbour, R., Dunn, W., Gordon, G., Grajeda, H., Guido, T., Hu, K., Huang, J., Johnson-Wood, K., Khan, K., Kholodenko, D., Lee, M., Liao, Z., Lieberburg, I., Motter, R., Mutter, L., Soriano, F., Shopp, G., Vasquez, N., Vandevert, C., Walker, S., Wogulis, M., Yednock, T., Games, D., Seubert, P., 1999. Immunization with amyloid-beta attenuates Alzheimer-disease-like pathology in the PDAPP mouse. Nature 400, 173-177.

Schipper, H.M., Bennett, D.A., Liberman, A., Bienias, J.L., Schneider, J.A., Kelly, J., Arvanitakis, Z., 2006. Glial heme oxygenase-1 expression in Alzheimer disease and mild cognitive impairment. Neurobiol Aging 27, 252-261.

Schliess, F., Gorg, B., Fischer, R., Desjardins, P., Bidmon, H.J., Herrmann, A., Butterworth, R.F., Zilles, K., Haussinger, D., 2002. Ammonia induces MK-801-sensitive nitration and phosphorylation of protein tyrosine residues in rat astrocytes. FASEB J 16, 739-741.

Schuessel, K., Leutner, S., Cairns, N.J., Muller, W.E., Eckert, A., 2004. Impact of gender on upregulation of antioxidant defence mechanisms in Alzheimer's disease brain. J Neural Transm 111, 1167-1182.

Schwamborn, J., Lindecke, A., Elvers, M., Horejschi, V., Kerick, M., Rafigh, M., Pfeiffer, J., Prullage, M., Kaltschmidt, B., Kaltschmidt, C., 2003. Microarray analysis of tumor necrosis factor alpha induced gene expression in U373 human glioblastoma cells. BMC Genomics 4, 46.

Scott, H., Pow, D., Tannenberg, A., Dodd, P., 2002. Aberrant expression of the glutamate transporter excitatory amino acid transporter 1 (EAAT1) in Alzheimer's disease. J Neurosci 22, RC206.

Seib, T.M., Patel, S.A., Bridges, R.J., 2011. Regulation of the System x(-) (C) cystine/glutamate exchanger by intracellular glutathione levels in rat astrocyte primary cultures. Glia.

Seifert, G., Huttmann, K., Binder, D.K., Hartmann, C., Wyczynski, A., Neusch, C., Steinhauser, C., 2009. Analysis of astroglial K+ channel expression in the developing hippocampus reveals a predominant role of the Kir4.1 subunit. J Neurosci 29, 7474-7488.

Seiler, N., 2002. Ammonia and Alzheimer's disease. Neurochem Int 41, 189-207.

Selmaj, K.W., Farooq, M., Norton, W.T., Raine, C.S., Brosnan, C.F., 1990. Proliferation of astrocytes in vitro in response to cytokines. A primary role for tumor necrosis factor. J Immunol 144, 129-135.

Senft, A.P., Dalton, T.P., Shertzer, H.G., 2000. Determining glutathione and glutathione disulfide using the fluorescence probe o-phthalaldehyde. Anal Biochem 280, 80-86.

Serres, S., Raffard, G., Franconi, J.M., Merle, M., 2008. Close coupling between astrocytic and neuronal metabolisms to fulfill anaplerotic and energy needs in the rat brain. J Cereb Blood Flow Metab 28, 712-724.

Seshadri, S., Beiser, A., Selhub, J., Jacques, P.F., Rosenberg, I.H., D'Agostino, R.B., Wilson, P.W., Wolf, P.A., 2002. Plasma homocysteine as a risk factor for dementia and Alzheimer's disease. N Engl J Med 346, 476-483.

Shah, V.P., Midha, K.K., Findlay, J.W., Hill, H.M., Hulse, J.D., McGilveray, I.J., McKay, G., Miller, K.J., Patnaik, R.N., Powell, M.L., Tonelli, A., Viswanathan, C.T., Yacobi, A., 2000. Bioanalytical method validation--a revisit with a decade of progress. Pharm Res 17, 1551-1557.

Shanker, G., Aschner, M., 2001. Identification and characterization of uptake systems for cystine and cysteine in cultured astrocytes and neurons: evidence for methylmercury-targeted disruption of astrocyte transport. J Neurosci Res 66, 998-1002.

Sharbir, G.A., 2004. HPLC method development and validation for pharmaceutical analysis. Pharm Technol 16, 37-49.

Shih, A.Y., Johnson, D.A., Wong, G., Kraft, A.D., Jiang, L., Erb, H., Johnson, J.A., Murphy, T.H., 2003. Coordinate regulation of glutathione biosynthesis and release by Nrf2-expressing glia potently protects neurons from oxidative stress. J Neurosci 23, 3394-3406.

Simard, M., Nedergaard, M., 2004. The neurobiology of glia in the context of water and ion homeostasis. Neuroscience 129, 877-896.

Simpson, I.A., Carruthers, A., Vannucci, S.J., 2007. Supply and demand in cerebral energy metabolism: the role of nutrient transporters. J Cereb Blood Flow Metab 27, 1766-1791.

Simpson, J., Ince, P., Lace, G., Forster, G., Shaw, P., Matthews, F., Savva, G., Brayne, C., Wharton, S., 2008. Astrocyte phenotype in relation to Alzheimer-type pathology in the ageing brain. Neurobiol Aging In Press.

Simpson, J.E., Ince, P.G., Lace, G., Forster, G., Shaw, P.J., Matthews, F., Savva, G., Brayne, C., Wharton, S.B., 2010. Astrocyte phenotype in relation to Alzheimer-type pathology in the ageing brain. Neurobiol Aging 31, 578-590.

Singleton, V.L., Rossi, J.A., 1965. Colorimetry of total phenolics with phosphomolybdic-phosphotungstic acid reagents. Am J Enol Vitic 16, 144-158.

Slosman, D.O., Ludwig, C., Zerarka, S., Pellerin, L., Chicherio, C., de Ribaupierre, A., Annoni, J.M., Bouras, C., Herrmann, F., Michel, J.P., Giacobini, E., Magistretti, P.J., 2001. Brain energy metabolism in Alzheimer's disease: 99mTc-HMPAO SPECT imaging during verbal fluency and role of astrocytes in the cellular mechanism of 99mTc-HMPAO retention. Brain Res Brain Res Rev 36, 230-240.

Small, G.W., Ercoli, L.M., Silverman, D.H.S., Huang, S.C., Komo, S., Bookheimer, S.Y., Lavretsky, H., Miller, K., Siddarth, P., Rasgon, N.L., Mazziotta, J.C., Saxena, S., Wu, H.M., Mega, M.S., Cummings, J.L., Saunders, A.M., Pericak-Vance, M.A., Roses, A.D., Barrio, J.R., Phelps, M.E., 2000. Cerebral metabolic and cognitive decline in persons at genetic risk for Alzheimer's disease. Proceed Nat Acad Sci 97, 6037-6042.

Smith, C.C., Bowen, D.M., Francis, P.T., Snowden, J.S., Neary, D., 1985. Putative amino acid transmitters in lumbar cerebrospinal fluid of patients with histologically verified Alzheimer's dementia. J Neurol Neurosurg Psychiatry 48, 469-471.

Smith, C.D., Carney, J.M., Starke-Reed, P.E., Oliver, C.N., Stadtman, E.R., Floyd, R.A., Markesbery, W.R., 1991. Excess brain protein oxidation and enzyme dysfunction in normal aging and in Alzheimer disease. Proc Natl Acad Sci U S A 88, 10540-10543.

Sofroniew, M.V., 2009. Molecular dissection of reactive astrogliosis and glial scar formation. Trends Neurosci 32, 638-647.

Sofroniew, M.V., Vinters, H.V., 2010. Astrocytes: biology and pathology. Acta Neuropathol 119, 7-35.

Sonnewald, U., Westergaard, N., Schousboe, A., 1997. Glutamate transport and metabolism in astrocytes. Glia 21, 56-63.

Steele, M., Stuchbury, G., Munch, G., 2007. The molecular basis of the prevention of Alzheimer's disease through healthy nutrition. Exp Gerontol 42, 28-36.

Steele, M.L., Robinson, S.R., 2011. Reactive astrocytes give neurons less support: implications for Alzheimer's disease. Neurobiol Aging.

Stuart, C.A., Ross, I.R., Howell, M.E., McCurry, M.P., Wood, T.G., Ceci, J.D., Kennel, S.J., Wall, J., 2011. Brain glucose transporter (Glut3) haploinsufficiency does not impair mouse brain glucose uptake. Brain Res 1384, 15-22.

Styren, S.D., Kamboh, M.I., DeKosky, S.T., 1998. Expression of differential immune factors in temporal cortex and cerebellum: the role of alpha-1-antichymotrypsin, apolipoprotein E, and reactive glia in the progression of Alzheimer's disease. J Comp Neurol 396, 511-520.

Suh, J.H., Shenvi, S.V., Dixon, B.M., Liu, H., Jaiswal, A.K., Liu, R.M., Hagen, T.M., 2004. Decline in transcriptional activity of Nrf2 causes age-related loss of glutathione synthesis, which is reversible with lipoic acid. Proc Natl Acad Sci U S A 101, 3381-3386.

Suh, S.W., Aoyama, K., Matsumori, Y., Liu, J., Swanson, R.A., 2005. Pyruvate administered after severe hypoglycemia reduces neuronal death and cognitive impairment. Diabetes 54, 1452-1458.

Suh, S.W., Bergher, J.P., Anderson, C.M., Treadway, J.L., Fosgerau, K., Swanson, R.A., 2007. Astrocyte glycogen sustains neuronal activity during hypoglycemia: studies with the glycogen phosphorylase inhibitor CP-316,819 ([R-R*,S*]-5-chloro-N-[2-hydroxy-3-(methoxymethylamino)-3-oxo-1-(phenylmet hyl)propyl]-1H-indole-2-carboxamide). J Pharmacol Exp Ther 321, 45-50.

Suk, K., 2005. Regulation of neuroinflammation by herbal medicine and its implications for neurodegenerative diseases. A focus on traditional medicines and flavonoids. Neurosignals 14, 23-33.

Surh, Y.J., 2008. NF-kappa B and Nrf2 as potential chemopreventive targets of some anti-inflammatory and antioxidative phytonutrients with anti-inflammatory and antioxidative activities. Asia Pac J Clin Nutr 17 Suppl 1, 269-272.

Suzuki, A., Stern, S.A., Bozdagi, O., Huntley, G.W., Walker, R.H., Magistretti, P.J., Alberini, C.M., 2011. Astrocyte-neuron lactate transport is required for long-term memory formation. Cell 144, 810-823.

Swardfager, W., Lanctot, K., Rothenburg, L., Wong, A., Cappell, J., Herrmann, N., 2010. A meta-analysis of cytokines in Alzheimer's disease. Biol Psychiatry 68, 930-941.

Takano, T., Tian, G.F., Peng, W., Lou, N., Libionka, W., Han, X., Nedergaard, M., 2006. Astrocyte-mediated control of cerebral blood flow. Nat Neurosci 9, 260-267.

Tanaka, K., Watase, K., Manabe, T., Yamada, K., Watanabe, M., Takahashi, K., Iwama, H., Nishikawa, T., Ichihara, N., Kikuchi, T., Okuyama, S., Kawashima, N., Hori, S., Takimoto, M., Wada, K., 1997. Epilepsy and Exacerbation of Brain Injury in Mice Lacking the Glutamate Transporter GLT-1 Science 276, 1699-1702.

Tarkowski, E., Blennow, K., Wallin, A., Tarkowski, A., 1999. Intracerebral production of tumor necrosis factor-alpha, a local neuroprotective agent, in Alzheimer disease and vascular dementia. J Clin Immunol 19, 223-230.

Thimmulappa, R.K., Mai, K.H., Srisuma, S., Kensler, T.W., Yamamoto, M., Biswal, S., 2002. Identification of Nrf2-regulated genes induced by the chemopreventive agent sulforaphane by oligonucleotide microarray. Cancer Res 62, 5196-5203.

Tietze, F., 1969. Enzymic method for quantitative determination of nanogram amounts of total and oxidized glutathione: applications to mammalian blood and other tissues. Anal Biochem 27, 502-522.

Tilleux, S., Hermans, E., 2008. Down-regulation of astrocytic GLAST by microglia-related inflammation is abrogated in dibutyryl cAMP-differentiated cultures. J Neurochem 105, 2224-2236.

Tobinick, E., 2008. Perispinal etanercept produces rapid improvement in primary progressive aphasia: identification of a novel, rapidly reversible TNF-mediated pathophysiologic mechanism. Medscape J Med 10, 135.

Tobinick, E., 2009. Tumour necrosis factor modulation for treatment of Alzheimer's disease: rationale and current evidence. CNS Drugs 23, 713-725.

Tobinick, E., Gross, H., Weinberger, A., Cohen, H., 2006. TNF-alpha modulation for treatment of Alzheimer's disease: a 6-month pilot study. Med Gen Med 8, 25.

Toyo'oka, T., Furukawa, F., Suzuki, T., Saito, Y., Takahashi, M., Hayashi, Y., Uzu, S., Imai, K., 1989. Determination of thiols and disulfides in normal rat tissues and hamster pancreas treated with N-nitrosobis(2-oxopropyl)amine using 4-(aminosulfonyl)-7-fluoro-2,1,3-benzoxadiazole and ammonium 7-fluoro-2,1,3-benzoxadiazole-4-sulfonate. Biomed Chromatogr 3, 166-172.

Toyo'oka, T., Imai, K., 1983. High-performance liquid chromatography and fluorometric detection of biologically important thiols, derivatized with ammonium 7-fluorobenzo-2-oxa-1,3-diazole-4-sulphonate (SBD-F). J Chromatogr 282, 495-500.

Tsacopoulos, M., Evequoz-Mercier, V., Perrottet, P., Buchner, E., 1988. Honeybee retinal glial cells transform glucose and supply the neurons with metabolic substrate. Proc Natl Acad Sci U S A 85, 8727-8731.

Tumani, H., Shen, G., Peter, J.B., Bruck, W., 1999. Glutamine synthetase in cerebrospinal fluid, serum, and brain: a diagnostic marker for Alzheimer disease? Arch Neurol 56, 1241-1246.

Tuppo, E., Arias, H., 2005. The role of inflammation in Alzheimer's disease. Int J Biochem Cell Biol 37, 289-305.

Um, M.Y., Choi, W.H., Aan, J.Y., Kim, S.R., Ha, T.Y., 2006. Protective effect of Polygonum multiflorum Thunb on amyloid beta-peptide 25-35 induced cognitive deficits in mice. J Ethnopharmacol 104, 144-148.

Unschuld, P.U., 1986. Medicine in China. A History of Pharmaceutics. University of California Press, Berkely.

van Exel, E., Eikelenboom, P., Comijs, H., Frolich, M., Smit, J.H., Stek, M.L., Scheltens, P., Eefsting, J.E., Westendorp, R.G., 2009. Vascular factors and markers of inflammation in offspring with a parental history of late-onset Alzheimer disease. Arch Gen Psychiatry 66, 1263-1270.

Vannucci, S.J., Maher, F., Simpson, I.A., 1997. Glucose transporter proteins in brain: delivery of glucose to neurons and glia. Glia 21, 2-21.

Vanzani, M.C., Iacono, R.F., Caccuri, R.L., Berria, M.I., 2005. Immunochemical and morphometric features of astrocyte reactivity vs. plaque location in Alzheimer's disease. Medicina (B Aires) 65, 213-218.

Vargas, M.R., Johnson, J.A., 2009. The Nrf2-ARE cytoprotective pathway in astrocytes. Expert Rev Mol Med 11, e17.

Vega, C., Pellerin, L., Dantzer, R., Magistretti, P.J., 2002. Long-term modulation of glucose utilization by IL-1 alpha and TNF-alpha in astrocytes: Na+ pump activity as a potential target via distinct signaling mechanisms. Glia 39, 10-18.

Vesce, S., Rossi, D., Brambilla, L., Volterra, A., 2007. Glutamate release from astrocytes in physiological conditions and in neurodegenerative disorders characterized by neuroinflammation. Int Rev Neurobiol 82, 57-71.

Vitvitsky, V., Thomas, M., Ghorpade, A., Gendelman, H.E., Banerjee, R., 2006. A functional transsulfuration pathway in the brain links to glutathione homeostasis. J Biol Chem 281, 35785-35793.

Voskuhl, R.R., Peterson, R.S., Song, B., Ao, Y., Morales, L.B., Tiwari-Woodruff, S., Sofroniew, M.V., 2009. Reactive astrocytes form scar-like perivascular barriers to leukocytes during adaptive immune inflammation of the CNS. J Neurosci 29, 11511-11522.

Voutsinos-Porche, B., Knott, G., Tanaka, K., Quairiaux, C., Welker, E., Bonvento, G., 2003. Glial glutamate transporters and maturation of the mouse somatosensory cortex. Cereb Cortex 13, 1110-1121.

Wang, Z.T., Ng, T.B., Yeung, H.W., Xu, G.J., 1996. Immunomodulatory effect of a polysaccharide-enriched preparation of Codonopsis pilosula roots. Gen Pharmacol 27, 1347-1350.

Warburg, O., Wind, F., Negelein, E., 1927. The Metabolism of Tumors in the Body. J Gen Physiol 8, 519-530.

Waterhouse, A.L., 2002. Determination of total phenolics. In: Wrolstad, R.E. (Ed.), Current protocols in food chemistry. John Wiley & Sons, Inc., New York.

Wharton, S.B., O'Callaghan, J.P., Savva, G.M., Nicoll, J.A., Matthews, F., Simpson, J.E., Forster, G., Shaw, P.J., Brayne, C., Ince, P.G., 2009. Population variation in glial fibrillary acidic protein levels in brain ageing: relationship to Alzheimer-type pathology and dementia. Dement Geriatr Cogn Disord 27, 465-473.

Wild, A.C., Moinova, H.R., Mulcahy, R.T., 1999. Regulation of gamma-glutamylcysteine synthetase subunit gene expression by the transcription factor Nrf2. J Biol Chem 274, 33627-33636.

Wilhelmsson, U., Bushong, E.A., Price, D.L., Smarr, B.L., Phung, V., Terada, M., Ellisman, M.H., Pekny, M., 2006. Redefining the concept of reactive astrocytes as

cells that remain within their unique domains upon reaction to injury. Proc Natl Acad Sci U S A 103, 17513-17518.

Williams, R.H., Maggiore, J.A., Reynolds, R.D., Helgason, C.M., 2001. Novel approach for the determination of the redox status of homocysteine and other aminothiols in plasma from healthy subjects and patients with ischemic stroke. Clin Chem 47, 1031-1039.

Wilms, H., Rosenstiel, P., Sievers, J., Deuschl, G., Lucius, R., 2001. Cerebrospinal fluid from patients with neurodegenerative and neuroinflammatory diseases: no evidence for rat glial activation in vitro. Neurosci Lett 314, 107-110.

Winston, D., Maimes, S., 2007. Herbs for Strength, Stamina and, Stress Relief. Healing Arts Press, Rochester.

Ye, Z.C., Rothstein, J.D., Sontheimer, H., 1999. Compromised glutamate transport in human glioma cells: reduction-mislocalization of sodium-dependent glutamate transporters and enhanced activity of cystine-glutamate exchange. J Neurosci 19, 10767-10777.

Ye, Z.C., Sontheimer, H., 1999. Glioma cells release excitotoxic concentrations of glutamate. Cancer Res 59, 4383-4391.

Yoshiba-Suzuki, S., Sagara, J., Bannai, S., Makino, N., 2011. The dynamics of cysteine, glutathione and their disulphides in astrocyte culture medium. J Biochem 150, 95-102.

Yu, N., Martin, J.L., Stella, N., Magistretti, P.J., 1993. Arachidonic acid stimulates glucose uptake in cerebral cortical astrocytes. Proc Natl Acad Sci U S A 90, 4042-4046.

Zerarka, S., Pellerin, L., Slosman, D., Magistretti, P.J., 2001. Astrocytes as a predominant cellular site of (99m)Tc-HMPAO retention. J Cereb Blood Flow Metab 21, 456-468.

Zhang, R.X., Li, M.X., Jia, Z.P., 2008. Rehmannia glutinosa: review of botany, chemistry and pharmacology. J Ethnopharmacol 117, 199-214.

Zhao, R., Liu, S., Zhou, L., 2005. Rapid Quantitative HPTLC Analysis, on One Plate, of Emodin, Resveratrol, and Polydatin in the Chinese Herb Polygonum cuspidatum. Chromatographia 61, 311-314.

Zheng, W., Wang, S.Y., 2001. Antioxidant activity and phenolic compounds in selected herbs. J Agric Food Chem 49, 5165-5170.

Zonta, M., Angulo, M.C., Gobbo, S., Rosengarten, B., Hossmann, K.A., Pozzan, T., Carmignoto, G., 2003. Neuron-to-astrocyte signaling is central to the dynamic control of brain microcirculation. Nat Neurosci 6, 43-50.

Zou, J., Wang, Y.X., Dou, F.F., Lu, H.Z., Ma, Z.W., Lu, P.H., Xu, X.M., 2010. Glutamine synthetase down-regulation reduces astrocyte protection against glutamate excitotoxicity to neurons. Neurochem Int 56, 577-584.